

School of Molecular and Life Sciences

**Using Synchrotron Infrared Spectroscopy and X-ray
Fluorescence Microscopy to Explore Fingerprint Chemistry**

Rhiannon Boseley
0000-0002-7919-9977

**This thesis is presented for the Degree of
Doctor of Philosophy
of
Curtin University**

March 2022

Declaration

To the best of my knowledge and belief this thesis contains no material previously published by any other person except where due acknowledgment has been made.

This thesis contains no material which has been accepted for the award of any other degree or diploma in any university.

Human Ethics

The research presented and reported in this thesis was conducted in accordance with the National Health and Medical Research Council National Statement on Ethical Conduct in Human Research (2007) – updated March 2014. The proposed research study received human research ethics approval from the Curtin University Human Research Ethics Committee (EC00262), Approval Number HRE2018-0476.

Signature:

Date: 22/02/2022

Abstract

In a criminal justice system, fingerprints are an important form of trace evidence used to connect an individual with an object or crime scene. Their use in investigations is reliant on their successful recovery, however due to the lack of sensitivity and robustness of current detection methods, a large number of fingerprints remain undetected. Research has focused on the chemistry of fingerprint samples to help rationalise the performance of detection treatments, with variation in response shown to be affected by donor and time since deposition. Previously, bulk chemical analysis techniques or optical methods have been used to examine the composition of fingerprint residues and large scale fingerprint development studies have demonstrated how development performance can vary. Understanding how variation in the spatial distribution of chemical components affect development performance has however, been previously difficult to study. This thesis aims to add new knowledge to this research field, by bringing together chemical and spatial information through the use of chemical imaging, revealing the distribution of organic and inorganic material in latent fingerprints and how this can relate to fingerprint development. The findings expand the current understanding of fingerprint chemistry, to explain variation in latent fingerprint detection and identify novel strategies to increase detection capabilities.

A synchrotron light source was utilised to gain a unique view of fingerprint residues, providing exceptional detection limits, spatial resolution and spectral quality to analyse natural fingerprint samples. X-ray fluorescence microscopy (XFM) was applied to map the natural distribution of inorganic components within fingerprint residue. Endogenous trace metals (Fe, Cu, Zn), diffusible ions (Cl^- , K^+ , Ca^{2+}), and exogenous metals (Ni, Ti) were detected across fourteen fingerprint donors. Further, the incorporation of a multimodal approach using XFM alongside infrared microspectroscopy (IRM) demonstrated for the first time the colocalization of endogenous metals within the hydrophilic organic components of fingerprint residue.

XFM was also used to explore the forensic processes of transfer and persistence, by linking trace metal profiles to contact with metal objects. Fingermarks were taken before and after brief handling of forensically significant items. The results reveal increased metal content after contact, and critically, a characteristic pattern of increased metal content dependent on the object. Persistence studies indicated that these metals are removed as easily as they are transferred, with a reduction in elemental content after hand washing prior to deposition or water immersion post deposition. Interestingly, particular metals (Ti, Zn, Fe) remain after water immersion, suggesting potential chemical targets for novel detection methods. Preliminary work using X-ray absorption near edge structure spectroscopic mapping highlighted the potential use of this technique to differentiate between different chemical forms of metals and metal ions in latent fingermarks. It is anticipated that these findings can now be used to assist the interpretation of the transfer and persistence of fingerprint evidence and direct future work for the advancement of trace metal detection tests and fingerprint development procedures.

The degradation of fingerprint residue is known to have a detrimental effect on development performance. The rate of degradation has been previously explored with bulk chemical analyses, but little is known about chemical alterations within specific regions of the fingerprint. Attenuated total reflectance (ATR) IRM with a synchrotron IR source was used to provide spatio-temporal resolution of chemical changes within fingerprint droplets, as a function of time since deposition, under ambient temperature conditions. Natural fingerprint droplets were imaged on the micron scales at hourly intervals within the first 7 – 13 hours after deposition, revealing that substantial dehydration occurred within the first 8 hours. Changes to lipid material was more varied, with the variation in the initial chemical composition and morphology of the droplet expected to influence the rate of change of the droplet over time.

The dehydration of fingerprint residue was revealed to be the most significant chemical and physical change seen in the immediate hours following deposition. Despite this, there remains uncertainty in the volume of water in a fingerprint and its potential rate of dehydration. The strength of the absorption of Terahertz/Far-

infrared (THz/Far-IR) radiation by water vapour molecules was exploited, using THz/Far-IR gas-phase spectroscopy to measure the volume of water in a fingerprint. Upon heating, water confined in natural fingerprints was evaporated to fill a vacuum chamber equipped with multipass optics. The amount of water vapour was then quantified by high-spectral resolution analysis, and fingerprints were observed to lose approximately 14 – 20 μg of water. The combination of both ATR-FTIR and Far-IR gas-phase techniques highlights important implications for experimental design in fingerprint research, and operational practices used by law enforcement agencies.

Acknowledgements

I would like to take this opportunity to thank the many people who have assisted me throughout my time as a PhD student. This thesis would not have been possible without the incredible support of the people around me.

I would particularly like to thank my supervisory team for their guidance and encouragement. To Simon, I am so grateful for your ability to turn any result, challenge or mistake into a positive, particularly when it's a late night synchrotron shift. It has been such an important thing to learn in the early stages of research and something I hope I can continue in the future, the last 4 years would have been a lot more difficult without having you by my side. To Mark, for introducing me to the world of synchrotron science, and always going above and beyond to help me understand what is going on, or how I should write about it.

To the team at the Australian synchrotron, Daryl and Pimm my amazing co-supervisors, thank you for sharing your wisdom and passion for everything synchrotron. To Pimm for always providing Daniel's Donuts when I needed a sugar hit and your enthusiasm when I needed a good dance. To Dom, for your patience with the Far-IR, managing what felt like the impossible task of measuring the water content in a fingerprint, and for always being up to chat all things F1. Also a big thank you to all of you for running remote experiments when we were locked within fortress WA.

To the members of the Forensic Research Group, I have been very lucky to have such a friendly and supportive group throughout this experience. Special mentions to Talia for surviving Dundee with me (just!), for teaching me how to adult and for going to every store trying to find the perfect pair of jeans. And to Josh, for always being around when I needed to vent, get lunch or needed advice on something.

To Ashley and Karina, I'm so grateful to have been through this experience with both of you. Thank you for not killing me when I wanted to stay up all night to finish off the last scan, for finding food that I would eat without complaining and for committing to a dance even when it was being filmed.

To the wonderful technical staff at Curtin who are always so happy to help; to Chappy for your endless tech support and regular sudoku puzzles, to Grant for our extensive AFL chats & to Tomoko for your incredible baked goods and laughs when I'm in the teaching labs.

To my family, for your endless love and encouragement throughout my entire university journey; to Mum and Dad thank you for always having faith that I was capable of anything, this thesis would not have been possible without your support. To my sister Kiera, for always being there to keep me on top of the world outside of uni, and to Nanny & Poppy for always putting me in a good mood at the end of the week with a cup of tea and a good chat. To my puppy Alice, for your cuddles when I needed them and for sitting right by my side as I wrote every word.

To my partner Ash, thank you for always believing in me and for putting up with the crazy rollercoaster of emotions and stress that I bring upon myself, thank you for being an escape where I can relax and take my mind off everything. To AM and KC, for our friendship and all the laughs when I needed them most. And finally to Jess and our wonderful team of girls at Riverton Calisthenics Club, thank you for being my outlet for creativity and for putting a smile on my face at training each week.

I would also like to acknowledge the support of the Australian Government for providing me with a Research Training Program stipend and the Australian Institute of Nuclear Science and Engineering (AINSE) for the Post-Graduate Research Award which funded this research.

Contribution of Others

The following have contributed to the thesis, with contributions being listed in the form of CRediT (Contributor Roles Taxonomy) statements for each chapter (see <https://www.elsevier.com/authors/journal-authors/policies-and-ethics/creditauthor-statement>)

Chapters 1 to 7:

Professor Simon W. Lewis (Principal Supervisor): Project administration, Supervision, Conceptualisation, Writing - Review & Editing.

Dr Mark J. Hackett (Co-Supervisor): Supervision, Conceptualisation, Writing - Review & Editing.

Dr Daryl Howard (Associate Supervisor): Supervision, Investigation, Methodology, Writing - Review & Editing.

Dr Jitraporn Vongsvivut (Associate Supervisor): Supervision, Investigation, Methodology, Writing - Review & Editing.

Chapter 4:

Portions of this chapter have been published in *Analytical Chemistry* see Appendix for details.

Dr Buddhika Dorakumbura, Dr Martin de Jonge, Dr Mark Tobin, Dr Tracey Ho and Professor Wilhelm Van Bronswijk,: Investigation, Writing - Review & Editing.

Chapter 5:

Portions of this chapter have been published in *Analytical Chemistry* and the *Analyst* see Appendix for details.

Dr Buddhika Dorakumbura, Dr Martin de Jonge, Dr Mark Tobin, Dr Tracey Ho and Professor Wilhelm Van Bronswijk,: Investigation, Writing - Review & Editing.

Chapter 6:

Portions of this chapter have been published in the *Analyst* see Appendix for details.
Dr Dominique Appadoo: Investigation, Methodology, Writing - Review & Editing.

Publications

This dissertation contains work which has been submitted for publication in the following peer reviewed journals:

Rhiannon E. Boseley, Buddhika N. Dorakumbura, Daryl L. Howard, Martin D. de Jonge, Mark J. Tobin, Jitraporn Vongsivut, Tracey T. M. Ho, Wilhelm van Bronswijk, Mark J. Hackett, and Simon W. Lewis. Revealing the Elemental Distribution within Latent Fingermarks Using Synchrotron Sourced X-ray Fluorescence Microscopy. *Analytical Chemistry* **2019** 91 (16), 10622-10630

DOI: [10.1021/acs.analchem.9b01843](https://doi.org/10.1021/acs.analchem.9b01843)

A preprint of this article can be viewed on Chem Rxiv at:

[10.26434/chemrxiv.7987247.v1](https://doi.org/10.26434/chemrxiv.7987247.v1)

Rhiannon E. Boseley, Daryl L. Howard, Mark J. Hackett, and Simon W. Lewis. The transfer and persistence of metals in latent fingermarks. *Analyst* **2022** 147 (3), 387-397 DOI: <https://doi.org/10.1039/D1AN01951A>.

A preprint of this article can be viewed on Chem Rxiv at:

[10.26434/chemrxiv-2021-kvtmv](https://doi.org/10.26434/chemrxiv-2021-kvtmv)

Rhiannon E. Boseley, Jitraporn Vongsivut, Mark J. Hackett, and Simon W. Lewis. Monitoring the chemical changes in fingerprint residue over time using synchrotron infrared spectroscopy. *Analyst*, **2022** 147 (5) , 799-810

DOI: <https://doi.org/10.1039/D1AN02293H>

A preprint of this article can be viewed on Chem Rxiv at:

[10.26434/chemrxiv-2021-qsbtD](https://doi.org/10.26434/chemrxiv-2021-qsbtD)

In addition, the following peer reviewed articles were published during the course of this dissertation:

Sorour Shahbazi, **Rhiannon Boseley**, Braden Grant, Dechao Chen, Thomas Becker, Oluwasesan Adegoke, Niamh Nic Daéid, Guohua Jia, Simon W. Lewis. Luminescence detection of latent fingermarks on non-porous surfaces with heavy-metal-free quantum dots. *Forensic Chemistry*, **2020** 18, 100222

DOI: [10.1016/j.forc.2020.100222](https://doi.org/10.1016/j.forc.2020.100222)

Joshua A. D'Uva, Nicholas Brent, **Rhiannon E. Boseley**, Daniana Ford, Georgina Sauzier, Simon W Lewis. Preliminary investigations into the use of single metal deposition II (SMD II) to visualise latent fingermarks on polyethylene 'zip-lock' bags in Western Australia. *Forensic Chemistry* **2020** 18, 100229.

DOI: [10.1016/j.forc.2020.100229](https://doi.org/10.1016/j.forc.2020.100229)

Giada Truccolo, **Rhiannon Boseley**, Simon Lewis, William Gee. Forensic applications of rare earths: Anticounterfeiting materials and latent fingerprint developers. In *Handbook on the Physics and Chemistry of Rare Earths*, **2020** 57, 45-117.

DOI: [10.1016/bs.hpcre.2020.07.001](https://doi.org/10.1016/bs.hpcre.2020.07.001)

The following article was also published during the course of this dissertation:

Rhiannon Boseley, Daryl Howard, Jitraporn Vongsvivut, Mark Hackett, Simon Lewis. Leaving a mark on forensic science: how spectroscopic techniques have revealed new insights in fingerprint chemistry. *Spectroscopy Europe*, **2022** 22

DOI: <https://doi.org/10.1255/sew.2022.a8>

Conference Presentations

Selected aspects of the work contained within this thesis have been presented, or have been accepted for presentation, at the following conferences:

Oral Presentations

Leaving a Mark on Forensic Science: Using synchrotron infrared spectroscopy and X-ray fluorescence microscopy to explore fingerprint chemistry, Australian Nuclear Science and Technology Organisation User Meeting, 2021 (online)

Using Synchrotron Sourced Microscopy to Explore Fingerprint Chemistry, Virtual XFM & IRM Microscopy Workshop at the Australian Synchrotron, 2021 (online)

➤ Invited Presentation

Using Synchrotron Sourced Microscopy to Explore Fingerprint Chemistry, 10th Annual Forensic Science Symposium, Florida International University, 2021 (online)

Using Synchrotron Sourced Microscopy to Explore Fingerprint Chemistry, Australian Synchrotron User Meeting, 2020 (online)

Using Synchrotron Sourced Microscopy to Explore Fingerprint Chemistry, Royal Australian Chemical Institute Research & Development Topics Conference, Adelaide, 2019

Revealing The Spatial Distribution of Chemical Species within Latent Fingerprints using Synchrotron Sourced Microscopy, Curtin University School of Molecular and Life Sciences Rapid Fire Seminar Series, Perth 2019

Exploring The Spatial Distribution of Chemical Species within Latent Fingerprints using Infrared Microscopy, Australian Synchrotron User Meeting, Melbourne 2018

Revealing the Spatial Distribution of Chemical Species Within Latent Fingerprints Using Synchrotron Sourced Microscopy, Australian New Zealand Forensic Science Society Symposium, Perth, 2018

Poster Presentations

Revealing the Elemental Distribution Within Latent Fingermarks Using Synchrotron Sourced X-ray Fluorescence Microscopy, Australian New Zealand Forensic Science Society - Western Australian Forensic Science Forum, Perth 2021

Using Synchrotron Sourced Microscopy to Explore Fingermark Chemistry, Australian Society of Molecular Imaging Symposium, 2021 (online)

- Outstanding Poster Presentation Prize

Revealing the Elemental Distribution Within Latent Fingermarks Using Synchrotron Sourced X-ray Fluorescence Microscopy, Royal Society of Chemistry Twitter Conference, 2019 (online)

Revealing the Elemental Distribution Within Latent Fingermarks Using Synchrotron Sourced X-ray Fluorescence Microscopy, Australian Synchrotron User Meeting, Melbourne 2018

- 1st Place Student Poster Prize
- 2nd Place Student Poster Slam

Table of Contents

<i>Declaration</i>	<i>i</i>
<i>Human Ethics</i>	<i>i</i>
<i>Abstract</i>	<i>ii</i>
<i>Acknowledgements</i>	<i>v</i>
<i>Contribution of Others</i>	<i>vii</i>
<i>Publications</i>	<i>viii</i>
<i>Conference Presentations</i>	<i>x</i>
<i>Table of Contents</i>	<i>xii</i>
<i>List of Figures</i>	<i>xvi</i>
<i>List of Tables</i>	<i>xxiii</i>
<i>List of Abbreviations</i>	<i>xxiv</i>
Chapter 1: Introduction	1
1.1 <i>Fingermarks as Forensic Evidence</i>	2
1.2 <i>Fingerprint Composition</i>	3
1.2.1 <i>Eccrine Components of Fingerprint Residue</i>	3
1.2.2 <i>Sebaceous Substituents of Fingerprint Residue</i>	5
1.2.3 <i>Other Contaminants Present in Fingerprint Residue</i>	6
1.3 <i>Factors Affecting Fingerprint Composition Post Deposition</i>	7
1.3.1 <i>Fingerprint Residue</i>	9
1.3.2 <i>Substrate Surface</i>	9
1.3.3 <i>Sample Environment</i>	10
1.4 <i>Fingerprint Development</i>	11
1.4.1 <i>Porous Fingerprint Development Methods</i>	12
1.4.2 <i>Non-porous Fingerprint Development Methods</i>	15
1.4.3 <i>Other Fingerprint Development Methods</i>	16
1.4.4 <i>Challenges with Fingerprint Development</i>	17
1.5 <i>Analytical Methods Used to Explore Fingerprint Chemistry</i>	18
1.5.1 <i>Chromatography Techniques</i>	18

1.5.2 Microscopy Techniques.....	19
1.5.3 Chemical Imaging Techniques	20
1.6 Using Synchrotron Light to Explore Fingerprint Chemistry.....	23
1.6.1 Infrared Spectroscopy	25
1.6.2 X-ray Fluorescence Microscopy	31
1.7 Exploiting Fingerprint Transfer for Forensic Science.....	36
1.8 Aims and Overview	38
Chapter 2: Sample Collection, Experimental Methods and Instrumentation	40
2.1 Introduction	41
2.2 Experimental Considerations.....	41
2.3 Fingerprint Collection.....	42
2.4 Donor Information.....	42
2.5 Substrate Surface Selection	43
2.6 Instrumentation.....	44
2.6.1 X-ray Fluorescence Microscopy	44
2.6.2 X-ray Absorption Near Edge Structure Imaging	46
2.6.3 Infrared Spectroscopy	46
2.6.4 Optical Microscopy	49
2.7 Fingerprint Development.....	49
2.7.1 1,2 – Indanedione	50
2.7.2 Powdering.....	51
2.7.3 Cyanoacrylate Fuming	51
2.7.4 Acid Nile Blue	52
2.7.5 Single Metal Deposition II.....	52
2.8 Photography of Developed Fingerprints.....	54
2.9 Fingerprint Grading.....	55
2.10 Statistical Analysis	57
2.11 Human Ethics Approval	57
Chapter 3: Exploring Donor Fingerprint Chemistry	58

3.1 Introduction	59
3.2 Methodology	62
3.2.1 Fingerprint Deposition	62
3.2.2 Donor Information	63
3.3 Results & Discussion	64
3.3.1 Comparison of Development Performance for Charged and Uncharged Fingermarks	65
3.3.2 Understanding Donor Chemistry and Classifying Donor Performance ...	70
3.4 Conclusions	74
Chapter 4: Using Synchrotron XFM to Reveal and Characterise Elemental Distribution in Latent Fingermarks, and to Further Understand Inter-Donor Variation	75
4.1 Introduction	76
4.2 Methodology	79
4.2.1 Fingerprint Deposition	79
4.3 Results and Discussion.....	80
4.3.1 XFM Reveals the Inorganic Distribution in Natural Fingermarks	80
4.3.2 Sources of Variation in Elemental Content of Latent Fingermarks: Interdonor Variability	82
4.3.3 Combining XFM and IRM to co-locate the Organic and Inorganic Materials in Latent Fingermarks.....	87
4.4 Conclusions	92
Chapter 5: The Transfer And Persistence Of Metals In Latent Fingermarks	94
5.1 Introduction	95
5.2 Methodology	96
5.2.1 Fingerprint Deposition	96
5.2.2 Image Analysis and Statistical Analysis	98
5.3 Results & Discussion	98
5.3.1 Sources of Variation in Elemental Content of Latent Fingermarks: Metal-contact Contamination	99
5.3.2 Elemental Composition of Latent Fingermarks before and after Handling a Gun Barrel or Ammunition Cartridge.....	101

5.3.3 <i>Transfer and Persistence of Elemental Contaminants from Party Sparklers and the Effect on Subsequent Deposition in Latent Fingermarks...</i>	109
5.3.4 <i>Persistence of Elemental Content of Natural Fingermarks: Daily Activity</i>	114
5.3.5 <i>Persistence of Elemental Content of Natural Fingermarks: Effect of Water Immersion</i>	116
5.4 <i>Conclusions</i>	119
Chapter 6: <i>Monitoring the Chemical Changes in Fingermark Residue Over Time using Synchrotron Infrared Spectroscopy</i>	121
6.1 <i>Introduction</i>	122
6.2 <i>Methodology</i>	125
6.2.1 <i>Fingermark Deposition: Synchrotron ATR-IRM.....</i>	125
6.2.2 <i>Fingermark Deposition: Synchrotron THz/Far-IR Spectroscopy.....</i>	126
6.3 <i>Results and Discussion.....</i>	128
6.3.1 <i>The Chemical and Morphological Changes in Eccrine and Lipid Material within Natural Latent Fingermarks in the first 13 hours following Deposition.</i>	128
6.3.2 <i>Measuring the Volume of Water Lost through Evaporation of Latent Fingermarks</i>	138
6.4 <i>Conclusions</i>	141
Chapter 7: <i>Conclusions and Recommendations for Future Work</i>	143
7.1 <i>Conclusions</i>	144
7.1.1 <i>Using Chemical Imaging Methods to Explore the Distribution of Elemental Material</i>	145
7.1.2 <i>Morphological and Chemical Changes in Fingermarks over time</i>	147
7.1.3 <i>Comparing Analytical Data to Results of Fingermark Development.....</i>	148
7.2 <i>Summary.....</i>	151
Chapter 8: <i>References</i>	153
Appendix.....	188

List of Figures

Figure 1.1: Schematic of Sear’s “Triangle of Interaction”, referring to the influence of fingerprint composition, substrate surface and substrate environment on fingerprint residues.	8
Figure 1.2: Flowchart showing an example of a fingerprint development treatment decision process.....	12
Figure 1.3: Schematic adapted from Wilmott et al. showing the key components of a synchrotron source including the direction of the electron flow through the insertion devices of a wiggler (a) and undulator (b)	24
Figure 1.4: Types of molecular vibrations. Note that + denotes movement out of the page and – denotes movement into the page	26
Figure 1.5: Schematic showing the process of X-ray Fluorescence.....	32
Figure 2.1: Example of the XFM emission spectra collected from a natural fingerprint sample, counts per channel as a function of X-ray energy (green) the X-ray spectrum fit (red) and the estimated background (magenta).	45
Figure 3.1: Diagram showing set up for deposition substrates	63
Figure 3.2: Representative donor (donor 19) showing an increase in material from uncharged (top) to charged (bottom) fingerprints developed with superglue fuming (a), post treated with acid Nile blue (b), black powder (c), SMD II (d) and 1,2-indanedione (e)	66
Figure 3.3: Graph displaying the sum of grades for each development method for uncharged and charged fingerprints	69
Figure 3.4: Representative “poor” donor (donor 18) uncharged (top) and charged (bottom) fingerprints developed with superglue fuming (a), post treated with acid Nile blue (b), black powder (c), SMD II (d) and 1,2-indanedione (e)	71

Figure 3.5: Representative “good” donor (donor 3) uncharged (top) and charged (bottom) fingermarks developed with superglue fuming (a), post treated with acid Nile blue (b), black powder (c), SMD II (d) and 1,2-indanedione (e) 72

Figure 3.6: Representative “mid” donor (donor 6) uncharged (top) and charged (bottom) fingermarks developed with superglue fuming (a), post treated with acid Nile blue (b), black powder (c), SMD II (d) and 1,2-indanedione (e) 73

Figure 4.1: Large area XFM scan of natural fingermark from donor 6, deposited on Ultralene Thin Film. Concentration scale bar (ng cm^{-2}) 81

Figure 4.2: Typical results for zinc distribution within natural fingermarks collected from fourteen donors on silicon nitride slides (D1,6,10 17-21) and mylar (D3, 12-16). Concentration scale bar (ng cm^{-2}) 84

Figure 4.3: Typical results for zinc distribution within natural fingermarks collected from fourteen donors on mylar on two separate occasions (deposit 1 left, deposit 2 right). Concentration scale bar (ng cm^{-2}) 85

Figure 4.4: Iron, titanium, and zinc distribution within a natural fingermark from donor 6 deposited on silicon nitride and imaged using XFM. Composite image (right) demonstrates the colocalization of these metals within the fingermark matrix. Concentration scale bar (ng cm^{-2}) 86

Figure 4.5: Calcium, chlorine, copper, potassium, and zinc distribution within a natural fingermark from donor 6 deposited on silicon nitride and imaged using XFM. Composite image (right) demonstrates the colocalization of these metals within the fingermark matrix; box outlined in the composite image displays area of crystal-like structures (a) seen in particular donors, likely to be salt crystals. Concentration scale bar (ng cm^{-2}) 86

Figure 4.6: A natural fingermark deposited from donor 6 on silicon nitride imaged with an optical microscope sample overview (a) and imaging area (b), XFM zinc distribution (c) and FTIR-FPA imaging with false colour image generated by integrating over the O-H stretching band ($3000\text{-}3500\text{ cm}^{-1}$) for water representative

of eccrine material (d) and the C-H stretching band for lipid material (2800-3000 cm^{-1}) (e) 88

Figure 4.7: Natural fingermark from Donor 1, deposited on a silicon nitride slide. Bright field optical image of the area investigated with FTIR-FPA imaging (a) with false colour image generated by integrating over the O–H stretching band for the eccrine material (3000 - 3500 cm^{-1}) (b) FTIR spectra of eccrine material obtained using the conventional FTIR spectroscopy (d) and the corresponding elemental distribution maps imaged using XFM (c). XFM concentration scale bar (ng cm^{-2}) ... 90

Figure 4.8: Natural fingermark from Donor 20 (top) and Donor 21 (bottom), deposited on a silicon nitride slide. Bright field optical image of the area investigated with FTIR-FPA imaging (a) with false colour image generated by integrating over the O–H stretching band for the eccrine material (3000 - 3500 cm^{-1}) (b) FTIR spectra of eccrine material obtained using the conventional FTIR spectroscopy (d) and the corresponding elemental distribution maps imaged using XFM (c). XFM concentration scale bar (ng cm^{-2}) 91

Figure 5.1: Copper and nickel distribution in a fingermark deposited from Donor 18 on silicon nitride and imaged using XFM. Natural deposit (left) and fingermark from hand in contact with Australian currency (right). Concentration Scale Bar (ng cm^{-2})..... 100

Figure 5.2: Elemental maps of fingermarks taken from a representative donor following regular activity (left), handling a gun barrel for 30 seconds (middle) and handling an ammunition cartridge case (right) 102

Figure 5.3: Scatter plots of the average elemental areal density calculated from fingermark samples taken following regular activity, handling a gun barrel for 30 seconds and handling an ammunition cartridge case for 30 seconds. Plots marked * indicate P-value <0.05 from Wilcoxon matched-pairs signed rank test. Each donor is represented by an individual colour outlined in Table 5.1. 104

Figure 5.4: XANES mapping of a fingermark taken after handling of a gun barrel reveals transfer of two different chemical forms of Fe. (a) Total Fe map taken at

7.4keV showing deposition of Fe along fingermark ridges, but also one Fe hotspot adjacent to a ridge (blue arrow), (b-d) principal component analysis was used to identify differences in the chemical form of Fe, with the image of PC1 scores closely reflecting total Fe distribution (b), while the PC2 scores image highlights that the Fe particle located adjacent to the ridge (blue arrow) displays a distinctly different pattern of spectral variance (c). The specific variables contributing most to the sources of variance described by PC1 and 2 are shown in the PC loadings (d). Analysis of normalised XANES spectra (e) taken from regions of interest (f), support the existence of different chemical forms of Fe across the fingermark. Specifically, the hot particle adjacent to the ridge presents a spectrum (blue trace in panel e) resembling elemental Fe, while the other traces resemble Fe³⁺ (1s – 3d pre-edge maxima at 7114.5 eV). 107

Figure 5.5: XANES mapping of a fingermark taken after handling of a gun barrel demonstrated only donor 12 had two forms of iron identified (a) Total Fe map taken at 7.4keV showing deposition of Fe along fingermark ridges (b-c) principal component analysis was used to identify differences in the chemical form of Fe, here the image of PC1 and PC2 scores closely reflect total Fe distribution (b). Analysis of normalised XANES spectra (d) taken from representative regions of interest from the 4 samples measured from donors 3,12,13 and 15, with donor 12 showing the two forms of Fe identified in Figure 5.4 108

Figure 5.6: Elemental maps of fingermarks taken from a representative donor following regular activity (left), handling a party sparkler for 30 seconds (middle) and handling a party sparkler for 30 seconds followed by washing hands (right).. 111

Figure 5.7: Scatter plots of the average elemental areal density calculated from fingermark samples taken following regular activity, handling a party sparkler for 30 seconds, or handling a party sparkler for 30 seconds and then washing the hands. Plots marked * indicate P-value <0.05 from Wilcoxon matched-pairs signed rank test. Each donor is represented by an individual colour outlined in Table 5.1 113

Figure 5.8: Zinc distribution within a natural fingermark from donor 6 deposited on Mylar and imaged using XFM. Fingermarks taken at 6 time points throughout the

day after daily cosmetic application (15 minutes, 1 hr, 2 hr, 3 hr, 6 hr, 10 hr.
 Concentration scale bar (ng cm^{-2}) 115

Figure 5.9: Water immersion experiments showing the removal of metals from
 fingermarks deposited by Donor 6, original fingermarks (left) rinsed fingermarks
 visualised on the same colour scale as the original fingermarks (middle) rinsed
 fingermarks on a maximum colour scale (right) 118

Figure 6.1: (a) Macro-ATR cantilever fitted with the 1 mm Ge crystal, fingermark is
 deposited onto centre of crystal and (b) the optical microscope image of the
 corresponding fingermark on the Ge crystal..... 125

Figure 6.2: Representative example of time-course (7 hour) changes in lipid and H_2O
 content during air-drying of a natural fingermark, as revealed by ATR-FTIR mapping
 approach (a). False colour ATR-FTIR maps were generated by integrating over the
 $\nu(\text{C-H})$ stretching bands ($2800\text{-}3000\text{ cm}^{-1}$) as a marker of lipid material (top row) and
 $\nu(\text{O-H})$ stretching bands of H_2O ($3000\text{-}3500\text{ cm}^{-1}$) as a marker for eccrine material
 (middle row). Overlay images are displayed in the bottom row. Scale bar $20\text{ }\mu\text{m}$. The
 relative changes in lipid and H_2O content as a function of air-drying time can also be
 visualised as the normalised average band area calculated across the entire droplet
 (b). Representative sample corresponds to Donor 1 (D1). 129

Figure 6.3: Representative examples of ATR-FTIR spectra collected from a natural
 fingermark after 1 hour, 4 hours, and 7.5 hours of air-drying period (from the same
 dataset presented in Figure 6.2, donor 1). Representative spectra are presented
 from image regions enriched in lipid material or water (using H_2O content as a
 marker of eccrine components). The most pronounced changes in lipid
 concentration are highlighted in (a) $\nu(\text{C-H})$ stretching band ($2800\text{-}3000\text{ cm}^{-1}$) and (b)
 $\nu(\text{C=O})$ stretching band ($1715\text{-}1750\text{ cm}^{-1}$)..... 130

Figure 6.4: 3 droplets mapped within the same fingermark from Donor 6, droplets
 marked in the false colour ATR-FTIR map generated by integrating over $\nu(\text{O-H})$
 stretching bands of H_2O ($3000\text{-}3500\text{ cm}^{-1}$) (a), the relative changes in H_2O content as
 a function of air-drying time for each droplet is visualised as the normalised average
 band area calculated across the entire droplet (b). Intra-droplet variation is evident,

as can be seen in the plot of an average droplet spectrum with the line thickness weighted to the standard deviation calculated from 147 spectra within droplet 3 as identified in A (c) and the average spectrum from the 12 donors in this study, weighted to the standard deviation (d) 131

Figure 6.5: Time-dependent changes in H₂O content (as a marker of eccrine material) and lipid content during air-drying of natural fingermarks was measured for 12 individual fingermarks (donors 1 – 12), using the same ATR-FTIR approach. As expected, a strong time-dependent decrease in H₂O content was observed in donors 1-10 (cyan), with exceptions observed in donors 11 and 12. The H₂O content was measured as the integrated area across $\nu(\text{O-H})$ absorbance bands (3000 – 3500 cm⁻¹), and lipid content (red) was measured across $\nu(\text{C-H})$ absorbance bands (2800 – 3000 cm⁻¹). The average band area was calculated across the entire fingermark droplet..... 133

Figure 6.6: Temperature and relative humidity data recorded within the laboratory space for the same period as the ATR-FTIR data reported in Figure 6.5. Evaporation rate does not appear to relate to the temperature and humidity changes measured in this study. 134

Figure 6.7: Analysis of intra-donor variance in triplicate fingermarks from donor 12. (a) False colour ATR-FTIR maps were generated by integrating over the $\nu(\text{C-H})$ stretching bands (2800-3000 cm⁻¹) as a marker of lipid material (top row) and $\nu(\text{O-H})$ stretching bands of H₂O (3000-3500 cm⁻¹) as a marker for eccrine material (middle row). Overlay images are displayed in the bottom row. (b) The relative changes in lipid and H₂O contents as a function of air-drying time can also be visualised as the normalised average band area calculated across the entire droplet. Scale bar 20 μm 137

Figure 6.8: THz/Far-IR gas phase spectra showing H₂O pure-rotational spectral lines for calibration samples, highlighting the linear response between band intensity and volume of water from which the gas phase sample was generated (0.25 μL , 0.5 μL , 0.875 μL , 1.25 μL , and 1.5 μL). The selected spectral region shows the rotational transitions of H₂O at 202.47cm⁻¹, 202.69cm⁻¹ and 202.92cm⁻¹ 140

Figure 6.9: (a) The volume of water contained in a latent fingerprint was quantified from the calibration curve (black dots, $R^2 = 0.9932$) using the rovibrational transition of H_2O at 202.69 cm^{-1} . (b) The volume of water was calculated for natural fingerprints ($n = 4$), fingerprints with hands left in the air for 30 minutes ($n = 4$), and fingerprints after wearing gloves for 10 minutes ($n = 5$). Volume shown for each data point in panel A, is for a set of 10 fingerprints deposited onto a sample substrate. The volume of water for each sample was therefore, divided by 10, to give an average water volume per fingerprint (as shown in panel B). Error bars in A, and B are equal to 2σ 140

List of Tables

Table 1.1: Summary of chemical imaging methods	21
Table 2.1: Donor information	43
Table 2.2: SMD II stock solution preparation	53
Table 2.3: Camera settings optimised to each detection method	54
Table 2.4: Photography enhancement conditions	55
Table 2.5: Fingerprint grading scheme	56
Table 3.1: Summary of fingerprint development treatments used in this study	60
Table 3.2: Details of the donors used in this study	64
Table 3.3: Summary of grading for uncharged fingerprints	67
Table 3.4: Summary of grading for charged fingerprints	67
Table 4.1: Details of the donors used in this study	79
Table 4.2: Components detected in latent fingerprints using XFM and their likely endogenous/exogenous source	82
Table 5.1: Details of the donors used in this study	97
Table 5.2: Average copper and nickel areal density measured from the particulate hotspots as shown in Figure 5.1 and the ratio of these metals in an Australian silver coloured coin.	100
Table 6.1: Details of the donors used in this study	126
Table 6.2: THz/Far-IR fingerprint sample types	127
Table 7.1: Summary of development class for uncharged fingerprints and corresponding chemical imaging information	150

List of Abbreviations

AFM	Atomic Force Microscopy
ANSTO	Australian Nuclear Science and Technology Organisation
ANZPAA	Australia New Zealand Policing Advisory Agency
ATR	Attenuated Total Reflectance
CAST	Centre of Applied Science and Technology
DNA	Deoxyribonucleic Acid
Far-IR	Far Infrared
FTIR	Fourier Transform Infrared
GC-MS	Gas Chromatography Mass Spectrometry
IFRG	International Fingerprint Research Group
IND	1,2 - Indanedione
IR	Infrared
IRM	Infrared Microspectroscopy
KB	Kirkpatrick–Baez
LA-ICP-MS	Laser Ablation Inductively Coupled Plasma Mass Spectrometry
LC-MS	Liquid Chromatography Mass Spectrometry
LUMO	Lowest Unoccupied Molecular Orbital
MALDI-MS	Matrix Assisted Laser Desorption Ionization Mass Spectrometry
MALDI-MSI	Matrix Assisted Laser Desorption Ionization Mass Spectrometry Imaging
MCT	Mercury Cadmium Telluride
NCFS	National Centre for Forensic Studies

NIFS	National Institute of Forensic Science
ORO	Oil Red O
PCA	Principal Component Analysis
PD	Physical Developer
QCM	Quartz Crystal Microbalance
S/N	Signal to Noise
SEM	Scanning Electron Microscopy
SIMS	Secondary Ion Mass Spectrometry
SMD	Single Metal Deposition
THz	Terahertz
TMDT	Trace Metal Detection Test
TOF-SIMS	Time of Flight Secondary Ion Mass Spectrometry
UV	Ultra Violet
VMD	Vacuum Metal Deposition
XANES	X-ray Absorption Near Edge Structure Spectroscopy
XFM	X-ray Fluorescence Microscopy
XPS	X-ray Photoelectron Spectroscopy
XRF	X-ray Fluorescence
2D	Two Dimensional

Chapter 1

Introduction



1.1 Fingermarks as Forensic Evidence

In forensic science, the transfer of trace evidence during the course of criminal activity can provide vital investigative information that links people, locations and/or objects. Latent fingermarks are an important type of trace evidence as they are easily transferred and characteristic to an individual, with the marks left following contact between the fingertip and a surface frequently utilised for identification purposes.¹ The residue left on contact is often invisible to the naked eye, requiring chemical or physical treatment to enable detection. Despite ongoing research to improve fingermark visualisation procedures, there remains significant detection challenges due to the chemical variability of fingermark residue.²

The composition of latent fingermarks is not static, and changes with time, which is an important consideration given that evidence is not normally collected immediately following transfer.³⁻⁵ Although experimentally challenging, it is important to characterise the nature of material that is transferred from a person's fingertips to the fingermark and for how long that material persists. Likewise, it is of immense value to identify how the chemical composition of a latent fingermark is influenced by physical activities prior to fingermark deposition.⁶⁻⁹ Chemical investigation of fingermark residues can assist in improving methods for the visual enhancement of fingermark samples, as well as improving the fundamental processes involved in the interpretation of fingermark evidence.

Commonly, investigations into the fingermark recovery process aim to improve the visualisation of fingermarks for identification purposes. More recently, the activity level surrounding the transfer of latent fingermarks has become an area of interest to fingermark researchers. A new approach by de Ronde *et al.* has redirected fingermark research to explore the activity leading to fingermark transfer, providing an objective view on whether the fingermark may be attributed to criminal activity.⁹⁻¹² By conducting fundamental research into processes such as transfer and persistence, there is potential to exploit the chemical and physical characteristics of fingermarks to improve their interpretation and evidential value in forensic investigations.

1.2 Fingermark Composition

Fingermark residue is made primarily of a mixture of secretions from the eccrine and sebaceous glands, often contaminated with constituents picked up through contact during daily activity. The exact initial composition can vary, influenced greatly by the donor, deposition conditions and surface characteristics.¹³⁻¹⁴ Donor traits such as age, biological gender, ethnicity, health and personal habits like cosmetic use and smoking impact the composition of material present on the fingertips and subsequently deposited in a fingermark.^{7, 15-22} Meanwhile characteristics such as deposition time and pressure and the porosity of the substrates surface can impact the behaviour of residue pertaining to its transfer and persistence.²³

1.2.1 Eccrine Components of Fingermark Residue

Eccrine glands are present on the palmar surface of the hands and the fingertips, thus it is expected their secretions make up a portion of fingermark residue. Eccrine glands produce sweat, an aqueous mixture containing amino acids, salts and proteins.²⁴⁻²⁵ The composition of eccrine sweat can vary greatly across donors, however there are common components present.

Quantitative studies have demonstrated a similar amino acid profile within fingermarks to eccrine sweat, with serine, glycine and alanine found to be the most abundant amino acid constituents.^{15, 26-27} The total amino acid concentration has been measured to be somewhere between 0.30 and 2.59 mg/L, with the amino acid profile shown to be variable between donors.²⁷⁻²⁸ Proteins and peptides have been studied in fingermark residue, van Dam *et al.* reported the use of matrix assisted laser desorption/ionization mass spectrometry (MALDI MS) to target dermcidin using immunolabeling, and demonstrated the dotted pore pattern located across the ridge.²⁹ The method has also been used to detect other protein and peptide compounds, with Ferguson *et al.* suggesting the method can be used to determine a chemical profile to deduce the biological gender of the donor.^{19, 30}

Eccrine sweat can contain minerals found in the blood, with a number of inorganic ions including chloride, magnesium, potassium and iron detected within eccrine

residues.^{15, 31} Sodium and chloride ions are expected to be present in greatest concentrations, with variation in sweat composition due to donor, sweat rate and environmental conditions.²⁴ Early research on eccrine sweat used body perspiration to establish the basic understanding of fingerprint chemistry until Cuthbertson *et al.*, under the instruction of the United Kingdom Atomic Weapons Establishment, reported specifically on latent fingerprint residues.³²⁻³⁴ Analysis of the water soluble components of fingerprint residue suggested the presence of metal ions including chloride, calcium, sodium and potassium, with considerable variation in chloride content, influenced by donor age.¹⁵

The water soluble ion content in fingerprint residues can impact on the fingerprint development process, with some detection treatments such as cyanoacrylate fuming considered to be influenced by the presence of chloride ions.³⁵ Some donors secrete a higher concentration of metal ions, which when in excess in fingerprint residue can cause corrosion of metal surfaces, leaving behind a visible fingerprint.³⁵⁻³⁷ Attempts to exploit the presence of these metal ions for chemical imaging purposes have demonstrated the distribution of particular metal ions across the fingerprint ridges. Time-of-flight secondary ion mass spectrometry (TOF-SIMS) has been used to successfully image fingerprints, often targeting sodium and potassium as ions of interest.³⁸⁻⁴⁰ Bailey *et al.* highlighted the use of X-ray photoelectron spectroscopy (XPS) detecting sodium, calcium, chloride and potassium in natural fingerprint samples and Worley *et al.* used micro-X-ray fluorescence to image the potassium and chlorine in fingerprints groomed for increased eccrine content.⁴¹⁻⁴² Across these methods there were noticeable variations in metal ion content between donors, reinforcing results of previous bulk chemistry studies on fingerprint residue.

The water fraction of a fingerprint is expected to make up a significant portion by mass, however there have been many conflicting reports on just how much water is within a fingerprint and its rate of evaporation.⁴³⁻⁴⁵ There are inherent challenges when attempting to measure the water present within a fingerprint due to the small quantities and variability of material present and influence from the surrounding environment. Attempts have been made using microbalances to measure the mass of this material and its change over time with great disparity in the findings.^{43, 45}

Keisar *et al.* calculated the mass of a fingermark to be between 2 – 9 µg, based on the weight of a smaller subsection of the mark, whilst Croxton measured a mass range of 0.33 – 29 µg.^{6, 43, 46} The water content is of interest to fingermark researchers as it is known to have a direct impact on fingermark detection, with dried, aged fingermarks showing weaker performance when detected with some operational methods.^{35, 47-49} Early reports of significant mass loss in fingermark residue suggested that 98-99% of initial fingermark mass loss is due to water evaporation, however Kent *et al.* has suggested the water fraction makes up less than 20% and Keisar *et al.* found significant variation in water content anywhere between 20% and 70% by mass.⁴³⁻⁴⁴

1.2.2 Sebaceous Substituents of Fingermark Residue

The sebaceous glands are accountable for the majority of the water-insoluble material present within fingermark residue. The glands are present over a greater proportion of the body compared to eccrine glands, and are usually attached to hair follicles so are frequently found on the scalp and face.²⁴ Though these glands are not present on the fingertips sebaceous material is often encountered within fingermark residue due to habitual contact with other areas of the body.^{15, 25} Due to the transferrable nature of this material the amount of lipids detected within fingermarks is understood to vary greatly, with additional variation seen due to substrate effects and environmental exposure.^{13, 23, 26}

The sebaceous glands produce an oily mixture of lipids called sebum, which is made up of squalene, fatty acids, wax esters, and triglycerides. The lipid composition of latent fingermarks has been studied with chromatographic analysis, with a number of groups identifying squalene as the most predominant lipophilic compound in fingermark residue.^{13-14, 16, 50-51} A number of oxidation by-products correlated to squalene precursors have been characterised, with suggestions their composition can be used to predict the time since deposition of the mark.⁵²⁻⁵⁴ Hydrolysis of sebum forms a number of fatty acids present in fingermark residues, Archer *et al.* investigated fatty acids such as palmitic acid, palmitoleic acid and oleic acid, with compositional changes after fingermark deposition shown to be affected by lighting and storage conditions.⁵⁰

One of the greatest challenges when analysing the lipid fraction of fingermark residue is the variation between samples. Sebum chemistry is influenced by donor traits such as age, biological gender and diet, and due to the multifaceted nature of the transfer of sebaceous material, the initial composition in fingermark residue can vary greatly.^{15, 19, 21-22} Frick *et al.* used gas-chromatography mass spectrometry (GC-MS) to explore the lipid fraction of fingermarks from over 100 donors.¹⁴ The findings compared the relative concentrations of lipid components including squalene, cholesterol, fatty acids and wax esters, highlighting the inherent variability of lipid material deposited in fingermark residue. Variation between donors and within multiple samples from the same donor makes correlation of donor traits across a large sample size difficult, the study concludes that the prospect of exploiting this chemical information for identification purposes cannot be used operationally until challenges with fingermark sampling protocols are better understood.^{13-14, 55}

1.2.3 Other Contaminants Present in Fingermark Residue

Contaminants within fingermark residue present an intriguing alternate target to extrapolate donor information for a forensic investigation.⁶ Skin debris is valuable as it can be a source for DNA, dead skin cells are often sloughed from the skin surface through contact with adhesive or rough surfaces.⁵⁶⁻⁵⁸ A number of drug metabolites have been identified within fingermark residue, secreted through the body and transferred from the surface of the hands.⁵⁹⁻⁶² These drugs have been exploited as chemical targets for chemical imaging, with recent studies aiming to differentiate between metabolites which have been deposited naturally within fingermark residue or transferred exogenously.^{8, 63}

Material can also be transferred to the fingertip and combined with fingermark residue through daily activity. Cosmetic and consumer products including moisturisers, sunscreens, hand sanitisers, make-up and hair products have all been identified in fingermark residues.^{7, 64-67} The presence of these materials can influence the chemistry of the residue, affecting degradation rates and potentially interfering with detection processes. However, some exogenous contaminants such as explosive and gun shot residues have proven useful in providing contextual information about

the donors activity prior to deposition.⁶⁸⁻⁷² Trace metal detection tests target the metal ions present in these residues and are often applied directly to the hands to identify recent handling of metal objects including firearms.⁷³⁻⁷⁷ Recent work by Xing *et al.* has explored the secondary transfer of these contaminants within latent fingerprints and palmprints on paper substrates.⁷⁸ The detection of secondary transfer of metal particles to fingerprint residue can provide valuable information at an identification and activity level, which would be of greater value when interpreting forensic data.

1.3 Factors Affecting Fingerprint Composition Post Deposition

Following the deposition of a fingerprint it is well recognised there are changes which chemically alter the residue.^{3, 5, 79} Sears *et al.* proposed the concept of the “triangle of interaction”, shown in Figure 1.1, which refers to how the substrate surface, the surrounding environment and the chemistry of the residue itself can affect the composition of fingerprint residue over time.⁸⁰ The rate of chemical and physical changes can impact the persistence of fingerprint material and its detectability, but also have the potential to be used to estimate the time since deposition.⁸¹⁻⁸³ Several studies have attempted to predict the age of a fingerprint by investigating the chemical composition and degradation over time.^{13, 84} Using chromatographic analysis the ratio of components, the presence of oxidation products and the change in chemical profile have all been explored as potential approaches to date fingerprint samples.⁵²⁻⁵⁴

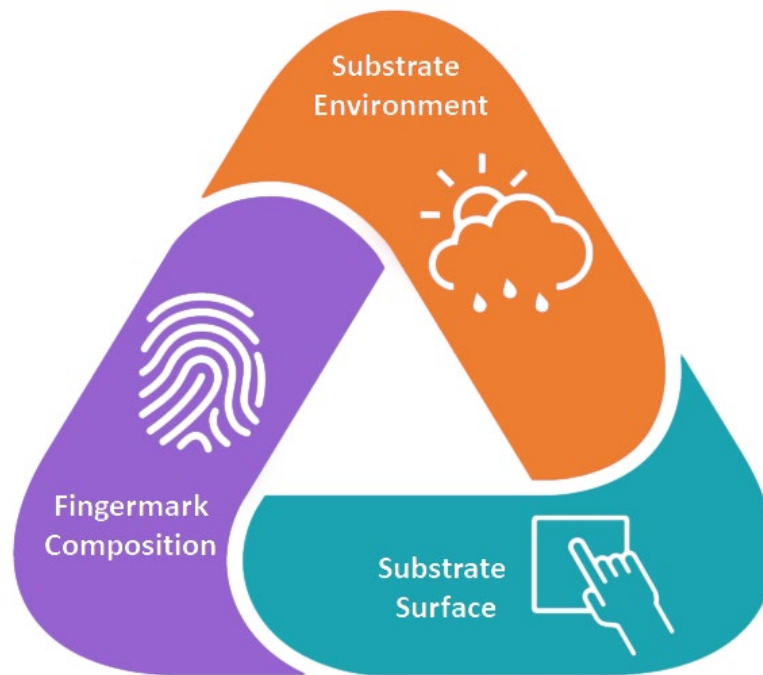


Figure 1.1: Schematic of Sear's "Triangle of Interaction", referring to the influence of fingerprint composition, substrate surface and substrate environment on fingerprint residues.⁸⁰

The physical changes in fingerprint samples have been observed when detecting fingerprint residues, with aged fingerprints performing differently when treated with particular enhancement methods including powdering, cyanoacrylate fuming and lipid sensitive reagents.^{35, 47, 49, 85-87} Physical changes have also been examined through the use of optical methods such as microscopy, with the ridge patterns shrinking as the deposit dries.⁸⁸ There are significant challenges when attempting to predict time since deposition using these approaches, a multitude of factors can affect the initial starting material as well as the rate of degradation.^{3, 5, 79, 89} Considerations of the effects of the triangle of interaction on fingerprint residue must be taken when conducting fingerprint research.^{80, 90} The International Fingerprint Research Group has guidelines to address the implications of these effects on fingerprint studies, with suggestions on donor pool size, substrate types and environmental conditions.⁹¹

1.3.1 Fingermark Residue

The rate of degradation of a fingermark is greatly impacted by the initial composition of the residue.^{5, 79, 92} As discussed previously, fingermark residue is a complex mixture which can vary between individuals based on a number of factors including donor characteristics and the donor activity leading to deposition.^{13, 26, 93} Intradonor variation refers to the disparities between fingermarks given from the same donor, influenced by the donors activities as well as deposition pressure, time and angle.^{13-14, 23, 26} The summation of these factors impact the chemistry of fingermark residue starting material and its subsequent aging process.

Following deposition, residue can interact with components within the fingermark. Squalene is a prominent compound within fingermark residue and is expected to play a protective role for certain fatty acids, providing a pathway for preferential degradation, delaying the depletion of the remaining fingermark compounds from initial degradation.^{53, 79, 94} The eccrine and sebaceous materials are present as an emulsion, as such the oxidation and deterioration of material is prolonged compared to rates for the individual standard compounds.⁹⁵⁻⁹⁷ Since it is a combination of the material present which can influence the rate of degradation, the initial fingermark residue has a considerable effect on the degradation process. Attempts have been made to minimise the variation in starting material for fingermark research, by instructing donors to wash their hands, limiting activity prior to deposition and controlling deposition force.^{14, 23, 80, 98} However, in their review, Girod *et al.* concluded that it may be impossible to overcome interdonor variation and is likely that aging models would need to be prepared on an individual basis to accurately estimate the time since deposition.³

1.3.2 Substrate Surface

The substrate surface influences the chemistry of the fingermark and its subsequent enhancement methods. Surfaces are often grouped into porous, non-porous and semi-porous categories. The absorption and diffusion of residues into the surface depend on their porosity and smoothness.⁹⁹ Porous surfaces such as paper and cardboard absorb a portion of the fingermark which can later be targeted by

particular detection methods. Eccrine components, such as amino acids, readily absorb into porous surfaces due to hydrogen bonding with cellulose in the substrate.^{15, 35} Meanwhile lipid material is transferred through adhesive forces, dependent on the smoothness and temperature of the surface. Almog *et al.* used a fluorescent dye and fluorescent microscope to observe the fingerprint cross section, demonstrating how the decrease in porosity of the surface reduces the rate of absorption of residue.⁹⁹ Smooth, non-porous surfaces such as glass, metal or plastic do not exhibit absorption, instead the residue remains in place on the surface of the substrate until physically removed or chemically degraded.^{83, 88}

The persistence of fingerprint residue directly correlates to the surface substrate.^{2, 100-101} The absorption of fingerprint material into a porous surface acts to trap the residue ensuring the residue can remain for extended periods of time, with fingerprints several decades old detected using chemical treatments.^{87, 102} The degradation of material is accelerated on non-porous surfaces, with squalene and cholesterol more susceptible to degradation and the rate of evaporation of water increased as the material is exposed to the surrounding environment.^{13, 84} Fingerprint residue can also be chemically altered by the surface, metals such as aluminium and brass undergo corrosion at the fingerprint site.^{37, 103} Recently, Chadwick *et al.* demonstrated the effect of the substrate surface on the success of fingerprint development, revealing that it is more likely a fingerprint will be appropriately developed on a porous surface, with improved development quality on paper substrates compared to non-porous surfaces.² This result is likely due to the behaviour of the residue, with the absorption of the fingerprint into a porous surface, where as residues on non-porous surfaces are more likely to be damaged through handling and environmental exposure prior to development.

1.3.3 Sample Environment

The surrounding environment has significant impact on the degradation of fingerprint residue. Environmental factors such as temperature, humidity, light and wind all have an effect on the persistence of material.^{5, 47, 82} Increases in temperature can accelerate the evaporation of aqueous material, whilst also speeding up the rate

of oxidation of lipids, such as squalene and cholesterol and the degradation of amino acids.^{84, 104-107} Meanwhile the exact temperature a fingermark is stored at can determine the degradation pathways, with Wolstenholme *et al.* demonstrating the degradation of oleic acid to be temperature dependent.¹⁰⁸ Exposure to UV light has proven to have an effect on the rate of degradation of lipid material, with Archer *et al.* reporting oxidation by-products in higher abundance for squalene, cholesterol and fatty acids compared to when stored in the dark.⁵⁰

Submersion in water can wash away the aqueous residues within a fingermark, leaving the lipid material behind. Dorakumbura *et al.* showed how the rate of degradation of squalene increased when submersed in water, however enhancement methods have been used to successfully enhance lipid material which has been wetted.^{52, 109-111} Increased humidity has been known to impact fingermark development, the presence of water vapour can dissolve water soluble components, whilst also speeding up lipid oxidation processes.^{32, 47, 112} Storage of fingermark samples open to airflow have increased exposure to oxygen and ozone, by limiting this exposure and storing samples in enclosed containers or office cupboards the oxidation of lipid material can be prolonged.^{96, 113}

There are many compounding factors influencing the surrounding environment, which in an experimental setting can be controlled.⁸² Unfortunately, in a realistic scenario information on the environment is unknown and predicting the effects the environment may have on fingermark degradation is unreasonable. Therefore, it is important that investigation of environmental effects on fingermark degradation happen solely on a fundamental level, to assist in the interpretation of fingermark evidence.

1.4 Fingermark Development

The successful detection of fingermark evidence can be crucial to providing investigative information to a criminal case. Thus the decision on how to process a fingermark sample is an important decision made by crime scene investigators.² There are a number of considerations to take into account when selecting the appropriate enhancement treatment process.¹¹⁴⁻¹¹⁶ The destructiveness, ease of use,

cost and required equipment or training are often considered by a department when selecting a routine treatment method, but factors intrinsic to the substrate can be crucial to the selection of an appropriate method.^{15, 117-119} The background colour, surrounding environment and the porosity of the surface are important factors to consider. The schematic shown in Figure 1.2 outlines an example of the decision process when selecting a fingerprint treatment method.

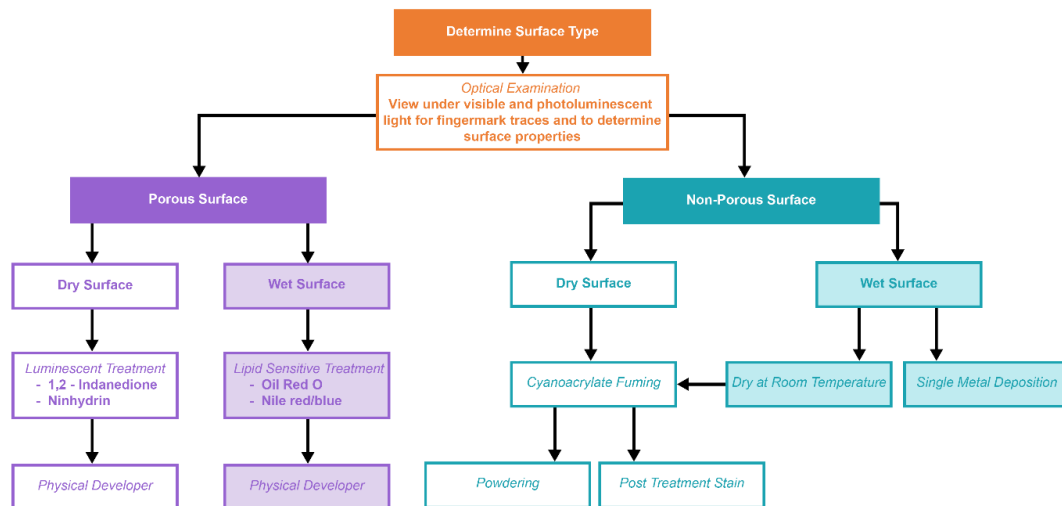


Figure 1.2: Flowchart showing an example of a fingerprint development treatment decision process. ^{115-116, 118}

1.4.1 Porous Fingerprint Development Methods

Eccrine material can be a particularly good chemical target for fingerprint enhancement due to its longevity on porous surfaces. The amino acids present bind with the cellulose in surfaces like paper and conserve the fingerprint pattern, providing opportunity to detect fingerprints long after deposition.^{15, 99} Reagents, including ninhydrin and 1,2-indanedione have been developed to react with the amino acids found in fingerprint residue to produce a brightly coloured or luminescent product.¹²⁰ The sensitivity of these methods have demonstrated high quality development across a wide range of donors and different formulations have been developed for use in a range of jurisdictions.^{35, 118, 121-124}

Since its initial serendipitous discovery as a fingerprint treatment, ninhydrin (2,2-dihydroxyindane-1,3-dione) has become the most widely used method for the

development of fingermarks on white or light coloured porous surfaces.^{28, 125-126} Fingermarks are submersed in a solution of ninhydrin for a few seconds before heating the substrate to speed up the reaction between ninhydrin and the amino acids to produce the colour Ruhemann's purple.^{35, 127} Dependent on the chemistry of the amino acids present within the residue the developed mark can appear red to deep violet in colour.³⁵ Modifications to this method have introduced metal salts as a post-treatment, in conjunction with cooling of the specimen, to produce a fluorescent product.^{28, 128-129} This can overcome the difficulties of visualising ninhydrin treated marks on dark coloured or patterned surfaces.^{15, 28, 129}

Significant research was carried out into analogues of ninhydrin to identify a reagent that would be able to provide both coloured and luminescent fingermarks, without the need for post-treatments.^{120, 130} Of the compounds investigated, 1,2-indanedione has emerged as the most effective treatment to date for targeting amino-acid components within fingerprint residue on coloured or patterned surfaces.^{122, 131-132} This reagent is applied similarly to ninhydrin, by typically submersing the fingerprint in a solution for a short period before heating the sample to accelerate the reaction.^{35, 118, 121} The product formed in this reaction has been termed Joullie's Pink, and is a bright, pink coloured product which exhibits fluorescence when excited with a 505 nm light source and viewed through a 550 nm barrier filter.¹¹⁸ This method has shown superior performance, with Bouzin *et al.* demonstrating the sensitivity of 1,2-indanedione, detecting fingerprints aged up to 80 years old, however there are still particular jurisdictions who are apprehensive to operational use due to the issues with development environment.^{102, 120, 122} There is evidence to suggest that humidity and temperature can impact the performance of 1,2-indanedione, with areas encountering high temperature and humidity conditions producing a better quality fingerprint.¹²⁴ The introduction of zinc-chloride to the working solution can improve the stability of the compound in solution, whilst improvement was seen in this method further work is still being carried out to optimise the method for cooler, low humidity environments.^{35, 122}

Lipid material is an alternative chemical target for the development of fingerprint residue. This material can be advantageous as a target due to its stability in harsher

environments, such as water exposure.¹³³ The oily nature of lipid material allows the hydrophobic residues to remain on a surface, trapping the fingerprint even after submersion in water.¹¹⁵ Traditionally, sebaceous secretions have been treated using physical developer (PD), a method used operationally to develop fingerprints on wetted surfaces using colloidal silver nitrate to develop a dark grey fingerprint.^{35, 134} The theory behind PD has been debated, with the understanding that it is a complex mechanism involving a mixture of eccrine and sebaceous secretions.^{110, 135-137} Despite its challenging development process and damaging temperament to discolour background surfaces, physical development treatment has proved useful in treating challenging samples, developing fingerprint samples up to 90 years old.^{87, 138} It has also provided a basis for the evolution of single and multi-metal deposition methods.

139-140

Alternatively, lipid secretions can be targeted by Oil Red O (ORO), a lipid sensitive dye adapted from methods in biology where the dye is used for staining lipoproteins.¹⁴¹ Rawji *et al.* compared Oil Red O and physical developer, highlighting the simplicity of the ORO procedure and enhanced development quality on white and thermal papers.¹⁴² However, ORO has been reported to only offer superior development when sebaceous rich deposits are used, with natural and aged samples producing fingerprints of poorer quality.^{35, 143-144} The methods produce red (ORO) and grey (PD) coloured fingerprints, meaning brightly coloured or patterned surfaces are challenging for visual contrast.^{35, 118}

Nile red is a histochemical stain which targets neutral lipids and provides increased sensitivity and photoluminescent properties to overcome contrast issues.¹⁴⁵⁻¹⁴⁶ Nile red has been used to treat fingerprints on wetted porous substances, however there are concerns over the toxicity of the solvents required for solubilisation.¹⁴⁵ Recent progress has adapted a safer and more cost effective alternative utilising Nile blue A, which when dispersed in aqueous solution hydrolyses to form Nile red.¹⁴⁷ Successful development of latent fingerprints using aqueous Nile blue solution on porous surfaces has been reported by Frick *et al.*, with the pH lowered using dilute sulfuric acid demonstrating a brighter fluorescent product due to the increased yield in Nile red.¹⁴⁷⁻¹⁴⁸ An alternate approach to overcome the immiscibility of Nile red in aqueous

solutions was reported by de la Hunty *et al.*, where an aqueous microemulsion incorporating Nile red, which is safer and more cost effective than conventional methods, was prepared, revealing superior development compared to the published aqueous Nile blue method.¹³³

1.4.2 Non-porous Fingerprint Development Methods

Substantial research has focussed on the evolution of development methods for porous surfaces, comparably non-porous surfaces are often treated with one of two methods, powdering or superglue fuming. These methods are preferable in an operational setting due to their cost effectiveness and ease of use.¹⁵ Both methods provide adequate contrast of the fingerprint ridge against the surface however, the development quality is concomitant to the state of the residue present.^{35, 48} Due to the nature of a non-porous surface the fingerprint is fragile and environmental exposure or length of time since deposition can be detrimental to development performance.^{2, 49}

Fingerprint powdering involves dusting the fingerprint with granular micron-sized particles.⁴⁸ The adhesion of the powder to the fingerprint is dependent on the particle size and shape, surface chemistry and electrostatic charge, with auto-adhesion ensuring the build up of particles following the first layer of powder deposition.³⁵ There are a number of fingerprint powders designed to suit a range of non-porous surface types including coloured, magnetic and fluorescent powders.¹⁴⁶ Once treated, powdered fingerprints can be photographed *in-situ* or be lifted using an appropriate medium to provide additional contrast.¹¹⁸

Cyanoacrylate fuming, or superglue fuming, is a method used to enhance the visibility and stability of fingerprint residue.¹⁴⁶ The fingerprint is placed inside a chamber with cyanoacrylate vapours which polymerise to form a rigid three dimensional matrix of the fingerprint.¹⁴⁹ The cyanoacrylate polymer interacts with the bases present within fingerprint residues, with weak bases present in eccrine material shown to promote polymer growth.¹⁵⁰⁻¹⁵¹ For this reason wet surfaces are not appropriate for this treatment, and should be dried to avoid development of the background. Humidity levels can impact the development processes of cyanoacrylate fuming, operationally

this is often controlled by humidity and temperature controlled development chambers.^{35, 47, 152} Following successful cyanoacrylate development coloured and fluorescent post-treatment stains can be used sequentially to further enhance the contrast and visibility of the fingerprint.¹⁵³⁻¹⁵⁴

1.4.3 Other Fingerprint Development Methods

The majority of fingerprint treatments are applied to either porous or non-porous surfaces, however there are a number of methods capable of treating fingerprints across a range of both types of surfaces, one of which is vacuum metal deposition (VMD). The process is often applied to non-porous and semi-porous substrates, and has been successful in treating marks on challenging surfaces such as polymer banknotes or after exposure to harsher environmental conditions.^{118, 155-157} VMD involves the evaporation of gold, which deposits as a thin monolayer across the fingerprint and substrate, the fingerprint residue diffuses the gold from its surface, leaving the top surface of the fingerprint exposed.³⁵ Subsequent treatment by zinc (or previously cadmium) fuming enhances the fingerprint ridge, by preferentially condensing on the exposed gold, providing a nucleation site for the zinc and producing a light coloured fingerprint against a dark background.^{35, 118, 158} Often “reverse development” is encountered, meaning the fingerprint is treated with zinc rather than the background, groups have theorised this phenomenon to either the interaction with inorganic constituents within fingerprint residue, particularly if the fingerprint is left to dry out, or to the amount of gold deposited initially.¹⁵⁸⁻¹⁶¹ Despite the success of this method, it is not used in all jurisdictions due to requirements for specialised equipment and an experienced operator.^{115, 118}

Advances in nanotechnology has seen a rise in nanoparticle treatments for fingerprint development.¹⁶²⁻¹⁶³ The size of these particles can be advantageous for improved development, however safety concerns over their use in powdered form must be considered, nanoparticles dispersed in solution is one approach taken to overcome this.¹⁶⁴ Single metal deposition (SMD) II is a method deriving from physical developer which uses gold nanoparticles in a colloidal solution to preferentially develop the fingerprint ridges.¹⁶⁵ The process involves a two-step procedure: an

initial gold nanoparticle deposition bath followed by a reinforcement solution where gold salts undergo *in-situ* reduction to further enhance the development contrast.^{109, 165-167} This step differentiates the method from its predecessor, multi-metal deposition, which uses a silver reduction bath. The method is advantageous in its ability to develop fingerprints across a range of porous and non-porous surfaces, however like physical developer the exact mechanism of the initial gold deposition process is still disputed.^{109, 168}

1.4.4 Challenges with Fingerprint Development

Despite the wide range of fingerprint development methods currently available, there remains numerous challenges in successfully developing latent fingerprints. Recently, Chadwick *et al.* highlighted the variability in sensitivity and selectivity of current detection methods, stating the substrate and donor play a significant role in successful fingerprint development.² Their work also emphasised that current operational methods do not detect all available fingerprints and reinforced the need for research to be conducted to better understand the fundamentals of fingerprint detection.

Sear's triangle of interaction model was suggested to aid in the decision making process when selecting an appropriate development procedure.⁸⁰ However, this theory can also be used retrospectively to help rationalise the behaviour of development methods. What is apparent is the significance of fingerprint chemistry, which as discussed previously can be directly affected by the substrate and surrounding environment.^{3, 5} In a research context the substrate and environmental conditions can be controlled and monitored, however, the chemistry of fingerprint residue is multifaceted and more variable.⁸² Exploring the fundamentals of fingerprint chemistry will improve the overall understanding of fingerprint development, and can improve the detection and interpretation of fingerprint evidence.

1.5 Analytical Methods Used to Explore Fingermark Chemistry

Improving the understanding of fingermark chemistry can assist in the advancement of fingermark detection procedures. Currently there are a number of visualisation methods used operationally with detection mechanisms that are not fully understood. By expanding the theory behind these techniques their performance can be better explained, leading to the improvement of methods and the creation of novel evidence-based techniques. Several studies have investigated fingermark chemistry using a range of analytical methods.^{3, 5, 169} Often this has involved direct measurement of bulk chemical composition of the fingermark sample using chromatography techniques, which provide a wealth of chemical information, but destroy the sample and any spatial information in the process. Meanwhile optical imaging methods, such as microscopy, are often non-destructive and can retain information on the distribution of material within the sample but are limited in their chemical specificity. Recent work has aimed to obtain the benefits of chemical specificity in addition to spatially resolved information by using chemical imaging methods.^{41, 95, 169-170} The use of such methods, which provide spatially resolved chemical information, has substantial potential to broaden the understanding of fingermark chemistry.

1.5.1 Chromatography Techniques

Chromatography offers excellent chemical specificity and sensitivity when analysing fingermark residues and has been applied in several studies to analyse the molecular composition of fingermark residue. Gas chromatography – mass spectrometry (GC-MS) is commonly used to identify the volatile compounds present within fingermark residue.^{13, 22-23, 50, 55, 84, 92, 105, 171} By comparing the mass spectra with that of standard compounds and the national standards database, a number of compounds present in fingermark residue have been identified.^{13, 16, 171-172} Liquid chromatography – mass spectrometry (LC-MS) is another chromatography technique and was used by de Puit *et al.* as an appropriate method to analyse the amino acid fraction of fingermark residue, identifying full amino acid profiles across a range of donors.^{27, 52} These methods can provide a chemical-specific view on the degradation of fingermark residue, with Dorakumbura *et al.* identifying a range of oxidation by-products which

form as a function of time since fingerprint deposition.⁵² Attempts to use these chemical profiles as an approach to dating the time since deposition of a fingerprint has been suggested, however a major challenge is the variation in starting material and the destructive nature of the method.^{52, 79, 173-174} Further work has investigated the effects of the surrounding environment on fingerprint chemistry, as well as attempts to link the chemical profile of a fingerprint to particular donor traits.^{3, 5, 22} Whilst chromatography methods can provide valuable bulk chemical information on the chemical constituents present, spatially resolved chemical information is not provided, meaning the information gained is limited to one dimension. It is hoped that investigation of spatially resolved chemical information may shed key insight on relationships between donor traits and fingerprint composition, donor activity and fingerprint composition, and how the chemistry of fingerprints changes during ageing.

1.5.2 Microscopy Techniques

Microscopy is used in forensic science to examine the physical properties of fingerprint residue, to visualise untreated fingerprints and investigate substrate surface properties. Optical microscopy is a non-destructive method, and can be used to explore the physical properties of the substrate surface and its interactions with fingerprint residues, as well as following fingerprint treatment to investigate development mechanisms.^{35, 88, 99, 175-177} There are different forms of microscopy which have been applied to fingerprint samples including bright field, dark field, phase contrast and scanning electron microscopy (SEM), Moret *et al.* reported a comparison of their performance, with limitations dependent on the substrate surface.¹⁷⁸ Dorakumbura *et al.* recently demonstrated the use of Atomic Force Microscopy (AFM) to explore physical properties such as the surface adhesion and topography of fingerprint droplets and Popov *et al.* used the technique to examine the migration of residue across the surface.¹⁷⁹⁻¹⁸⁰ AFM has also been used to investigate the substrate surface topography and its impact on fingerprint development, as well as metal corrosion from fingerprint residues.¹⁸¹⁻¹⁸² Microscopy is a valuable method capable of retaining spatial information, and has been used to demonstrate the physical changes of fingerprint residue over time, Scruton *et al.* and

Thomas *et al.* have both used optical microscopy to demonstrate how the shape or fingerprint droplets and ridges change over a period of time.^{88, 175, 183} Whilst this information is important for fingerprint research, it provides limited chemical information in comparison to bulk techniques such as chromatography.

1.5.3 Chemical Imaging Techniques

As an alternative to microscopy techniques and bulk chemical analyses, there is a suite of chemical imaging methods which can provide correlative chemical and spatial information.^{41, 169-170} Each method provides a unique perspective to explore fingerprint chemistry, providing a distinct set of capabilities and limitations which have been highlighted in Table 1.1. By applying a range of chemical imaging methods there is opportunity to develop a more comprehensive view of fingerprint chemistry.

Table 1.1: Summary of chemical imaging methods

Chemical Imaging Technique	Detection Method	Advantages	Disadvantages
Infrared microspectroscopy (IRM) ^{67, 95, 101, 184-190}	Molecular infrared absorption	<ul style="list-style-type: none"> - Potential for “good” spatial resolution (3 – 10 μm) - Moderate chemical sensitivity - Analysis of natural fingerprints - Non-destructive 	<ul style="list-style-type: none"> - Limited chemical specificity - Requires a specialised light source (synchrotron or quantum cascade laser) to achieve acceptable S/N at best possible spatial resolution
Matrix - assisted laser desorption ionization mass spectral imaging (MALDI-MSI) ^{8, 19, 30, 60, 65-66, 108, 191-192}	Molecular protonation	<ul style="list-style-type: none"> - Good chemical specificity - Can distinguish overlapping fingerprints based on chemical profile 	<ul style="list-style-type: none"> - Limited spatial resolution (10 μm at best, routinely $\sim 50 \mu\text{m}$) - Requires chemical pre-treatment of samples - Experiment often conducted under vacuum
Raman microspectroscopy ^{59, 61, 69, 95, 193}	Molecular Raman scattering	<ul style="list-style-type: none"> - High spatial resolution ($\sim 500 \text{ nm}$) - Relatively non-destructive 	<ul style="list-style-type: none"> - Moderate detection limits - Not sensitive to water - Issues with auto-fluorescence
Laser ablation - inductively coupled plasma - mass	Elemental ionisation	<ul style="list-style-type: none"> - Good detection limits (ppb) - Isotope specificity 	<ul style="list-style-type: none"> - Limited spatial resolution (10 μm)

spectrometry (LA-ICP-MS) ¹⁹⁴			- Redistribution of mobile ions during sample preparation
Secondary ions mass spectrometry (SIMS) ^{38-40, 70, 195}	Elemental ionisation	- Good detection limits (ppm-ppb) - High spatial resolution (<100 nm) - Surface sensitive	- Experiment conducted under vacuum - Surface sensitive (only reveals top-atomic layer of a deposit which can be several microns thick)
Scanning Electron Microscopy (SEM) ^{35, 88, 112, 152, 178, 196-198}	Electron beam or X-ray spectroscopy	- Good spatial resolution (< 1 μm) - Good sensitivity (typically 0.1 at%)	- Some surfaces require sample pre-treatment - Experiment conducted under vacuum - Small imaging area
X-ray fluorescence microscopy (XFM) ⁴²	Elemental X-ray fluorescence	- Good spatial resolution (1 μm or less) - Good detection limits (nM) - Analysis of natural fingermarks	- Requires a synchrotron light source to achieve optimal resolution and detection limits
X-ray photoelectron spectroscopy (XPS) ¹⁹⁹⁻²⁰⁰	Elemental photoemission	- High spatial resolution (<100 nm) - Good detection limits (ppm) - Surface sensitive	- Experiment conducted under vacuum - Surface sensitive (only reveals top-atomic layer of a deposit which can be several microns thick)

Recent advances in scientific capabilities have increased accessibility to advanced analytical methods that provide spatially resolved chemical analyses, such as the techniques presented in Table 1.1. Each method has benefits with respect to the level of information it can provide, however, only a handful of techniques offer the opportunity to analyse natural fingerprint samples, without any chemical alteration, treatments, or solvent extractions prior to measurement. *In-situ* label free measurements, when and where possible, can give a more realistic representation of the chemical species naturally present in fingerprint residue. Further the capability to analyse samples *in-situ* at ambient temperature and pressure, without the need for vacuum conditions (which often results in loss of loosely bound elemental content, or loss of morphology) is important when analysing organic material such as latent fingerprints.²⁰¹

1.6 Using Synchrotron Light to Explore Fingerprint Chemistry

A synchrotron, which is a type of particle accelerator, produces an intense (bright), broadband light source. The broadband nature of synchrotron light provides access to a wide range of the electromagnetic spectrum, from the far-infrared to high energy X-rays.²⁰²⁻²⁰³ In practice, scientists can essentially use synchrotron light as an incredibly bright, “tunable” light source to couple with various spectroscopic measurements.

Synchrotron light is generated with an electron beam at facilities which are set up similarly to that presented in Figure 1.3.²⁰⁴ Using thermionic emission, an electron gun emits electrons which are accelerated to 99.9997% of the speed of light by the linear accelerator.²⁰⁵ The linear accelerator or linac increases the speed of the electrons through intermittent exposure to a series of oscillating electric potentials.²⁰⁶ The electrons are then transferred to the booster ring where the ramping of magnetic fields and radio frequency cavities quickly accelerates the electron beam to an energy of 3 GeV.²⁰⁷ The storage ring then converts this electron beam to synchrotron light using a series of straight sections containing insertion devices and bending magnets. Insertion devices consist of magnets known as wigglers and undulators shown in Figure 1.3(a and b); these devices contribute to the

high flux and brightness between each bending magnet and are named for the action of the beam through their magnetic field. The bending magnets circulate the beam around the storage ring, as the electron beam is deflected off the bending magnets electromagnetic radiation is emitted tangentially to the electron beam, this radiation is passed through a series of optics to focus and tune the synchrotron light down to the beamline for experimental use.²⁰⁴

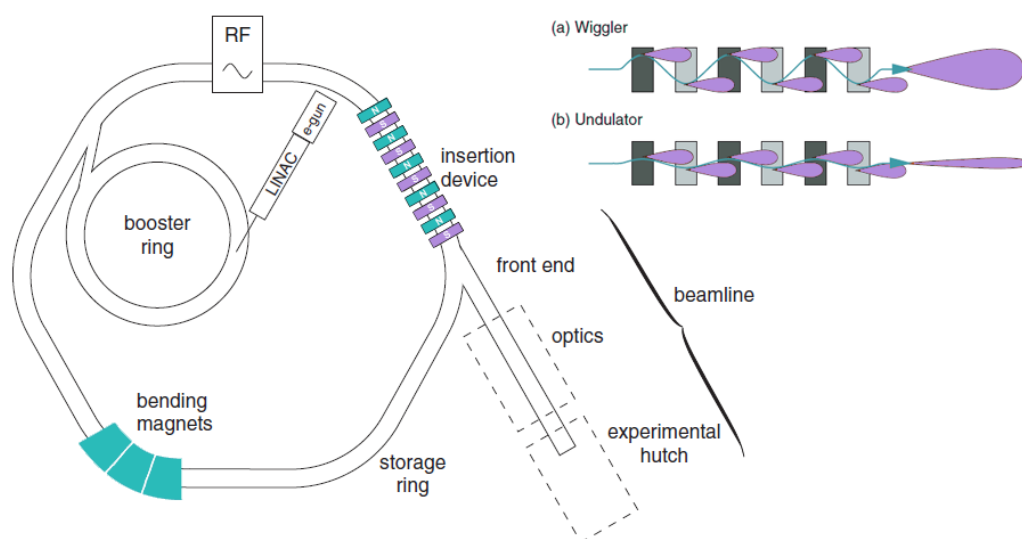


Figure 1.3: Schematic adapted from Wilmott et al. showing the key components of a synchrotron source including the direction of the electron flow through the insertion devices of a wiggler (a) and undulator (b).²⁰⁴

The synchrotron provides a light source with high brightness and highly collimated light, which allows experiments to be conducted which would not otherwise be possible using a conventional benchtop globar source.²⁰⁸ One advantage of this is the improved detection limits, which are effective in detecting the trace amounts of material present within a biological sample, such as latent fingerprints.^{170, 201, 209} This means that chemical species can be mapped within individual droplets in fingerprint samples, giving an exceptional view of their chemistry. To make meaningful conclusions about fingerprint chemistry it is important to assess a number of fingerprint donors, due to the inherent chemical variability of fingerprint residue discussed throughout this chapter.⁹¹ Due to the high brightness of a synchrotron light source, spectroscopic measurements can be made within a sufficiently quick data

collection time, achieving acceptable signal to noise ratios (S/N), to facilitate analysis of sufficient replicates and/or time resolved studies.²⁰⁸

1.6.1 Infrared Spectroscopy

The infrared (IR) region of the electromagnetic spectrum runs from 12800 cm^{-1} to 10 cm^{-1} , a wide range that is often split into the near-IR ($12800\text{ cm}^{-1} - 4000\text{ cm}^{-1}$), mid-IR ($4000\text{ cm}^{-1} - 400\text{ cm}^{-1}$) and far-IR ($400\text{ cm}^{-1} - 10\text{ cm}^{-1}$).²¹⁰⁻²¹¹ In general, the near-IR region corresponds to overtones of molecular vibrations, the mid-IR corresponds to the fundamentals of molecular vibrations, while the Far-IR region typically contains absorbance bands associated with rotational transitions.²¹⁰⁻²¹¹ Information can then be inferred about the chemical species present within a molecule, and/or molecular structure based upon the absorption specific wavelengths of light.²¹² Samples can be analysed as solids, solutions, neat-liquids, or in the gas phase. As the far-IR region is typically (but not always) used to analyse rotational modes, the majority of experiments conducted in the far-IR are gas-phase experiments.²¹⁰

For a molecule to absorb IR radiation and be measurable as an IR spectrum it requires a net dipole as it vibrates or rotates. Figure 1.4 displays the different types of vibrational transitions which can occur within a molecule when IR radiation is absorbed, vibrational transitions can occur between any bond with at least two atoms, meaning larger molecules can have a multitude of transitions occurring simultaneously. The energy levels of these transitions are quantized, meaning that there are a restricted number of transitions possible.²¹⁰ For gases there are several rotational energy levels for each vibration, which are characterised by a spectrum of discrete fine lines. Meanwhile for neat liquids, solutions and solids rotation is restricted and the close proximity of neighbouring molecules (and therefore intermolecular bonding) give the vibrational transitions a broader band shape in the corresponding spectrum.²¹⁰ Scientific advances have focused primarily in the mid-infrared with development of a wide range of instrumentation to measure the molecular vibrations in this region. Progress in the far-infrared has been slower, however this region has shown promise for gas and condensed phase experiments.

^{211, 213}

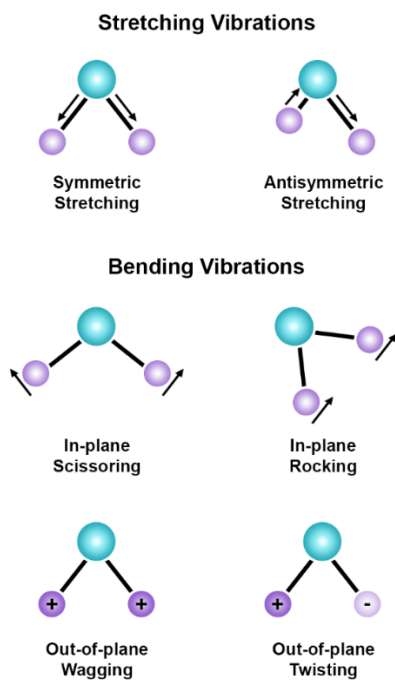


Figure 1.4: Types of molecular vibrations. Note that + denotes movement out of the page and – denotes movement into the page.^{210, 212}

The vast majority of infrared spectra are now routinely collected through the use of an interferometer and Fourier transform, referred to as Fourier transform infrared spectroscopy (FTIR). In FTIR a whole single beam spectrum is measured simultaneously, without the use of a diffraction grating, which offers the advantages of increased signal to noise ratio and improved data collection times.²¹⁴ A key part of an FTIR spectrometer is the interferometer, where the infrared beam is split at right angles into a transmitted and reflected beam and directed towards a stationary and movable mirror, these beams are reflected and then recombined to show interference. The movement of the mirror can control the degree of this interference as a function of the beam's cosine wave, which is detected as an interferogram. Using Fourier transform calculations the interferogram (recorded in time-domain) is converted back to a spectrum (frequency domain).²¹⁵

1.6.1.1 FTIR Microspectroscopy

The advent of FTIR spectroscopy revolutionised analysis of the mid-IR, enabling rapid collection of a mid-IR spectrum to quickly investigate chemical composition. Further, FTIR can be coupled with an infrared transmitting microscope to provide chemical knowledge whilst retaining valuable spatial information.²¹⁶⁻²¹⁷ Numerous acronyms exist for the collection of spatially resolved FTIR spectra, with the aid of some form of microscope optics – this thesis will use the acronym infrared microscopy (IRM) when referring to the collection of spatially resolved FTIR spectra. In IRM the infrared beam is focused to a small spot on the sample using apertures and a microscope objective, with diffraction limited resolution possible.²¹⁵⁻²¹⁶ When confining the beam to a sufficiently small size to achieve diffraction limited spatial resolution, high photon flux (brightness) is essential.²¹⁸ Unfortunately, conventional global sources used in most benchtop laboratory instruments do not provide sufficient brightness to achieve diffraction limited resolution and therefore suffer from poor signal to noise ratio when working at or near the diffraction limit.^{184, 218-220} In order to achieve diffraction limited spatial resolution with spectra displaying acceptable S/N and collected within an experimentally reasonable time frame, the high brightness of synchrotron light is often used.^{184, 218-220} In order to facilitate IRM over larger sample areas there is often the addition of a motorised sample stage, or a multiple pixel array detector.²¹⁵ This allows an IR spectrum to be collected at multiple points across the sample, which can be combined to generate a chemical map (or image if using an array detector).

1.6.1.2 ATR-FTIR Spectroscopy

There are several “modes” through which an FTIR spectrum can be recorded, typically transmittance, reflectance, or attenuated total internal reflectance (ATR). The selection of measurement mode requires consideration of the desired surface specificity, and the thickness, smoothness and opacity of the sample.²¹⁵ As their name suggests, transmittance spectra are recorded from measurement of light intensity that has transmitted through the sample, while reflectance is a measurement of light scattered or reflected off the surface. Attenuated total

reflectance (ATR) is an alternative method which provides measurement of an absorbance spectrum comparable to that collected in transmittance mode, but without the requirement of a sufficiently thin sample to allow light transmission.²¹⁷ An ATR-FTIR measurement takes advantage of light directed at a critical angle, meeting the interface of two materials with differing refractive indices. The two materials are a crystal with high refractive index (the ATR crystal) and the sample. At the point where the angle of incidence is above the critical angle of the crystal and sample, the IR beam is internally reflected within the crystal, and this phenomenon is called total internal reflectance.²¹⁷ These conditions result in an evanescent wave on the crystal surface, which when brought into contact with a sample is absorbed by the IR active molecules and then reflected to the detector.²²¹⁻²²²

Most materials used in the ATR crystal must have high refractive index to ensure total internal reflection, governed by equation 1. Typical materials and their refractive index include diamond ($n= 2.42$), silicon ($n= 3.42$) and germanium ($n= 4.00$).²¹⁵ At the point where total internal reflectance occurs an evanescent wave is produced on the crystal surface, and the oscillating electric field of the evanescent wave can interact with the oscillating dipole of sample molecules at the crystal surface, enabling measurement of the ATR-FTIR (spectrum).²²¹

Equation 1: *The equation for the depth of penetration (d_p) of the evanescent wave, which is defined as the distance where the strength of the electric field decays to e^{-1} .*^{184, 217, 222}

$$d_p = \frac{\lambda}{2\pi n_1 \left(\sin^2 \theta - \left(\frac{n_2}{n_1} \right)^2 \right)^{0.5}}$$

d_p = depth of penetration
 n_1 = refractive index of the ATR crystal
 n_2 = refractive index of the sample
 θ = angle of incidence
 λ = wavelength of light

The application of ATR with IRM, sometimes referred to as ATR-FTIR microspectroscopy, has advantages over traditional transmission and reflectance modes. ATR is applicable over a range of liquid, solid and semi-solid samples, negating the issues with opacity seen with transmission modes.²¹⁷ The sample preparation required is relatively simple, with the ATR crystal being brought into contact with the sample, this process can also be non-destructive if care is taken.^{215,}

²²³ An additional advantage of ATR, is that the high refractive index of the crystal effectively increases the numerical aperture when ATR-FTIR is coupled with microscopy (ATR-IRM), and therefore, improves the diffraction limited resolution that can be obtained.²¹⁶ Kazarian *et al.* have made numerous critical advantages in ATR-IRM methodology, showcasing it as a powerful non-destructive tool for chemical characterisation in the biological, pharmaceutical and forensic science fields.^{216, 224-228}

The incorporation of synchrotron IR light for ATR-IRM can provide the best possible spectral resolution, Miller *et al.* highlighted its relevance for biological systems revealing improved signal to noise ratios.²¹⁸ Additionally, capabilities are expanded with the use of a Ge ATR crystal, Chan *et al.* demonstrated its application, which provides a high numerical aperture for the microscope, thus improving the imaging spatial resolution.²¹⁶ Vongsvivut *et al.* combined the two, using a synchrotron sourced ATR-FTIR microscope fitted with a Ge ATR crystal, to map a range of biological and environmental samples with sub-micron pixel size.¹⁸⁴ The brightness of the synchrotron light source, coupled with the improved resolution of the Ge ATR set up optimises the microscopy capabilities of IRM, with successful imaging of individual cells shown in tissue samples.¹⁸⁴

1.6.1.3 FTIR Spectroscopy in the Gas Phase

To measure a gas or vapour sample using FTIR spectroscopy (e.g. in mid or far infrared range, to observe rotational modes) a gas cell fitting is added. A gas cell provides an adequate path length to account for the dilute concentrations of a gas compared to a solid or liquid sample.²¹⁵ The cell is under vacuum prior to introducing the sample using a series of valves and a pressure gauge, the IR beam is then passed through appropriate infrared transparent windows into the cell, through the sample and to the detector. Gas cells can be fitted with a series of mirrors to reflect the beam inside the cell increasing the path length of the beam which, as per Beer's law, will improve the absorbance of low concentration samples.²¹⁰ The spectra measured in the gas phase are characteristically different due to the increased space between gas

molecules, which allows them to undergo both vibrational and rotational transitions resulting in an additional spectral features.²¹⁵

The brightness of synchrotron radiation is suited to gas phase studies due to its high spectral resolution capabilities.²¹³ The high flux improves the S/N at wavenumbers within the Far-IR and Terahertz (THz) region, enabling studies to be conducted on condensed phase samples.²²⁹ The high S/N in the Far-IR range permits the evaluation of discrete fine lines indicative of molecular rotational modes, as observed in molecules such as water, which can be identified in this region without overlapping of vibrational modes from functional groups such as hydroxyl groups of carbohydrates or N-H stretching of amino-acids which is experienced in the Mid-IR region.²¹⁰ The setup at the ANSTO Australian Synchrotron THz/Far-IR Spectroscopy beamline is equipped with two ambient temperature gas cells, one which is used to study stable gas species, whilst the second can be coupled to a furnace to study short lived species generated by pyrolysis.²¹³ By analysing gas samples in the THz/Far-IR region greater detail is revealed, with vibrational and rotational transitions reported using these methods within a range of fields including geology, biology, atmospheric chemistry and astrophysical sciences.²¹³

1.6.1.4 Past applications of infrared spectroscopy to study fingerprint residues

FTIR spectroscopy has been utilised in fingerprint research to demonstrate how variation in molecular chemistry can be indicative of donor traits such as age and biological gender and to estimate time since fingerprint deposition.^{18, 101, 190, 226} Commonly fingerprint samples have been analysed by IRM methods (either mapping or imaging), to retain spatial information to better understand the behaviour and distribution of material within fingerprint residues.²²⁶ The first reports using IRM for the analysis of latent fingerprints were reported in 2001 from the Lawrence Berkeley National Laboratory, where Wilkinson *et al.* suggested the use of synchrotron sourced IRM to explore the distribution and changes in fingerprint chemistry.²³⁰⁻²³¹ This was followed by Williams *et al.* who published the use of traditional global sourced IRM to image a small section of fingerprint ridges in reflectance mode.²³² Subsequent studies using this method explored the effects of gender, temperature

and time on the composition of fingermarks from children, with Antoine *et al.* comparing to the composition of adult fingermarks.^{18, 190}

The addition of ATR-FTIR has broadened the application of IR spectroscopy to a wider number of substrate surfaces and further improves the spatial resolution, which is important when working with small volumes of complex biological mixtures such as fingermarks.²¹⁶ Girod *et al.* reported this with ATR yielding improved spectral quality compared to reflectance mode on aluminium and glass surfaces.¹⁰¹ A number of studies have demonstrated the use of ATR-FTIR microspectroscopy to identify contaminants in fingermark residue, and explore fingermark composition.^{7, 233-235} Ricci *et al.* placed the fingermark directly on to a ZnSe crystal, using ATR-IRM to show the lipid and amino acid material present in fingermark residue from 5 donors and monitoring the changes with time and temperature.¹⁸⁷

Fritz *et al.* further explored the use of synchrotron sourced IRM, imaging fingermarks in reflection mode on polished stainless steel and transmission mode on ZnSe substrates.¹⁸⁵ The study showed the capabilities of working at diffraction limited spatial resolutions to help differentiate between glandular secretions and skin debris. In a recent study, Dorakumbura *et al.* made use of the advances in synchrotron science using synchrotron sourced ATR-IRM to improve signal to noise ratios and spatial resolution capabilities to the micron scale. This setup allows the characterisation of eccrine and sebaceous material within individual droplets in fingermark residue, giving fingermark researchers an unprecedented view of fingermark chemistry (specifically the distribution of individual lipid droplets relative to eccrine material).⁹⁵

1.6.2 X-ray Fluorescence Microscopy

X-ray Fluorescence Microscopy (XFM) (or sometimes referred to as XRF) is an analytical technique used to map the elemental distribution of materials.²³⁶ Elemental quantification is possible with benchtop (or even portable hand-held) XRF spectrometers, however, bright light sources are required to provide sufficient S/N and sufficient detection limits when analysing small sample areas (e.g., analysis at

the micron level). For this reason, most XFM measurements are conducted at synchrotron facilities.²³⁷

The process of generating an XRF spectrum is similar for both a bulk XRF measurement or XFM. In general, the sample is bombarded with high energy X-rays which can excite electrons within the atoms present in the sample as shown in Figure 1.5.²³⁸ Specifically, if the energy is great enough to overcome the binding energy of an inner orbital electron, the electron can be excited to an unoccupied molecular orbital with higher energy (e.g., the lowest unoccupied molecular orbital, LUMO), or it can be ejected from the atom (e.g., the atom is ionised).²¹⁰ In both cases, excitation and ejection of a core electron leaves behind a core-hole, and the atom is in an excited (unstable) electronic configuration. To return the atom to its stable ground state, an electron is transferred from a higher energy orbital to fill the vacancy of the inner orbital. This electron transfer has an inherent energy difference, moving from a higher energy to a lower energy orbital, the residual energy is emitted as fluorescence, with a wavelength characteristic of the atom.^{236, 239}

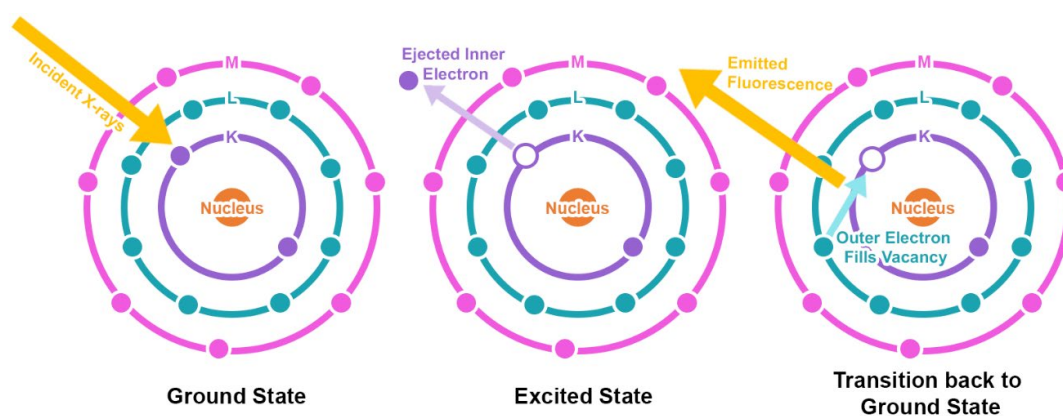


Figure 1.5: Schematic showing the process of X-ray Fluorescence.^{236, 238}

Synchrotron sourced XFM is well suited to study elemental distributions in latent fingerprints (and biological samples in general), owing to its ability to provide quick data collection at micron or sub-micron level spatial resolution and nM detection limits.^{170, 201, 209, 238, 240-241} Further, XFM offers the capability to analyse samples *in-situ* at ambient temperature and pressure, without the need for vacuum conditions.^{201, 241} Although a suite of other techniques also offer elemental mapping capabilities, such as laser ablation inductively coupled plasma mass spectrometry (LA-ICP-MS),^{209,}

²⁴²⁻²⁴⁴ secondary ions mass spectrometry (SIMS),²⁴⁵⁻²⁴⁶ and X-ray photoelectron spectroscopy (XPS),¹⁹⁹ these techniques are either surface sensitive, require analysis under vacuum conditions, or can be destructive to the fingerprint sample.

1.6.2.1 X-ray Optics and Detectors

In XRF a spectrometer measures the total fluorescence emitted from the sample. The total spectrum measured consists of a mixture of X-rays characteristic of the atoms present within the sample, as well as scatter from the incident energy source.²³⁶ Mathematical fitting algorithms are used to separate spectral components to identify the intensity of individual fluorescence lines atoms, which can then be converted to elemental concentration by comparison against standards.²³⁸

Several options for X-ray detectors exist, including the Maia 384-element detector array and Vortex silicon drift detectors. The majority of studies undertaken at the ANSTO Australian Synchrotron utilise the Maia detector, with upgrades to the Vortex detector currently underway.²⁴⁷ The Maia detector is designed with a 0.5 mm diameter aperture which allows the beam to pass through the detector on to the sample in a backscatter configuration, to allow greater opportunities for sample size and scanning ranges. The sensor consists of a monolithic silicon planar array, with 384 detector elements, each connecting to independent analogue channels.²⁴⁷ When undertaking XFM a full emission spectrum is taken at each point across the sample, which is used to generate a map of the overall distribution of elemental material.²⁴⁸ The Maia detector can be used in event-mode, meaning that the position of the photon event is tagged with the identity of the detector element used to record it, to improve the efficiency of data acquisition.²⁴⁹ This allows the dwell time per pixel to decrease, allowing users to select the optimal image size and dwell time for the sample, to capture high definition images whilst retaining adequate spatial information with real-time elemental deconvolution and image projection.²⁵⁰⁻²⁵¹ Diffraction limited spatial resolution is rarely achieved in most XFM experiments. Typically, XFM experiments use a set of X-ray optics to define the spot size, which is on the order of 1 – 2 μm if using a Kirkpatrick–Baez (KB) mirror pair, or on the order of 50 – 200 nm if using zone plate optics. The KB mirror shape is adjusted by two

adjustable moments applied to a trapezoidal-shaped mirror. Horizontal and vertical mirrors are made from silicon with platinum and rhodium strips, the radius of curvature and ellipticity of these mirrors are controlled independently to focus the beam.²⁵¹ Alternatively, a hard X-ray Fresnel zone-plate nanoprobe can be applied in conjunction with laser interferometer sample position encoding. At the Australian Synchrotron the nanoprobe can be fitted with two different sized zone plates, which are optimised for different X-ray energies. This setup is ideal for diffraction-limited focusing, however it is a less efficient focussing method than KB mirrors, resulting in substantially less flux within the focussed spot, and therefore higher noise levels. To compensate, mapping experiments with a zone plate require longer data collection times to provide adequate S/N, but this often makes the experiment impractical within a reasonable time frame. The zone plate capability has been decommissioned for users on the XFM beamline at the ANSTO Australian Synchrotron, with the KB mirror pair routinely used collectively with the Maia detector.²⁴⁷

1.6.2.2 X-ray Absorption Near Edge Structure Spectroscopy

The XFM beamline at the ANSTO Australian Synchrotron also has the capabilities to perform X-ray absorption near-edge structure (XANES) spectroscopy imaging which can be used to investigate the chemical state of the elemental material.²⁴⁷ It involves mapping a single element in a sample as a function of the element's incident energy across the element's absorption edge. A 2D map of the elemental profile is generated, as performed in XFM, however in this case at the completion of the 2D map the incident energy is changed and the map repeated for the selected energies. The outcome is a stack of images of the sample across an energy range, this can provide information on the element's chemical forms, such as oxidation state and binding molecules. At this stage the method has been used primarily on biological samples, demonstrating the distribution of Fe, Cu and Zn within cells and tissue samples.²⁵²⁻²⁵⁵

1.6.2.3 Past applications of elemental mapping to study fingerprint residues

While a large number of studies have explored the distribution of organic material within latent fingerprints, using methods such as IRM, MALDI-MSI and Raman

spectroscopy, there has been less work conducted to investigate the inorganic material. While naturally there are small amounts of metal ions present in eccrine secretions, inorganic material is also often transferred to the hands on contact with firearms or metal objects.^{76, 256} This makes the identification of elemental material in fingermarks of potential interest to forensic researchers, however research in this area has been hampered by accessibility to instrumentation with the appropriate sensitivity, spatial resolution and imaging conditions required for fingermark samples. Primarily, research using methods such as XPS, TOF-SIMS and LA-ICP-MS has been used to explore the contaminants present in fingermark residue, or following fingermark development, to improve ridge quality by increasing the elemental material present.^{70, 194, 199, 257} Elemental mapping of natural fingermarks has been limited to surface-sensitive methods where the ridge is detected due to contrast against a surface, such as that reported by Thandauthapani *et al.* where TOF-SIMS was used to image the sodium, potassium and chloride ion distribution in fingermarks on stainless steel, however this method did require samples to be placed in a vacuum chamber setup, potentially disrupting the fingermark sample.

XFM provides the opportunity to image the elemental content of fingermarks, with good sensitivity and in atmospheric conditions, limiting sample damage.²⁴¹ Wilkinson *et al.* first suggested the use of synchrotron XRF to map the electrolytes present in children's fingermarks in 2002, however no further work was reported using the method until Worley *et al.* revealed the use a benchtop XRF device to image fingermark samples.^{42, 230} Detecting the elemental material in natural fingermarks was difficult due to the limitations of the benchtop device, detecting only the chlorine, potassium and sulfur content in a fingermark from one donor, no elemental content was detected for additional donors, expected to be below the detection limits of the device.⁴² Further experiments saw improvements in detectability after purposely increasing the elemental content on the hands, following application of lotion and sunscreen as well as contact with food and saliva.⁴² This suggests the potential application of the method, if advances in technology provide improved sensitivity, which could be provided by synchrotron sourced XFM.

1.7 Exploiting Fingermark Transfer for Forensic Science

There is great value in the investigation of fingermark chemistry for the improvement of fingermark detection, however it can also be exploited to determine donor specific information.⁶ The composition of latent fingermarks is known to contain contaminants, some of which are transferred through donor activity prior to fingermark deposition. The multifaceted potential of fingermark evidence has recently been revealed, with fingermarks no longer limited to information used in identification, but now also in gaining contextual activity level information.⁹⁻¹²

Evaluating a fingermark in the context of activities that resulted in the fingermark deposition itself, or activities undertaken prior to deposition, is a decision left ultimately to the court.²⁵⁸ A thorough understanding of transfer mechanisms, including how physical activities influence subsequent chemical composition of latent fingermarks, in addition to chemical persistence within latent fingermarks could therefore aid forensic scientists in assigning evidential values to improve the interpretation of fingermark evidence in relation to the activity level.²⁵⁹⁻²⁶⁰ Such studies have been conducted to explore the transfer mechanisms involved in DNA and textile fibre trace evidence.^{56, 261-267} The studies involved experiments where participants were directly or indirectly brought into contact with an item, with variables including donor, recipient and extent of contact considered to explore their effect on transfer processes.^{261, 263-265} Recently, de Ronde and co-workers have investigated the deposition of latent fingermarks in an activity level context for a variety of criminal scenarios.⁹⁻¹²

Metal contaminants have been utilised for the identification of iron on the hands after handling a metal firearm, with researchers using coloured indicators to reveal the presence of iron on the suspect's hands to demonstrate the use of firearms.^{76-77, 256, 268} The detection of secondary transfer of iron in fingermark residue provides information at both an identification and activity level, which may add value when interpreting forensic data. Furthering the understanding of transfer mechanisms for contaminants in fingermark residue can assist in advancing the connection between the activity level and fingermark evidence.^{8, 62-63} Bradshaw *et al.* have recently

utilised MALDI-MSI to gain contextual information on a donor in operational case work.¹⁹² Using this method metabolites were identified in a fingerprint detected through powdering methods. These metabolites were indicative of drug and alcohol consumption which was important information for this case. Further work has explored donor lifestyle information by identifying organic active ingredients from foods, alcohols and cosmetic products, which can aid in building a suspect profile.⁶⁵

The modern direction for fingerprint research to provide contextual information is a growing field. There is a need for more fundamental research to better understand the materials that are transferred to and persist within fingerprints, with scope to develop improved and/or targeted strategies to detect contaminants using various coloured or fluorescent indicators. Whilst analytical methods such as MALDI-MSI can provide information on the organic contaminants present within fingerprint residue, the application of a wider range of analytical techniques can provide an improved picture of fingerprint contaminants and their potential to provide activity level information.

1.8 Aims and Overview

This thesis aims to use synchrotron science to further the understanding of fingerprint chemistry and demonstrate the capabilities of synchrotron sourced X-rays and IR light to analyse fingerprint residues. Advanced analytical instrumentation will be used to investigate the distribution, transfer and persistence of organic and inorganic materials within latent fingerprints. The results will assist future research in the advancement of fingerprint visualisation methods to improve the rate of recovery for criminal investigations.

Therefore, the overall aims of the project will be to:

- Expand the current understanding of fingerprint chemistry and how donor chemical variation can contribute to the inconsistencies seen in fingerprint development performance (Chapter 3)
- Explore the capabilities of synchrotron sourced XFM to reveal the distribution of elemental material in natural latent fingerprints (Chapter 4);
- Investigate the fundamental forensic processes of transfer and persistence and how this relates to the chemical composition of fingerprint residues (Chapter 5);
- Use IR spectroscopy to monitor the changes in fingerprint residues in the immediate hours following deposition (Chapter 6);

As per the IFRG guidelines this study will adhere to the requirements suggested for fingerprint research, a full discussion of the experimental considerations is outlined in Chapter 2, followed by an overview of the experimental methods and instrumentation used throughout this study. Chapter 3 begins by investigating the donor variation in fingerprint chemistry, with five visualisation techniques chosen to demonstrate the diversity in response to chemical and physical treatments due to the chemical differences in fingerprint residues. This will also act as a screening process to ensure an adequate representation of donor chemistries are selected for subsequent studies to provide an accurate representation of the variation expected amongst the general population.

Chapters 4 and 5 explore the use of synchrotron sourced XFM, providing for the first time micron resolution elemental mapping of the natural inorganic material in latent fingermarks. This will provide valuable information on the inorganic chemistry of fingermark residues. When combined in a multi-modal XFM/IRM workflow the association between inorganic and organic materials in fingermark residues can be captured, providing an unprecedented view of fingermark chemistry. Further, Chapter 5 will explore the fundamental processes of transfer and persistence, aligning directly with the priorities outlined by the recent Research and Innovation Roadmap reported by the National Institute of Forensic Science (NIFS), which is a directorate within the Australia New Zealand Policing Advisory Agency (ANZPAA).²⁶⁰ Investigations into the transfer and persistence of metallic material from forensically significant items will provide valuable information regarding the activity level of the donor, providing the opportunity to look beyond the identification information, to gaining crucial contextual information from fingermark evidence.

Chapter 6 will make use of synchrotron sourced IRM for its improved data acquisition times and spatial resolution to monitor the changes in organic residues. Fingermark droplets from natural fingermark samples will be monitored in the first 13 hours following deposition. Eccrine and sebaceous material will be characterised by spectroscopic marker bands previously identified using this method and changes in these bands will be measured to visualise the change in morphology and chemical composition within the droplet. This will demonstrate the rate of change within a fingermark in the immediate hours after deposition, a time period rarely explored in previous studies. Additionally the capability of gas phase THz/Far-IR spectroscopy will be assessed in an attempt to measure the volume of water evaporated from fingermark residues. This is a challenging experimental concept due to the small volumes and dynamic material being measured, however the sensitivity of the pure-rotational water vapour transitions in the Far-IR offers a unique opportunity to contribute to answering this ambitious scientific endeavour.

Chapter 2

Sample Collection, Experimental Methods and Instrumentation



2.1 Introduction

This chapter outlines the experimental methods used throughout this study. It begins with a discussion of the experimental considerations made to work with fingerprint samples, including information on fingerprint collection procedures and donor information. The instrumentation used in the subsequent chapters is outlined, with any adaptations to the generic setup conditions specified within the relevant chapter. Finally, there is an overview of the fingerprint development methods used in chapter 3, including reagent information and preparation methods.

2.2 Experimental Considerations

The inherent variability in fingerprint chemistry is a challenge for researchers, considerations must be made to ensure an achievable level of consistency, which allows reasonable conclusions to be drawn. The IFRG aims to standardise research methodology by providing guidelines for developing and testing methods for fingerprint recovery.⁹¹ This helps to ensure the operational effectiveness of the technique, but should also be considered in fundamental studies to ensure an appropriate representation of the general population.

The IFRG suggests an appropriate number of donors should be used to account for interdonor chemical variation (5-15), where possible a larger donor pool will provide a more accurate representation of this. In this study, there were limitations on donor numbers used due to availability of the instrumentation, compromises were made in areas such as image size and resolution to ensure an appropriate number of donors were used to provide significant results. For consistency, all donors were instructed on the appropriate procedures when depositing samples outlined in section 2.3. Chemical imaging was undertaken on natural fingerprint samples to provide the most realistic representation of fingerprint residue and substrate surface was kept consistent throughout comparison studies, see relevant chapter for experiment specific information.

Care was taken to ensure consistency in environmental conditions where possible, with fingerprint samples primarily stored in an office environment under ambient

lighting in an air-conditioned office space, unless otherwise stated. Due to unforeseen circumstances of the COVID-19 pandemic, a portion of the chemical imaging work was conducted remotely and samples were sent by air to the ANSTO – Australian Synchrotron (Clayton, Victoria). Care was taken during packaging of samples to ensure the samples remained intact and were labelled to avoid contact on handling.

Despite the preventative measures taken to limit the variation in fingerprint residues, there is an inevitable level of variability when working with biological materials. However, by following the recommendations outlined by the IFRG, this research will be conducted following an appropriate method to allow legitimate conclusions to be established based on the data presented.

2.3 Fingerprint Collection

Fingerprint donors were instructed to provide natural fingerprints by lightly pressing the finger on the substrate surface for ~5 seconds. Natural fingerprints, which have not been intentionally groomed for increased material, were used throughout this study unless otherwise stated. Care was taken to ensure that the donor had not washed their hands, eaten or come into contact with chemicals in the 30 minutes prior to sample collection to reduce contamination and ensure a natural build-up of surface secretions.

2.4 Donor Information

In this study 21 donors were selected to participate. An overview of the donor information is provided in Table 2.1. Due to donor availability not all donors participated in every study and a specific donor list can be found within each chapter. Donors provided information on cosmetic use, which refers to the daily use of products including sunscreen, moisturisers, make-up and hair products.

Table 2.1: Donor information

Donor No.	Age*	Biological Gender	Cosmetic Use
1	77	Male	None Reported
2	27	Female	None Reported
3	22	Male	None Reported
4	24	Male	None Reported
5	41	Male	None Reported
6	23	Female	Yes
7	55	Male	Yes
8	48	Male	None Reported
9	26	Female	Yes
10	40	Female	Yes
11	34	Female	None Reported
12	23	Female	Yes
13	23	Female	Yes
14	36	Male	None Reported
15	23	Male	Yes
16	23	Female	Yes
17	50	Male	None Reported
18	32	Male	None Reported
19	34	Female	Yes
20	23	Female	Yes
21	32	Female	None Reported

*Age is taken from date of first sample deposited

2.5 Substrate Surface Selection

Substrate surfaces were selected as per the relevant instrumentation and experimental requirements. Fingerprint development within Chapter 3 was carried out on both porous, Nu World Stone (China) sectioned water-proof paper, and non-porous surfaces, glass microscope slides (VWR International, Leuven); these surfaces were selected to be most compatible across multiple development methods used throughout this experiment. Chapters 4 and 5 outline XFM experiments which were conducted using silicon nitride slides (Melbourne Centre for Nanofabrication, Australia) and mylar film (Sietronics Pty Ltd, Australia). These surfaces are best suited for the instrument set up as they are made of light elements which do not interfere with the X-ray spectrum collected and are relatively thin which reduces scatter, larger

scan areas were imaged on mylar film as the size of the silicon nitride window is limited. Chapter 6 involves ATR-IRM experiments with fingermarks deposited directly onto the Ge crystal (Bruker Optik GmbH, Ettlingen, Germany), Ge was selected to allow the highest possible spatial resolution from the ATR set up, variation in this surface is likely to demonstrate alternate performance in droplet behaviour due to surface topography, however consideration was taken on the impact of the surface selection on resolution for fundamental experiments.

2.6 Instrumentation

2.6.1 X-ray Fluorescence Microscopy

Elemental mapping of fingerprint residue was conducted on the XFM beamline at the ANSTO Australian Synchrotron. The instrumental setup follows the method published by Summers et al,²⁶⁹ which is routinely used at this beamline.^{247, 251} A Kirkpatrick–Baez mirror microprobe with a monochromatic incident beam of energy 15.8 keV is focused to a $\sim 1 \mu\text{m}$ spot on the sample ($1 \mu\text{m}$ at $1\text{-}\sigma$, $2 \mu\text{m}$ at $2\text{-}\sigma$). X-ray emissions were collected using the low-latency, 384 channel Maia detector in event mode to improve data acquisition times. The sample was oriented normal to the incident beam and with the detector positioned in backscatter geometry to allow for improved sensitivity. The sample was raster scanned through the beam, imaging parameters are specified below. Calibration of the data against a standard of known composition, elemental foils (Micromatter, Canada), as well as taking into account the composition and density of the substrate, the air path between the sample and the detector and the approximate composition of the sample provided elemental quantification. For full details of this process please refer to Summers *et al.*²⁶⁹

In the studies described in Chapters 4 and 5, the sample was scanned through the beam with an effective dwell time of either 0.1 ms per effective step size (image pixel size) of $1 \mu\text{m}$, or dwell time 0.7 ms per effective step size (image pixel size) of $2 \mu\text{m}$. A three point moving average was used to increase signal-to-noise ratio and enhance image contrast. For full details of this process, please refer to Summers *et al.*²⁶⁹ The XFM spectra collected is analysed using dynamic analysis, an approach reported by Ryan et al., to resolve the elemental spectral signatures present whilst rejecting

artefacts due to overlapping elements and detector effects.²⁷⁰⁻²⁷² An example of the spectra collected is shown in Figure 2.1, with the counts per channel as a function of X-ray energy shown in green and the fit selected for this data shown in red, with Cl, K, Ca, Ti, Mn, Fe, Co, Ni, Cu, Zn, Br measured at the K- α emission and Ba, Pb and Bi measured at the L- α emission. Data was analysed by extracting elemental maps as TIFF files of per-pixel elemental areal density in ng cm^{-2} and then importing into ImageJ v1.50i.

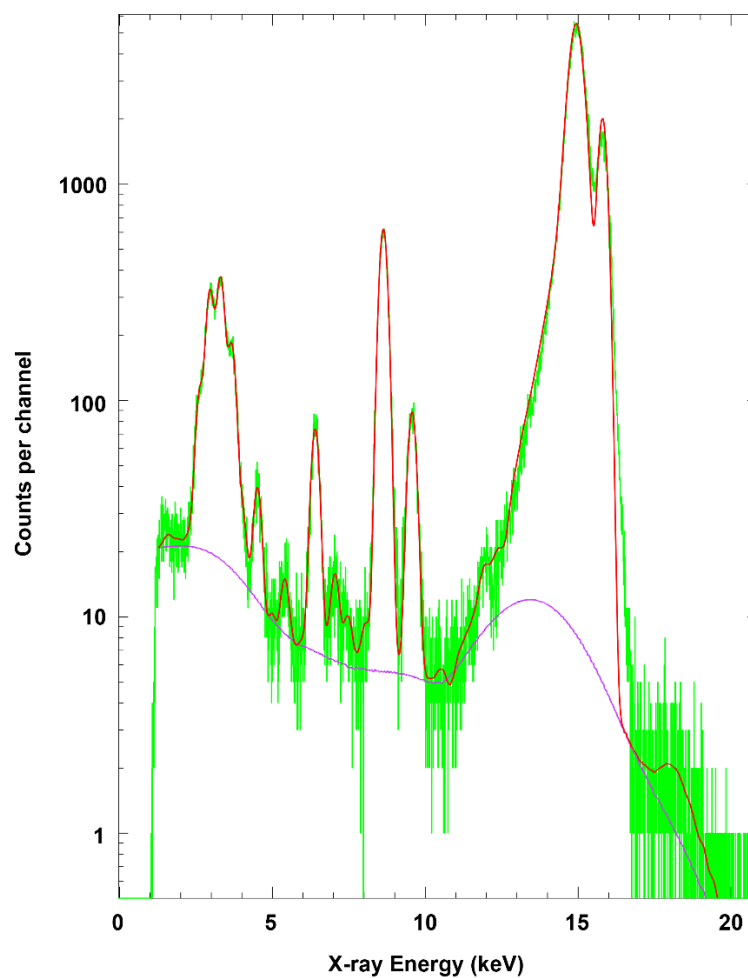


Figure 2.1: Example of the XFM emission spectra collected from a natural fingerprint sample, counts per channel as a function of X-ray energy (green) the X-ray spectrum fit (red) and the estimated background (magenta).

2.6.2 X-ray Absorption Near Edge Structure Imaging

To investigate the chemical form of Fe in latent fingerprints, a “XANES-stack” of X-ray fluorescence elemental maps were recorded using the XFM beamline setup specified in section 2.5.1. 105 incident energies across the Fe K-edge were measured using the following step sizes: 7050 – 7100 (pre-edge region, 5 eV steps), 7100 – 7106 (pre-edge region, 2eV steps), 7106 – 7140 white line, 0.5 eV steps), 7140 – 7160 (post-edge 2eV steps), 7160 – 7200 (post-edge, 5 eV steps) and 7380 – 7400 (post-edge, 5 eV steps). Images were collected starting at the highest energy (7400 eV). This process is similar to those already reported in the literature for Fe, Cu, and Zn.²⁵²⁻²⁵⁵

To investigate the chemical form of Fe in latent fingerprints, a “XANES-stack” of X-ray fluorescence elemental maps were collected as per the method outlined in section 2.5.2. Spectra were calibrated such that the lowest energy maximum in the first-derivative spectrum of elemental Fe occurs at 7112.0 eV. In addition to analysis of micro-XANES spectra from selected regions of interests within the elemental maps, principal component analysis (PCA) was undertaken for the full XANES-stack, using Mantis 2.3.02.

2.6.3 Infrared Spectroscopy

2.6.3.1 Synchrotron Sourced ATR-IRM

Synchrotron ATR-IRM experiments were conducted on the Infrared Microspectroscopy (IRM) beamline at the ANSTO – Australian Synchrotron (Clayton, Victoria). The FTIR instrument on the IRM beamline consists of a Bruker Hyperion3000 microscope coupled to a Bruker Vertex V80v FTIR spectrometer, with a liquid nitrogen cooled narrow-band mercury cadmium telluride (MCT) detector (Bruker Optik GmbH, Ettlingen, Germany). The MCT detector could be maintained at liquid nitrogen cooled temperatures for a period of 12 – 14 hours, after which re-cooling is required. In some occasions, changes to optical alignment and signal amplitudes may occur after re-cooling the detector due to the nature of the highly collimated synchrotron-IR beam that makes it sensitive to the vibration of detecting

element inside the MCT detector during the change of the dewar temperature, this limits time-course studies to a maximum of 13 hours to avoid the potential fluctuation of the synchrotron signals after 13 hours. The ATR-FTIR accessory was equipped with a germanium (Ge) hemispherical crystal ($n_{\text{Ge}} = 4.0$), which has a 1 mm diameter active sensing area. Spectral maps were acquired using a 20 \times objective (NA = 0.60; Bruker Optik GmbH, Ettlingen, Germany), with an effective spot size of 1.88 μm on the sample surface and a step interval of 1 μm between the measurement points. It was previously determined that this optical configuration yielded a spatial resolution of $\sim 2.95 \mu\text{m}$, for chemical images constructed using absorbance intensities at $\sim 2925 \text{ cm}^{-1}$ located close to the $\nu(\text{C-H})$ bands ($2800\text{-}3000 \text{ cm}^{-1}$) and the $\nu(\text{O-H})$ stretching band ($3000\text{-}3500 \text{ cm}^{-1}$) used in this study.¹⁸⁴ A background spectrum of the clean Ge-ATR crystal was measured using 256 co-added scans and 8 cm^{-1} spectral resolution. Each sample spectrum was recorded using 4 co-added scans and 8 cm^{-1} spectral resolution. The experiment was performed under ambient room conditions without nitrogen purge and with opened purge box, to ensure a natural evaporation of water in the fingermarks throughout the measurement. All the raw FTIR spectra were ATR and atmospheric compensation corrected and analysed using Bruker OPUS v8.0 and CytoSpec 2.00.03 software (CytoSpec Inc., Boston, MA, USA). Images were further processed with ImageJ 1.50i software.

2.6.3.2 Terahertz Far-Infrared Spectroscopy

Far-infrared experiments described in Chapter 6 used a furnace to heat a 300 mm long Qz tube with a 20 mm inner diameter coupled to 10 L glass gas-cell via the gas-manifold located on a mobile gas-handling vacuum (MGHV) system. The optical configuration of the spectrometer consisted of a 12.5 mm aperture, a 6 μm multilayer Mylar beam splitter, and a 4.2 K Si bolometer from Infrared Laboratories equipped with a PE window and a 13 μm thick stretched PE film cold filter ($< 800 \text{ cm}^{-1}$). The spectra were recorded at 0.01 cm^{-1} spectral resolution, at a scanner speed of 2.5316 cm/s (40 kHz), and the pre-amplifier gain on the Si bolometer was set to 200. Sets of 10 scans were accumulated yielding a signal-to-noise (S/N) ratio of approximately 194.

The gas-cell is made of borosilicate glass, and with variable path-length gold-coated optics, M35V, from Infrared Analysis; the cell has a nominal single path-length of 625 mm, and the number of times the light can be bounced off its mirrors can be varied from 4 up to 56 times in multiples of 4, yielding an optical path-length from 2.5 m to 35 m. For this spectral region, the gas-cell was equipped with PE wedged windows, and the path-length set to 2.5 m. The gas-cell was placed on the sample compartment of a Bruker IFS125/HR FT spectrometer. The quartz tube was heated to 70 (+/-0.5)°C using the furnace while the gas cell was heated to 70 (+/-5)°C using heating tapes.

The complete system consisting of the furnace, MGHV system and gas-cell was first evacuated to its base pressure ($< 1 \times 10^{-3}$ mbar). Prior to inserting a sample, the furnace was isolated from the vacuum and was brought up to atmospheric pressure and purged with dry N₂(g) from the pressurised boil-off of the N₂(ℓ) tanks. The flow of the purged N₂(g) was halted during sample insertion to prevent any H₂O in the fingermarks from being sublimed; then, the furnace was sealed and isolated after sample insertion while the sample line was evacuated to base-pressure. After the system (excluding the furnace) was brought back to base pressure, a measured amount (~ 5 mbar) of the warm gas mixture consisting of H₂O(g) mainly from the rod, fingerprints and the purged N₂(g) was allowed to flow from the furnace into the gas cell for analysis.

All raw FTIR spectra were measured and analysed using Bruker OPUS v8.0. A background spectrum was first recorded, and was used to calculate the absorbance spectrum of each sample. For the background spectra, a cleaned glass rod was inserted in the quartz tube, and the warm gas mixture consisting mainly of H₂O(g) from the rod and the dry N₂(g) was allowed to flow from the furnace into the gas cell for analysis the gas-cell was filled with 5.01 mbar of N₂(g).

The absorbance spectrum of each sample was first normalised to the pressure when the background spectrum was recorded (5.01 mbar) before the background absorbance was subtracted from the sample absorbance to yield the true absorbance of H₂O coming from the fingerprint samples only (sample = H₂O droplets and fingerprints).

2.6.3.3 Benchtop FTIR Microspectroscopy with Thermal IR Source

Multimodal studies in Chapter 4 included the use of the offline FTIR microscope available at the IRM beamline at the ANSTO Australian Synchrotron. The procedure follows the method outlined by Dorakumbura *et al.* to image fingermark samples in transmission mode using a Bruker Hyperion 3000 FTIR microscope with a liquid nitrogen cooled 64×64 Focal Plane Array (FPA) detector and a matching $15\times$ objective and condenser (NA = 0.40), coupled to a Bruker Vertex 70 FTIR spectrometer with an internal Global™ IR source (Bruker Optik, Ettlingen, Germany).⁹⁵ The sample chamber was purged with dry nitrogen prior to scanning to reduce spectral contribution of atmospheric water vapour and CO₂. FPA-FTIR images were acquired within a $4000 - 800 \text{ cm}^{-1}$ spectral region. The FPA consists of a 64×64 pixel array, where the physical pixel size is $40 \text{ }\mu\text{m}$. At $15 \times$ magnification the effective pixel size is $2.67\mu\text{m}$. In this study, the FPA data were collected with 2×2 pixel binning of the 64×64 pixel array to yield a final pixel size of $5.3 \text{ }\mu\text{m}$ per spectrum. For each FTIR image, high-quality FTIR spectral images were collected at 8 cm^{-1} resolution, with 32 coadded scans, Blackman-Harris 3-Term apodization, Power-Spectrum phase correction, and a zero-filling factor of 2 using OPUS 7.2 imaging software (Bruker). Background measurements were taken prior to sample spectral images by focusing on a clean surface area of the substrate without the fingermark. All spectra were analysed using OPUS v8.0 software and CytoSpec 2.00.03 software. Images were further processed with ImageJ 1.50i software.

2.6.4 Optical Microscopy

Optical images were collected using an optical stereomicroscope (Leica MZ7.5, Leica Microsystems Pty Ltd, NSW, Australia) at the IRM beamline at the ANSTO Australian Synchrotron.

2.7 Fingermark Development

In chapter 3, fingermark samples were taken from a number of donors to explore their donor chemistry using a range of development procedures. The following section outlines the details of each development procedure including reagent

information, solution preparation and development methodology. After a minimum of 24 hours split fingerprint samples were separated and treated with one of the following development methods.

2.7.1 1,2 – Indanedione

1,2-Indanedione is a chemical treatment commonly used to develop fingerprints on porous surfaces such as paper. The method used in this study is adapted from the National Centre for Forensic Studies (NCFS), with the use of petroleum spirits used as the carrier solvent due to chemical availability.¹¹⁸

Reagents and equipment: Reagents were sourced from the following suppliers: 1,2-indanedione (Reddy Chemtech); ethyl acetate (UNIVAR APS); glacial acetic acid (Ajax Finechem); absolute ethanol and anhydrous zinc chloride (Sigma Aldrich); and carrier solvent petroleum spirits bp 40-60 (VWR Chemicals). Reagents were used as received and of analytical grade unless otherwise stated.

Solution preparation: The stock solutions were prepared by dissolving indanedione (2.3 g) in ethyl acetate (480 mL) and adding acetic acid (20 mL). The zinc chloride stock solution was prepared by dissolving zinc chloride (8 g) in ethanol (200 mL). The working solution (IND-Zn) combines the indanedione stock solution (130 mL) with the carrier solvent, petroleum spirits (870 mL) and adding the zinc chloride (4mL) stock solution.

Sample development: The samples were developed by submerging in the working solution (~200 mL) in a glass tray for 5 – 10 seconds, the sample was then air dried and stored in an envelope in a laboratory cupboard to age overnight. Samples were not treated in a heat press to accelerate development in this study, as per the method suggested by NCFS, due to the nature of the substrate; this paper can be damaged when applying heat and adequate development is shown after leaving the fingerprints to age overnight in an enclosed space.

2.7.2 Powdering

Samples on non-porous surfaces were treated using magnetic black powder. This powder was selected due to availability, ease of use and cleanliness in the laboratory space. Samples were treated as per training by the Western Australian Police Force.

Reagents and equipment: Magnetic black powder was sourced from (Criminal Research Products, Southport NC) and dusted using a magnetic brush (Sirchie, Youngsville NC).

Sample development: Fingermarks were treated with black magnetic powder by picking up the powder with a magnetic brush and swirling the powder in a circular motion across the fingerprint sample. Excess powder was removed from the sample by tapping the edge of the glass side against the lab bench.

2.7.3 Cyanoacrylate Fuming

Cyanoacrylate fuming was conducted with a custom built chamber, which was not temperature or humidity controlled. The available laboratory conditions have demonstrated appropriate development on non-porous surfaces following the procedure outlined below.²⁷³

Reagents and equipment: Loctite 401 (60 % w/w ethyl-2-cyanoacrylate; Bunnings Warehouse) was used as superglue and the chamber was built from a sealed terrarium glass container (Ikea Socker Greenhouse, 35cm x 45 cm x 22 cm).

Sample development: The sample was placed inside the terrarium. A small piece of aluminium foil (Capri Heavy Duty Catering Foil, China) was folded to contain the superglue (~1.5g) which was placed in the centre of the samples and the chamber was sealed with tape for 2 hours for fuming. Following development the chamber was opened and the samples removed and placed inside a laboratory cupboard to cure overnight.

2.7.4 Acid Nile Blue

Acid Nile blue was used as a post cyanoacrylate treatment to provide improved contrast against the surface by producing a fluorescent fingerprint. The procedure was developed in house as per the procedure below.

Reagents and equipment: Reagents were sourced from the following suppliers: Nile Blue A (Sigma-Aldrich, USA) and sulfuric acid (Ajax Finechem). Reagents were used as received and of analytical grade unless otherwise stated.

Solution preparation: The acid Nile blue working solution was prepared following the method developed by Crocker.¹⁴⁸ Nile Blue A (0.005 g, 6.8 μmol) was dissolved in sulfuric acid (100 mL, 0.3 M) and heated to 95 °C for 1 hour with constant stirring. The solution was cooled to room temperature and stored in an aluminium wrapped Schott bottle in a laboratory cupboard to avoid photo degradation.

Sample development: At least 24 hours after superglue fuming fingerprints were treated using acid Nile blue. The samples were developed by submersing in the working solution (100 mL) in a glass tray for 20 minutes with intermittent swirling of the solution across the samples. The samples were rinsed with deionised water, air dried, photographed and stored in a laboratory cupboard to avoid light exposure.

2.7.5 Single Metal Deposition II

SMD II was used to treat fingerprints on porous surfaces, the method was initially reported by Bécue and Moret and has been adapted for an Australian context by Newland *et al.*^{109, 165}

Reagents and equipment: Reagents were sourced from the following suppliers: citric acid monohydrate; hydroxylamine hydrochloride; L-aspartic acid; gold (III) chloride trihydrate; trisodium citrate dihydrate; Tween 20; and sodium hydroxide (Sigma-Aldrich, USA); Reagents were used as received and of analytical grade unless otherwise stated.

Solution Preparation: SMD II development requires two solution baths, the first involves a gold nanoparticle colloidal solution and the second a solution of gold salts

dissolved in deionised water. Both solutions were prepared using the stock solutions described in Table 2.2.

Table 2.2: *SMD II stock solution preparation*

Stock Solution	Preparation
A	Tetrachloroauric acid trihydrate (0.5 g) dissolved in deionised water (5 mL)
B	Trisodium citrate dihydrate (1.70 g) dissolved in deionised water (85 mL)
C	Sodium hydroxide (0.120 g) and L-aspartic acid (0.380 g) dissolved in deionised water (25 mL)
D	Citric acid monohydrate (31.5 g) dissolved in deionised water (150 mL)
E	Hydroxylamine hydrochloride (1.0 g) dissolved in deionised water (50 mL)

The SMD II gold nanoparticle solution was prepared by adding solution A (1 mL) to deionised (DI) water (460 mL) and heating to boiling point under constant stirring. Solution B (42 mL) and solution C (420 µL) were combined and quickly added to the boiling solution. The solution was heated under constant stirring until a colour change was observed to produce a deep red coloured solution. The solution was cooled, diluted with deionised water to a final volume (2.5 L) and the surfactant, Tween 20 (2.5 mL) was added under stirring. The solution was stored at 4 °C in a polypropylene container in a refrigerator.

The gold salt solution is prepared immediately prior to use in the development procedure by combining solution A (200 µL) and solution E (200 µL) and adding to deionised water (200 mL).

Sample development: The SMD II gold nanoparticle stock solution (300 mL) was removed from the refrigerator and left to warm to room temperature. To lower the pH of the gold nanoparticle solution, Solution D (9 mL) was added. Prior to development, fingerprint samples were rinsed by submerging in deionised water for 3-5 minutes. The samples were then transferred to the gold nanoparticle solution bath and submersed for 20 minutes under constant orbital shaking on a PathTech Basic Orbital Mixer set at approximately 50 RPM. The samples were rinsed in

deionised water for 3-5 minutes and then transferred to a second glass dish, containing a freshly prepared gold salt solution. Again the samples were submersed for 20 minutes under constant orbital shaking at approximately 50 RPM. Finally, the samples were rinsed in deionised water again for 3-5 minutes before being left to dry on paper towels at room temperature.

2.8 Photography of Developed Fingermarks

Developed fingermark samples were digitally recorded using a Nikon D300 camera on manual exposure mode fitted with a 60 mm lens and mounted at 35 cm above the sample using a Firenze Mini Repro stand. Photographs were taken under optimised conditions for each development method to best visualise each set of fingermarks, these details are outlined in Table 2.3. Samples requiring illumination utilised dual incandescent light globes mounted on either side of the camera or a Rofin Polilight© PL500 (Rofin, Australia) set to the specified light wavelength.

Table 2.3: *Camera settings optimised to each detection method*

Detection Treatment	Lighting	Camera Filter	Shutter Speed	Aperture	ISO
1,2-Indanedione	505 nm light	550 nm	2 sec	f/11	200
Powdering	2 incandescent globes	None	1/15 sec	f/11	200
Superglue Fuming	4 incandescent globes	None	1/15 sec	f/11	200
Acid Nile Blue	505 nm light	550 nm	6 sec	f/11	200
SMD II	2 incandescent globes	None	1/15 sec	f/11	200

Digital images were recorded to a desktop computer using Nikon Camera Control Pro (version 2.31.0) and saved according to the date photographed and sample number. Where required images were enhanced using Adobe Photoshop CC to improve the visibility of fingermark ridge detail. Enhancement details are described in Table 2.4, all enhancement was kept consistent across all samples and each development treatment.

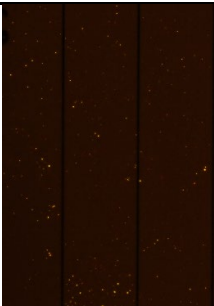
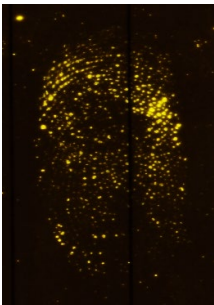
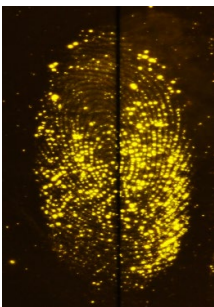

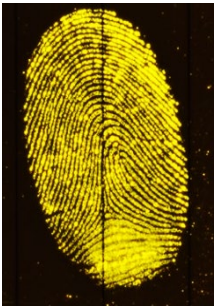
Table 2.4: *Photography enhancement conditions*

Technique	Filter	Brightness	Contrast	Exposure	Gamma Correction
1,2-Indanedione	None	None	None	None	None
Powdering	B&W	20	40	+0.30	0.80
Superglue Fuming	B&W	75	50	None	None
Acid Nile Blue	None	100	50	None	None
SMD II	B&W	30	70	+1.00	0.40

2.9 Fingermark Grading

To assess development performance following photographic enhancement the fingermarks were graded following the system used by Fritz and Frick which is adapted from the United Kingdom Home Office Police Scientific Branch.²⁷⁴⁻²⁷⁵ Outlined in Table 2.5 the grading system assesses the fingermark contrast against the background and quality of ridge detail on a scale of 0-4. The use of a grading system is subjective to human observation and bias, however is appropriate in this study as it is relative to donor performance.

Table 2.5: *Fingermark grading scheme*

Grading	Friction Ridge Detail	Contrast of Ridge Detail	Photographic Example
0	No Development	No Contrast	
1	Signs of contact but less than 1/3 of continuous fingerprint ridge.	Poor Contrast	
2	1/3 to 2/3 of continuous fingerprint ridge.	Moderate Contrast	
3	More than 2/3 of continuous fingerprint ridge but not a "perfect" fingerprint	Good Contrast	
4	Full development; whole fingerprint continuous ridges	Very Good Contrast	

2.10 Statistical Analysis

In chapter 5 Graphpad Prism v9.2.0 was utilised for data visualisation and statistical analysis. Average elemental areal density for each fingerprint donor is presented as scatter plots. Statistical testing was used to identify differences in elemental profile between the median group intensities using a non-parametric Wilcoxon matched pairs test for all donors ($n = 7$). This type of test was selected to consider the unique elemental profile of each donor, accounting only for the change in profile due to the transfer from contact with metal surfaces. Significance was defined at the 95 % confidence limit ($p < 0.05$).

2.11 Human Ethics Approval

This research involved the collection of samples from human participants, which required low risk ethics approval by the Curtin University Human Research Ethics Committee. Ethics approval (HRE2018-0476) was granted on the 20th of July 2018. Requirements of this approval include the participants access to an information sheet, which outlines the purpose of the study, participant rights and contact information if the participant wishes to enquire further or withdraw their involvement. If willing to volunteer the participant will provide formal consent by signing the provided consent form. An example of the information sheet and consent form can be seen in the Appendix. By abiding by the conditions provided by the ethics committee the privacy and safety of the donors involved is ensured.

Chapter 3

Exploring Donor Fingerprint Chemistry



3.1 Introduction

Despite a multitude of current operational detection techniques a significant number of fingermarks remain undetected, as recently demonstrated by Chadwick *et al.*² The reasons for this are multidimensional, due in large part to the complex chemistry of fingermark residue. The influence of the donor, substrate and surrounding environment each impact the resulting residue, making treatment conditions for each sample highly variable.⁸⁰ It is therefore important when conducting fingermark research to take into account how these factors can influence the study.

The IFRG Guidelines suggest procedures to consider when conducting fingermark research to limit the effects of external factors on the experiment.²⁷⁶ Whilst substrate surfaces and environmental conditions such as light exposure, temperature and humidity can be controlled, donor variation is inevitable. Differences in chemical composition between donors as well as between multiple depositions from the same donor have been highlighted in a number of studies as mentioned in section 1.2. Girod *et al.* and Frick *et al.* both utilised GC-MS to demonstrate the differences in the bulk chemistry of fingermark residue, identifying a range of different compounds as well as variations in the ratio of commonly occurring compounds.^{14, 92} Girod *et al.* went a step further and grouped 25 donors based on their chemical composition into “poor” and “rich” lipid donor groups.⁹² Poor donors were found to contain a lower volume of total lipid material as well as lower volumes of individual classifying compounds. Meanwhile rich donors had a more diverse range of lipid compounds and increased volumes.

A similar concept has been adapted to classifying fingermarks following development. A number of studies have demonstrated the variation in fingermark development due to differences in donor chemistry.^{93, 277} In theory using a maximum number of donors can provide a more realistic view of the general population, however in experimental scenarios there are limitations on the size of a donor pool.⁹⁰ To overcome the constraints on donor numbers, Sears *et al.* recommend that testing be conducted prior to the main study to assess the development traits of the donor pool.⁸⁰ A larger range of potential donors should be evaluated to find those who

provide varying development levels. By including a number of “good”, “medium” and “poor” donors there is an expectation that there will be a reasonable representation of the range of fingerprint chemistry encountered in the general population.

This chapter involves a preliminary assessment of the fingerprint donor pool who were selected for chemical imaging studies in the subsequent experimental chapters. Classifying the donor pool based on their development performance from a number of visualisation techniques ensures that subsequent work will include a range of donors representative of the expected chemical variation of fingerprint residue. A number of fingerprint treatments (summarised in Table 3.1) were selected to target a range of components in fingerprint residue to thoroughly explore the chemistry of the donor pool. These reagents were chosen based on their frequency of use operationally, ease of use and access to appropriate reagents and facilities. Considerations were made to ensure the use of both lipid and eccrine sensitive reagents to allow for comparison in donor chemistry as well as treatment methods which would physically target a combination of the material deposited on the surface. Surface compatibility was also considered to ensure both porous and non-porous substrates were explored.

Table 3.1: *Summary of fingerprint development treatments used in this study*

Detection Treatment	Residue Target	Surface
1,2-Indanedione/zinc chloride	Amino Acids	Porous
Powdering	Physical Adhesion	Non-Porous
Superglue Fuming	Basic (eccrine) material	Non-Porous
Acid Nile Blue	Lipids	Porous/Non-Porous
Single Metal Deposition II	Combination of material*	Porous/Non-Porous

* Development mechanism research ongoing

1,2-indanedione/zinc chloride was selected for its sensitivity to a number of amino acid compounds in fingerprint residue which react to produce a bright pink fluorescent fingerprint.^{120, 131-132} Amino acids are typically abundant in eccrine material, making this reagent suitable to target eccrine rich deposits on porous surfaces. Globally the optimal conditions for 1,2-indanedione have been debated due

to the influence of the working environment (temperature, humidity), however within an Australian context this technique has demonstrated superior development and is used successfully to develop fingerprints, commonly on paper surfaces.^{121-122, 124}

Powdering and cyanoacrylate (superglue) fuming were selected as they are commonly used operational methods.^{35, 118} Fingerprint powdering occurs through a physical adhesion between the powder and the fingerprint residue, where the particles are preferentially deposited on the mark through a combination of adhesion to grease in the residue as well as electrostatic charge and surface chemistry of the powder.⁴⁸ This method allows the detection of the bulk fingerprint residue, meaning it is sensitive to a wider range of donor material regardless of their fingerprint chemistry.

Often fingerprints are treated by superglue fuming, to visualise the mark and to increase the stability of the residue for further treatment. The process is used operationally due to its simplicity and capability to simultaneously develop a large number of items.^{35, 118} The development mechanism is base initiated, with weak bases present in eccrine sweat capable of initiating cyanoacrylate polymerisation.^{35, 150-151} Increased levels of humidity can improve the performance of superglue fuming, with temperature and humidity controlled chambers often used operationally.^{47, 112, 150}

An advantage of the superglue fuming method is not only to develop the fingerprint, but to allow for sequential treatment with post-treatment stains. In this study superglue fuming was followed by the lipid sensitive treatment acid Nile blue to produce a fluorescent fingerprint.¹⁴⁸ The advantages of selecting this treatment were two-fold, to improve the contrast of the fingerprint as well as targeting the lipid components of the residue. Acid Nile blue is a method adapted from aqueous Nile blue to improve the sensitivity of the method, by increasing the yield of Nile red, the fluorescent product.¹⁴⁷ The treatment though yet to be used operationally has demonstrated promising results, often used directly on porous substrates however, when used as a post treatment stain acid Nile blue is capable of providing improved contrast on non-porous surfaces.²⁷³

Finally single metal deposition (SMD) II was selected as an emerging method currently being studied at Curtin University.^{86, 109, 165} The method uses a two step procedure which involves the deposition of gold nanoparticles in a solution bath followed by the *in-situ* reduction of gold in a reinforcement bath to improve fingerprint contrast.^{165, 167} The treatment is based on previous metal deposition methods such as physical developer and multi-metal deposition.¹³⁹ Despite ongoing research into the treatment mechanism there is still some debate over the chemical target within a fingerprint. This treatment thus provides an opportunity to look at fingerprint residue with an emerging development method and explore its behaviour across a number of donors with differing fingerprint chemistry.^{109, 165}

By combining the results of the development using these selected visualisation techniques a broad understanding of the chemistry of the donor pool is gained. The aim is to ensure a donor pool with the appropriate representation of the general population as per recommendations by Sears *et al.* will be used in subsequent chemical imaging studies throughout this thesis.⁸⁰

3.2 Methodology

3.2.1 Fingerprint Deposition

Two sets of split fingerprints were collected from 13 donors, split fingerprints (samples which can be split in half) were used in this study to limit intradonor variation. Donors were first instructed to rub their hands together to try and evenly distribute exogenous material across both hands. Fingerprints from the three middle fingers of the left hand were placed over the centre of two glass microscope slides (VWR International, Leuven) and fingerprints from the three middle fingers of the right hand were placed over the centre of a dotted line on sectioned water-proof paper (Nu World Stone, China), see diagram in Figure 3.1. One set of natural, uncharged fingerprints were collected following ordinary activity, ensuring the donor had not washed their hands, eaten or been in contact with chemicals for 30 minutes prior. Directly after the collection of uncharged marks, one set of charged fingerprints were collected, referring to fingerprints groomed for increased lipid content. Donors were asked to rub their face/head/neck with their hands prior to

rubbing their hands together and depositing fingermarks. The fingermarks were collected by placing the middle three fingers on the substrate for approximately 5 seconds. In this study pressure was not monitored, however donors were instructed about the deposition process and asked to use a light pressure when placing their fingers on the substrate. Fingermarks were stored in an enclosed box on an office shelf with limited airflow and light exposure for a minimum of 24 hours before development.

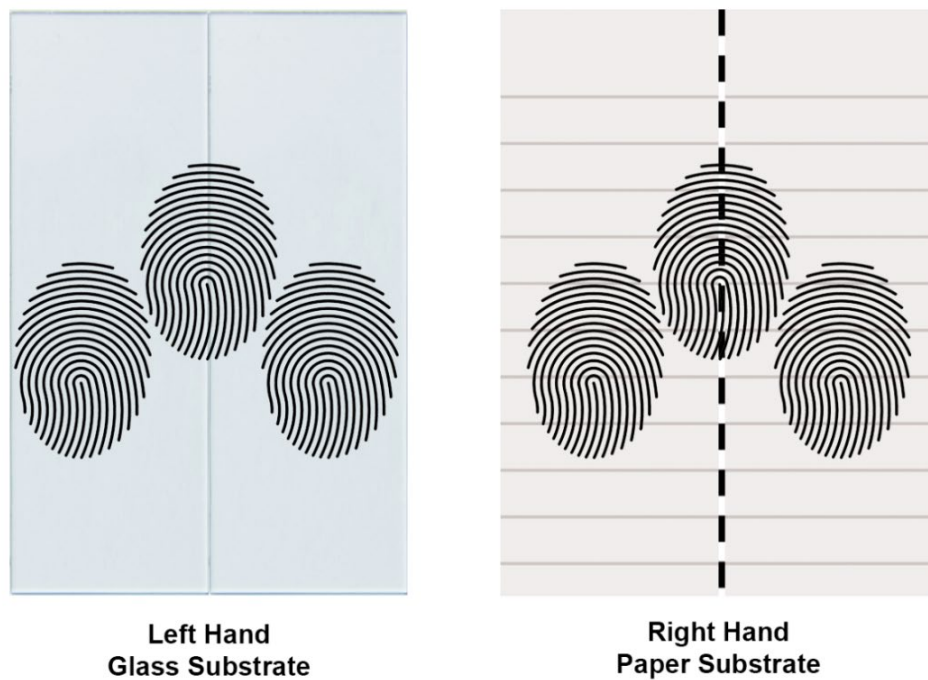


Figure 3.1: *Diagram showing set up for deposition substrates.*

3.2.2 Donor Information

13 donors were available to take part in this study, donor information can be seen in Table 3.2. After a minimum of 24 hours the fingerprint samples were split and each treated with one of the selected development methods outlined in Table 3.1. Full descriptions of development procedures are summarised in section 2.6.

Table 3.2: *Details of the donors used in this study*

Donor No.	Age	Biological Gender	Cosmetic Use
1	77	Male	None Reported
3	22	Male	None Reported
4	24	Male	None Reported
6	23	Female	Yes
12	23	Female	Yes
13	23	Female	Yes
14	36	Male	None Reported
15	23	Male	Yes
16	23	Female	Yes
17	50	Male	None Reported
18	32	Male	None Reported
19	34	Female	Yes
20	23	Female	Yes

3.3 Results & Discussion

In this study a range of fingerprint development methods were utilised to explore the behaviour of the selected donor pool. The donors provided a set of uncharged and charged split fingerprints which were developed using superglue fuming followed by acid Nile blue, magnetic black powder, SMD II and 1,2-indanedione/zinc chloride. The results presented here summarise the findings with an overview of the fingerprint grading as per the system used by Fritz and Frick, adapted from the scheme used by the UK Home Office Centre for Applied Science and Technology (CAST) described in section 2.8.²⁷⁴⁻²⁷⁵

The IFRG guidelines outline considerations to be made when conducting fingerprint research.²⁷⁶ Whilst the guidelines are aimed at research exploring novel or modified development methods, fundamental studies, such as that presented here, should aim to consider these guidelines where possible. A summary of the experimental considerations for this study can be found in section 2.2. The surfaces selected were optimised to be compatible across the scope of the development methods, with glass slides (VWR International, Leuven) selected as the non-porous surface and water-proof paper made from a calcium carbonate and polyethylene blend (Nu World

Stone, China) selected as the porous surface. Both uncharged and charged fingermarks were utilised in this study to demonstrate the effects of intentionally grooming fingermarks for increased lipid content on these development methods.

3.3.1 Comparison of Development Performance for Charged and Uncharged Fingermarks

Table 3.3 and 3.4 present an overview of the fingermark gradings for each development method for uncharged (Table 3.3) and charged (Table 3.4) fingermarks across the donor set. The variation in grading is notable and suggests at first glance that an appropriate representation of realistic interdonor variation is evident within the donor pool. Donors were classified as good, poor or mid level developers, separately for charged and uncharged samples. Classification was based upon a total sum of their grades across all development methods (Sum of grades: $0 < \text{Poor} \leq 10 < \text{Mid} < 15 \leq \text{Good}$). Comparing the data in Table 3.3 and 3.4 it is clear that there is improved grading of charged fingermarks, with no fingermarks graded 0 for the charged prints, compared to 9 uncharged samples. There is also a rise in the number of donors classified as “good” following the charging of fingermarks, rising from 3 good uncharged donors to 7 good charged donors. Looking at a representative sample (Donor 19) in Figure 3.2, an increase in the development of marks for all 5 detection treatments is shown, suggesting an increase in material present within the sample detectable by each of the treatments. This reinforces the differences in performance when fingermarks are groomed, and supports the recommendation by the IFRG guidelines to utilise uncharged fingermarks as a more realistic sample when possible.

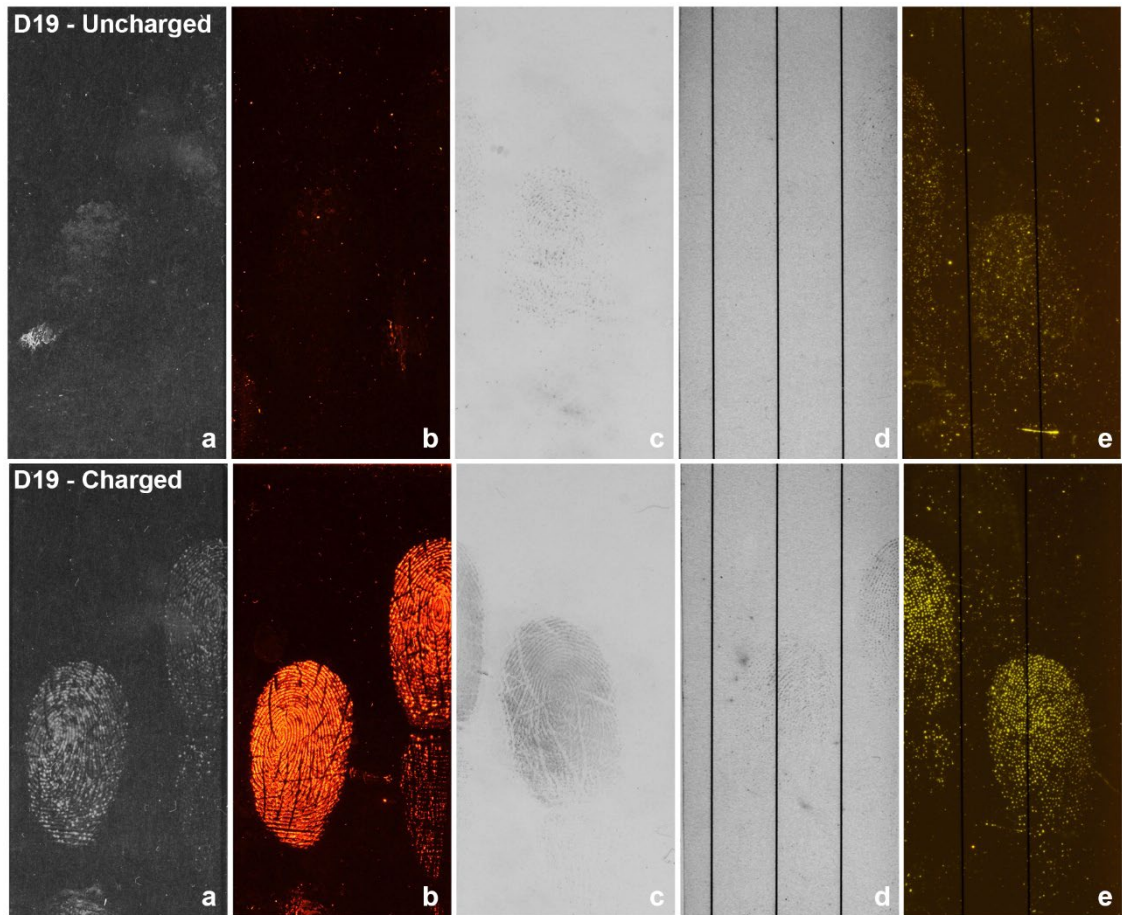


Figure 3.2: Representative donor (donor 19) showing an increase in material from uncharged (top) to charged (bottom) fingerprints developed with superglue fuming (a), post treated with acid Nile blue (b), black powder (c), SMD II (d) and 1,2-indanedione (e).

Table 3.3: Summary of grading for uncharged fingermarks

Donor	Superglue	Nile Blue*	Powdering	SMD II	Indanedione	Class
1	0	0	1	1	3	Poor
3	4	3	3	4	4	Good
4	3	3	4	2	3	Good
6	3	0	4	3	3	Mid
12	2	1	3	4	3	Mid
13	3	3	2	2	4	Mid
14	3	1	3	3	3	Mid
15	3	3	4	3	3	Good
16	0	0	1	1	2	Poor
17	3	3	3	2	3	Mid
18	1	0	1	1	1	Poor
19	0	0	1	0	1	Poor
20	2	2	3	2	3	Mid

Table 3.4: Summary of grading for charged fingermarks

Donor	Superglue	Nile Blue*	Powdering	SMD II	Indanedione	Class
1	2	3	3	2	3	Mid
3	3	3	3	4	4	Good
4	3	4	3	2	3	Good
6	3	4	3	2	3	Good
12	3	3	3	4	4	Good
13	2	3	2	3	3	Mid
14	3	4	4	3	4	Good
15	3	4	3	4	4	Good
16	2	3	2	1	1	Poor
17	2	2	3	1	3	Mid
18	1	4	3	1	1	Poor
19	3	4	3	1	2	Mid
20	4	4	3	2	3	Good

* Nile Blue refers to acid Nile blue which was processed subsequently to superglue fuming

The fingerprint grading data is presented as number of fingerprints per grade in the graph in Figure 3.3 to directly compare the development methods for both charged and uncharged marks. Though this study had not aimed to compare development methods, by looking at these values it can suggest the chemical nature of the fingerprint samples provided. For example, when looking at the performance of acid Nile blue there is a large difference in grading when comparing the charged and uncharged marks, with 7:0 grade 4 marks and 0:5 grade 0 marks for charged and uncharged marks respectively. The increase in grade following the increase of lipid material indicates this method relies on the presence of lipid material to develop a mark. Acid Nile blue is a modified method based on aqueous Nile blue, a method proposed by Frick *et al.* which targets lipid material. It is not unexpected that the method demonstrates similar characteristics, showing improved development for fingerprints groomed for increased lipid material.

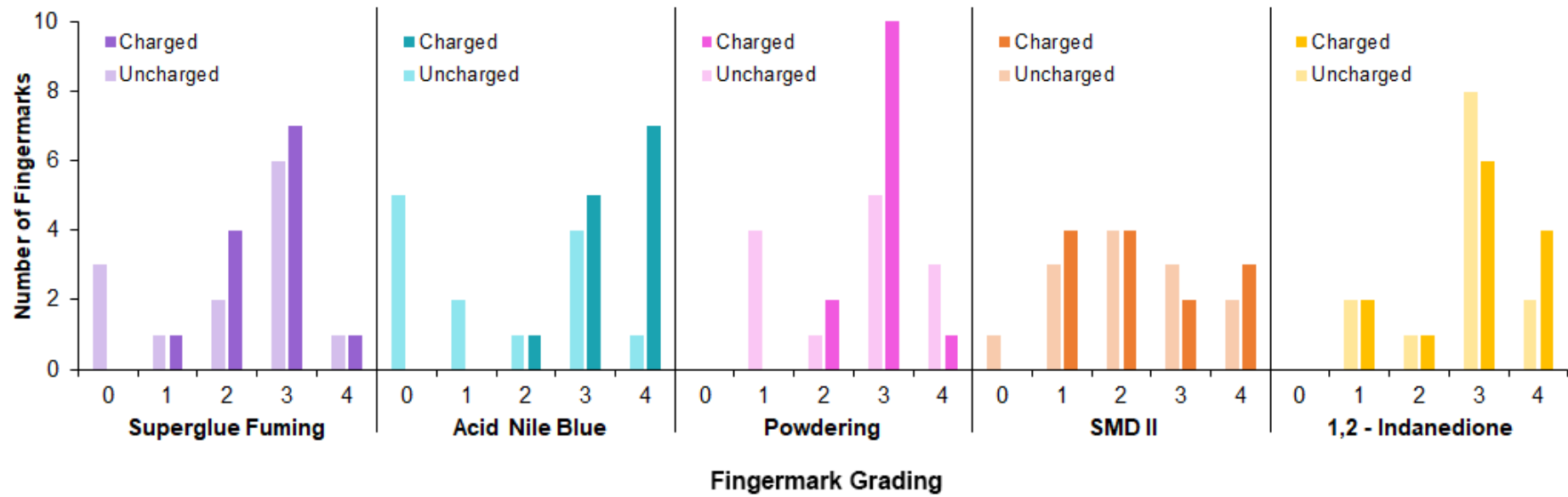


Figure 3.3: Graph displaying the sum of grades for each development method for uncharged and charged fingermarks.

1,2-Indanedione/zinc chloride is the most consistent method across both uncharged and charged samples. This method is a sensitive amino acid reagent, targeting the eccrine component of the fingerprint. Eccrine material would be expected to appear within both charged and uncharged sets of marks as it is present on the fingertips as secretions from the eccrine glands.⁸⁰

3.3.2 Understanding Donor Chemistry and Classifying Donor Performance

It was apparent that a number of donors performed better across all treatments. Comparing donors 3 and 18 in Figure 3.4 and 3.5 there is a clear difference in their overall development. It is expected that the “good donors”, those that appeared to consistently provide high quality development across each treatment, are expected to have richer chemistry, depositing a natural mixture of lipid and eccrine material which can be targeted by each of the development treatments. In contrast, donors, such as that represented by donor 18, can be considered “poor donors”, as it appears they deposit less residue overall. Improvement in these “poor donors” appeared with grooming, with all “poor donor” charged marks showing increased performance with acid Nile blue, however it is important to consider the uncharged natural fingerprint as the realistic sample.

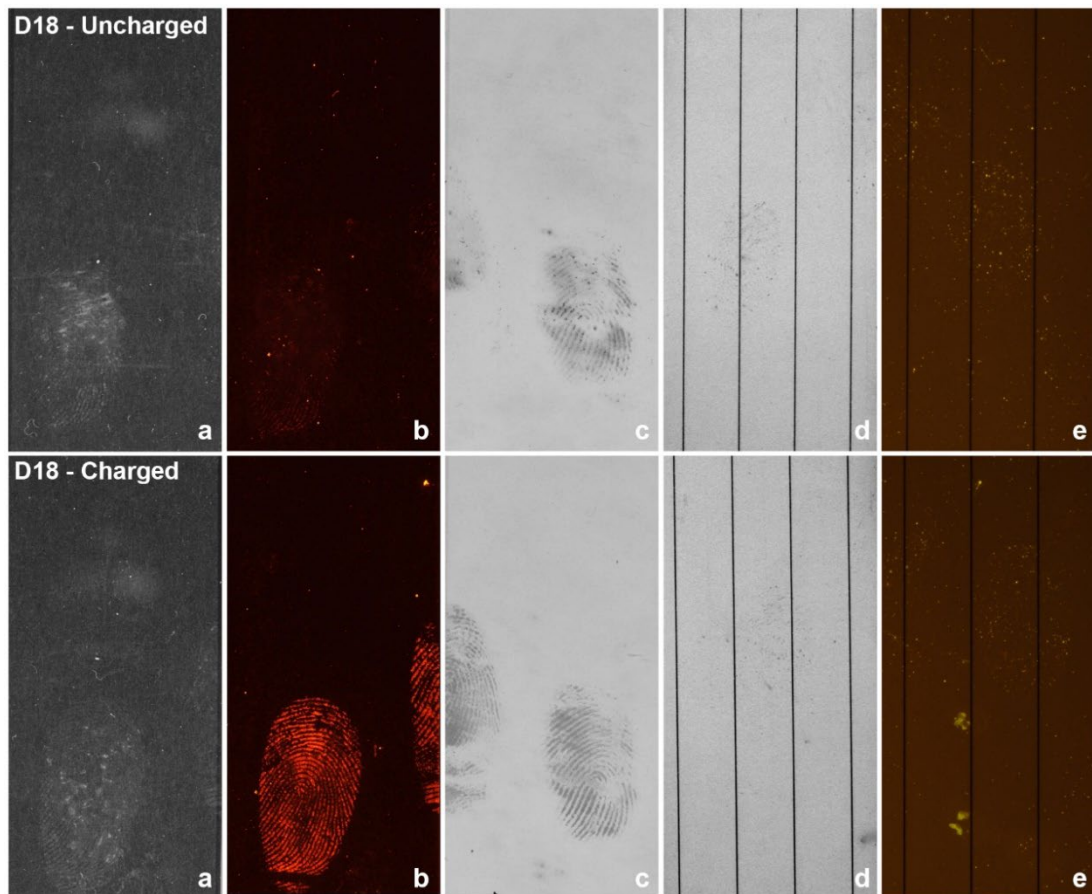


Figure 3.4: Representative “poor” donor (donor 18) uncharged (top) and charged (bottom) fingermarks developed with superglue fuming (a), post treated with acid Nile blue (b), black powder (c), SMD II (d) and 1,2-indanedione (e).

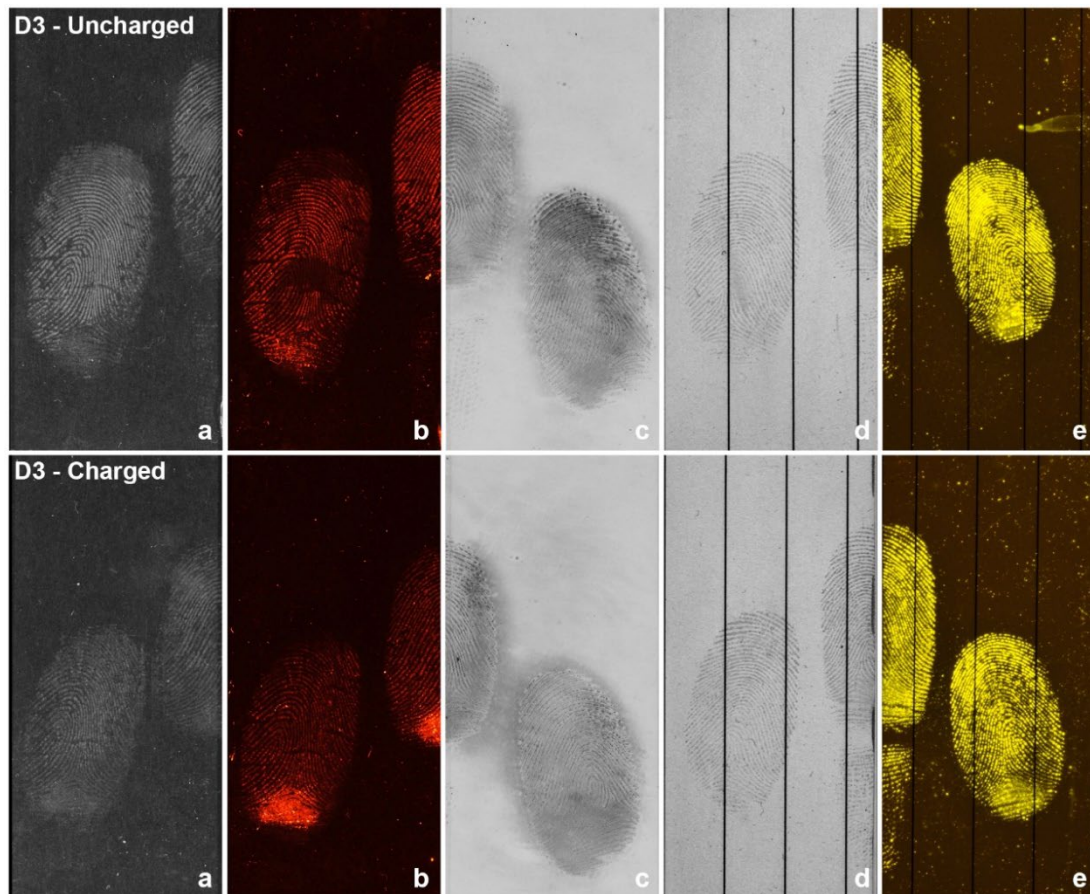


Figure 3.5: Representative “good” donor (donor 3) uncharged (top) and charged (bottom) fingermarks developed with superglue fuming (a), post treated with acid Nile blue (b), black powder (c), SMD II (d) and 1,2-indanedione (e).

A number of donors were graded between these groups of good and poor donors, these samples are interesting to explore the chemistry of the marks. Within this group of samples 1,2-indanedione/zinc chloride provided more consistent development, suggesting that eccrine material appears to be abundant within fingerprint residue across these donors. The lipid material appeared more variable, with Figure 3.6 showing the development of donor 6, one of these mid-performing donors who appeared to provide high quality development with each treatment except for acid Nile blue. This indicates that this donor may naturally deposit eccrine material with a limited amount of lipid material. Comparing the uncharged mark to the charged sample it is obvious the contact with lipid rich areas of the body alter the chemistry of fingerprint residue. The charged mark appears to have a substantial increase in lipid material, providing a developed mark graded 4 compared to the

uncharged mark graded 0 when treated with acid Nile blue. This emphasises how contact with other parts of the body to groom a fingermark with sebaceous material increases the lipid content on the fingers, reinforcing the concept that habitual touching of the face or other parts of the body throughout the day can change the chemistry of the fingermark deposited, leading to intradonor variation.²⁷⁸ This adds to the complexity of fingermark chemistry, suggesting that the lipid material is likely to be more convoluted than the eccrine counterpart.

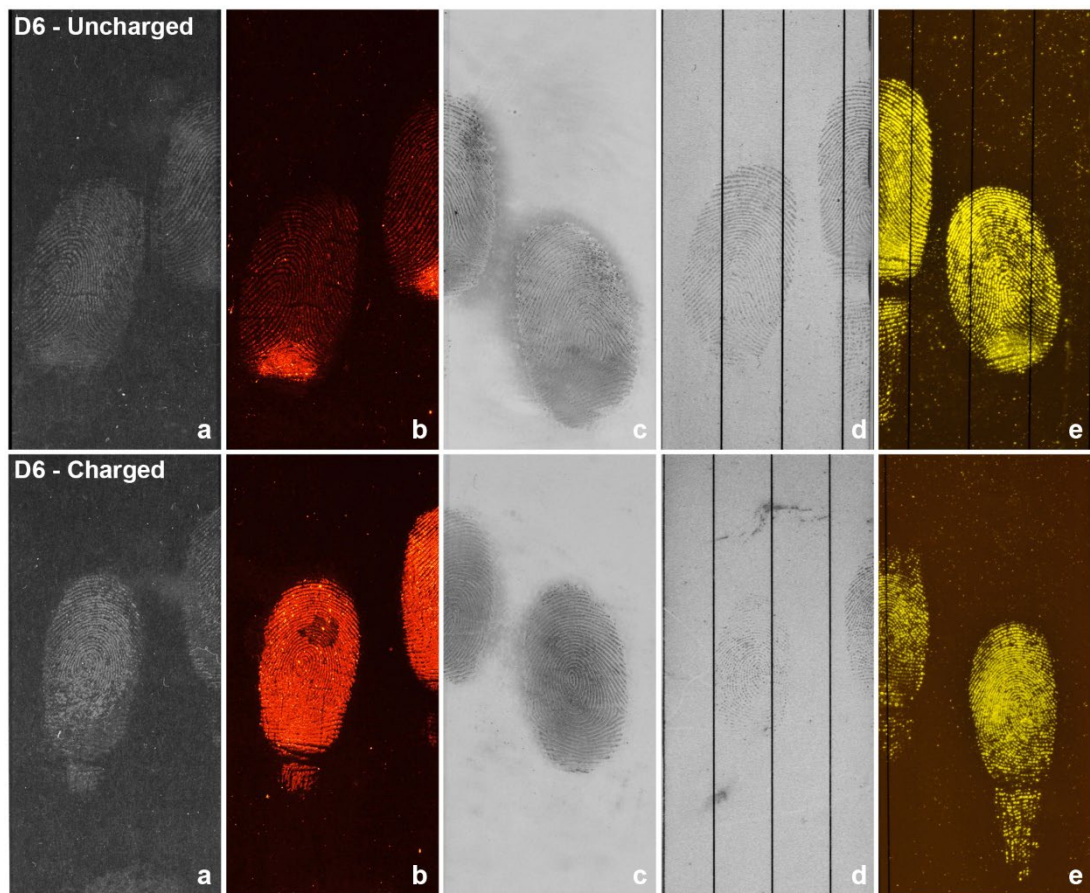


Figure 3.6: Representative “mid” donor (donor 6) uncharged (top) and charged (bottom) fingermarks developed with superglue fuming (a), post treated with acid Nile blue (b), black powder (c), SMD II (d) and 1,2-indanedione (e).

The remaining development methods, superglue fuming, black powder and SMD II didn't provide any additional information about the chemistry of the selected donors. Black powder and superglue fuming appeared to perform similarly, developing marks from most mid-good donors. These methods performed poorly for weaker donors as there was less material to adhere to. SMD II comparably

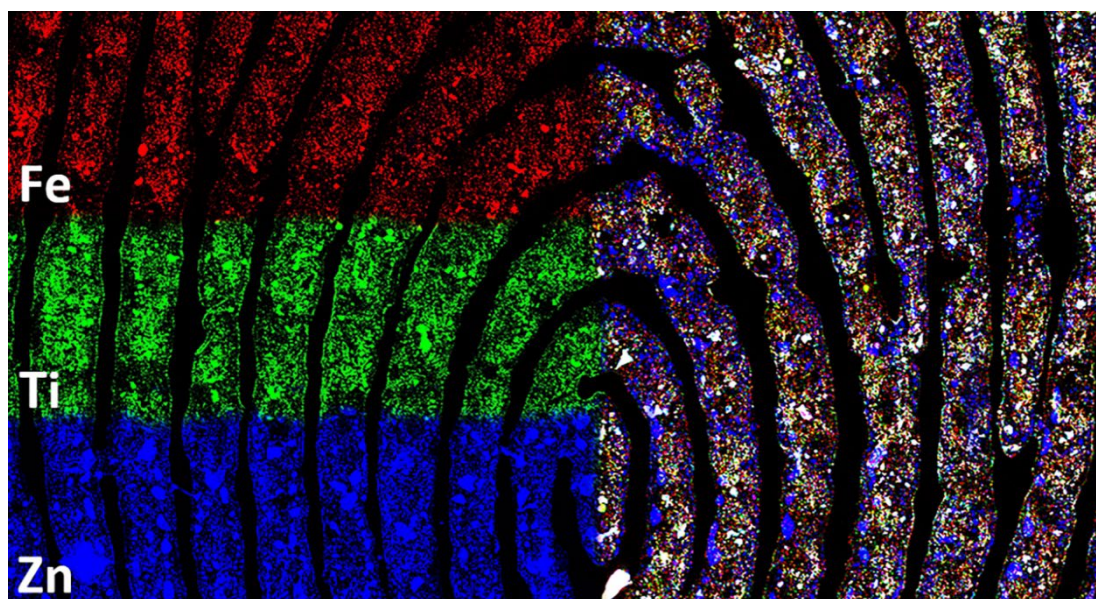
demonstrated inferior performance, with lack of contrast between the substrate appearing to have substantial effect on the grading of the mark. This is a newly developed technique and is still undergoing research to exhibit its potential as a viable method.

3.4 Conclusions

This chapter demonstrates the characteristics of the selected donor pool, showcasing the inherent variability of fingerprint development. The 13 donors selected provide an appropriate range of development performance, believed to be representative of a larger population. Using 5 fingerprint visualisation methods, 1,2-indanedione/zinc chloride, powdering, SMD II and superglue fuming followed by post-treatment staining with acid Nile blue, the fingerprints were graded and compared to classify the donor's performance. An improvement was seen in development following the grooming of fingerprints for increased lipid material, reinforcing that uncharged fingerprints are a more realistic example of fingerprints found as evidence and should be used where possible to provide a more accurate sample of fingerprint residue. The classification of poor, mid and good donor groups within the selected pool provides the necessary grouping to ensure an appropriate sample set for chemical imaging studies presented in the subsequent experimental chapters in this thesis. It was important to ensure the succeeding chapters included a range of donors within each of these classifications, to provide a realistic example of the variation expected within fingerprint residue. This would allow deeper and more authentic conclusions to be made regarding fingerprint chemistry, by encompassing a broad range of the potential chemistries across the population.

Chapter 4

Using Synchrotron XFM to Reveal and Characterise Elemental Distribution in Latent Fingermarks, and to Further Understand Inter-Donor Variation



Portions of this chapter have been published in the following articles:

Rhiannon E. Boseley, Buddhika N. Dorakumbura, Daryl L. Howard, Martin D. de Jonge, Mark J. Tobin, Jitraporn Vongsvivut, Tracey T. M. Ho, Wilhelm van Bronswijk, Mark J. Hackett, and Simon W. Lewis. Revealing the Elemental Distribution within Latent Fingermarks Using Synchrotron Sourced X-ray Fluorescence Microscopy. *Analytical Chemistry* **2019** 91 (16), 10622-10630

DOI: [10.1021/acs.analchem.9b01843](https://doi.org/10.1021/acs.analchem.9b01843)

Rhiannon Boseley, Daryl Howard, Jitraporn Vongsvivut, Mark Hackett, Simon Lewis. Leaving a mark on forensic science: how spectroscopic techniques have revealed new insights in fingerprint chemistry. *Spectroscopy Europe*, **2022** 22

DOI: <https://doi.org/10.1255/sew.2022.a8>

4.1 Introduction

Understanding the chemical composition and distribution of fingerprint residue may help explain the variation in response to latent fingerprint visualisation methods. Such knowledge can then be used to direct research to improve current techniques and identify new detection strategies. The majority of research in the literature describes investigation of organic components of fingerprint residue, leaving the elemental distribution less well understood. The chemistry of latent fingerprint residue heavily impacts the ability to detect and visualise latent fingerprints; by expanding research into the analysis of the inorganic material within fingerprint residues, the gaps in fingerprint chemistry can begin to be filled.²

Fingerprints are a mixture of the natural secretions from the glands present in the skin and any surface contaminants present. The natural secretion is made up of a combination of components originating from the eccrine and sebaceous glands, and while one type of secretion may predominate, there can be no purely eccrine or purely sebaceous deposit.⁹⁵ Eccrine secretions (sweat) contain a variety of hydrophilic organic and inorganic materials such as amino acids, proteins, ions (Cl^- , K^+ , Na^+ , Mg^{2+}) and trace metals (Fe, Cu, Zn), and these components have the potential to be transferred when depositing latent fingerprints.^{15, 25, 178} A better knowledge of elemental distribution within latent fingerprints is important to increase the understanding of the effects ions and transition metals may have on the underlying chemistry of current methods of detection.

For example, the amino acid reagent 1,2-indanedione uses the addition of a low concentration solution of zinc chloride as a Lewis acid catalyst to improve the detection response in conditions of low humidity.¹²³⁻¹²⁴ Spindler et al. suggests that the trace metals present within commercial paper could contribute to this reaction, implying that the zinc content in fingerprint residue could also influence this development.¹²⁴ Researchers have previously exploited the presence of metals in fingerprint residue for detection, using heightened temperatures to accelerate metal corrosion to develop marks on metallic surfaces.^{36-37, 103, 279} Exogenous metals have also been targeted directly on the hands through the use of trace metal detection

tests (TMDT) following the handling of metal items such as firearms.^{73-75, 280} The reactivity of elemental species suggests that they may affect fingermark development, and this reinforces the need to better understand the presence and distribution of these ions within fingermark residue. In addition to understanding the elemental distribution within fingermarks, the distribution of specific elements in relation to organic components of the fingermark is also of specific interest. Indeed, it is the interaction between metal ions and organic molecules that can have pronounced effects on detection methods.^{35, 116, 124} Despite the importance of knowing elemental distribution in relation to the distribution of organic molecules in fingermarks, studies into the topic have been limited.

Several studies have used direct chemical imaging methods, such as MALDI-MSI,^{19, 30, 41, 65, 108} Raman microscopy,^{95, 193} and FTIR microspectroscopy^{67, 101, 185} to investigate spatial distribution of organic constituents, but few studies have investigated the distribution of inorganic constituents in fingermarks,⁴² and prior to this thesis, no study had investigated both organic and inorganic constituents in natural fingermarks under atmospheric conditions. The relative scarcity of literature aiming to understand the elemental distribution likely reflects the previous unavailability of direct elemental mapping techniques.^{38-40, 199-200}

A number of alternative techniques offer elemental mapping capabilities, as outlined in Chapter 1 (Section 1.5.3). Some of these methods, such as LA-ICP-MS, SIMS and XPS are surface sensitive, often require analysis under vacuum conditions and can be destructive to the fingermark, limiting their application for the analysis of fingermark samples.^{38-41, 70, 194, 199-200, 244, 257} LA-ICP-MS and SIMS offer superior detection limits (in the PPM – PPB range) however with respect to spatial resolution, the state-of-the-art LA-ICP-MS can achieve 1 μm , but more routinely is typically limited to 10's of microns^{195, 209, 242-244} While SIMS and XPS can routinely provide high spatial resolution, the measurement is limited to the sample surface (i.e., surface sensitivity on the order of tens of nm's).^{195, 199, 245-246} Therefore, for samples such as fingermarks that are a 3 dimensional structure (e.g., comprised of organic droplets several microns thick), the high surface sensitivity of SIMS and XPS is less suited to detect elements internal to the surface (e.g., within an eccrine droplet).

In contrast to XPS, and SIMS; XFM is capable of analysis at ambient pressure (vacuum not required). Advances in brightness of third generation synchrotron light sources and upgrades in detector technology and electronics now make rapid, direct elemental mapping possible.¹⁷⁰ XFM is therefore, well suited to study elemental distributions in latent fingerprints, owing to its ability to provide quick data collection at micron or sub-micron level spatial resolution, and nM detection limits.^{201, 209, 240} These advances have thrust XFM using synchrotron light sources into a wide-range of scientific areas to map trace elemental content, including material sciences,²⁸¹ life sciences,^{269, 282-283} and cultural heritage studies.²⁸⁴⁻²⁸⁵ Previous research has demonstrated the use of XFM imaging of sebaceous fingerprints to provide critical information on elemental distribution; however, the instrumentation available in that study did not have the sensitivity required to detect trace metals at micron spatial resolution, which is especially important if attempting to study association between inorganic and organic components.⁴² The brightness of synchrotron sourced X-rays typically provides an improvement in spatial resolution and detection limits of at least an order of magnitude compared to non-synchrotron benchtop X-ray fluorescence instruments.²⁸⁶⁻²⁸⁷

In this work, IRM was used in combination with XFM to characterize the location of organic and inorganic constituents in fingerprint residue to better understand the chemical complexity of natural fingerprints and how it may impact methods of fingerprint detection. This chapter consists of three distinct studies. In Study 1, the capabilities of XFM were investigated as a technique for analysing fingerprint residues, imaging for the first time the natural distribution of elemental material at sub-micron resolution. Study 2 reveals the variation of inorganic components in fingerprint residue across a set of donors, with suggestion that the observed variation is a combination of endogenous and exogenous metals transferred to, and distributed within, latent fingerprints. Lastly, Study 3 involves the development of a multi-modal XFM/IRM workflow, which was applied to reveal the association between organic and inorganic components; specifically, endogenous elemental components were located in the eccrine material, while a broader distribution of exogenous metals was observed.

4.2 Methodology

4.2.1 Fingermark Deposition

Fingermarks were collected from fourteen donors; information on each of the donors can be found in Table 4.1. The donors gave natural deposits by gently pressing their index finger down for 5–10 seconds on silicon nitride slides (Melbourne Centre for Nanofabrication, Australia), Ultralene Thin Film (SPEX Sample Prep, USA) and Mylar, Gum (Sietronics, Australia). Fingermarks were imaged using XFM as described in section 2.5.1. Multimodal studies were conducted using benchtop thermal source FTIR microscopy and optical microscopy (instrumental information is outlined in sections 2.5.3.3 and 2.5.4).

Table 4.1: *Details of the donors used in this study*

Donor No.	Age	Biological Gender	Cosmetic Use
1	77	Male	None Reported
3	22	Male	None Reported
6	23	Female	Yes
10	40	Female	Yes
12	23	Female	Yes
13	23	Female	Yes
14	36	Male	None Reported
15	23	Male	Yes
16	23	Female	Yes
17	50	Male	None Reported
18	32	Male	None Reported
19	34	Female	Yes
20	23	Female	Yes
21	32	Female	None Reported

4.3 Results and Discussion

This study used XFM to characterize the elemental distribution within latent fingermarks, at $\sim 2 \mu\text{m}$ spatial resolution, to address specific research questions: what is the spatial distribution of inorganic components within natural fingermarks (4.3.1); how might the elemental content and distribution change between fingermark donors (4.3.2); are exogenous sources of metals and ions readily transferred to fingermarks (e.g., inorganic components of cosmetics) (4.3.2); and which elements co-localise with eccrine or sebaceous material (4.3.3).

4.3.1 XFM Reveals the Inorganic Distribution in Natural Fingermarks

XFM elemental mapping was used to determine the distribution, and variation in the distribution, of inorganic ions and metals in a series of natural fingermarks deposited by fourteen donors. A representative example of XFM elemental maps from a natural fingermark from one donor (donor 6) is presented in Figure 4.1. In general, the elemental distribution across the sample was found to follow the ridge pattern detail of a latent fingermark, as can be seen in Figure 4.1. Numerous ions and metals were detected in the fingermarks, and these are characterized in Table 4.2. Many of the ions and metals that were detected are likely to be endogenous diffusible ions excreted through the eccrine glands as sweat (for example, Cl^- , K^+ , Ca^{2+}). In contrast, several exogenous metals were detected (Bi, Ni, Ti), which most likely originate from exogenous sources such as contact with metal alloys or cosmetics.^{15, 32, 70} Other metals that were detected (Fe, Cu, Zn) may originate from endogenous or exogenous sources. Fe, Cu and Zn are all metals present within the body through dietary intake, they play an important role in cell and brain function, with involvement in numerous protein and enzyme pathways.²⁸⁸⁻²⁹⁰ These metals have been measured in human sweat samples and so it is not unexpected that they would be detected at trace levels in fingermark samples.²⁹¹ Alternatively, exogenous sources of these metals could include cosmetic products, food residues and through contact with metallic objects, which may potentially be exploited for forensic purposes, such as the presence of gun shot residues or illicit substances.⁶ Perhaps not unexpectedly, elements associated with topical skin applications (cosmetics, sun protectants) were identified

in the fingermarks from multiple donors. Titanium and zinc oxides are often added as ingredients to cosmetics to provide sun protection by physically reflecting UV radiation.²⁹²⁻²⁹³ A number of other inorganic substances are added to cosmetic products as colourants including zinc oxide, titanium dioxide, iron oxides, bismuth oxychloride and copper.²⁹⁴ These products are frequently applied using the hands, leaving traces on the fingers, and deposited in fingermark residues; a number of studies have explored the organic components of these substances deposited in fingermark samples.^{7, 295-296} The inclusion of these exogenous substances adds to the complexity of fingermark chemistry, but also has the potential to be exploited to indicate donor traits.

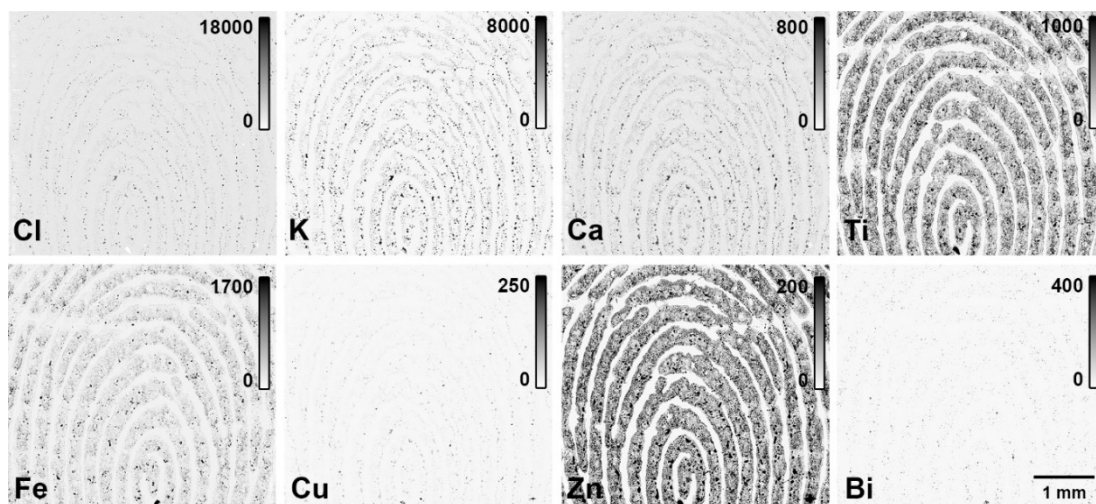


Figure 4.1: Large area XFM scan of natural fingermark from donor 6, deposited on Ultralene Thin Film. Concentration scale bar (ng cm^{-2}).

Table 4.2: *Components detected in latent fingerprints using XFM and their likely endogenous/exogenous source*

Inorganic Component	Source	Potential Origin
Cl ⁻	Endogenous	Sweat
K ⁺	Endogenous	Sweat
Ca ²⁺	Endogenous	Sweat
Ti	Exogenous	Cosmetics
Bi	Exogenous	Cosmetics
Fe	Endogenous/Exogenous	Cosmetics/Sweat
Ni	Exogenous	Currency
Cu	Endogenous/ exogenous	Currency/Sweat
Zn	Endogenous/ exogenous	Cosmetics/Sweat

4.3.2 Sources of Variation in Elemental Content of Latent Fingerprints: Interdonor Variability

Research has previously demonstrated that a high level of interdonor variability exists with respect to organic composition and distribution within fingerprints.^{14, 92, 95, 98} Despite the well characterized heterogeneity in organic composition of fingerprints, the variability in inorganic composition has been less studied due to the previous unavailability of suitable techniques. The capability of XFM for rapid, micron level spatial resolution elemental mapping was used in this study (for the first time) to assess interdonor variability in elemental composition and distribution within natural fingerprints. The variation in inorganic material within fingerprint residue across multiple donors (fourteen separate donors) revealed by XFM is presented in Figure 4.2. It should be noted that donors 6 and 20 were known cosmetic users and demonstrated much higher levels of zinc and titanium in comparison to other donors. As can be seen in Figure 4.2, using Zn as an example, high interdonor variability was observed.

This study also compared intradonor variability, referring to the variability between deposits from the same individual. Samples were taken at two time points

throughout the same day from each donor, as shown in Figure 4.3. The differences between each sample increases the complexity of fingerprint residue as seen through variation in the amount of metallic material deposited. Intradonor variability has proven to be a challenge when sampling fingerprints, particularly for research purposes, and demonstrates the necessity of research protocols, such as the International Fingerprint Research Group guidelines, to account for the variation in fingerprint residue and provide more consistent and reliable research conditions.⁹¹

Zn is expected to be secreted from eccrine pores, and therefore, endogenous Zn is expected to be found in natural fingerprints.¹⁵ Figure 4.2 clearly demonstrates, however, that the fingerprints obtained from users of cosmetics contain substantially larger amounts of Zn than non- or light cosmetic users. This suggests exogenous Zn, found in cosmetics, may be a large source of the observed interdonor variation. This is supported by specific metal colocalizations in the fingerprints from donor 6, a known heavy cosmetic user (Figure 4.4). Specifically, regions of high Zn content were found to colocalize with high Ti content. Ti is not an endogenous metal in fingerprints and, therefore, can only be sourced from an exogenous source, such as cosmetics.²⁹²⁻²⁹⁴ Interestingly, although Ti and Zn were found to colocalize in the fingerprints of cosmetic users, Fe did not show the same level of hot spot colocalization. Strong colocalization of ions Ca^{2+} , Cl^- , and K^+ with metals Cu and Zn were also observed in natural fingerprints (Figure 4.5). Closer examination of the ion distribution revealed that the Cl^- and K^+ deposits have distinct star shaped morphology, which likely indicates the presence of crystalline material within the fingerprint residue.³⁵ Similar findings were reported by Dorakumbura *et al.* where Raman spectroscopy showed small salt crystals at the centre of an eccrine droplet.⁹⁵ The presence of sodium chloride deposited in eccrine sweat has also been suggested as a potential reactive species in fingerprint residue, as a possible target for metal deposition methods and in cyanoacrylate polymerization.^{35, 116} Since chloride appears to be deposited across a fingerprint ridge, this research reinforces the potential for chloride ions to be interacting with these development techniques.

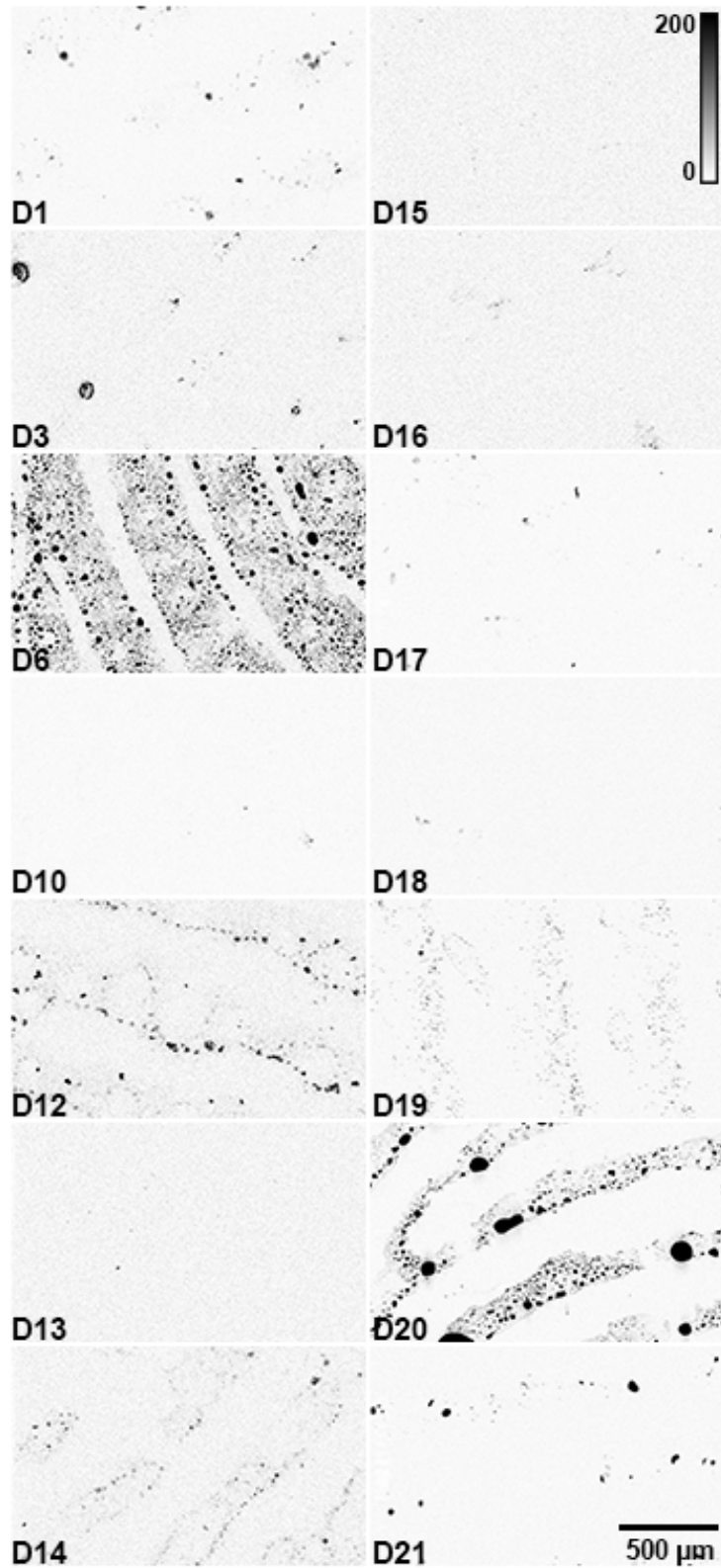


Figure 4.2: Typical results for zinc distribution within natural fingermarks collected from fourteen donors on silicon nitride slides (D1,6,10 17-21) and mylar (D3, 12-16). Concentration scale bar (ng cm^{-2}).

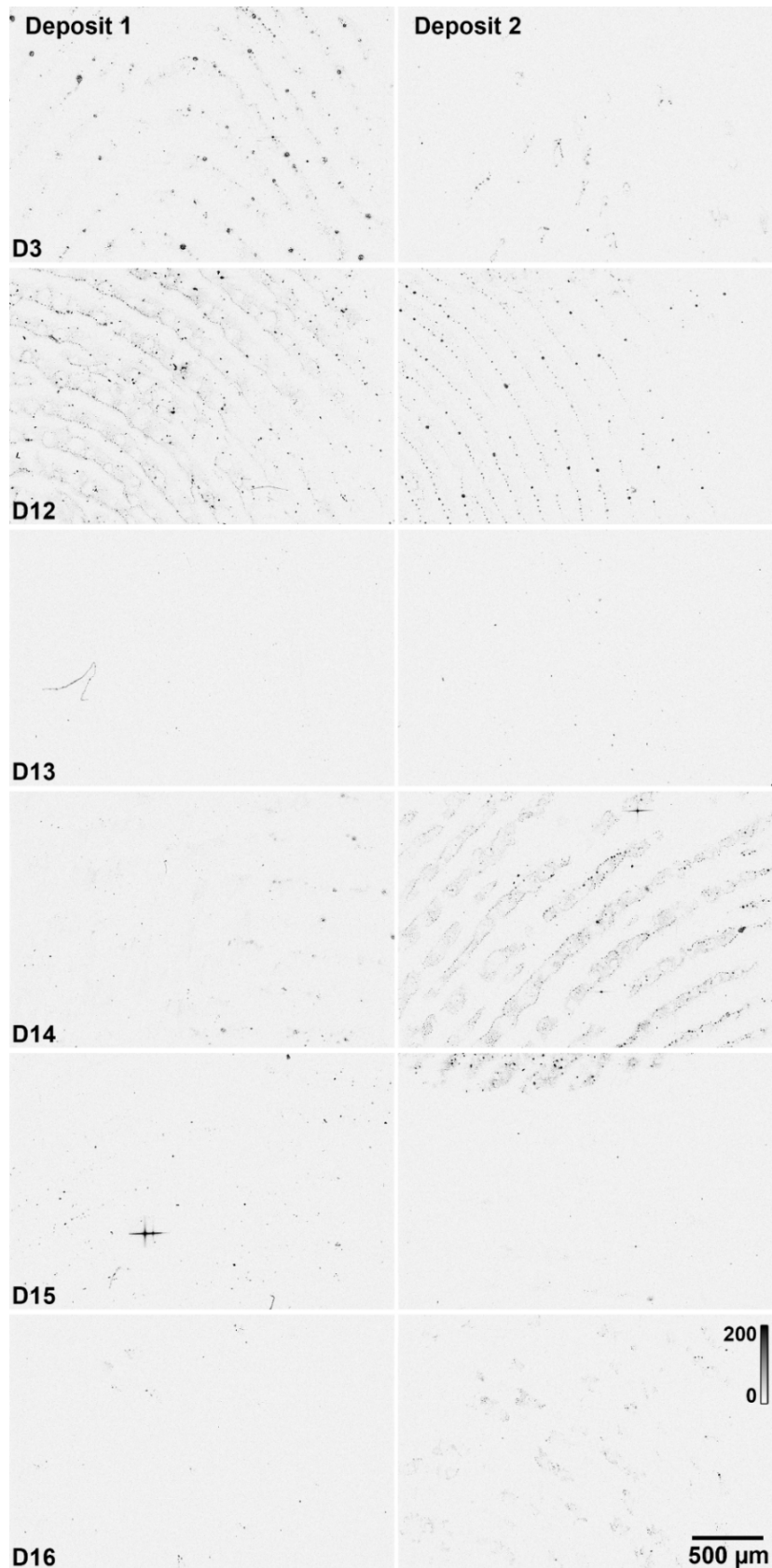


Figure 4.3: Typical results for zinc distribution within natural fingerprints collected from fourteen donors on mylar on two separate occasions (deposit 1 left, deposit 2 right). Concentration scale bar (ng cm^{-2}).

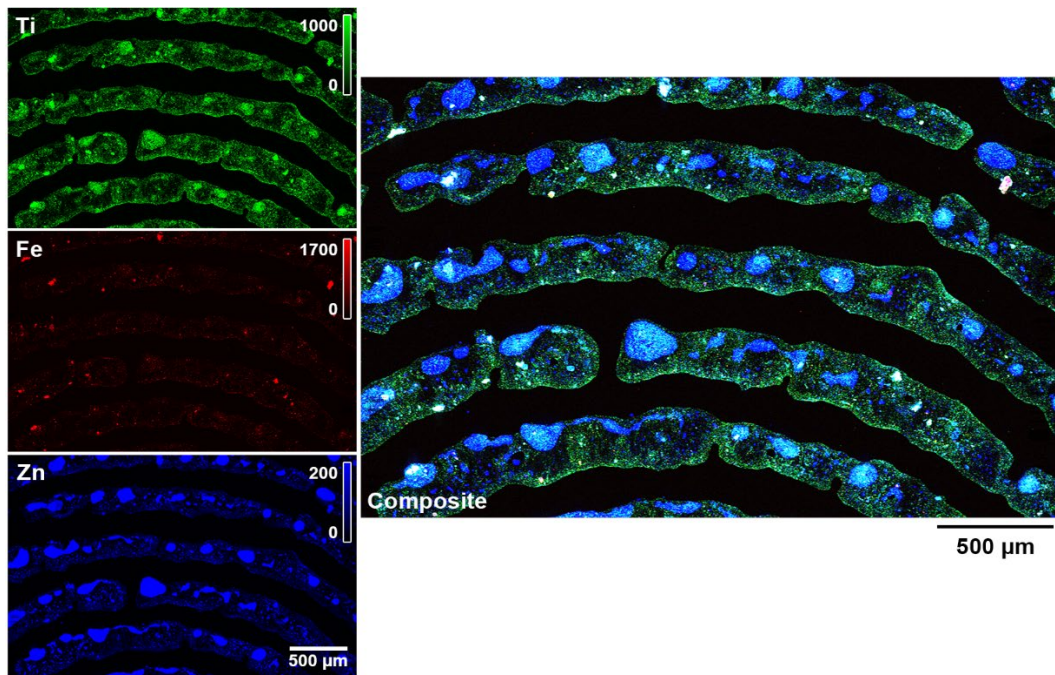


Figure 4.4: Iron, titanium, and zinc distribution within a natural fingermark from donor 6 deposited on silicon nitride and imaged using XFM. Composite image (right) demonstrates the colocalization of these metals within the fingermark matrix. Concentration scale bar (ng cm^{-2}).

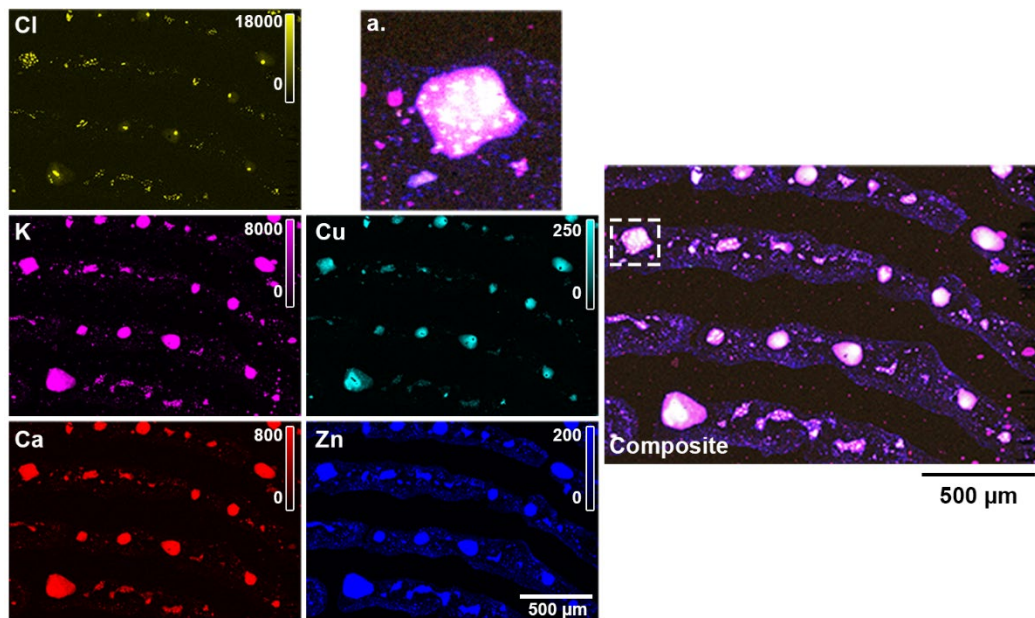


Figure 4.5: Calcium, chlorine, copper, potassium, and zinc distribution within a natural fingermark from donor 6 deposited on silicon nitride and imaged using XFM. Composite image (right) demonstrates the colocalization of these metals within the fingermark matrix; box outlined in the composite image displays area of crystal-like structures (a) seen in particular donors, likely to be salt crystals. Concentration scale bar (ng cm^{-2}).

4.3.3 Combining XFM and IRM to co-locate the Organic and Inorganic Materials in Latent Fingermarks

The previous section explored the use of XFM elemental mapping to investigate the distribution of inorganic material in latent fingermarks. Whilst this information is valuable to understanding fingermark chemistry, there is great potential in combining this data in a multimodal approach, in particular to associate the distribution of inorganic with organic material. Here the co-localization of eccrine and sebaceous material is presented with inorganic elements, by combining data from the IRM and XFM beamlines. The combination of these methods has proven valuable in biomedical studies, with Miller *et al.* and Summers *et al.* demonstrating the success of multi-modal imaging to identify the elemental distribution and protein structures in brain tissue from the same sample.^{269, 297-298} The instrumentation available at synchrotron facilities provides the opportunity to image the distribution of organic and inorganic material in the same fingermark sample. This will offer a unique view of fingermark chemistry, and for the first time relate the distribution of elements to the organic components in natural fingermarks. This can help to understand the association of these materials and their influence on the chemical changes in fingermark residue and their response to chemical development treatments.

When conducting experiments across multiple analytical instruments, a number of considerations need to be made involving substrate surface and image timing. The sample was deposited on silicon nitride slides as they were appropriate for all imaging methods; alternatively Mylar, which was used in some XFM studies presented in this thesis, was too rough to conduct infrared transmission experiments. Transmission mode was selected using a focal plane array detector, to provide a larger scale imaging area, as a wider field of view was required to allow for matching physical attributes within the sample during analysis. After an initial optical image was taken, the sample was imaged using the thermal source benchtop IR microscope, to measure the organic distribution across the sample. Subsequently, the elemental material was imaged on the XFM beamline, as the inorganic material is expected to be more stable over time.

Here, for the first time, synchrotron sourced XFM, used in combination with IRM, has been used to demonstrate the distribution of the elemental components within fingerprint residue relative to organic material. Figure 4.6 shows the same sample imaged on the optical microscope, IRM and XFM. The results indicate that the inorganic material, represented by zinc in Figure 4.6c, and the organic, both eccrine and lipid material (Figure 4.6d and 4.6e), identified by integrating across the O-H stretching band ($3000\text{-}3500\text{ cm}^{-1}$) and C-H stretching region ($2800\text{ - }3000\text{ cm}^{-1}$) respectively, co-locate across the sample, with bright spots matching across the images. These hot spots appear to correlate with droplets within the optical image, suggesting that areas detected by XFM to have increased elemental content are likely to be endogenous, and secreted through the eccrine or sebaceous glands. In this case, the elemental material appeared to collocate similarly within both eccrine and sebaceous materials, however at this resolution it is difficult to distinguish due to the imaging requirements to image the fingerprint on a large scale.

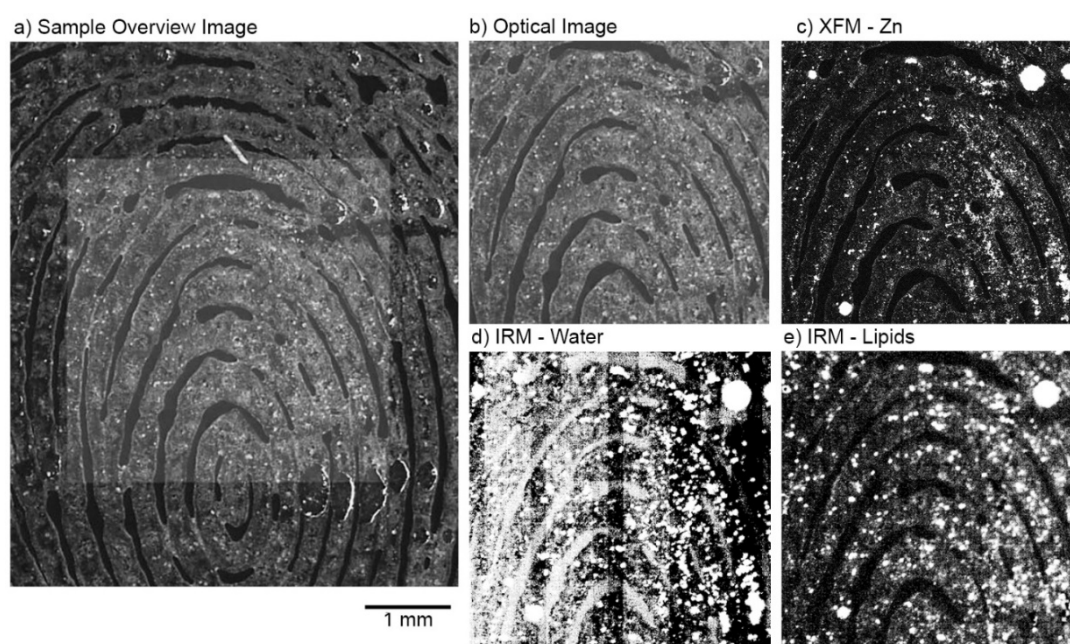


Figure 4.6: A natural fingerprint deposited from donor 6 on silicon nitride imaged with an optical microscope sample overview (a) and imaging area (b), XFM zinc distribution (c) and FTIR-FPA imaging with false colour image generated by integrating over the O-H stretching band ($3000\text{-}3500\text{ cm}^{-1}$) for water representative of eccrine material (d) and the C-H stretching band for lipid material ($2800\text{-}3000\text{ cm}^{-1}$) (e).

Previous work by Dorakumbura *et al.* explored the distribution of organic components at the microscale using synchrotron sourced ATR-IRM and Raman spectroscopy, demonstrating that eccrine and sebaceous material exist in an emulsion like residue.⁹⁵ This meant that it is not unexpected that eccrine and sebaceous material were found to have similar distribution at the macro-scale, however on the micron and sub-micron scale there can be distinct differences in their distributions. The experiment was repeated at increased spatial resolution by decreasing the imaging area to account for the limitations of the instrument. Figure 4.7 displays a FTIR false-colour distribution of eccrine material (Figure 4.7b) overlaid on the bright field image (Figure 4.7a). The false-colour FTIR image was generated using a spectroscopic marker band ($3000 - 3500 \text{ cm}^{-1}$) presented in Figure 4.7d, which corresponds to the O-H stretching vibration, characteristic of eccrine components, water, lactic acid or urea.⁹⁵ Figure 4.7c reveals the elemental distribution in the same natural fingerprint that was analysed with IRM, and demonstrates the presence of chlorine, potassium, calcium, copper and zinc. The similarity in location and morphology allows co-localisation of elemental distribution with eccrine components within the fingerprint residue. Based on the observed co-localisation it is apparent that the eccrine material of natural fingerprints is enriched in inorganic components; this pattern of colocalization was observed across two additional donors (Figure 4.8). Fingerprint regions enriched in sebaceous material were not found to be enriched with inorganic material (e.g., Ca, Cl, Cu, K, and Zn).

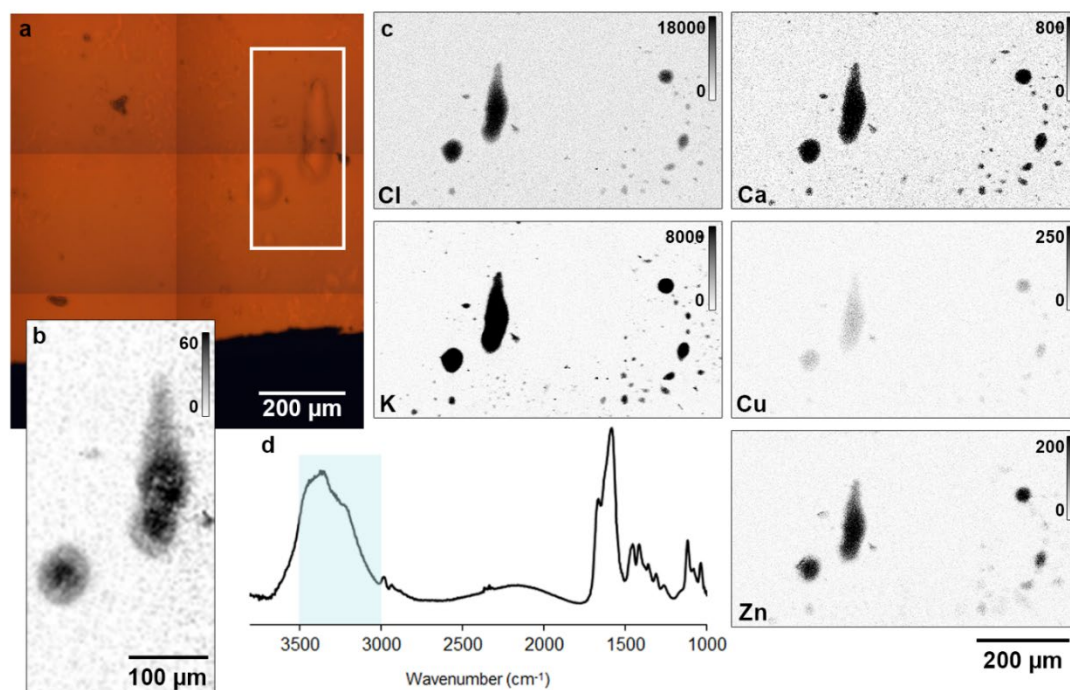


Figure 4.7: Natural fingerprint from Donor 1, deposited on a silicon nitride slide. Bright field optical image of the area investigated with FTIR-FPA imaging (a) with false colour image generated by integrating over the O–H stretching band for the eccrine material ($3000 - 3500 \text{ cm}^{-1}$) (b) FTIR spectra of eccrine material obtained using the conventional FTIR spectroscopy (d) and the corresponding elemental distribution maps imaged using XFM (c). XFM concentration scale bar (ng cm^{-2}).

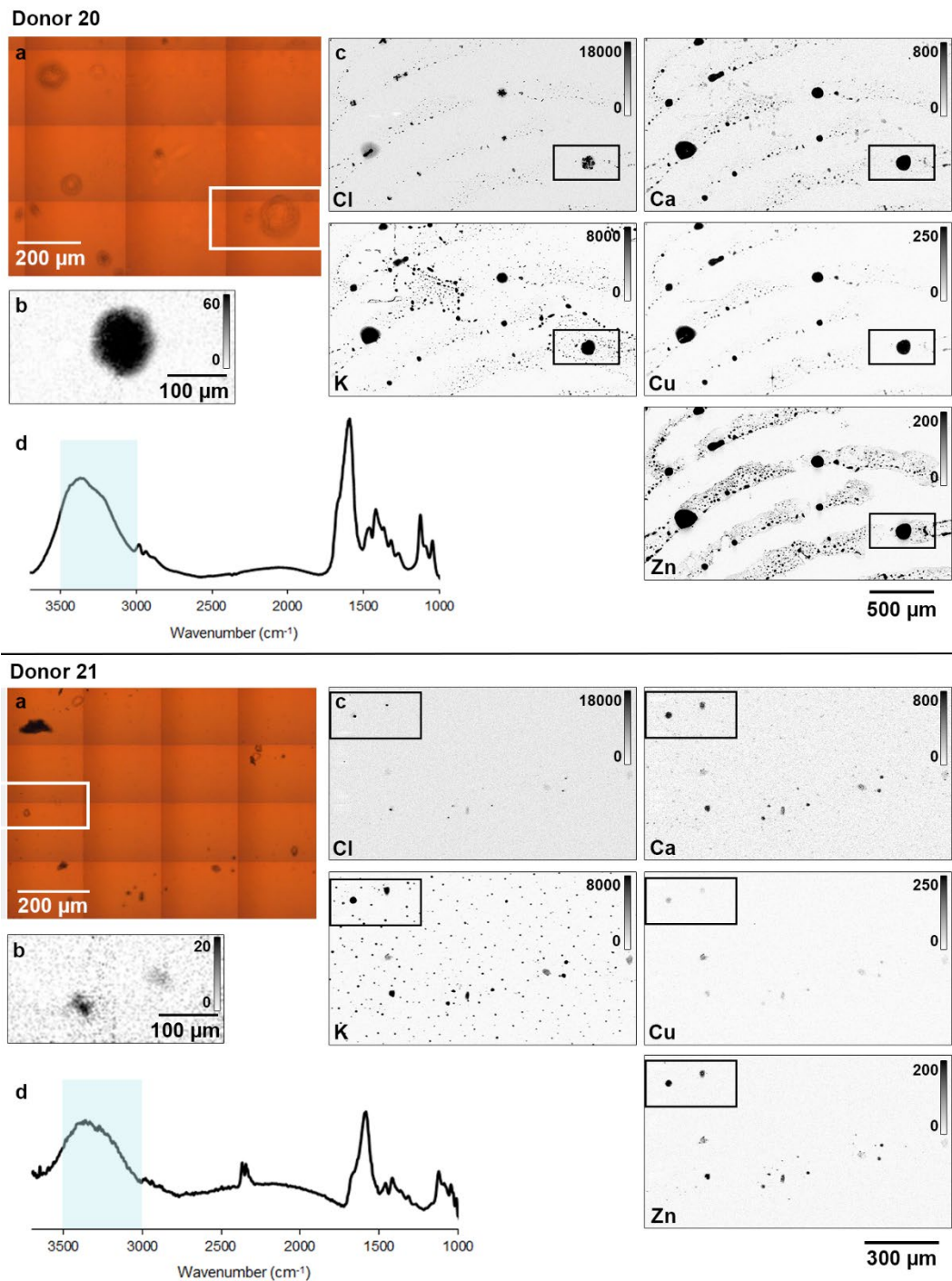


Figure 4.8: Natural fingermark from Donor 20 (top) and Donor 21 (bottom), deposited on a silicon nitride slide. Bright field optical image of the area investigated with FTIR-FPA imaging (a) with false colour image generated by integrating over the O–H stretching band for the eccrine material ($3000 - 3500 \text{ cm}^{-1}$) (b) FTIR spectra of eccrine material obtained using the conventional FTIR spectroscopy (d) and the corresponding elemental distribution maps imaged using XFM (c). XFM concentration scale bar (ng cm^{-2}).

Metal ions have previously been established to have an impact on the ability of detection reagents to recover and successfully visualise latent fingerprints, with a number of studies specifically focussing on the interactions of metal ions with organic components of fingerprints and the detection reagents.^{35, 116, 124} Amino acid (eccrine material) detection reagents 1,2-indanedione and ninhydrin, are both known to interact with metal salts.^{116, 124} Researchers have shown that the addition of zinc chloride to the 1,2-indanedione working solution improves the colour and luminescence of the detected fingerprint, and it is also well established that the addition of zinc and nickel salts as a post treatment for ninhydrin alter the colour of the developed fingerprint.^{116, 124} In this study, the observation of Zn co-localised with eccrine material may explain in part the variation in detection of latent fingerprints using 1,2-indanedione and ninhydrin. Specifically, the enrichment in Zn that is observed in cosmetic users provides a new avenue to investigate, specifically, to identify if the fingerprints of cosmetic users are more readily detected by 1,2-indanedione and ninhydrin methods, on the basis of their Zn enrichment.

4.4 Conclusions

This study has demonstrated the capabilities for direct elemental mapping techniques, such as XFM, to study the trace elements present within latent fingerprints. Using this capability, this research begins to explore the elemental distribution within fingerprint residue to begin to better understand the effects these ions have on the underlying chemistry of current methods of detection. Specifically, this work demonstrates that the distribution of endogenous inorganic components within latent fingerprints are localised to eccrine organic material. Such an observation suggests that variation in metal ion content may account for variation in the ability to detect latent fingerprints, especially reagents targeting eccrine material and in which metal ion chemistry is known to affect the detection chemistry. Further, the presence of exogenous material in particular donors reinforces the influence of daily activities, such as cosmetic use, on fingerprint chemistry.

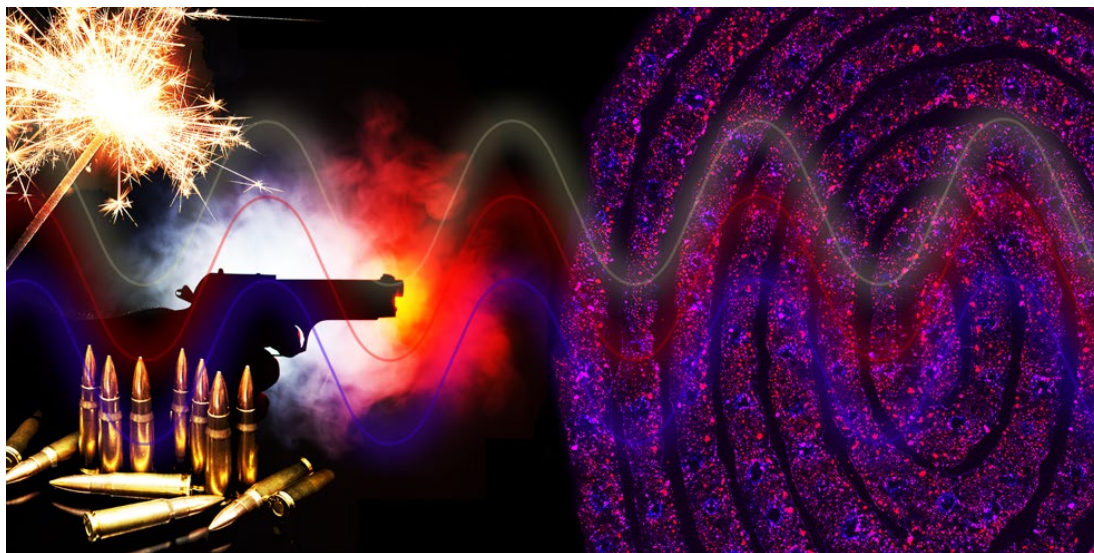
Due to the necessity of a synchrotron facility to undertake the measurements described in this study, routine application for forensic testing is unlikely. However,

direct application of the techniques presented in this study to select forensic cases is achievable. Possibly of greater value is the knowledge gained relating to greater understanding of the chemical complexity of latent fingerprints, which this and future studies will provide. Such insight may provide the necessary founding for the development of new, routinely applicable methods to detect latent fingerprints or identify chemical traits within the fingerprint (e.g., presence of cosmetics).

These findings highlight only a fraction of the potential studies for which XFM and direct elemental mapping can be applied to study the chemistry of fingerprints. Classical analytical techniques such as LC-MS and GC-MS, and more recently mapping techniques such as FTIR and Raman microscopy, have been invaluable in increasing understanding of the organic chemical composition of latent fingerprints and how it affects detection methods. On the basis of this study, it is anticipated that direct elemental mapping can play a similar role to reveal the complexities through which metal ions influence fingerprint chemistry, and subsequently improve detection capability.

Chapter 5

The Transfer And Persistence Of Metals In Latent Fingermarks



Portions of this chapter have been published in the following articles:

Rhiannon E. Boseley, Buddhika N. Dorakumbura, Daryl L. Howard, Martin D. de Jonge, Mark J. Tobin, Jitraporn Vongsivut, Tracey T. M. Ho, Wilhelm van Bronswijk, Mark J. Hackett, and Simon W. Lewis. Revealing the Elemental Distribution within Latent Fingermarks Using Synchrotron Sourced X-ray Fluorescence Microscopy. *Analytical Chemistry* **2019** 91 (16), 10622-10630

DOI: [10.1021/acs.analchem.9b01843](https://doi.org/10.1021/acs.analchem.9b01843)

Rhiannon E. Boseley, Daryl L. Howard, Mark J. Hackett, and Simon W. Lewis. The transfer and persistence of metals in latent fingermarks. *Analyst* **2022** 147(3), 387-397 DOI: <https://doi.org/10.1039/D1AN01951A>

5.1 Introduction

During the course of criminal activity the transfer of trace evidence creates a link between people, locations and/or objects, subsequently these traces can provide crucial investigative information. There is an increasing interest in studying the transfer and persistence of trace evidence, and the consequences that may have on the interpretation of that evidence at the activity level.^{9, 56, 261, 265-266} There are many factors that affect the degree of material transfer, including the source material, the recipient surface, as well as the strength and length of contact.^{80, 299} Latent fingerprints are an important type of trace evidence as they are easily transferred and can identify an individual using the ridge patterns. The composition of latent fingerprints is dynamic, known to change over time, which is discussed in detail in section 1.3. Since evidence is not normally collected immediately following transfer, the persistence of fingerprint residues needs to be considered.³⁻⁵ Investigating these processes to demonstrate how fingerprint composition is impacted by the donor's activity prior to deposition and the persistence of fingerprint material will assist with the interpretation of fingerprint evidence.⁶⁻⁹

The primary focus of forensic fingerprint examiners is the identification of an individual from a recovered fingerprint.^{4, 300} The court is responsible for deciding how to interpret fingerprint evidence, providing context on the activity that leads to the transfer of fingerprint residue.²⁵⁸ To assist the court with their interpretation a robust understanding of transfer and persistence mechanisms is needed, to assist forensic scientists in assigning evidential values for how these processes relate to fingerprint chemistry.²⁵⁹ Research has recently been conducted to explore the transfer mechanisms involved in DNA and textile fibre trace evidence.^{56, 261-267} These studies explored how variables including type of contact, donor, recipient and contact duration can effect transfer processes.^{261, 263-265} A similar approach has been taken by de Ronde *et al.* to investigate a variety of criminal activities leading to fingerprint deposition.⁹⁻¹² Here, work is presented to expand on these studies through the investigation of transfer and persistence of inorganic material (e.g., metal ions), in latent fingerprints.

Cosmetics, illicit substances and gunshot residues all contain metal ions, which can be detected in fingerprint residue through the use of coloured or fluorescent indicators.^{70, 73-75, 78, 256, 301} However, such methods do not offer high elemental specificity, and it is challenging to identify if non-specific and generic presence of metal ions can be linked to a particular physical activity, or if “false-positives” could occur from endogenous biological metal ions naturally secreted through the fingertips. Through detailed understanding of the specific metal ions that are transferred to and persist within fingerprints, there may be scope to develop improved and / or targeted strategies to detect metal ions using various coloured or fluorescent indicators.

In chapter 4, XFM was used to demonstrate that a range of metal ions can be detected in fingerprint residue. In this study, work using XFM elemental mapping is expanded to characterise the transfer and persistence of metals in fingerprints, following contact with metal objects of forensic interest. Further, X-ray absorption near edge structure (XANES) spectroscopic mapping has been used to help reveal the chemical form of metals that are transferred, which is critical information to enable future development of forensic detection strategies.

5.2 Methodology

5.2.1 Fingerprint Deposition

Fingerprints were collected from eight donors, donor information can be found in Table 5.1. Samples were imaged using the XFM beamline, full instrumental details can be found in section 2.5.1 and XANES information in section 2.5.2.

Table 5.1: *Details of the donors used in this study*

Donor No.	Age	Biological Gender	Cosmetic Use	Scatter Plot Colour
3	22	Male	None Reported	●
6	23	Female	Yes	●
12	23	Female	Yes	●
13	23	Female	Yes	●
14	36	Male	None Reported	●
15	23	Male	Yes	●
16	23	Female	Yes	●
18	32	Male	None Reported	n/a

5.2.1.1 Preliminary Study – Investigation of transfer of exogenous material from Australian currency

Prior to deposition Donor 18 was instructed to wash his hands to remove existing exogenous material, one hand was brought into contact with Australian silver-coloured coins, with gentle rubbing, whilst the other was not. Fingermark impressions were taken from both hands on silicon nitride slides (Melbourne Centre for Nanofabrication, Australia) and imaged using XFM.

5.2.1.2 Further studies into metal transfer from forensic objects

Seven donors (3, 6, 12-16) gave six deposits, 2 natural marks, 3 marks following contact with forensically significant items, and 1 mark after hand washing. Donors were instructed to gently press their finger down for 5–10 seconds on Mylar, 6um (Sietronics, Australia).

For deposits 2 and 3, donors were instructed to hold a gun barrel (Gecado Air Rifle Mod 30 -pitted, WA Police) in their left hand and cartridge case (REM 223, WA Police) in their right hand for 30 seconds, fingermarks were then taken from each hand. Deposit 5 was taken after 30 second contact with a party sparkler (Artwrap, China), the hands were then washed with soap (Kimberly-Clark, Roswell GA) and water, air dried and using the same finger, deposit 6 was taken. Deposits 1 and 4 were natural marks deposited prior to contact with samples.

5.2.1.3 Investigation of Daily Persistence of Exogenous Material

Donor 6 was selected as a known cosmetic user, to provide fingermarks throughout the day. Donor 6 conducted their regular morning routine, including applying a range of cosmetic items, a fingermark was taken on Mylar, 6um (Sietronics, Australia) 15 minutes after this process. The hands were then washed with soap (Kimberly-Clark, Roswell GA) and water at least once between each subsequent deposition at time points 1, 2, 3, 6 and 10 hours from the initial deposition.

5.2.1.4 Investigation of Elemental Displacement or Redistribution Following Immersion of Latent Fingermarks in Water

Fingermarks were collected from eight donors (Donors 1, 6, 10, 17, 18, 19, 20 and 21) on silicon nitride slides and imaged using XFM. The samples were then covered with deionized water for 30 minutes. The samples were dried and reimaged using XFM.

5.2.2 Image Analysis and Statistical Analysis

XFM elemental maps were exported as tiff images and analysed using ImageJ (1.5i). The average elemental areal density was calculated across the entire scan area, for the following elements: Cl, K, Mn, Fe, Co, Ni, Cu, Zn, Br, Ba, Pb and Bi. The average elemental areal density from each donor is presented as scatter plots generated using Graphpad Prism v9.2.0. Statistical testing was used to identify differences between the median group intensities for the following experimental group comparisons (natural vs barrel, natural vs cartridge, barrel vs cartridge) and (natural vs sparkler, natural vs sparkler and washed, sparkler vs sparkler and washed) using a non-parametric Wilcoxon matched pairs test for all 7 donors ($n = 7$). Significance was defined at the 95 % confidence limit ($p < 0.05$).

5.3 Results & Discussion

The physical activities a person engages in can influence the elemental composition of their fingermarks. Understanding how different physical activities manifest in altered elemental composition of fingermarks is therefore important knowledge in a forensic context. In addition to direct association between physical activities and the

subsequent elemental composition of fingermarks, understanding the persistence of trace elements can suggest a potential timeline for fingermark deposition. This study has utilised synchrotron sourced XFM to investigate the transfer and persistence of elemental material from forensically significant items to a latent fingermark deposit. In addition, XANES-mapping has been used to identify the different chemical forms of Fe that may be found in latent fingermarks.

5.3.1 Sources of Variation in Elemental Content of Latent Fingermarks: Metal-contact Contamination

Following on from studies in Chapter 4 looking at the inter-donor variation in elemental content and distribution within fingermarks, investigations were conducted to reveal how contact with metal surfaces would transfer material from the surface to the fingertips and then be deposited in a fingermark. Some donors analysed in Chapter 4 showed that Ni and Cu, major components of metal alloys, were sometimes found in high concentration and co-localised. This was hypothesised to reflect donor contact with metal surfaces, such as coins. The hypothesis was tested using contact between fingertips and Australian currency, specifically silver coins which comprise of 75% Cu and 25% Ni, as a case study. Donor 18 was instructed to wash their hands and then bring one hand into contact with silver-coloured coins, with gentle rubbing, while the other hand remained free of coin-contact. Latent fingermarks were taken from both hands for direct comparison to demonstrate the transfer of metals from the coin to the fingermark. The impression from the finger that had been in contact with the coin displayed higher levels of Cu and Ni, as shown in Figure 5.1. Not unexpectedly, the distribution of Cu and Ni was heterogeneous, with highly localised regions, resembling particles, displaying a co-localised enrichment of Cu and Ni (Figure 5.1). The approximate size of the Cu and Ni enriched particles ranged from $4 \times 8 \mu\text{m}^2$ to $50 \times 55 \mu\text{m}^2$. The areal density of Cu and Ni (ng cm^{-2}) was measured by drawing a region of interest around these hotspots to give a Cu / Ni ratio of 2.67, which is similar to that of Australian currency (Table 5.2). These results strongly suggest that the Cu and Ni in this fingermark originated from contact with the metal coin. By extension, this finding indicates that handling of Australian currency, or other metal surfaces may result in routine transfer of metals to

fingermark residue and be present within a latent fingermark. This inspired further experiments looking at what other forensically significant items could transfer elemental material to the fingermark following handling.

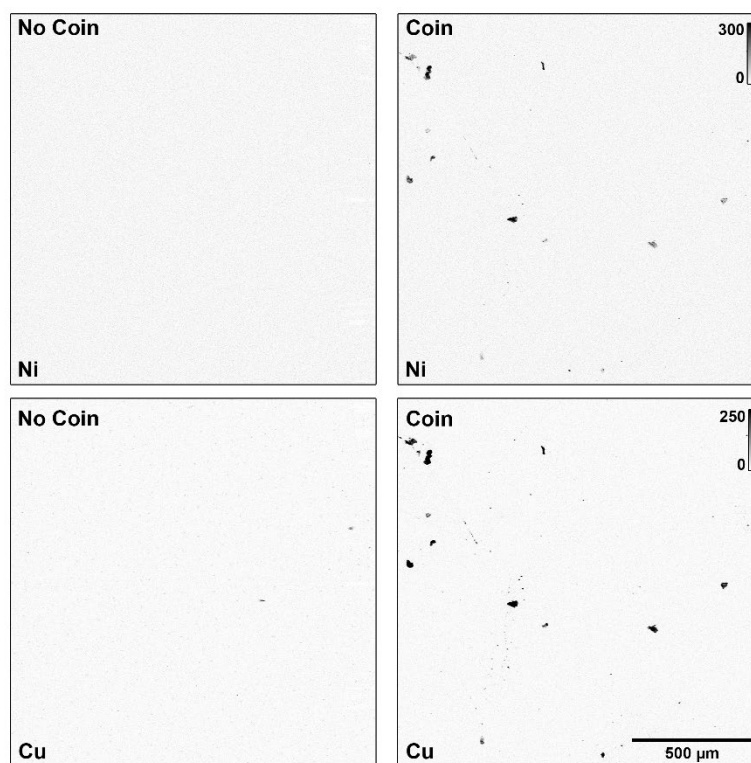


Figure 5.1: Copper and nickel distribution in a fingermark deposited from Donor 18 on silicon nitride and imaged using XFM. Natural deposit (left) and fingermark from hand in contact with Australian currency (right). Concentration Scale Bar (ng cm^{-2}).

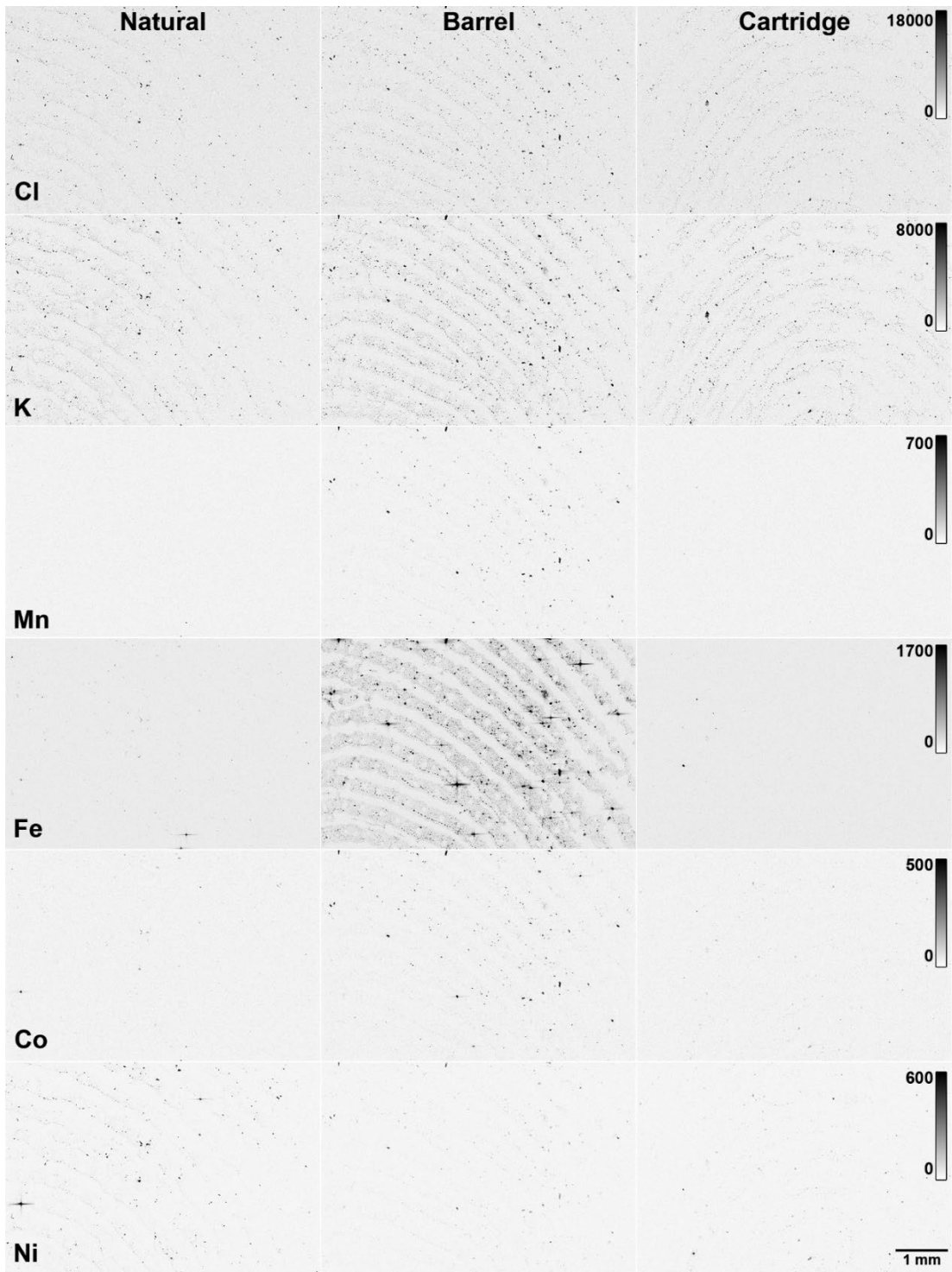
Table 5.2: Average copper and nickel areal density measured from the particulate hotspots as shown in Figure 5.1 and the ratio of these metals in an Australian silver coloured coin.

	Metal	Composition
No Contact	Cu	42.5 ng cm^{-2}
	Ni	36.3 ng cm^{-2}
	Cu/Ni	1.17
Coin Contact	Cu	284 ng cm^{-2}
	Ni	106 ng cm^{-2}
	Cu/Ni	2.67
Coin	Cu/Ni	3.00

5.3.2 Elemental Composition of Latent Fingermarks before and after Handling a Gun Barrel or Ammunition Cartridge

In this study, how the elemental content of latent fingermarks is influenced through handling metallic objects (gun barrel and ammunition cartridge) was investigated. XFM elemental maps were simultaneously recorded for Cl, K, Mn, Fe, Co, Ni, Cu, Zn, Br, Ba, Pb, and Bi, with a representative example presented in Figure 5.2 (not all elements were detectable in all fingermarks). It can be visibly seen in Figure 5.2 that following contact with the gun barrel there is a drastic increase in the trace amounts of Fe and Pb present. In general, the Fe and Pb appear to be diffusely localised along the ridge pattern of the fingermark however, a heterogeneous distribution of what appears to be small, particulate Fe and Pb hotspots can also be observed, potentially revealing small particles of gun shot residue (Figure 5.2).

Statistical analysis using a non-parametric Wilcoxon matched pairs test compared the elemental content of $n = 7$ fingermarks and confirmed that the increase in Fe and Pb after handling a gun barrel is significant. Interestingly, most metals displayed substantial variation in content between donors (as seen in Figure 5.3). It is possible that one source of the variation in elemental content observed between donors after handling a gun barrel cartridge is due to heterogeneity in the gun barrel.³⁰² Another source of the elemental variation could be explained by variation in the organic components in the natural fingermarks, allowing greater retention of elements from the metal gun barrel on the individual's fingertips. Future studies are required to investigate these potential sources of variation. In Chapter 4 multi-modal IRM and XFM were used in workflows to co-localise organic and inorganic fingermark constituents. Future studies are now planned, using multimodal IRM and XFM, to determine if variation in an individual's organic fingermark composition influences the retention of metal ions following metal-object handling. Nonetheless, irrespective of the heterogenous response in Mn, Co, and Bi, the results of this study have shown a consistent, and reproducible increase in Fe and Pb content in latent fingermarks following handling of a gun barrel.



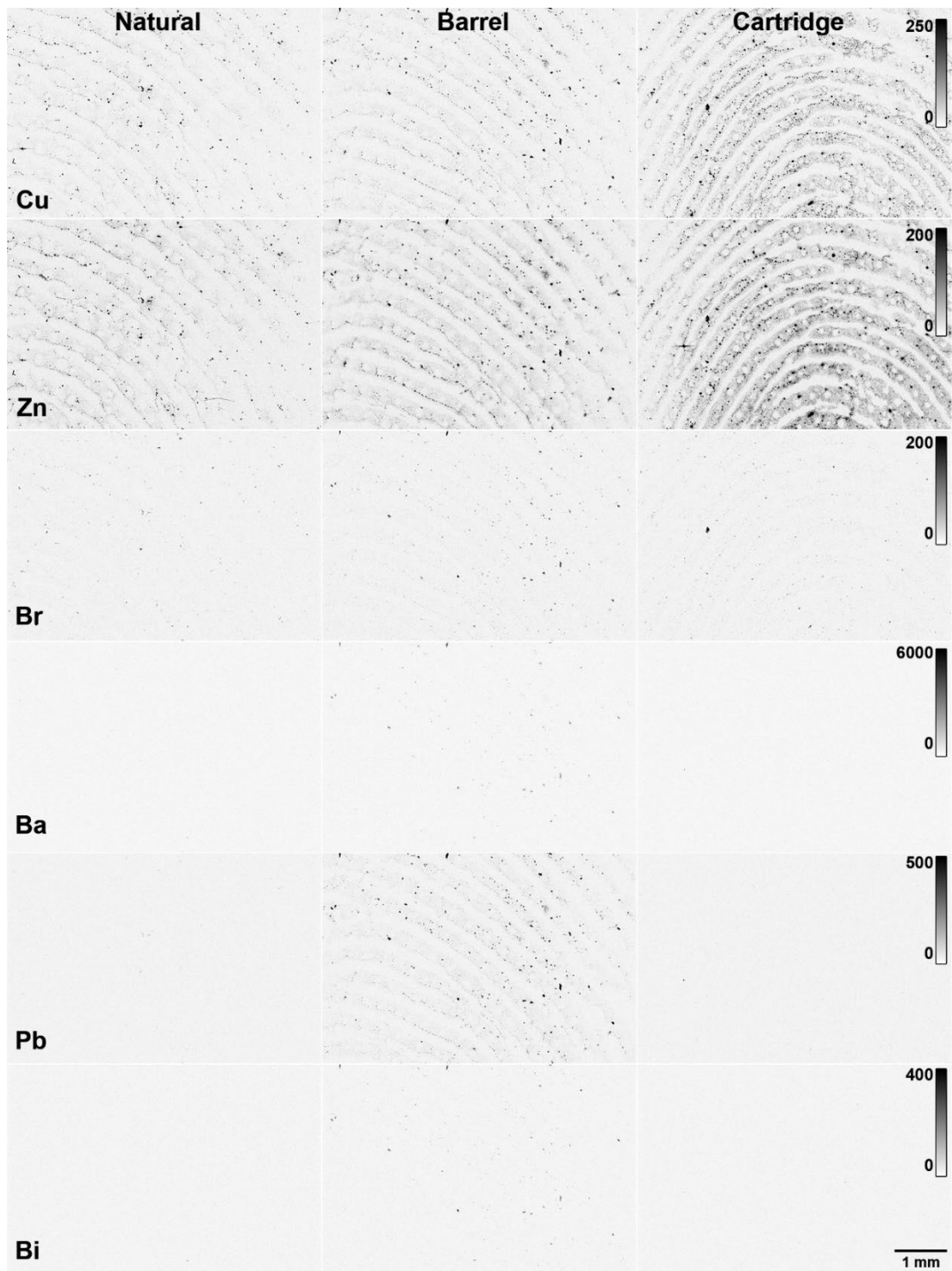


Figure 5.2: *Elemental maps of fingerprints taken from a representative donor following regular activity (left), handling a gun barrel for 30 seconds (middle) and handling an ammunition cartridge case (right).*

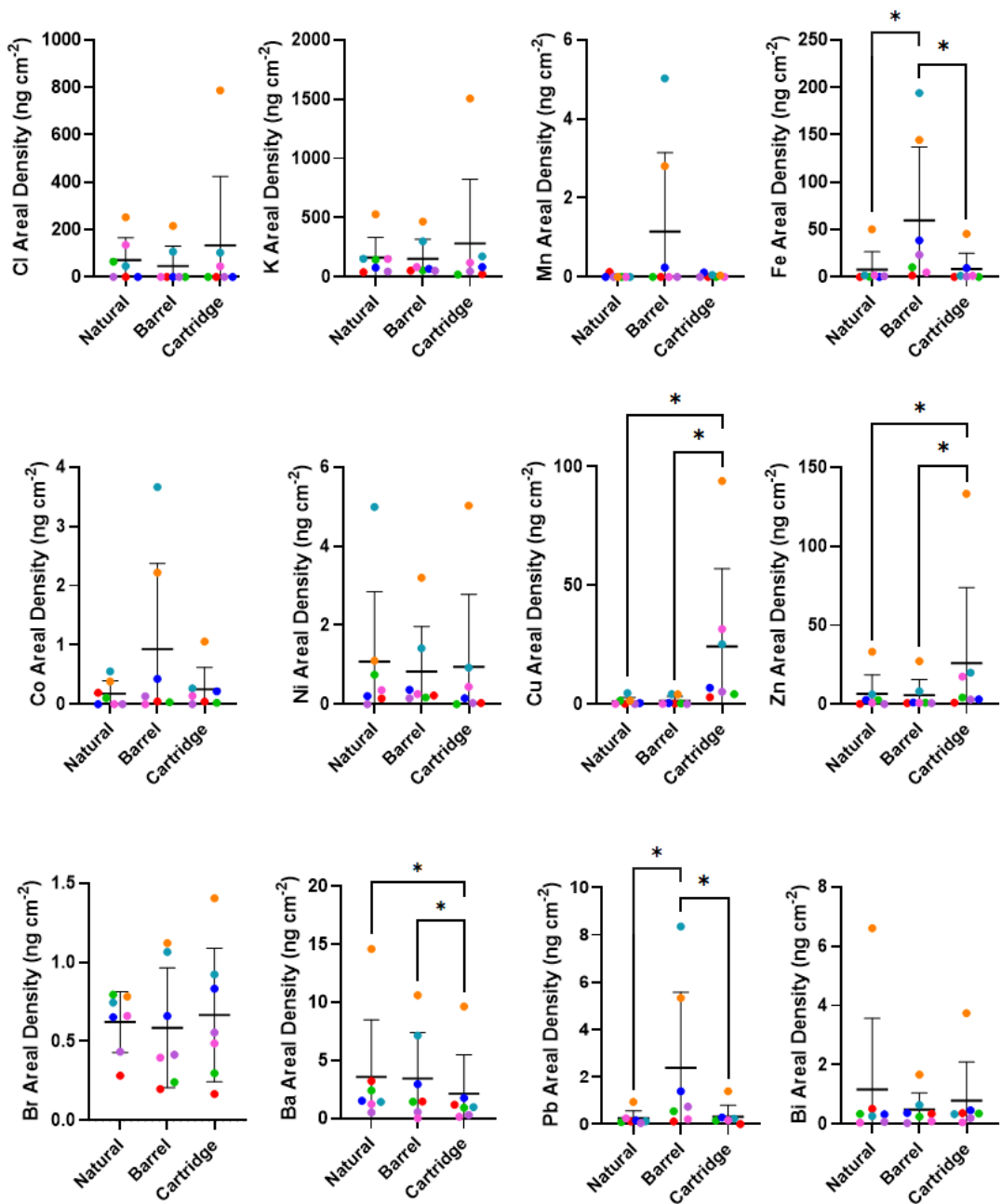


Figure 5.3: Scatter plots of the average elemental areal density calculated from fingermark samples taken following regular activity, handling a gun barrel for 30 seconds and handling an ammunition cartridge case for 30 seconds. Plots marked * indicate P -value < 0.05 from Wilcoxon matched-pairs signed rank test. Each donor is represented by an individual colour outlined in Table 5.1.

A representative example of elemental maps of a latent fingerprint obtained before and after handling an ammunition cartridge are also presented in Figure 5.2. Not surprisingly, an increase in metal ions can be observed as a result of handling the ammunition cartridge. It is important to note however, that different metal ions are enriched in the fingerprint after handling the ammunition cartridge (Cu, Zn) compared to the gun barrel (Fe, Pb). There is also a difference in the distribution of Cu and Zn (after handling the ammunition cartridge), compared to Fe and Pb (after handling the gun barrel). Specifically, the distribution of Cu and Zn appears to reflect a more homogenous localisation across the fingerprint ridges with a complete absence of the particulate hotspots that were observed for Fe and Pb after touching the gun barrel residue. This increase in Cu and Zn in the fingerprints after handling the ammunition cartridge was confirmed through statistical analysis from $n = 7$ different fingerprints (Figure 5.3).

Iron K-Edge X-ray absorption near edge structure (XANES) spectroscopic mapping was used to differentiate between chemical forms of iron deposited in a fingerprint after handling a gun barrel. As a preliminary study four samples which had been deposited following contact with a gun barrel were selected for XANES iron analysis. XANES mapping of fingerprints taken from donor 12 shown in Figure 5.4 identified two chemically different forms of Fe were present in a fingerprint taken after handling a gun barrel. A localised particulate hotspot of Fe appears brightly in the total Fe map (Figure 5.4a). Principal component analysis (PCA) of the XANES data showed that the PC1 scores image (Figure 5.4b) largely reflected the total Fe map, and therefore likely reflects data variance associated with total Fe content. However, the PC2 scores image (Figure 5.4c) highlighted a specific Fe hotspot, located between the ridge detail (blue arrow, Figure 5.4c) that contained a distinct difference in data variance compared to surrounding Fe hotspots. The representative PC loadings are presented in Figure 5.4d, highlighting the specific X-ray energies contribution scores plots and identifying that PC2 is specifically reflecting data variation at the white line feature. Based on the PC score images, average XANES spectra (Figure 5.4e) were generated from specific regions of interest (Figure 5.4f), which highlights the Fe particle located between the ridges (blue arrow, Figure 5.4c) is metallic Fe, while the

remaining Fe hotspots show spectra consistent with ferric iron (Fe^{3+}), as indicated by the maximum of the pre-edge feature ($1s - 3d$ transition), centred at 7114.5 eV.³⁰³ Without being exactly sure of the origin of the two different chemical forms of Fe, the results infer that the metallic Fe present is likely a solid steel particle taken directly from the surface of the gun barrel, whilst the Fe dispersed across the fingerprint ridge is expected to be an iron oxide, present on the surface due to steel pitting.³⁰⁴⁻³⁰⁵ Additional donors revealed Fe distribution characteristic of ferric ion, no further metallic ion particles were detected across the imaged regions. Figure 5.5d shows representative spectra from each of the 4 samples imaged as well as the two spectra identified from donor 12 in Figure 5.4. PCA analysis of the additional samples did not show variance across the sample, with the same Fe distribution identified in the total Fe image (Figure 5.5a) as in PC1 and PC2 from donor 15 (Figure 5.5 b-c).

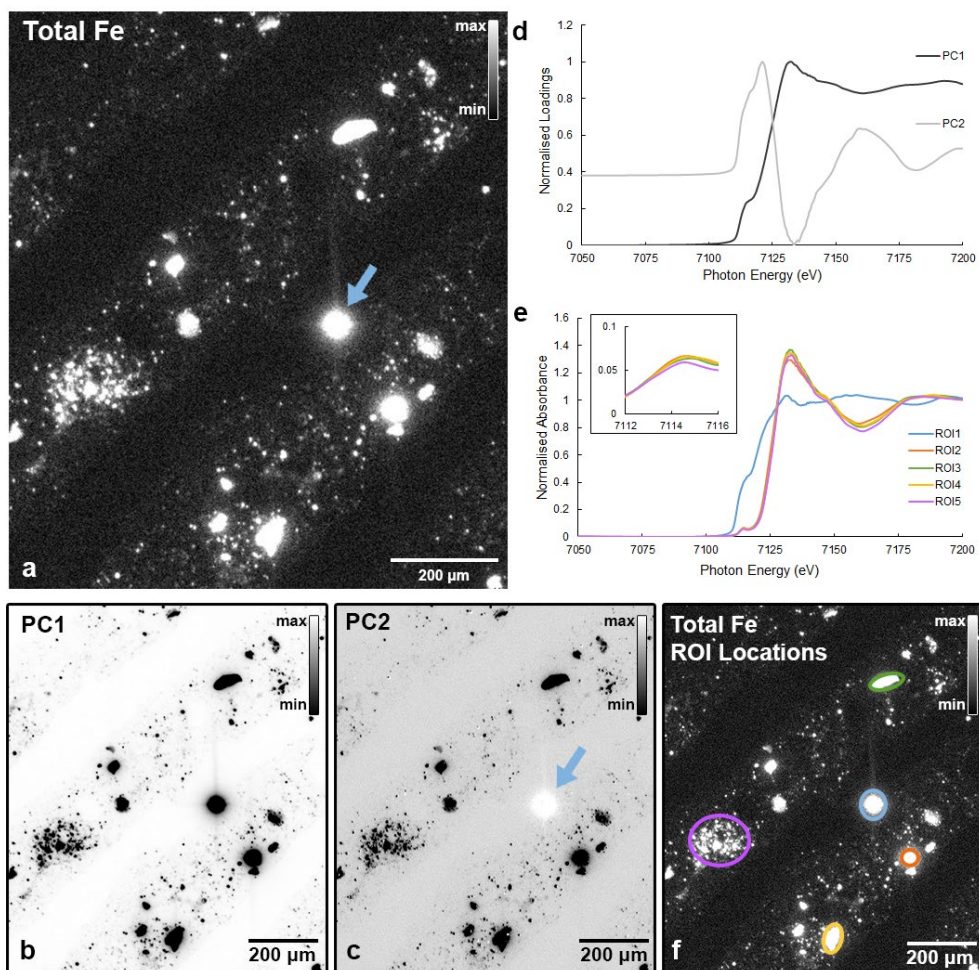


Figure 5.4: XANES mapping of a fingerprint taken after handling of a gun barrel reveals transfer of two different chemical forms of Fe. (a) Total Fe map taken at 7.4keV showing deposition of Fe along fingerprint ridges, but also one Fe hotspot adjacent to a ridge (blue arrow), (b-d) principal component analysis was used to identify differences in the chemical form of Fe, with the image of PC1 scores closely reflecting total Fe distribution (b), while the PC2 scores image highlights that the Fe particle located adjacent to the ridge (blue arrow) displays a distinctly different pattern of spectral variance (c). The specific variables contributing most to the sources of variance described by PC1 and 2 are shown in the PC loadings (d). Analysis of normalised XANES spectra (e) taken from regions of interest (f), support the existence of different chemical forms of Fe across the fingerprint. Specifically, the hot particle adjacent to the ridge presents a spectrum (blue trace in panel e) resembling elemental Fe, while the other traces resemble Fe^{3+} ($1s - 3d$ pre-edge maxima at 7114.5 eV).

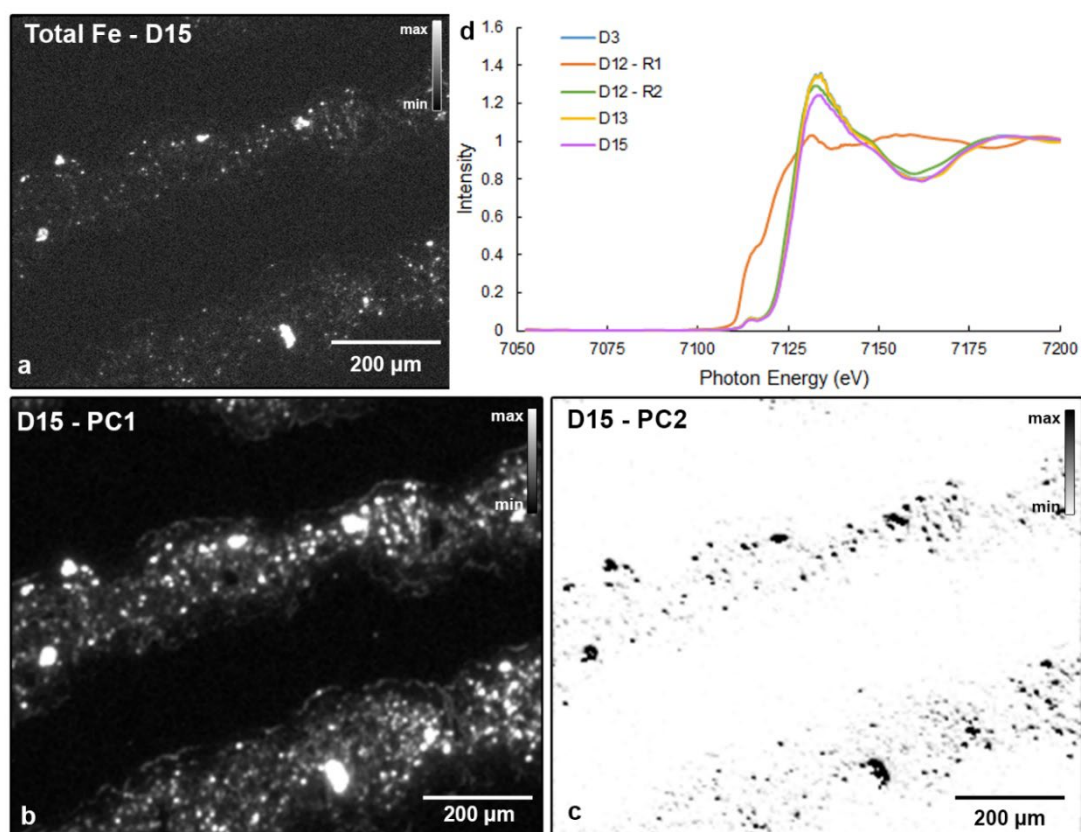


Figure 5.5: XANES mapping of a fingerprint taken after handling of a gun barrel demonstrated only donor 12 had two forms of iron identified. (a) Total Fe map taken at 7.4keV showing deposition of Fe along fingerprint ridges (b-c) principal component analysis was used to identify differences in the chemical form of Fe, here the image of PC1 and PC2 scores closely reflect total Fe distribution (b). Analysis of normalised XANES spectra (d) taken from representative regions of interest from the 4 samples measured from donors 3,12,13 and 15, with donor 12 showing the two forms of Fe identified in Figure 5.4.

In summary, the results of this study strongly suggest that the metals present in latent fingerprints can assist in connecting an individual to a particular object or class of objects, providing vital activity level information to a forensic case. Specifically, the results show that fingerprints become enriched in Fe and Pb after handling a gun barrel, while becoming enriched in Cu and Zn after handling an ammunition cartridge. The elemental composition of these metal objects can attribute to this differential enrichment. Ammunition cases are commonly made of brass, a combination of Cu and Zn whilst Fe is present in rust on the steel barrel and Pb

residue from bullet and primer mixtures is commonly found as gun shot residue.^{302, 304, 306} In addition, XANES-mapping has helped identify that at least two chemical forms of Fe may be present in latent fingerprints after handling a gun barrel, namely metallic Fe particles, and ferric iron (Fe^{3+}). These two chemical forms of Fe help explain the Fe distribution observed in the fingerprints, with localised particulate hotspots identified as metallic Fe, and the more diffuse Fe localised to ridges identified as Fe^{3+} . These results, therefore, provide strong evidence that analytical developments can help identify the presence of specific metal ions in latent fingerprints deposited at crime scenes may have specific forensic value in linking fingerprints to a past physical activity.

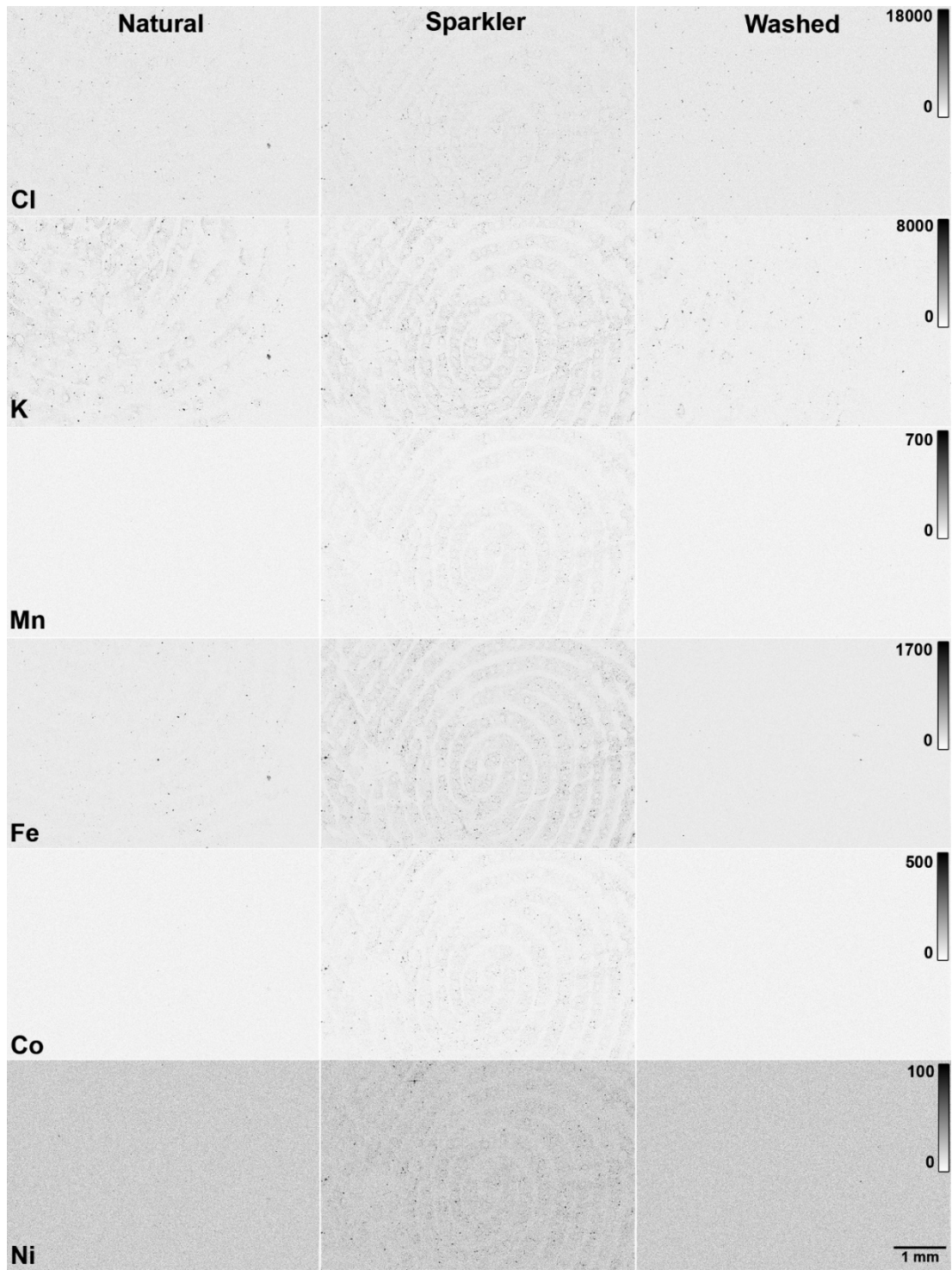
5.3.3 Transfer and Persistence of Elemental Contaminants from Party Sparklers and the Effect on Subsequent Deposition in Latent Fingerprints

To examine the persistence of exogenous metals and metal ions on the hands this experiment explored how hand washing, following the handling of objects, influences the profile of metal ions in latent fingerprints. Specifically, transfer and persistence of trace elements within latent fingerprints were investigated following contact with a party sparkler and subsequent hand washing.

Increased presence of certain elements in latent fingerprints can be observed following contact with unlit party sparklers (Figure 5.6). Specifically, an increase in Fe, Co, Ni, Br, and Ba is observable across the ridge pattern detail of fingerprints, and statistical analysis of $n=7$ donors confirmed these visual increases were significant (Figure 5.7). Interestingly, some donors showed an increase in Mn and Zn content, however this was not seen consistently and as already described is likely due to inconsistent retention of these metals associated with variation in organic residue present on the fingertips. Party sparklers have been the focus of recent forensic research due to their use in improvised explosive devices (IED). Work by D'Uva *et al.* has studied the elemental profile of these sparklers, using inductively coupled plasma-mass spectrometry (ICP-MS) to demonstrate the elemental profile of sparkler residue can indicate their potential source.³⁰⁷ The results shown here are consistent with this work, suggesting that barium which is found in highest concentration in

party sparklers, is easily transferred to the fingertips and deposited in fingermarks after handling.

To explore the persistence of party sparkler material on fingertips and how this may affect elemental composition of subsequent fingermarks, fingermarks were also recorded after hand-washing. In Figure 5.6 and Figure 5.7 it is noticeable that Ba, Br, Co, and Zn all significantly decreased in concentration after hand washing (noting that the decrease in Zn is most likely removable endogenous Zn). Statistical analysis confirmed these visual observations were significant (Figure 5.7). This finding suggests these elements are easily transferred, but also easily removed from the hands. Detection of an elevated profile of these metal ions in a latent fingermark may therefore indicate relatively recent handling of materials containing this elemental profile. Of interest, Ni and Br content were increased.



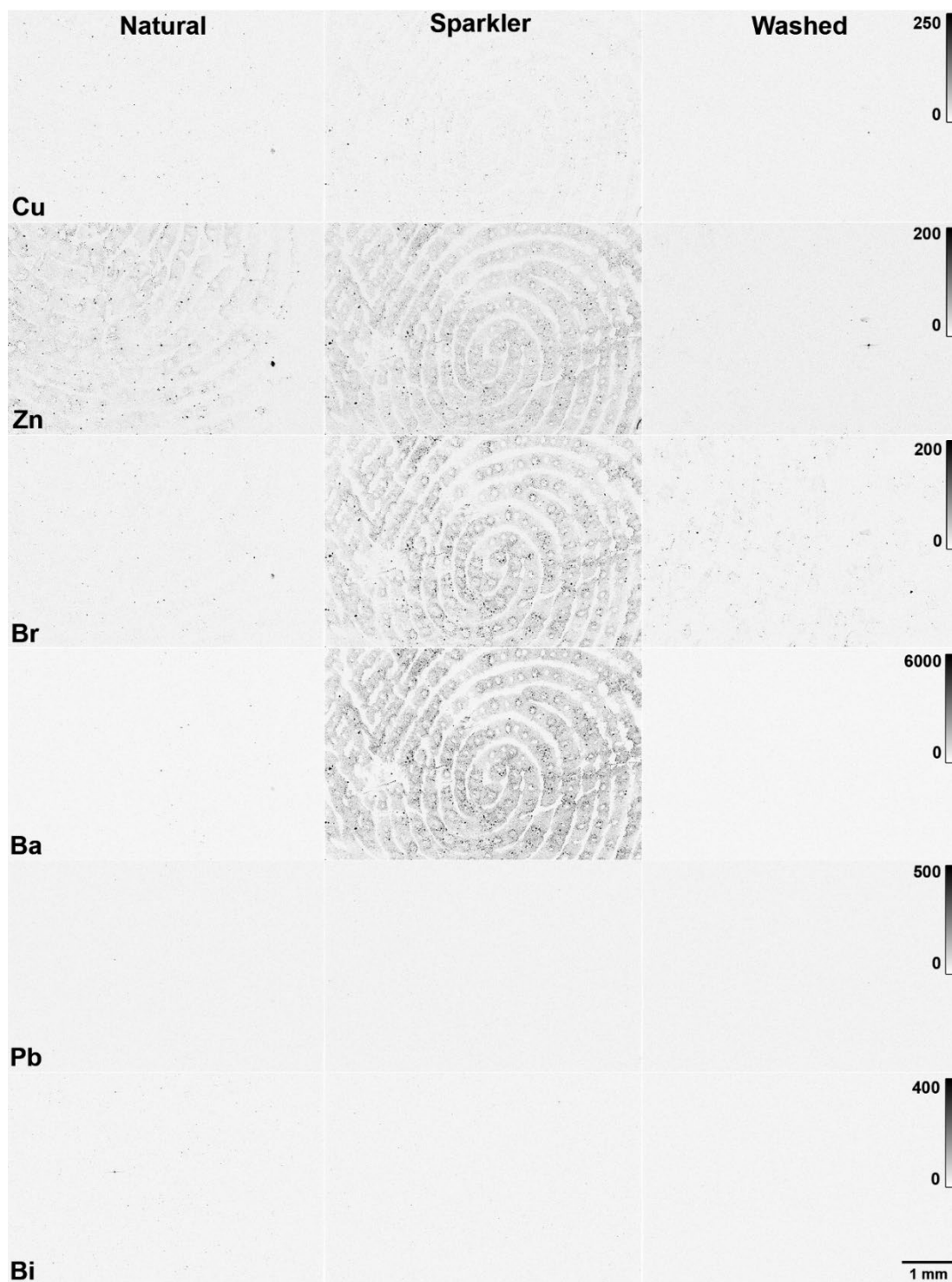


Figure 5.6: Elemental maps of fingermarks taken from a representative donor following regular activity (left), handling a party sparkler for 30 seconds (middle) and handling a party sparkler for 30 seconds followed by washing hands (right).

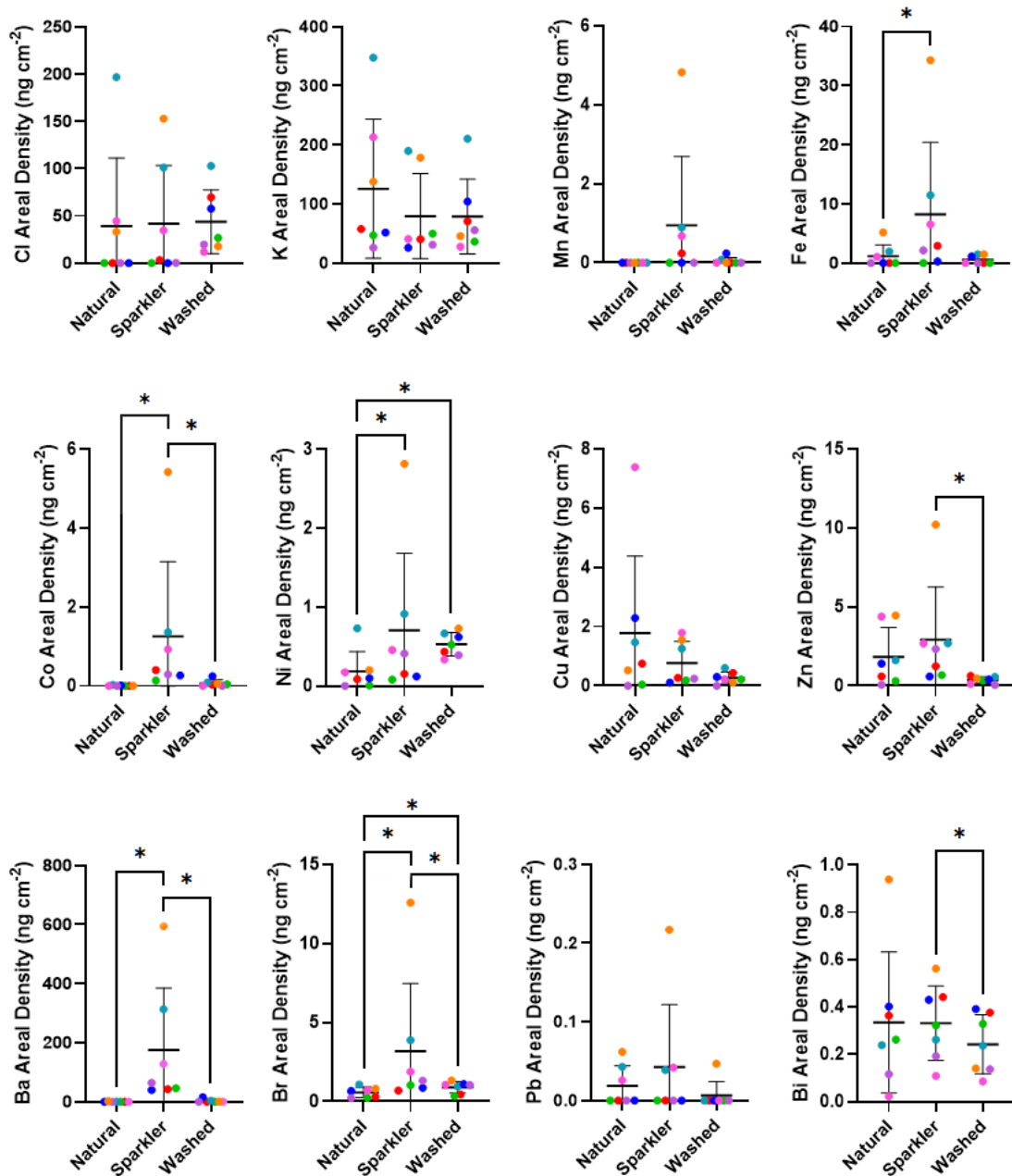


Figure 5.7: Scatter plots of the average elemental areal density calculated from fingerprint samples taken following regular activity, handling a party sparkler for 30 seconds, or handling a party sparkler for 30 seconds and then washing the hands. Plots marked * indicate P-value < 0.05 from Wilcoxon matched-pairs signed rank test. Each donor is represented by an individual colour outlined in Table 5.1.

5.3.4 Persistence of Elemental Content of Natural Fingermarks: Daily Activity

This persistence of elemental material was considered further, to investigate how exogenous material can change throughout the length of a day. Donor 6, a known cosmetic user, deposited fingermarks at various time points throughout the day, with regular hand washing. In the results presented in Figure 5.8 the zinc content appears to be consistent throughout the day, with slight variation, likely due to deposition pressure which was not controlled in this experiment. This was consistent across all metals deposited by this donor. The exogenous metals present are believed to be heavily attributed to their cosmetic use, however this would suggest a larger amount deposited following make up application. Habitual touching of the face could provide enough contact for the transfer of these metals, or the long-term use of these cosmetics may have led to build up on the surface of the skin of the hydrophobic components of these materials. This provides data which could be concerning for the health of these individuals who are heavy cosmetic users, but also indicates a potential chemical target, detecting these cosmetic residues to assist in identifying individual's behaviour. This should be noted when exploring the use of TMDT's, as donors who have increased elemental content in their fingermarks due to cosmetic residue may provide false positives to these tests. A wider range of donors with differing cosmetic use should be compared in a wide scale study to determine the effects of cosmetics on TMDT's.

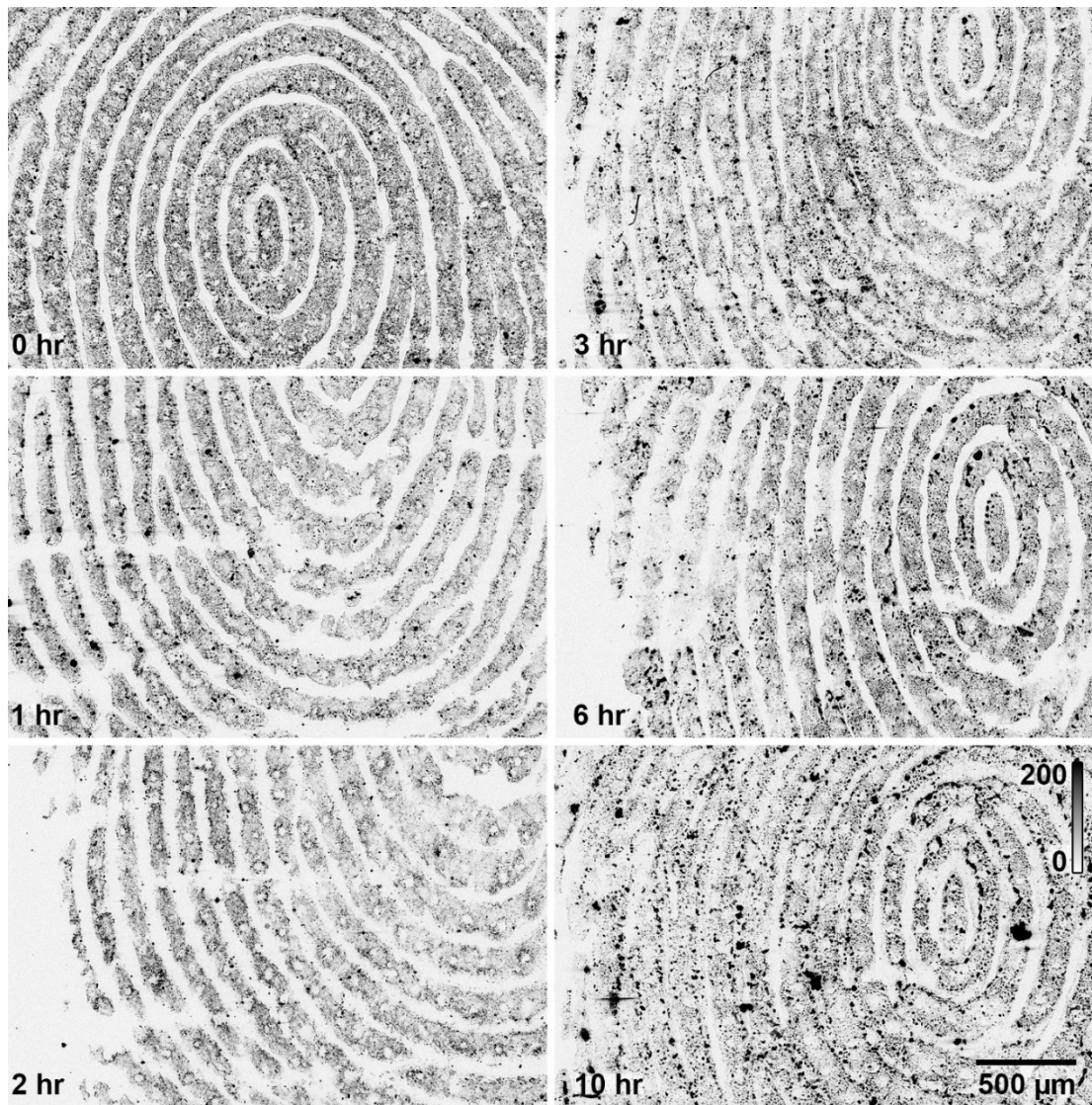


Figure 5.8: Zinc distribution within a natural fingerprint from donor 6 deposited on Mylar and imaged using XFM. Fingermarks taken at 6 time points throughout the day after daily cosmetic application (15 minutes, 1 hr, 2 hr, 3 hr, 6 hr, 10 hr. Concentration scale bar (ng cm^{-2}).

5.3.5 Persistence of Elemental Content of Natural Fingermarks: Effect of Water Immersion

The composition of a fingermark is not static; chemical and physical changes are influenced by environmental factors such as temperature, humidity and light exposure. In a true forensic context fingermarks may be exposed to a variety of factors, such as water immersion (either from exposure to the environment or criminal efforts to clean contaminated surfaces). It is therefore important to understand how exposure of fingermarks to water immersion affects the persistence of elemental content and distribution within the fingermark. Such knowledge may help explain the success or failure of different detection methods in varying conditions or be used to develop improved detection methods for certain scenarios.

Figure 5.9 shows Cl, K, Ca, and Cu were almost completely removed from the fingermark following water immersion. Water immersion substantially reduced the concentration but did not completely remove Zn from the fingermark. Interestingly, although a large proportion of Zn was removed from the fingermark during water immersion, the relative distribution of Zn after water immersion remained similar to that observed before water immersion. The levels of Fe and Ti in the fingermark were not visibly observed to change as a consequence of water immersion.

The removal of chloride ions through water immersion suggests that this ion cannot be targeted with water dispersive techniques. However, under certain circumstances fingermarks may be enriched in metals such as Zn and Fe or contain metals such as Bi and Ti as a result of cosmetic use. Most currently available fingermark detection methods are centred on an interaction or reaction between detection reagents and organic components of fingermarks. This current study not only reveals the possibility that metal ions in the fingermark may influence the chemical interactions between reagent and organic fingermark components, but also highlights that the metal ions themselves could be used as targets. This study revealed that even after immersion in water, a process that removes much of the water soluble eccrine material (which is targeted by current detection methods), metals ions of Fe, Ti, and Zn can remain. In particular, Fe and Ti appeared largely unaltered by water

immersion. Although it is likely that the presence of these metals at the concentrations observed in this study is from exogenous sources, the results highlight the potential to develop metal sensing settings. Such detection methods could include fluorescent or colour metal binding compounds, such as TMDT's currently used to detect the handling of metal objects.

In addition to acting as targets for fingerprint detection protocols, these findings on exogenous metal transfer indicate the potential to give information on donor traits, specifically cosmetic use. Although direct elemental mapping techniques themselves, such as XFM, are unlikely to ever become a routine fingerprint detection technique, the ability to reveal elemental content and distribution within a fingerprint can provide important identification information on donor behaviour, such as contact with exogenous metals prior to fingerprint deposition. In forensic cases of high importance, under certain circumstances largely governed by the surface fingerprints are deposited on, XFM analyses of latent fingerprints may provide valuable information on donor traits.

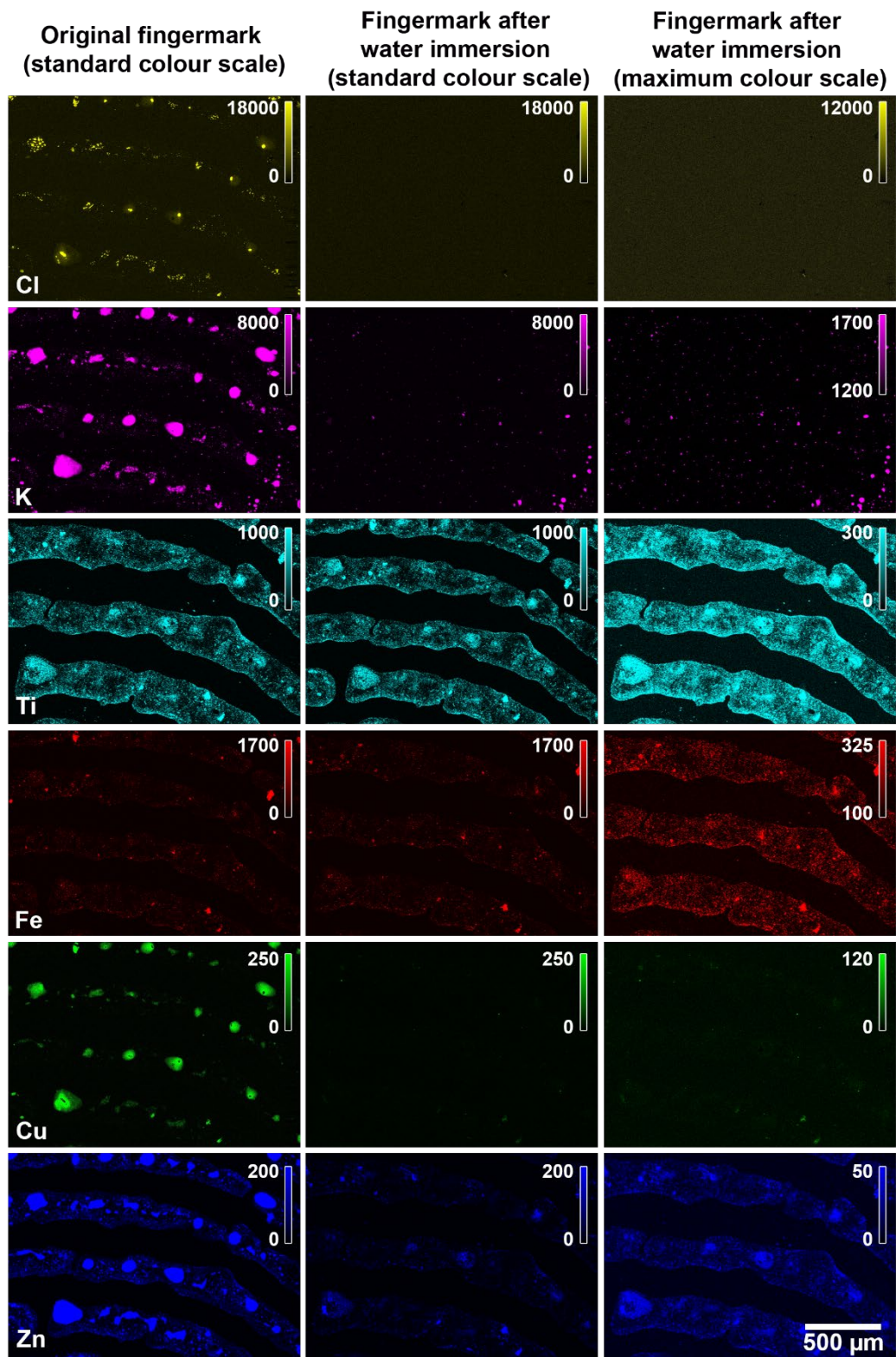


Figure 5.9: Water immersion experiments showing the removal of metals from fingerprints deposited by Donor 6, original fingerprints (left) rinsed fingerprints visualised on the same colour scale as the original fingerprints (middle) rinsed fingerprints on a maximum colour scale (right).

5.4 Conclusions

This study has used XFM to highlight the extent to which exogenous inorganic material may be transferred from objects onto a person's fingerprints. The results highlight that brief handling of metallic objects (gun barrel, ammunition cartridge) or inorganic material (party sparkler) results in robust transfer of metal ions or metallic fragments to an individual's hands, which are subsequently deposited in fingerprints. The ease of transfer of exogenous metals suggested by this study reinforces the complexity of fingerprint chemistry, implying that variation in fingerprint composition can be influenced by the activity level of the donor.

Interestingly, a brief period of hand washing appeared to successfully prevent the appearance of certain metal ions or metallic fragments in subsequent fingerprints. This finding may have important implications for future applications of forensic methods to detect metal ions or metallic particles, as this current study suggests their appearance in latent fingerprints likely indicates recent handling of metallic objects or inorganic compounds. Such information may be important to law enforcement agencies when trying to establish a timeline of events, in a similar fashion to textile fibre persistence. Pounds and Smalldon^{308, 309-310} Further the persistence of inorganic cosmetic residues on the hands of a donor throughout the day was explored, with 6 fingerprints taken on separate occasions on the same day. Elemental mapping demonstrated a consistent heightened level of metals and metal ions across multiple deposits, suggesting that increased elemental material might be indicative of a donor's behaviour. This cosmetic inorganic material was also seen to remain post water immersion, presenting a possibility of using metal ion sensing compounds as a new, niche opportunity to detect latent fingerprints exposed to environmental factors such as water exposure, in circumstances where traditional approaches fail.

This study has also highlighted the potential for future method development using X-ray techniques, specifically XANES spectroscopy, in order to differentiate between different chemical forms of metals and metal ions found in latent fingerprints. The knowledge of the chemical form of a metal ion is likely crucial information to guide the development of improved detection strategies. Lastly, it is unlikely that

synchrotron XFM will find routine use in the field of forensic science for fingerprint detection, however, the method could yield valuable information in select cases of high importance. More importantly, this study has identified a “profile” of metal ions that are transferred into latent fingerprints following specific physical activities, which can now form the basis for rationale design of targeted detection strategies (e.g. coloured or fluorescent metal ion sensors).

Chapter 6

Monitoring the Chemical Changes in Fingermark Residue Over Time using Synchrotron Infrared Spectroscopy



Portions of this chapter have been published in the following article:

Rhiannon E. Boseley, Jitraporn Vongsvivut, Mark J. Hackett, and Simon W. Lewis.

Monitoring the chemical changes in fingermark residue over time using synchrotron infrared spectroscopy. *Analyst*, **2022** 147 (5), 799-810

DOI: <https://doi.org/10.1039/D1AN02293H>

6.1 Introduction

Degradation of fingerprint residue has a major impact on the successful forensic detection of latent fingerprints.² Following deposition there are changes in morphology and the chemistry of fingerprint residue due to interaction with the surface, the sample environment, and the fingerprint residue itself.⁸⁰ The above factors can impact fingerprint chemistry at variable rates, hindering successful fingerprint development.⁸⁰ Whilst the surface and sample environment are conditions which can be controlled and monitored, the chemistry of fingerprint residue is multifaceted and more variable and therefore is an area of interest for fingerprint researchers.

Fingerprint residue is a combination of secretions from the eccrine and sebaceous glands, with additional contaminants picked up through contact during daily activity.^{3, 6, 25} The eccrine and sebaceous secretions often exist as a series or network of “droplets” within the fingerprint, sometimes resembling an oil-in-water (or water-in-oil) emulsion.⁹⁵ Once deposited, this residue is not static with a potential to move across a surface, and undergo chemical and physical changes. Sebaceous material is an oily mixture of lipids, which are known to degrade over time, and studies have attempted to correlate this rate of degradation to time since fingerprint deposition.^{50, 53, 96} However, as the lipids may originate from different sources, such as sebaceous glands or from physical contact with certain parts of the body, there can be large variation in the initial lipid content and composition, which makes age prediction of fingerprints challenging.^{5, 79} The eccrine constituents are an aqueous mixture containing amino acids, salts and proteins. The water content undergoes evaporation as one of the first signs of degradation, which can be a main driver towards altering the physical and chemical properties of the remaining residue.^{45, 88, 177, 183}

The water content in fingerprints decreases as a function of time since deposition, yet, fundamental knowledge, such as the exact amount of water contained in a fingerprint is not well known. The intrinsic difficulties in measuring the volumes of water in a fingerprint are due to the small amount of material deposited which can

vary as a function of its environment, influenced by variables such as temperature and humidity. It is well understood that the water content has a direct impact on fingerprint detection, with dried, aged fingerprints showing weaker performance when detected with some operational methods.^{35, 47-49, 160} Due to the impact of dehydration on the development process it is expected that the water content makes up a significant portion by mass of a fresh fingerprint. Studies have debated the fraction of water in a fingerprint and tried to investigate the rate of evaporation, with many concluding a wide range in values due to the inherent variability in material deposited.⁴³⁻⁴⁵ Keisar *et al.* and Croxton both reported the use of microbalances to measure the total mass of fingerprint residues and its variation over time, suggesting a total mass within 0.33 – 29 µg.^{43, 46} The rate of evaporation was also suggested by Bright *et al.* who investigated fingerprints under vacuum conditions, however these methods have relied on the total change in the mass of a fingerprint and do not provide information on chemical-specific changes, the values also vary greatly between donors, requiring large data sets to provide a more precise measure.⁴⁴⁻⁴⁵

An alternative approach has been to explore the chemical alteration within fingerprint residue, by directly measuring the chemical constituents present at different time points since deposition, using techniques such as GC-MS and LC-MS.^{5, 13, 50, 52-54, 96} Whilst each of these methods can provide valuable bulk chemical information on the degradation process, spatially resolved chemical information is not provided. A method or methods which can determine both chemical specificity and spatial information can provide a better overall picture of fingerprint residue as it ages.¹¹³

Recent advances in scientific capabilities have utilised methods such as AFM, ATR-IRM, and as presented in chapters 4 and 5, XFM to bring together spatial and chemical-specific information on fingerprint residue.^{95, 179} There are a number of advantages to these methods, particularly the capability to image fingerprints without any chemical alteration, treatments, or solvent extractions prior to measurement. *In-situ* label-free measurements, provide a more realistic depiction of the chemical species naturally present in fingerprint residue, and when coupled with microscopy they can localise chemical information to specific structural features of

fingermarks (e.g. ridge patterns, or individual droplets). Specific examples include a study by Ricci *et al.*, using ATR-IRM to study time-course chemical changes as fingermarks were heated from room temperature to 80 °C, collecting data at a spatial resolution of 50 µm, which allowed visualisation of the chemical changes along fingermark ridge details.¹⁸⁷ In a further study, Ricci *et al.*, again used ATR-IRM to identify specific chemical components associated with cosmetics at discrete locations within the fingermark.⁷ In recent studies, synchrotron-sourced ATR-IRM was used to identify the distribution of eccrine and sebaceous components present within a single droplet.⁹⁵ The application of these methods provides the opportunity to further understand the degradation of fingermark residue, by directly imaging the chemical and morphological changes of the eccrine and sebaceous material within a natural fingermark as a function of time since deposition.

In this study, the high photon flux (“brightness”) of the synchrotron-IR beam coupled with synchrotron ATR-FTIR, were exploited to enable collection of diffraction-limited ATR-IRM data with sufficient signal to noise ratio (S/N), within an experimentally realistic time frame.²¹⁸ According to previous investigations, the spatial resolution of the synchrotron ATR-IRM technique measured using the same acquisition parameters was 2.95 µm at 2925 cm⁻¹,¹⁸⁴ which is in good agreement with the original studies in this field.²¹⁶⁻²¹⁷

Although the ATR-IRM technique is well suited to study chemical composition in highly localised regions of the fingermark, due to the surface sensitivity of the measurement, it is less well suited to determine absolute water content in a fingermark. The high brightness and high collimation of synchrotron radiation in the Terahertz/Far-infrared (THz/Far-IR) region is capable of collecting high spectral resolution data with sufficient sensitivity to observe and record the pure-rotational water vapour transitions. High spectral resolution THz/Far-IR spectroscopy therefore provides an intriguing opportunity to estimate the total water content in fingermark residues by heating the sample and evaporating the water into the gas phase for high spectral resolution analysis. Taken together, the results from synchrotron-sourced ATR-IRM and THz/Far-IR gas-phase spectroscopy provide new insights into the chemical changes that occur within fingermarks as a function of time since

deposition, as well as an estimate of the total initial water content contained within a fingerprint.

6.2 Methodology

6.2.1 Fingerprint Deposition: Synchrotron ATR-IRM

Fingermarks for the IRM study were deposited directly onto the ATR germanium (Ge) hemispherical crystal by lightly pressing the centre of the fingertip on the centre of the crystal for 5 seconds (See Figure 6.1). Natural fingerprints were collected from 12 donors, donor information is provided in Table 6.1. Fingerprint droplets were mapped every ~hour for a period of 7-13 hours using the IRM as described in section 2.5.3.1.

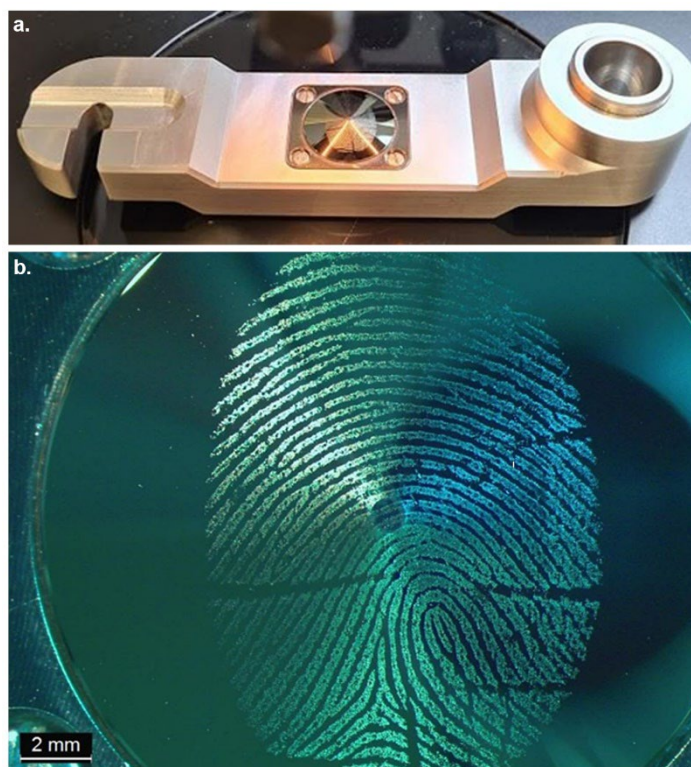


Figure 6.1: (a) Macro-ATR cantilever fitted with the 1 mm Ge crystal, fingerprint is deposited onto centre of crystal and (b) the optical microscope image of the corresponding fingerprint on the Ge crystal.

Table 6.1: *Details of the donors used in this study*

Donor	Age	Gender	Cosmetic Use
1	77	Male	None reported
2	27	Female	None reported
3	22	Male	None reported
4	24	Male	None reported
5	41	Male	None reported
6	23	Female	Yes
7	55	Male	Yes
8	48	Male	None reported
9	26	Female	Yes
10	40	Female	Yes
11	34	Female	None reported
12	23	Female	None reported

6.2.2 Fingermark Deposition: Synchrotron THz/Far-IR Spectroscopy

Fingermarks were studied using the Far-IR Spectrometer as per the method described in section 2.5.3.2. Fingermarks for this study were collected on a standard 200 mm long 5 mm in diameter chemistry glass rod, from donors 7 and 10 (see Table 6.1 for donor information). The glass rod was first cleaned with isopropanol and left to warm to room temperature prior to sample deposition. Then, the fingermarks were deposited by rolling the fingertips across a glass rod back and forth for 5 seconds. Three types of fingermarks were collected, and are outlined in Table 6.2; these types were decided based on the varying amounts of water that could be yielded.

Table 6.2: THz/Far-IR fingerprint sample types

Sample Type	Sample Preparation
Natural	Donor was instructed to go about their daily activities for 30 minutes, no washing of the hands in this time.
Air	Donor was instructed not to touch anything for 30 minutes, hands were open to atmosphere
Gloves	Donor was instructed not to touch anything for 20 minutes then wore nitrile gloves for 10 minutes

In order to quantify the amount of water detected in the donor fingerprints, a calibration curve was generated from carefully measured volumes of deionised water (0.25 μL , 0.5 μL , 0.875 μL , 1.25 μL , and 1.5 μL). The water was deposited in the middle of the glass rod using a 0.1 – 2.5 μL pipette.

6.3 Results and Discussion

6.3.1 The Chemical and Morphological Changes in Eccrine and Lipid Material within Natural Latent Fingermarks in the first 13 hours following Deposition.

In this study, the chemical and morphological changes of individual droplets within natural fingermarks were measured in the first 7 - 13 hours following sample deposition using synchrotron ATR-IRM. Specifically, spectroscopic marker bands of eccrine and sebaceous material were monitored (eccrine marker: O-H stretching ($3000-3500\text{ cm}^{-1}$), sebaceous marker: C-H stretching of lipids ($2800-3000\text{ cm}^{-1}$)), as per previous studies.⁹⁵

Twelve donors provided fingermark samples in which droplets containing eccrine and lipid material could be identified. Across each sample, it was noticeable that the fingermarks deposited by different donors showed diverse morphology and varied composition of lipid and eccrine material, which were consistent with past work.⁹⁵ Figure 6.2 shows a representative sample of a fingermark droplet provided by donor 1. This particular sample appears to be a central eccrine droplet surrounded with lipid material. Across a period of 7 hours, there is a noticeable change in lipid and eccrine concentration, based on the C-H stretching ($2800-3000\text{ cm}^{-1}$) and O-H stretching ($3000-3500\text{ cm}^{-1}$) bands, previously reported to be indicative of these substituents.⁹⁵ This sample shows an exponential decrease in the signal attributed to the eccrine material, based on the average intensity of the O-H stretching peak integrated across the droplet area. This trend can be further observed when looking directly at the spectra extracted from the images (Figure 6.3), where the peak intensity of the O-H stretching peak ($3000-3500\text{ cm}^{-1}$), and the O-H bending peak ($1540-1700\text{ cm}^{-1}$) can be clearly seen to decrease as the time since deposition increases. In contrast, the opposite trend is seen for sebaceous material, with a clear increase in peak intensity for the C-H stretching ($2800-3000\text{ cm}^{-1}$) band (Figure 6.3).

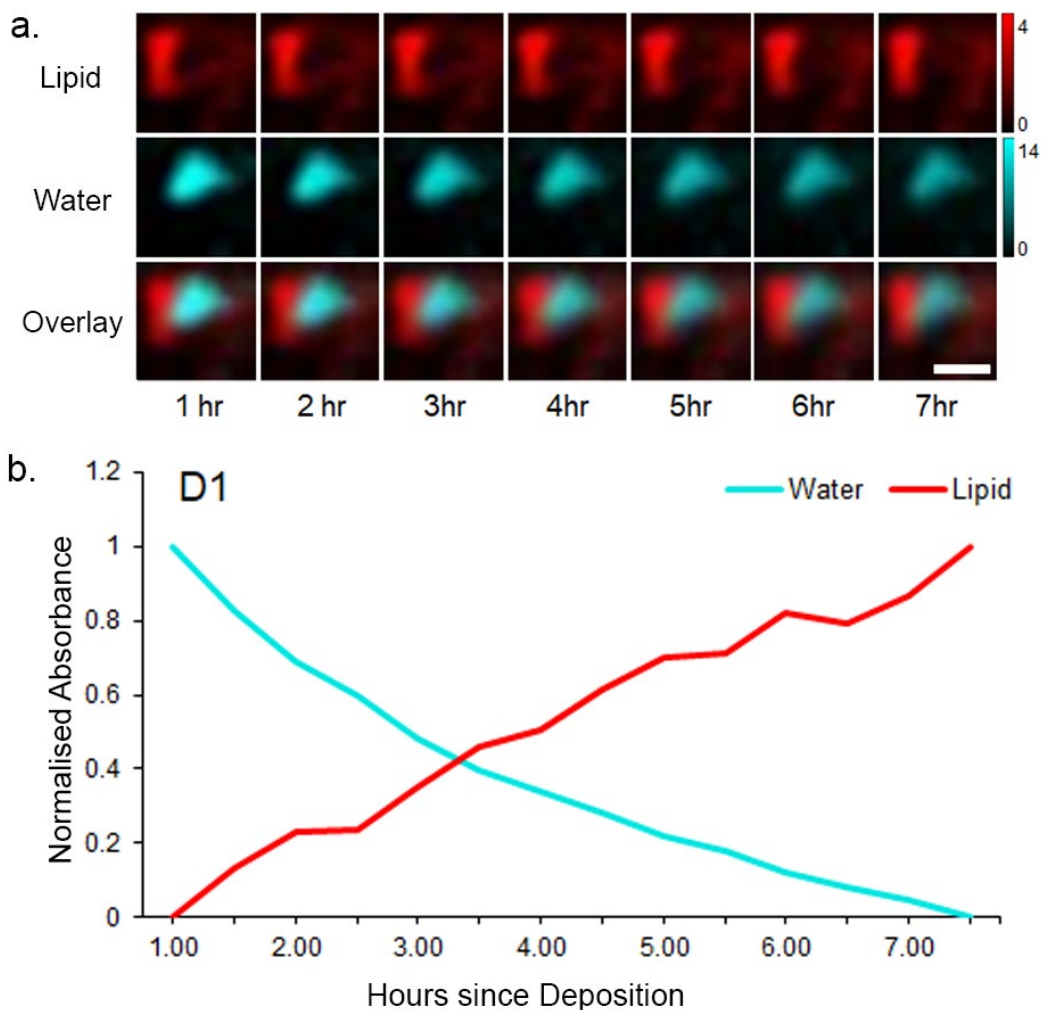


Figure 6.2: Representative example of time-course (7 hour) changes in lipid and H₂O content during air-drying of a natural fingerprint, as revealed by ATR-FTIR mapping approach (a). False colour ATR-FTIR maps were generated by integrating over the $\nu(\text{C-H})$ stretching bands ($2800\text{-}3000\text{ cm}^{-1}$) as a marker of lipid material (top row) and $\nu(\text{O-H})$ stretching bands of H₂O ($3000\text{-}3500\text{ cm}^{-1}$) as a marker for eccrine material (middle row). Overlay images are displayed in the bottom row. Scale bar $20\text{ }\mu\text{m}$. The relative changes in lipid and H₂O content as a function of air-drying time can also be visualised as the normalised average band area calculated across the entire droplet (b). Representative sample corresponds to Donor 1 (D1).

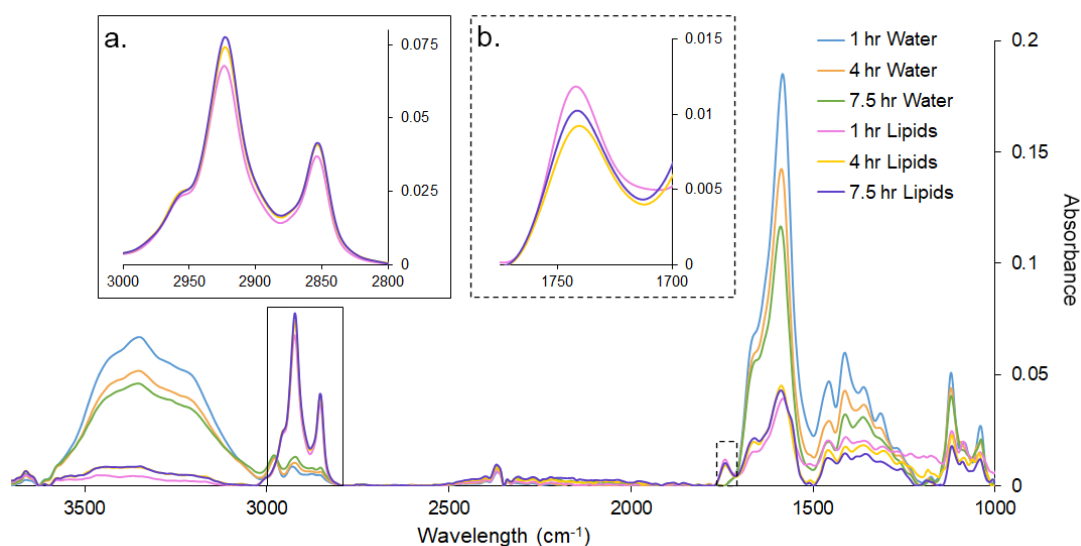


Figure 6.3: Representative examples of ATR-FTIR spectra collected from a natural fingermark after 1 hour, 4 hours, and 7.5 hours of air-drying period (from the same dataset presented in Figure 6.2, donor 1). Representative spectra are presented from image regions enriched in lipid material or water (using H₂O content as a marker of eccrine components). The most pronounced changes in lipid concentration are highlighted in (a) $\nu(\text{C-H})$ stretching band (2800-3000 cm^{-1}) and (b) $\nu(\text{C=O})$ stretching band (1715-1750 cm^{-1}).

To help put into context the inter-donor variance that was observed across 12 donors, intra-donor variance was examined (Figure 6.4). Intra-donor variance was examined across 3 droplets within the same fingermark (Figure 6.4a). The time-course chemical changes within the three droplets displayed a marked degree of similarity (Figure 6.4b), indicating relatively small intra-donor variation with respect to time-course changes. Although the response as a function of time was similar across all three droplets, intra-droplet variation is evident, as can be seen in the plot of an average droplet spectrum with the line thickness weighted to the standard deviation (Figure 6.4c, average and standard deviation calculated from 147 spectra within the droplet). For comparison the average spectrum from the 12 donors in this study, also weighted to the standard deviation is presented (Figure 6.4d).

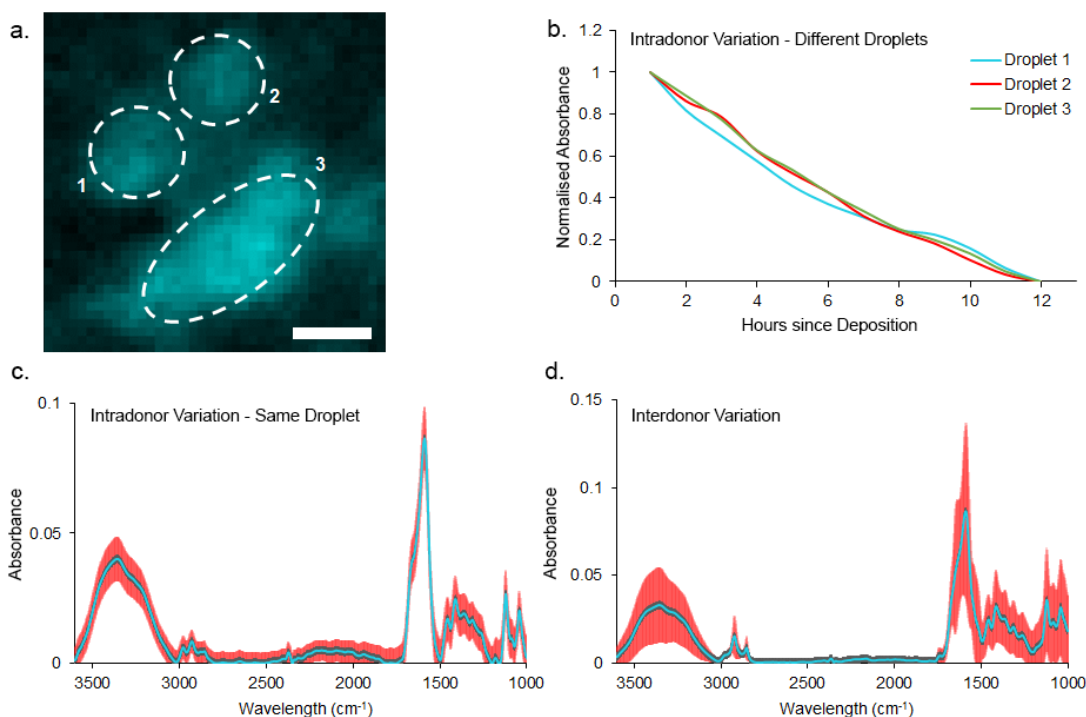


Figure 6.4: 3 droplets mapped within the same fingerprint from Donor 6, droplets marked in the false colour ATR-FTIR map generated by integrating over $\nu(\text{O-H})$ stretching bands of H_2O ($3000\text{--}3500\text{ cm}^{-1}$) (a), the relative changes in H_2O content as a function of air-drying time for each droplet is visualised as the normalised average band area calculated across the entire droplet (b). Intra-droplet variation is evident, as can be seen in the plot of an average droplet spectrum with the line thickness weighted to the standard deviation calculated from 147 spectra within droplet 3 as identified in A (c) and the average spectrum from the 12 donors in this study, weighted to the standard deviation (d).

A decrease in water content was observed across 10 donors over time, as represented in Figure 6.5, with the water content appearing to plateau after approximately 8 hours. As eccrine material is an aqueous mixture, the reduction in water content can be attributed to evaporation. This expands on recent work by Keisar *et al.*, which explored the evaporation of water within the first few minutes post fingerprint deposition.⁴³ Although demonstration that water evaporates from a fingerprint is not particularly surprising, a key observation from these results has been the evidence that water can continue to evaporate from a fingerprint sample at room temperature for at least 8 hours. Please note this study was conducted at

ambient temperature and humidity in an air-conditioned laboratory, the nitrogen purge was switched off and the purge box opened to replicate a natural evaporation of water in the fingerprint throughout the measurement. Temperature and humidity data was reported for 11 donors and is presented in Figure 6.6. These factors remained fairly consistent throughout the measurement and no trend was evident when comparing the rate of dehydration to temperature and humidity changes in this study.

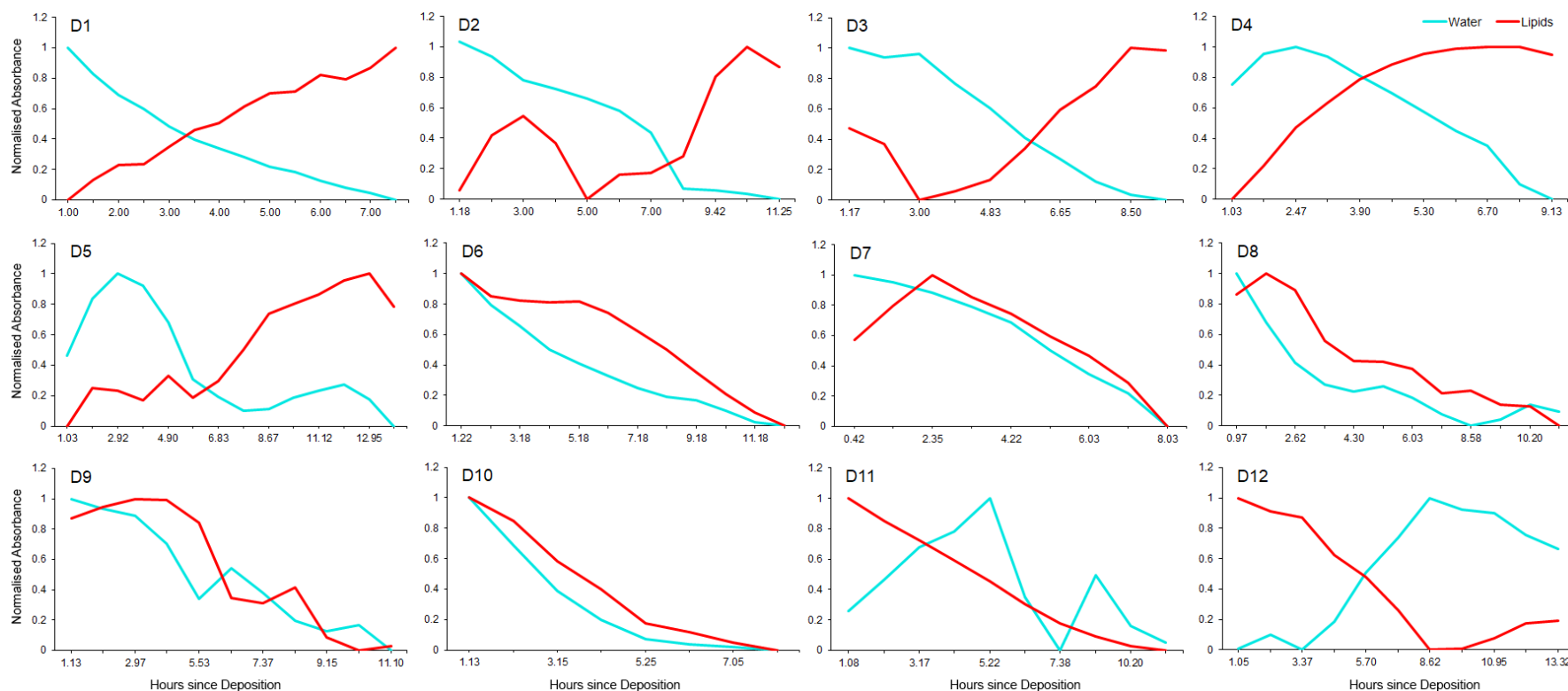


Figure 6.5: Time-dependent changes in H₂O content (as a marker of eccrine material) and lipid content during air-drying of natural fingermarks was measured for 12 individual fingermarks (donors 1 – 12), using the same ATR-FTIR approach. As expected, a strong time-dependent decrease in H₂O content was observed in donors 1-10 (cyan), with exceptions observed in donors 11 and 12. The H₂O content was measured as the integrated area across $\nu(\text{O-H})$ absorbance bands (3000 – 3500 cm^{-1}), and lipid content (red) was measured across $\nu(\text{C-H})$ absorbance bands (2800 – 3000 cm^{-1}). The average band area was calculated across the entire fingermark droplet.

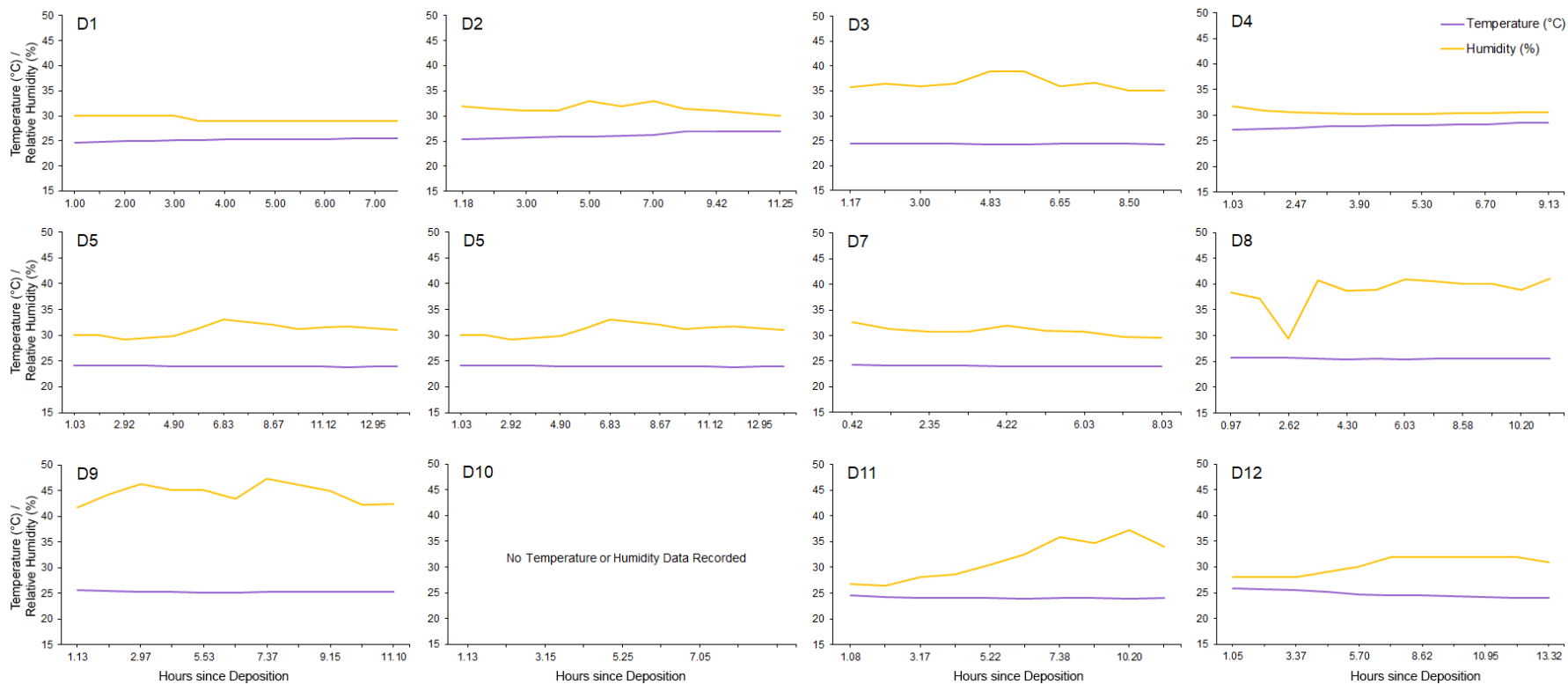


Figure 6.6: Temperature and relative humidity data recorded within the laboratory space for the same period as the ATR-FTIR data reported in Figure 6.5. Evaporation rate does not appear to relate to the temperature and humidity changes measured in this study.

In addition, the lipid concentration and distribution were observed to be more varied with greater disparity seen across donors compared to the eccrine material. The sample shown in Figure 6.2 demonstrates a relative increase in lipid material, this was consistent with 5 donors, whilst the remaining 7 donors decreased in overall lipid concentration. The discrepancies could be justified by the increase in concentration of the residual lipid content, and also the redistribution of lipid material that led to an increase in contact areas between the lipid material and the Ge crystal as a result of the water evaporation. Interestingly, a distinct pattern of changes in lipid composition was observed. The C-H stretching peaks ($2800-3000\text{ cm}^{-1}$) showed a gradual increase over the 8 hour period, suggesting an increase in lipid concentration. However, the C=O stretching region ($1715-1750\text{ cm}^{-1}$) decreased in the first 4 hours and then increased between 4 to 8 hours. These results could indicate initial degradation of lipid material before the potential oxidation of these compounds.

The oxidation of sebaceous lipids, such as squalene, cholesterol and unsaturated fatty acids, has previously been reported in studies aiming to predict fingerprint age.^{16, 53, 311} Many of the oxidation by-products formed are quite volatile and will promote further chemical alteration of the residue.^{79, 312} Factors influencing the starting material in fingerprint residue have been shown to have a major impact on the rate of degradation of these components, making it impossible to identify universal trends.^{3, 79} The findings reported here reinforce the challenges of calculating time since deposition, with significant variation appearing within the morphology and lipid composition of single droplets in fresh natural fingerprints. These studies focused on the first 13 hours since deposition, further work should be done to explore a longer time period to investigate whether further morphological and chemical changes can be observed on the macro scale with this method over longer time periods.

Noticeably, Donor 12 was an anomaly, with the O-H peak intensity increasing over the first 8 hours (Figure 6.5). To investigate further, measurements were repeated with this donor by taking triplicate fingerprint samples (Figure 6.7). The two repeat measurements behaved more consistently with the rest of the data for eccrine material, displaying a time-dependent decrease in the O-H peak, which can be

ascribed as water content in the eccrine material (Figure 6.7). The variation in response from donor 12 can be attributed to the high lipid content present in the initial fingerprint and the large size of the droplet. The droplet imaged in replicate 1 appeared to cover the entire imaged area, meaning the droplet size was $> 80 \times 80 \mu\text{m}^2$, whereas replicates 2 and 3 were smaller, fitting within a $75 \times 75 \mu\text{m}^2$ imaged area. It is understood that the morphological size of the original drop would appear to change the rate of evaporation of water within the sample. It is possible evaporation occurred outside the immediate imaged area, and thereby is not considered within the results. Amongst the triplicate samples from the single donor it was apparent that the lipid material also did not behave consistently, with two replicate measurements showing an increase and one a decrease in lipid material. These results did not appear to be related to droplet size or distribution adjacent to eccrine material, although previous work has demonstrated an increase in lipid degradation when fingerprints were stored in an aqueous environment.⁵² On a longer time scale, it is possible that the sebaceous material distributed amongst the aqueous material within a fingerprint could influence the rate of degradation. This emphasises how unpredictable the rate of change of a fingerprint is, even within the same donor, suggesting it near impossible to use the chemistry of the fingerprint to predict the time of deposition without knowing the initial chemistry of the residue.

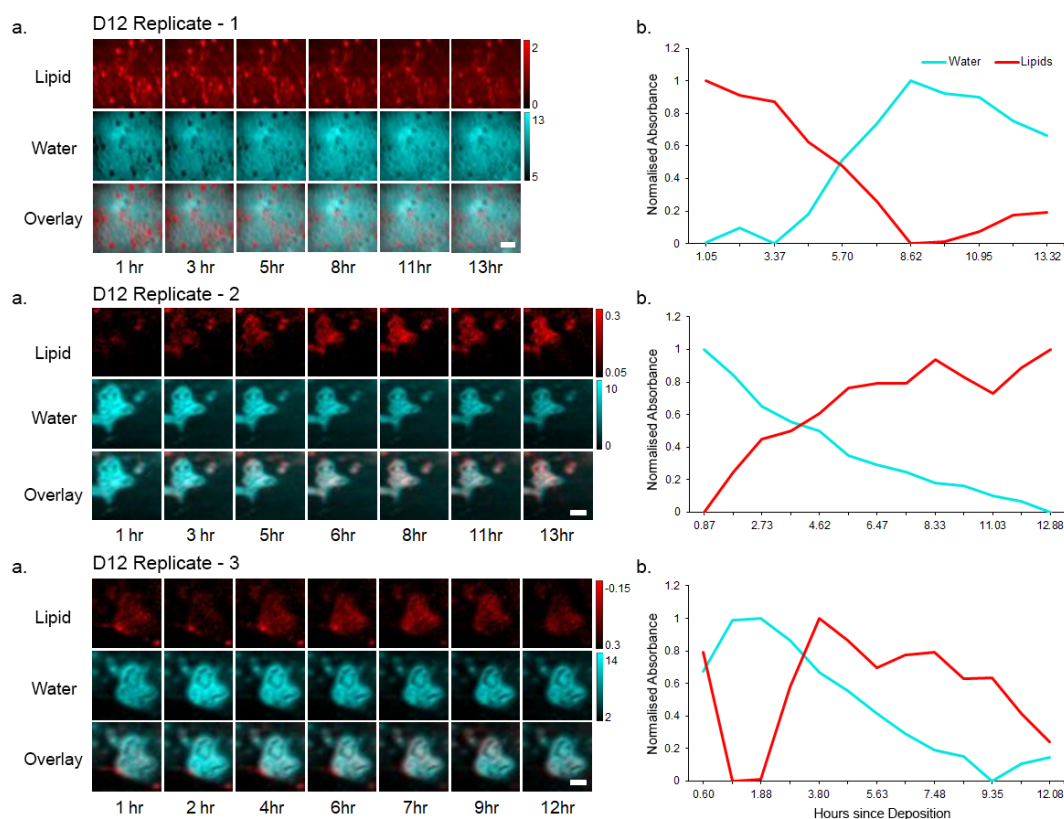


Figure 6.7: Analysis of intra-donor variance in triplicate fingermarks from donor 12. (a) False colour ATR-FTIR maps were generated by integrating over the $\nu(\text{C-H})$ stretching bands ($2800\text{-}3000\text{ cm}^{-1}$) as a marker of lipid material (top row) and $\nu(\text{O-H})$ stretching bands of H_2O ($3000\text{-}3500\text{ cm}^{-1}$) as a marker for eccrine material (middle row). Overlay images are displayed in the bottom row. (b) The relative changes in lipid and H_2O contents as a function of air-drying time can also be visualised as the normalised average band area calculated across the entire droplet. Scale bar $20\text{ }\mu\text{m}$.

This study is the first to report the use of chemical imaging techniques to demonstrate how fingermark chemistry changes at ambient temperature in the immediate hours following deposition, and has important implications for fingermark research. Specifically, the International Fingerprint Research Group (IFRG) provides guidelines when conducting fingermark research and recommends the use of fingermarks, which are left to age for a minimum of 24 hours before development.⁹¹ These guidelines have largely been developed from operational observations, and this current study therefore provides valuable experimental data to support the guidelines. The results shown here provide context for why fresh fingermarks should not be used for research into latent fingermark detection techniques, demonstrating

the changes in residue chemistry, specifically the evaporation of water content that can occur within the first 8 hours following deposition. By leaving fingerprints for 24 hours, researchers can provide a more realistic representation of what would be encountered in casework as it is unlikely for fingerprints to be collected within the hours immediately following transfer of material. It should be noted that this study was carried out on a germanium crystal substrate surface, it is likely that the rate of change in droplet morphology and chemistry is impacted by surface topography, this fundamental study demonstrates the potential change on a non-porous surface, variation in the rates of change on alternative surfaces, particularly porous and semi-porous surfaces, is expected and needs to be explored further. Whilst this study focused primarily on the first 13 hours following deposition, further work should be conducted to see whether additional changes can be seen in the morphology and chemical composition of the droplet for a longer time frame. Indeed, earlier work by Ricci *et al.*, has highlighted that upon heating, chemical changes do indeed occur in latent fingerprints across extended time periods, and there is substantial scope to further use ATR-IRM to investigate chemical changes to fingerprints under a variety of conditions of forensic interest.¹⁸⁷

6.3.2 Measuring the Volume of Water Lost through Evaporation of Latent Fingerprints

The results from the IRM work demonstrated that eccrine material in a fingerprint showed a substantial change in the first hours since deposition, thus impacting the chemical composition and the morphology of the mark as it ages. Whilst eccrine sweat is made up of 99% water, water is estimated to comprise anywhere between 20-70% of the total fingerprint residue, varying significantly between donors based on a range of factors.⁴³⁻⁴⁴ There are a number of challenges in measuring the volume of material deposited in fingerprint residue, with the inherent variability and influence from the surrounding environment, making it difficult to standardise an analytical approach. Recent work has utilised a quartz crystal microbalance (QCM) to determine the amount of water lost through evaporation from a fingerprint sample.⁶

⁴³ The results demonstrated that the majority of water content was evaporated in

the first few minutes following deposition, however the results shown here suggest there is a longer time period of evaporation.⁴³

High-spectral resolution gas-phase THz/Far-IR spectroscopy was used to estimate the total volume of water contained in a fingerprint. Fingerprints were heated to 70 °C, and the water content measured in the gas phase using a gas cell with 2.5 m optical path difference. The water content was determined using a linear calibration, developed from the rotational spectrum of water; a portion of the rotational spectrum void of strong and overlapping peaks was selected, in particular a peak located at 202.69 cm⁻¹ was chosen (see Figure 6.8). A plot of the absorbance intensities with respect to volume of H₂O deposited on the glass rod showed a linear relationship with an *R*² value of 0.9932. This linear relationship was then used to predict the volume of water in the fingerprint sample, outlined in Figure 6.9. Of the three sets of fingerprints taken the natural fingerprints had the lowest water content, between 14-20 µg (volume of water converted to mass of water, assuming a density of 1 g/mL). Two further samples were taken, fingerprints deposited after the hands were left in the air for 30 minutes, minimising contact with a surface and fingerprints deposited after wearing nitrile gloves for 10 minutes. These samples demonstrated increased water content, 60-79 µg and 77-101 µg respectively. The increase in water content could possibly be attributed to the loss of material on the surface of the hands in natural daily behaviour, by minimising contact with a surface the eccrine material is left to build up on the fingertip, potentially increasing the material deposited in this study. Wearing gloves can increase the amount of eccrine material produced by increasing the perspiration rate from the hands, and therefore the increase in water content calculated from these samples is not unexpected.⁸⁰

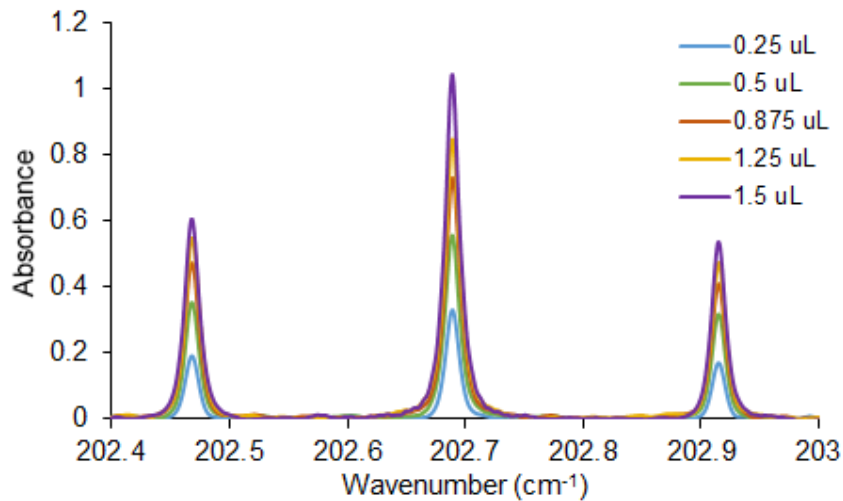


Figure 6.8: THz/Far-IR gas phase spectra showing H_2O pure-rotational spectral lines for calibration samples, highlighting the linear response between band intensity and volume of water from which the gas phase sample was generated (0.25 μL , 0.5 μL , 0.875 μL , 1.25 μL , and 1.5 μL). The selected spectral region shows the rotational transitions of H_2O at 202.47cm^{-1} , 202.69cm^{-1} and 202.92cm^{-1} .

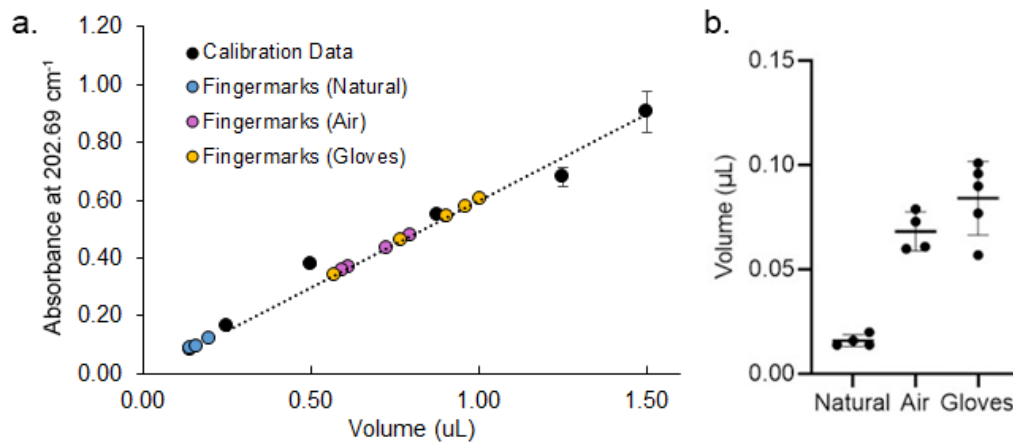


Figure 6.9: (a) The volume of water contained in a latent fingerprint was quantified from the calibration curve (black dots, $R^2 = 0.9932$) using the rovibrational transition of H_2O at 202.69 cm^{-1} . (b) The volume of water was calculated for natural fingerprints ($n = 4$), fingerprints with hands left in the air for 30 minutes ($n = 4$), and fingerprints after wearing gloves for 10 minutes ($n = 5$). Volume shown for each data point in panel A, is for a set of 10 fingerprints deposited onto a sample substrate. The volume of water for each sample was therefore, divided by 10, to give an average water volume per fingerprint (as shown in panel B). Error bars in A, and B are equal to 2σ .

The literature contains few reports concerning the determination of the mass of a fingerprint, which are often conflicting with respect to the volume of water present in fingerprint residue.^{6, 43, 45} This is most likely due to the challenge of working on the microscale with material so sensitive to change and influence from the surrounding environment. The measurements recorded in this study are higher than that reported by Keisar *et al.*, with their total fingerprint mass calculated to be between 2 – 9 µg.⁴³ Their approach measured a 0.2 cm² area of the fingerprint (~ 1/10th of the full fingerprint surface area) using a QCM, with the entire mass calculated using the Sauerbrey equation, not taking into account the inherent variability across a fingerprint.⁴³ Bleay *et al.* report studies which measured a fingerprint mass across a range of 0.33 and 29.00 µg, with large discrepancies not unexpected as the water content is anticipated to vary significantly between samples.⁶ The results shown here for natural fingerprints appear to lie at the upper range of this mass, suggesting the water content could comprise 40 – 70% of the total fingerprint mass at the time of deposition, a figure which aligns with recently proposed values in literature.⁴³ Further work should consider the correlative use of high-spectral resolution gas-phase THz/Far-IR spectroscopy alongside microbalance measurements, using an increased number of donors to improve the accuracy of this method and provide complementary data to assist in the determination of the volume of water lost through evaporation of fingerprint samples.

6.4 Conclusions

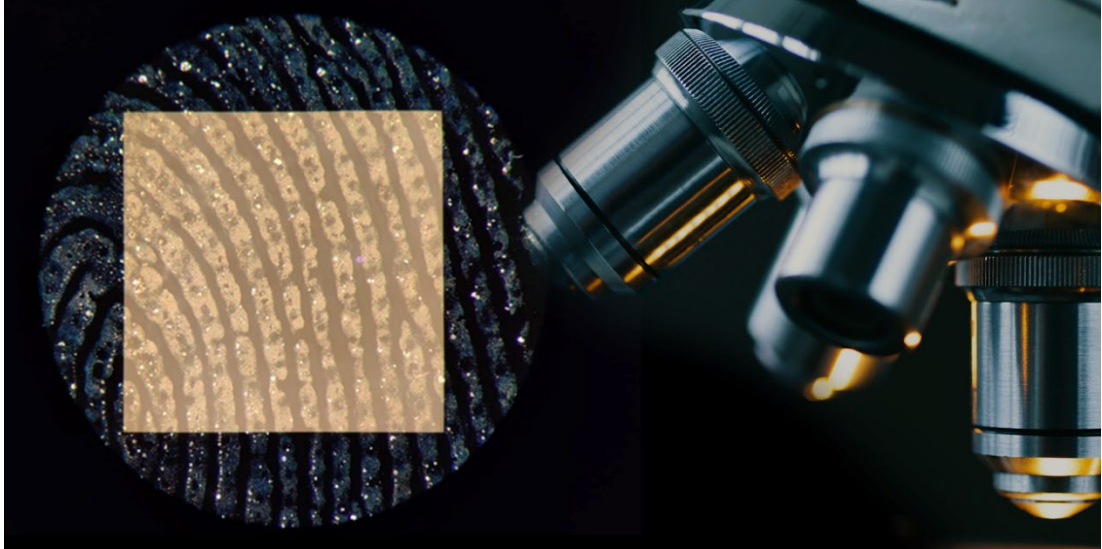
This study has reinforced the complexity of fingerprint chemistry using synchrotron FTIR spectroscopy in both mid-IR and THz/Far-IR spectral ranges. Single droplets within natural fingerprints from 12 donors were imaged using the synchrotron ATR-IRM technique. The variation in the initial chemical composition and morphology has demonstrated a significant impact on the rate of change of the droplet over time, highlighting the inherently complex nature of this biological material. Broadly, there is a noticeable change within the fingerprint sample in the immediate hours following deposition, with a decrease in water content seen within the first 8 hours. The lipid material is more multifaceted, with samples shown to both increase and decrease in lipid concentration following deposition due to the degradation and

redistribution of lipid material. The results challenge the suggestion that one can simply predict the age since deposition of a fingerprint. The variability of interdonor and intradonor fingerprint chemistry corroborates the unpredictable nature of the rate of change of fingerprint residue, particularly without knowledge of the initial material present. Imaging this change in the first few hours explicitly shows how dynamic fingerprint residue is, which must be considered in both operational and research contexts.

To determine the extent of change in water content, high-spectral resolution gas-phase THz/Far-IR spectroscopy was used to quantify the amount of water that could be evaporated from a fingerprint sample. The intensity of the rotational transitions of water vapour were measured to determine the approximate loss of water ranging between 14 to 101 μg for natural fingerprints and those which had been groomed for increased water content. The results appear to be within the same range as those recently reported for natural fingerprints;^{6, 46} however, given the highly variable nature of fingerprint material further work should be conducted with a wider range of donors to provide a more developed understanding of the potential of this method to measure water within fingerprint residue.

Chapter 7

Conclusions and Recommendations for Future Work



7.1 Conclusions

This thesis aimed to improve the fundamental understanding of fingerprint chemistry by exploring the distribution of organic and inorganic species in fingerprint residue. There are a number of development methods used operationally to detect latent fingerprints, however the majority of fingerprints are never successfully recovered from crime scenes and used in criminal investigations.² The detection of latent fingerprints relies on a range of chemical or physical treatments, which generally target the chemical differences between the fingerprint residue and the substrate. Current methods can be hindered by variation due to issues with sensitivity, selectivity and lack of robustness. In recent years forensic research has aimed to improve current techniques and develop new evidence-based detection methods. The work presented throughout this thesis adds to the fundamental understanding of fingerprint residue to underpin future work to improve fingerprint recovery.

Chemical variability is intrinsic to working with biological samples such as fingerprints. Each sample is influenced by interdonor and intradonor variation, contributing to the inevitable challenge of trying to replicate consistent samples. Further the effects of the “triangle of interaction”, referring to the impact of the surface, surrounding environment and chemistry of the residue itself, can impact the degradation of the fingerprint samples over time.⁸⁰ The IFRG guidelines assist researchers by suggesting procedures which should be followed to provide reliable and accountable results.⁹¹ Though these guidelines are directed towards fingerprint research into the development of new visualisation methods, the principles are important to consider when exploring the residue itself, and were referred to throughout the design of this study.

Chapter 3 contains an investigation into the chemistry of fingerprints provided by the donor pool used throughout this thesis. Fingerprint development using a range of lipid and amino acid sensitive reagents, as well as physical treatments was conducted to compare the performance of these donors and reveal the variation in their residue chemistry. Amongst 13 donors selected for this study a substantial

variation in development performance was seen. Donors were categorised as poor, mid or good donors, a method used previously by fingerprint researchers.^{80, 90, 92} Of the 13 donors, four were classified as poor, six as mid and three as good, based on their overall performance of uncharged fingerprints. This meant that there was an appropriate range of donor chemistry amongst the donor pool selected and would be a suitable representation of the greater population for subsequent studies. Development of charged fingerprints saw an improvement in performance across the selected treatments, particularly acid Nile blue, as a post cyanoacrylate fuming stain, suggesting the increased lipid content provided by grooming fingerprints does not provide an accurate example of natural fingerprint secretions and were omitted from use throughout subsequent studies.

Amongst the “mid” classified fingerprint donors there was an interesting level of variation in the development performance from particular treatments. This was likely to be the result of varying fingerprint chemistry, specifically from the residue composition or from the total volume of material deposited. Previous research has focused on fingerprint chemistry by either using fingerprint development treatments as a visual tool, or by analysis of the bulk chemistry of the residue to identify the total composition of the mark.^{2-3, 14, 92-93, 277} This thesis combined chemical-specific and spatial information through the use of chemical imaging methods to explore how fingerprint chemistry can vary between donor groups, and impact their recovery.

7.1.1 Using Chemical Imaging Methods to Explore the Distribution of Elemental Material

The majority of published literature studying the chemical composition of fingerprint residue has focused on the organic material, using bulk methods to extract and identify individual compounds present and monitor the changes over time. Less is understood about the inorganic material which, in part, is due to the previous lack of advanced instrumentation with the required sensitivity and spatial resolution to explore the natural elemental content in fingerprint samples. Chapter 4 demonstrates for the first time that synchrotron sourced XFM can be used to study

the trace elements present within natural fingermarks with micron spatial resolution. A range of endogenous and exogenous metals and metal ions were mapped across fingermarks from fourteen donors showing substantial variability between donors. These results can help to explain the variation in detectability, particularly in treatments where metal ion chemistry is known to impact development performance. Interestingly, donors who were heavy cosmetic users had increased elemental content, suggesting that donor behaviour can impact the inorganic composition. These results inspired work presented in Chapter 5, exploring the fundamentals of transfer and persistence, which aligns with the NIFS Research and Innovation Roadmap, which lists the development of latent fingermarks and the transfer, persistence and frequency of trace evidence as research priorities.²⁶⁰ Research in these areas is the key to constructing a more robust data set and expanding the knowledge base of these fundamental forensic science processes, which can improve the interpretation of trace evidence.

Chapter 4 also summarises the outcomes of multimodal studies combining information from XFM, IRM and optical microscopy, demonstrating that on the macro-scale hotspots within the elemental maps correlate to the organic residues. On a smaller scale, within individual eccrine droplets there is evidence that elemental material secreted primarily through the eccrine glands is responsible for the endogenous inorganic components within latent fingermarks. This observation helps to explain variation in fingermark development, particularly reagents targeting eccrine material and in which metal ion chemistry is known to affect the detection reagents.

In Chapter 5 further work was conducted at the XFM beamline to investigate the process of transfer by imaging the exogenous inorganic material transferred to a person's hands and deposited in their fingermarks. The results indicate that even after brief handling of metal objects there is sufficient transfer of metals and metal ions which can be detected using XFM. The handling of a metal gun barrel increased the iron and lead content deposited in fingermark samples, whilst contact with a cartridge case increased the zinc and copper content, and party sparklers increased the barium content in fingermarks from all seven donors. The ease of transfer of

exogenous metals to fingerprint samples reinforces the complexity of fingerprint residue, with the indication that donor activity prior to fingerprint deposition can greatly impact the chemistry of the residue deposited. Further, the persistence of these metals were explored, with a brief period of hand washing shown to remove elemental material from the hands and from subsequent fingerprints. Chapter 5 also includes an investigation of the persistence of metals in fingerprints exposed to aqueous environments, indicating that endogenous metals, found within the aqueous organic material, are easily removed from a fingerprint after water submersion. This provides important forensic information when attempting to establish a timeline of events, suggesting that metal ions present within fingerprint samples, may be indicative of recent handling of metal objects and no exposure to an aqueous environment.

7.1.2 Morphological and Chemical Changes in Fingerprints over time

In Chapter 6, the bright synchrotron IR-beam was used to measure the chemical and morphological changes in individual droplets from natural fingerprints. Using ATR-IRM fingerprint residues were mapped for the first 7 - 13 hours following fingerprint deposition, and spectroscopic marker bands of eccrine and sebaceous material were monitored. The results visually demonstrate the evaporation of water across all donors, with a consistent decrease in the O-H stretching band noticeable within the first 8 hours. This finding has important context for fingerprint researchers, providing empirical data to reinforce the recommendations by the IFRG on the use of aged fingerprints. Fingerprints should be aged prior to development to provide a more realistic example of fingerprint residue, as it is rare, operationally, that a fingerprint will be recovered within the first 8 hours. The sebaceous material presented as more complex, with greater variation in the concentration of lipid material over time, characterised by the C-H stretching band. The inconsistencies in the rate of change in lipid material across the twelve donors reinforces the challenges of trying to predict fingerprint age, particularly without knowledge of the initial residues deposited.

The change in water content within fingermark residue is an important factor affecting fingermark chemistry in the initial stages after deposition. Despite this, studies continue to debate the volume of water present in fingermark residues due to challenges with current instrumental capabilities to measure such small volumes of the dynamic material. Access to the THz/Far-IR spectroscopy beamline offered the opportunity to measure the total water content in fingermark residues by exploiting the sensitivity of the Far-IR region to pure-rotational water vapour transitions. In Chapter 6, by evaporating the water from a fingermark sample into the gas phase, the amount of water lost from fingermark material was measured to range between 14 to 101 μg for natural and charged fingermarks. This value lies within the range of recent work using quartz crystal microbalances to measure the change in mass of a fingermark, suggesting Far-IR spectroscopy as a potential tool to contribute to better understanding the water content in fingermark residues.^{6, 46} Further work is underway to expand the donor set used in this study to gain a broader view of the variation in water content in natural fingermarks, used in conjunction with supplementary analytical methods.

7.1.3 Comparing Analytical Data to Results of Fingermark Development

Much of the research conducted to date analysing the chemistry of fingermark residues is to help inform the understanding of the performance of latent fingermark treatments. Treatment performance is known to vary between donors and with time since deposition, with greater difficulties in successful development of older fingermarks. This has been explored using larger donor sets in the hope of connecting particular donor traits to explain this variation.^{93, 277} By comparison this thesis looks at an individual level, to see whether the chemistry of the residue influences the performance of development methods. In chapter 3 the donor pool used throughout this study was investigated to ensure an appropriate range of donors was used to represent the variation expected across the general population. Whilst this work was important to be done prior to chemical imaging, retrospectively the results of fingermark development can be considered and related back to the chemical imaging data.

Table 7.1 outlines the development class of uncharged fingerprints taken from donors who participated in chemical imaging studies and their corresponding results from XFM and IRM studies, summarised as visibility of inorganic material and visible changes in water and lipid material over time. Despite the use of 1,2-indanedione (which is known to interact with certain metal ions) within the selected donor set, there is no obvious correlation between elemental material and fingerprint development, with both good and poor donors demonstrating visible ridge detail when imaged using XFM.^{35, 116, 124} It is expected there may have been intradonor variation between the samples taken on two separate occasions. Future work should consider repeat experiments with samples taken from each hand, one for chemical imaging and one for fingerprint development, to limit the effect of intradonor variation. An interesting result is that 2 donors classified as “poor” due to low development performance showed visible elemental ridge detail, suggesting XFM may be capable of detecting the inorganic material deposited in fingerprints where chemical visualisation of the organic material is not possible. Specific targeting of the elemental material, in this case zinc, may provide future research direction to improve development performance and the advancement of detection methods.

Table 7.1: Summary of development class for uncharged fingermarks and corresponding chemical imaging information

Donor Code	Development Class	XFM - Visible Ridge Detail	IRM - Water	IRM - Lipids
1	Poor	Yes	Decrease	Increase
16	Poor	No		
18	Poor	No		
19	Poor	Yes		
6	Mid	Yes	Decrease	Decrease
12	Mid	Yes	Increase	Decrease
13	Mid	No		
14	Mid	Yes		
17	Mid	No		
20	Mid	Yes		
3	Good	Yes	Decrease	Increase
4	Good		Decrease	Increase
15	Good	No		

The number of donors within the initial testing pool available for IR imaging was limited to five, however within this group variation was seen in the changes in water and lipid material within the first 13 hours following deposition. Although fingerprint development was conducted at least 24 hours after deposition, as per the IFRG guidelines, the behaviour of the organic material within the first few hours is likely to have consequences for the residual fingerprint and its subsequent development.⁹¹ Within this data set there was no apparent trend relating the chemical changes in fingerprint residue seen in the infrared data to fingerprint development performance. The changes imaged through synchrotron IRM are on the microscale, imaging the chemical changes within individual droplets. Whilst it is expected that the trends seen in relation to dehydration rates within the first 8 hours following deposition are similar on the macro scale, further work investigating this across an entire fingerprint may provide a more appropriate view of how these chemical changes link to fingerprint performance. A challenge with undertaking such experiments are the time limitations in fingerprint imaging. The chemical changes imaged in Chapter 6 occurred within the first 7-13 hours which was measured by imaging the fingerprint sample at a rate of hours, however large area scans, such as

the data presented in the multimodal studies in Chapter 4, take a number of hours to collect therefore limiting the number of scans which can be taken immediately following deposition. Future work should look at the long-term chemical changes in a large scale fingerprint study, with concurrent samples taken and detected using development methods. Ongoing advances in instrument technology may provide the opportunity for future studies to investigate the changes occurring within the immediate hours following deposition.

In principle, it would be expected that chemical differences in fingerprint residues should directly relate to the performance of fingerprint development techniques, particularly those which rely on chemical-specific interactions. The findings presented here did not present any apparent trends connecting the results of fingerprint development with the elemental and organic imaging data. The most logical explanation would be due to intradonor variability, with fingerprint samples used in this study taken on separate occasions. Future work should be conducted using split fingerprints to allow chemical development and chemical imaging to be performed on samples taken from the same deposition to provide a more conclusive view of the connection between fingerprint composition and development performance. There is also space to further the understanding of the composition of fingerprint residues through the use of bulk analysis, to determine how varied the chemical composition is on an individual level.

7.2 Summary

In summary this thesis demonstrates the potential of synchrotron-sourced spectroscopic and chemical imaging methods for fundamental research into the chemistry of fingerprint residues. By using a combination of advanced analytical instrumentation, paired with synchrotron sourced X-rays and IR light, the understanding of the organic and inorganic materials present in a fingerprint has been broadened. Despite the methods being unlikely to be used operationally, they have provided a unique view of fingerprint chemistry, measuring fingerprint residues with greater detection limits, spatial resolutions and spectral quality than comparable benchtop methods. The results presented here provide insight for future

studies to expand the understanding of current fingerprint visualisation methods and lay the groundwork to developing novel evidence-based techniques to improve the recovery of fingerprint samples for criminal investigations.

Chapter 8

References

1. Barnes, J. G., Chapter 1: History. In *The fingerprint sourcebook*, National Insistute of Justice: 2011.
2. Chadwick, S.; Moret, S.; Jayashanka, N.; Lennard, C.; Spindler, X.; Roux, C., Investigation of some of the factors influencing fingermark detection. *Forensic Science International* 2018, 289, 381-389.
3. Girod, A.; Ramotowski, R.; Weyermann, C., Composition of fingermark residue: A qualitative and quantitative review. *Forensic Science International* 2012, 223 (1), 10-24.
4. Bleay, S. M.; Croxton, R. S.; De Puit, M., *Fingerprint Development Techniques : Theory and Application*. John Wiley & Sons, Incorporated: Newark, United Kingdom, 2018.
5. Cadd, S.; Islam, M.; Manson, P.; Bleay, S., Fingerprint composition and aging: A literature review. *Science & Justice* 2015, 55 (4), 219-238.
6. Bleay, S. M.; Bailey, M. J.; Croxton, R. S.; Francese, S., The forensic exploitation of fingermark chemistry: A review. *WIREs Forensic Science* 2021, 3 (4), e1403.
7. Ricci, C.; Kazarian, S. G., Collection and detection of latent fingermarks contaminated with cosmetics on nonporous and porous surfaces. *Surface and Interface Analysis* 2010, 42 (5), 386-392.
8. Costa, C.; Jang, M.; de Jesus, J.; Steven, R. T.; Nikula, C. J.; Elia, E.; Bunch, J.; Bellew, A. T.; Watts, J. F.; Hinder, S.; Bailey, M. J., Imaging mass spectrometry: a new way to distinguish dermal contact from administration of cocaine, using a single fingerprint. *Analyst* 2021, 146 (12), 4010-4021.
9. de Ronde, A.; Kokshoorn, B.; de Poot, C. J.; de Puit, M., The evaluation of fingermarks given activity level propositions. *Forensic Science International* 2019, 302, 109904.

10. de Ronde, A.; van Aken, M.; de Poot, C. J.; de Puit, M., A study into evaluating the location of fingerprints on letters given activity level propositions. *Forensic Science International* 2020, 315.
11. de Ronde, A.; van Aken, M.; de Puit, M.; de Poot, C., A study into fingerprints at activity level on pillowcases. *Forensic Science International* 2019, 295, 113-120.
12. de Ronde, A.; Kokshoorn, B.; de Puit, M.; de Poot, C. J., Using case specific experiments to evaluate fingerprints on knives given activity level propositions. *Forensic Science International* 2021, 320.
13. Weyermann, C.; Roux, C.; Champod, C., Initial Results on the Composition of Fingerprints and its Evolution as a Function of Time by GC/MS Analysis. *Journal of Forensic Sciences* 2011, 56 (1), 102-108.
14. Frick, A. A.; Chidlow, G.; Lewis, S. W.; van Bronswijk, W., Investigations into the initial composition of latent fingerprint lipids by gas chromatography–mass spectrometry. *Forensic Science International* 2015, 254, 133-147.
15. Lee, H. C.; Ramotowski, R.; Gaensslen, R. E., *Advances in Fingerprint Technology*. 2 ed.; 2001.
16. Mong, G.; Petersen, C.; Clauss, T. Advanced fingerprint analysis project fingerprint constituents; Pacific Northwest National Lab., Richland, WA, US: 1999.
17. Benton, M.; Chua, M. J.; Gu, F.; Rowell, F.; Ma, J., Environmental nicotine contamination in latent fingerprints from smoker contacts and passive smoking. *Forensic Science International* 2010, 200 (1), 28-34.
18. Antoine, K. M.; Mortazavi, S.; Miller, A. D.; Miller, L. M., Chemical Differences Are Observed in Children's Versus Adults' Latent Fingerprints as a Function of Time*. *Journal of Forensic Sciences* 2010, 55 (2), 513-518.
19. Ferguson, L. S.; Wulfert, F.; Wolstenholme, R.; Fonville, J. M.; Clench, M. R.; Carolan, V. A.; Francese, S., Direct detection of peptides and small proteins in

- fingermarks and determination of sex by MALDI mass spectrometry profiling. *Analyst* 2012, 137 (20), 4686-4692.
20. Zhou, Z.; Zare, R. N., Personal Information from Latent Fingerprints Using Desorption Electrospray Ionization Mass Spectrometry and Machine Learning. *Analytical Chemistry* 2017, 89 (2), 1369-1372.
 21. O'Neill, K. C.; Hinnert, P.; Lee, Y. J., Potential of triacylglycerol profiles in latent fingerprints to reveal individual diet, exercise, or health information for forensic evidence. *Analytical Methods* 2020, 12 (6), 792-798.
 22. van Helmond, W.; van Herwijnen, A. W.; van Riemsdijk, J. J. H.; van Bochove, M. A.; de Poot, C. J.; de Puit, M., Chemical profiling of fingerprints using mass spectrometry. *Forensic Chemistry* 2019, 16, 100183.
 23. Dorakumbura, B. N.; Buseti, F.; Lewis, S. W., Investigations into sampling approaches for chemical analysis of latent fingerprint residue. *Forensic Chemistry* 2019, 14, 100166.
 24. Baker, L. B., Physiology of sweat gland function: The roles of sweating and sweat composition in human health. *Temperature (Austin, Tex.)* 2019, 6 (3), 211-259.
 25. Frick, A. A.; Fritz, P.; Lewis, S. W., Chemistry of Print Residue In *Encyclopedia of Forensic Sciences*, Saukko, P. J.; Houck, M. M., Eds. Academic Press: Waltham, 2013; pp 92-97.
 26. Croxton, R. S.; Baron, M. G.; Butler, D.; Kent, T.; Sears, V. G., Variation in amino acid and lipid composition of latent fingerprints. *Forensic Science International* 2010, 199 (1), 93-102.
 27. de Puit, M.; Ismail, M.; Xu, X., LCMS Analysis of Fingerprints, the Amino Acid Profile of 20 Donors. *Journal of Forensic Sciences* 2014, 59 (2), 364-370.
 28. Hansen, D. B.; Joullié, M. M., The development of novel ninhydrin analogues. *Chemical Society Reviews* 2005, 34 (5), 408-417.

29. van Dam, A.; Aalders, M. C. G.; van de Braak, K.; Hardy, H. J. J.; van Leeuwen, T. G.; Lambrechts, S. A. G., Simultaneous labeling of multiple components in a single fingermark. *Forensic Science International* 2013, 232 (1), 173-179.
30. Francese, S., Techniques for Fingermark Analysis Using MALDI MS: A Practical Overview. In *Advances in MALDI and Laser-Induced Soft Ionization Mass Spectrometry*, Cramer, R., Ed. Springer International Publishing: Cham, 2016; pp 93-128.
31. Mitchell, H. H.; Hamilton, T. S., The dermal excretion under controlled environmental conditions of nitrogen and minerals in human subjects, with particular reference to calcium and iron. *J Biol Chem* 1949, 178 (1), 345-361.
32. Cuthbertson, F. The chemistry of fingerprints; Atomic Weapons Research Establishment, Report No. 013/69: Aldermaston, 1969.
33. Cuthbertson, F. The chemistry of fingerprints; Atomic Weapons Research Establishment, SSCD Memorandum SAC/8/65: Aldermaston, 1965.
34. Cuthbertson, F. J. R. M. The chemistry of fingerprints; Atomic Weapons Research Establishment: Aldermaston, 1972.
35. S. Bleay, V. S., R. Downham, H. Bandey, A. Gibson, V. Bowman, L. Fitzgerald, T. Ciuksza, J. Ramadani, and C. Selway, *Fingerprint source book v2.0*; Home Office Centre for Applied Science and Technology (CAST): 2017.
36. Sykes, S.; Bond, J. W., A Comparison of Fingerprint Sweat Corrosion of Different Alloys of Brass. *Journal of Forensic Sciences* 2013, 58 (1), 138-141.
37. Wightman, G.; O'Connor, D., The thermal visualisation of latent fingermarks on metallic surfaces. *Forensic Science International* 2011, 204 (1), 88-96.
38. Bailey, M. J.; Ismail, M.; Bleay, S.; Bright, N.; Elad, M. L.; Cohen, Y.; Geller, B.; Everson, D.; Costa, C.; Webb, R. P.; Watts, J. F.; de Puit, M., Enhanced imaging of developed fingerprints using mass spectrometry imaging. *Analyst* 2013, 138 (21), 6246-6250.

39. Szyrkowska, M. I.; Czerski, K.; Grams, J.; Paryjczak, T.; Parczewski, A., Preliminary studies using imaging mass spectrometry TOF-SIMS in detection and analysis of fingerprints. *The Imaging Science Journal* 2007, 55 (3), 180-187.
40. Thandauthapani, T. D.; Reeve, A. J.; Long, A. S.; Turner, I. J.; Sharp, J. S., Exposing latent fingermarks on problematic metal surfaces using time of flight secondary ion mass spectroscopy. *Science & Justice* 2018, 58 (6), 405-414.
41. Bailey, M. J.; Bright, N. J.; Croxton, R. S.; Francese, S.; Ferguson, L. S.; Hinder, S.; Jickells, S.; Jones, B. J.; Jones, B. N.; Kazarian, S. G.; Ojeda, J. J.; Webb, R. P.; Wolstenholme, R.; Bleay, S., Chemical Characterization of Latent Fingerprints by Matrix-Assisted Laser Desorption Ionization, Time-of-Flight Secondary Ion Mass Spectrometry, Mega Electron Volt Secondary Mass Spectrometry, Gas Chromatography/Mass Spectrometry, X-ray Photoelectron Spectroscopy, and Attenuated Total Reflection Fourier Transform Infrared Spectroscopic Imaging: An Intercomparison. *Analytical Chemistry* 2012, 84 (20), 8514-8523.
42. Worley, C. G.; Wiltshire, S. S.; Miller, T. C.; Havrilla, G. J.; Majidi, V., Detection of Visible and Latent Fingerprints Using Micro-X-ray Fluorescence Elemental Imaging *. *Journal of Forensic Sciences* 2006, 51 (1), 57-63.
43. Keisar, O.; Cohen, Y.; Finkelstein, Y.; Kostirya, N.; Ben-David, R.; Danon, A.; Porat, Z. e.; Almog, J., Measuring the water content in freshly-deposited fingermarks. *Forensic Science International* 2019, 294, 204-210.
44. Kent, T., Water content of latent fingerprints – Dispelling the myth. *Forensic Science International* 2016, 266, 134-138.
45. Bright, N. J.; Willson, T. R.; Driscoll, D. J.; Reddy, S. M.; Webb, R. P.; Bleay, S.; Ward, N. I.; Kirkby, K. J.; Bailey, M. J., Chemical changes exhibited by latent fingerprints after exposure to vacuum conditions. *Forensic Science International* 2013, 230 (1), 81-86.
46. Croxton, R. Analysis of Latent Fingerprint Components by Gas Chromatography-Mass Spectrometry. University of Lincoln, 2008.

47. Wargacki, S. P.; Lewis, L. A.; Dadmun, M. D., Enhancing the Quality of Aged Latent Fingerprints Developed by Superglue Fuming: Loss and Replenishment of Initiator. *Journal of Forensic Sciences* 2008, 53 (5), 1138-1144.
48. Sodhi, G. S.; Kaur, J., Powder method for detecting latent fingerprints: a review. *Forensic Science International* 2001, 120 (3), 172-176.
49. De Alcaraz-Fossoul, J.; Mestres Patris, C.; Balaciart Muntaner, A.; Barrot Feixat, C.; Gené Badia, M., Determination of latent fingerprint degradation patterns-- a real fieldwork study. *International Journal of Legal Medicine* 2013, 127 (4), 857-70.
50. Archer, N. E.; Charles, Y.; Elliott, J. A.; Jickells, S., Changes in the lipid composition of latent fingerprint residue with time after deposition on a surface. *Forensic Science International* 2005, 154 (2), 224-239.
51. Darke, D.; Wilson, J., The total analysis by gas chromatography of palmar and forehead lipids. AERE Report No. G 1979, 1528.
52. Dorakumbura, B. N.; Buseti, F.; Lewis, S. W., Analysis of squalene and its transformation by-products in latent fingermarks by ultrahigh-performance liquid chromatography-high resolution accurate mass Orbitrap™ mass spectrometry. *Forensic Chemistry* 2020, 17, 100193.
53. Mountfort, K. A.; Bronstein, H.; Archer, N.; Jickells, S. M., Identification of Oxidation Products of Squalene in Solution and in Latent Fingerprints by ESI-MS and LC/APCI-MS. *Analytical Chemistry* 2007, 79 (7), 2650-2657.
54. Frick, A. A.; Chidlow, G.; Goodpaster, J. V.; Lewis, S. W.; van Bronswijk, W., Monitoring compositional changes of the lipid fraction of fingermark residues deposited on paper during storage. *Forensic Chemistry* 2016, 2, 29-36.
55. Michalski, S.; Shaler, R.; Dorman, F. L., The Evaluation of Fatty Acid Ratios in Latent Fingermarks by Gas Chromatography/Mass Spectrometry (GC/MS) Analysis. *Journal of Forensic Sciences* 2013, 58 (s1), S215-S220.

56. van Oorschot, R. A. H.; Szkuta, B.; Meakin, G. E.; Kokshoorn, B.; Goray, M., DNA transfer in forensic science: A review. *Forensic Science International: Genetics* 2019, 38, 140-166.
57. van Oorschot, R. A. H.; Jones, M. K., DNA fingerprints from fingerprints. *Nature* 1997, 387 (6635), 767-767.
58. Oleiwi, A. A.; Morris, M. R.; Schmerer, W. M.; Sutton, R., The relative DNA-shedding propensity of the palm and finger surfaces. *Science & Justice* 2015, 55 (5), 329-334.
59. Day, J. S.; Edwards, H. G. M.; Dobrowski, S. A.; Voice, A. M., The detection of drugs of abuse in fingerprints using Raman spectroscopy I: latent fingerprints. *Spectrochimica Acta Part A: Molecular and Biomolecular Spectroscopy* 2004, 60 (3), 563-568.
60. Groeneveld, G.; de Puit, M.; Bleay, S.; Bradshaw, R.; Francese, S., Detection and mapping of illicit drugs and their metabolites in fingermarks by MALDI MS and compatibility with forensic techniques. *Scientific Reports* 2015, 5 (1), 11716.
61. Day, J. S.; Edwards, H. G. M.; Dobrowski, S. A.; Voice, A. M., The detection of drugs of abuse in fingerprints using Raman spectroscopy II: cyanoacrylate-fumed fingerprints. *Spectrochimica Acta Part A: Molecular and Biomolecular Spectroscopy* 2004, 60 (8), 1725-1730.
62. Ismail, M.; Stevenson, D.; Costa, C.; Webb, R.; de Puit, M.; Bailey, M., Noninvasive Detection of Cocaine and Heroin Use with Single Fingerprints: Determination of an Environmental Cutoff. *Clinical Chemistry* 2018, 64 (6), 909-917.
63. Jang, M.; Costa, C.; Bunch, J.; Gibson, B.; Ismail, M.; Palitsin, V.; Webb, R.; Hudson, M.; Bailey, M. J., On the relevance of cocaine detection in a fingerprint. *Scientific Reports* 2020, 10 (1), 1974.
64. Chadwick, S.; Neskoski, M.; Spindler, X.; Lennard, C.; Roux, C., Effect of hand sanitizer on the performance of fingerprint detection techniques. *Forensic Science International* 2017, 273, 153-160.

65. Hinners, P.; O'Neill, K. C.; Lee, Y. J., Revealing Individual Lifestyles through Mass Spectrometry Imaging of Chemical Compounds in Fingerprints. *Scientific Reports* 2018, 8 (1), 5149.
66. Bradshaw, R.; Bleay, S.; Wolstenholme, R.; Clench, M. R.; Francese, S., Towards the integration of matrix assisted laser desorption ionisation mass spectrometry imaging into the current fingermark examination workflow. *Forensic Science International* 2013, 232 (1), 111-124.
67. Banas, A.; Banas, K.; Breese, M. B. H.; Loke, J.; Heng Teo, B.; Lim, S. K., Detection of microscopic particles present as contaminants in latent fingerprints by means of synchrotron radiation-based Fourier transform infra-red micro-imaging. *Analyst* 2012, 137 (15), 3459-3465.
68. Rowell, F.; Seviour, J.; Lim, A. Y.; Elumbaring-Salazar, C. G.; Loke, J.; Ma, J., Detection of nitro-organic and peroxide explosives in latent fingermarks by DART- and SALDI-TOF-mass spectrometry. *Forensic Science International* 2012, 221 (1), 84-91.
69. Emmons, E. D.; Tripathi, A.; Guicheteau, J. A.; Christesen, S. D.; Fountain, A. W., Raman Chemical Imaging of Explosive-Contaminated Fingerprints. *Applied Spectroscopy* 2009, 63 (11), 1197-1203.
70. Szykowska, M. I.; Czerski, K.; Rogowski, J.; Paryjczak, T.; Parczewski, A., Detection of exogenous contaminants of fingerprints using ToF-SIMS. *Surface and Interface Analysis* 2010, 42 (5), 393-397.
71. Love, C.; Gilchrist, E.; Smith, N.; Barron, L., Detection of anionic energetic material residues in enhanced fingermarks on porous and non-porous surfaces using ion chromatography. *Forensic Science International* 2013, 231 (1), 150-156.
72. Gilchrist, E.; Smith, N.; Barron, L., Probing gunshot residue, sweat and latent human fingerprints with capillary-scale ion chromatography and suppressed conductivity detection. *Analyst* 2012, 137 (7), 1576-1583.

73. Trace Metal Detection Technique in Law Enforcement. National Institute of Law Enforcement Criminal Justice: U.S. Government Printing Office, Washington, D.C. , 1970.
74. Bleay, S. M.; Grove, L. E.; Kelly, P. F.; King, R. S. P.; Mayse, K.; Shah, B. C.; Wilson, R., Non-invasive detection and chemical mapping of trace metal residues on the skin. *RSC Advances* 2014, 4 (37), 19525-19528.
75. Xing, Z.; Lu, S.; Wang, A.; Yang, R., A subsequent procedure for further deciphering weapons after application of the Trace Metal Detection Test (TMDT): Proof of concept. *Forensic Science International* 2020, 310, 110253.
76. Almog, J., Firearms: identification of handling of firearms/trace metal detection. In *Wiley Encyclopedia of Forensic Science*, 2009.
77. Almog, J.; Glattstein, B., Detection of firearms imprints on hands of suspects: study of the PDT-based field test. *Journal of Forensic Science* 1997, 42 (6), 993-996.
78. Xing, Z.; Yang, R.; Liu, W.; Zhang, H., A modified trace metal detection test for secondary imprints on porous substrates: A preliminary study. *Forensic Science International* 2019, 296, 28-38.
79. Frick, A. A.; Girod-Frais, A.; Moraleda, A.; Weyermann, C., Latent Fingermark Aging: Chemical Degradation Over Time. In De Alcaraz-Fossoul J. (eds) *Technologies for Fingermark Age Estimations: A Step Forward*, Springer, Cham.: 2021.
80. Sears, V. G.; Bleay, S. M.; Bandey, H. L.; Bowman, V. J., A methodology for fingermark research. *Science & Justice* 2012, 52 (3), 145-160.
81. Baniuk, K., Determination of age of fingerprints. *Forensic Science International* 1990, 46 (1), 133-137.
82. Wertheim, K., Fingerprint age determination: Is there any hope? *Journal of Forensic Identification* 2003, 53 (1), 42-49.

83. Cohen, Y.; Rozen, E.; Azoury, M.; Attias, D.; Gavrielli, B.; Elad, M. L., Survivability of Latent Fingerprints Part I: Adhesion of Latent Fingerprints to Smooth Surfaces. *Journal of Forensic Identification* 2012, 62 (1), 47-53.
84. Girod, A.; Spyratou, A.; Holmes, D.; Weyermann, C., Aging of target lipid parameters in fingermark residue using GC/MS: Effects of influence factors and perspectives for dating purposes. *Science & Justice* 2016, 56 (3), 165-180.
85. Barnett, P. D.; Berger, R. A., The Effects of Temperature and Humidity on the Permanency of Latent Fingerprints. *Journal of the Forensic Science Society* 1976, 16 (3), 249-254.
86. D'Uva, J.; Brent, N.; Boseley, R.; Ford, D.; Sauzier, G.; Lewis, S., Preliminary investigations into the use of single metal deposition II (SMD II) to visualise latent fingermarks on polyethylene 'zip-lock' bags in Western Australia. *Forensic Chemistry* 2020, 18, 100229.
87. Bleay, S.; Fitzgerald, L.; Sears, V.; Kent, T., Visualising the past – An evaluation of processes and sequences for fingermark recovery from old documents. *Science & Justice* 2019, 59 (2), 125-137.
88. Scruton, B.; Robins, B. W.; Blott, B. H., The deposition of fingerprint films. *Journal of Physics D: Applied Physics* 1975, 8 (6), 714-723.
89. Girod, A.; Ramotowski, R.; Lambrechts, S.; Misriela, P.; Aalders, M.; Weyermann, C., Fingermark age determinations: Legal considerations, review of the literature and practical propositions. *Forensic Science International* 2016, 262, 212-226.
90. Kent, T., Standardizing protocols for fingerprint reagent testing. *Journal of Forensic Identification* 2010, 60 (3), 371-379.
91. International Fingerprint Research Group. Guidelines for the Assessment of Fingermark Detection Techniques. *Journal of Forensic Identification* 2014, 64 (2), 174-200.

92. Girod, A.; Weyermann, C., Lipid composition of fingermark residue and donor classification using GC/MS. *Forensic Science International* 2014, 238, 68-82.
93. Fritz, P.; Frick, A. A.; van Bronswijk, W.; Beaudoin, A.; Bleay, S.; Lennard, C.; Lewis, S. W., Investigations into the Influence of Donor Traits on the Performance of Fingermark Development Reagents. Part 1: 1,2-Indanedione-Zinc Chloride. *Journal of Forensic Identification* 2017, 67 (3), 410-425.
94. Shimizu, N.; Ito, J.; Kato, S.; Otoki, Y.; Goto, M.; Eitsuka, T.; Miyazawa, T.; Nakagawa, K., Oxidation of squalene by singlet oxygen and free radicals results in different compositions of squalene monohydroperoxide isomers. *Scientific Reports* 2018, 8 (1), 9116.
95. Dorakumbura, B. N.; Boseley, R. E.; Becker, T.; Martin, D. E.; Richter, A.; Tobin, M. J.; van Bronswijk, W.; Vongsvivut, J.; Hackett, M. J.; Lewis, S. W., Revealing the spatial distribution of chemical species within latent fingermarks using vibrational spectroscopy. *Analyst* 2018, 143 (17), 4027-4039.
96. Pleik, S.; Spengler, B.; Ram Bhandari, D.; Luhn, S.; Schäfer, T.; Urbach, D.; Kirsch, D., Ambient-air ozonolysis of triglycerides in aged fingerprint residues. *Analyst* 2018, 143 (5), 1197-1209.
97. Johnston, A.; Rogers, K., A study of the intermolecular interactions of lipid components from analogue fingerprint residues. *Science & Justice* 2018, 58 (2), 121-127.
98. Gorka, M.; Augsburger, M.; Thomas, A.; Bécue, A., Molecular composition of fingermarks: Assessment of the intra- and inter-variability in a small group of donors using MALDI-MSI. *Forensic Chemistry* 2019, 12, 99-106.
99. Almog, J.; Azoury, M.; Elmaliah, Y.; Berenstein, L.; Zaban, A., Fingerprints' third dimension: the depth and shape of fingerprints penetration into paper-cross section examination by fluorescence microscopy. *Journal of forensic sciences* 2004, 49 (5), 981-985.

100. O'Neill, K. C.; Lee, Y. J., Effect of Aging and Surface Interactions on the Diffusion of Endogenous Compounds in Latent Fingerprints Studied by Mass Spectrometry Imaging. *Journal of Forensic Sciences* 2018, 63 (3), 708-713.
101. Girod, A.; Xiao, L.; Reedy, B.; Roux, C.; Weyermann, C., Fingermark initial composition and aging using Fourier transform infrared microscopy (μ -FTIR). *Forensic Science International* 2015, 254, 185-196.
102. Bouzin, J. T.; Merendino, J.; Bleay, S. M.; Sauzier, G.; Lewis, S. W., New light on old fingermarks: The detection of historic latent fingermarks on old paper documents using 1,2-indanedione/zinc. *Forensic Science International: Reports* 2020, 2, 100145.
103. Bond, J. W., Visualization of Latent Fingerprint Corrosion of Metallic Surfaces. *Journal of forensic sciences*. 2008, 53 (4), 812-822.
104. Kim, Y.; Choi, W.-s.; Jeon, B.; Choi, T. H., The Effect of Temperature and Exposure Time on Stability of Cholesterol and Squalene in Latent Fingermarks Deposited on PVDF Membrane. *Journal of Forensic Sciences* 2020, 65 (2), 458-464.
105. Richmond-Aylor, A.; Bell, S.; Callery, P.; Morris, K., Thermal Degradation Analysis of Amino Acids in Fingerprint Residue by Pyrolysis GC-MS to Develop New Latent Fingerprint Developing Reagents*. *Journal of Forensic Sciences* 2007, 52 (2), 380-382.
106. De Paoli, G.; Lewis Sr., S. A.; Schuette, E. L.; Lewis, L. A.; Connatser, R. M.; Farkas, T., Photo- and Thermal-Degradation Studies of Select Eccrine Fingerprint Constituents. *Journal of Forensic Sciences* 2010, 55 (4), 962-969.
107. Johnston, A.; Rogers, K., The Effect of Moderate Temperatures on Latent Fingerprint Chemistry. *Applied Spectroscopy* 2017, 71 (9), 2102-2110.
108. Wolstenholme, R.; Bradshaw, R.; Clench, M. R.; Francese, S., Study of latent fingermarks by matrix-assisted laser desorption/ionisation mass spectrometry imaging of endogenous lipids. *Rapid Communications in Mass Spectrometry* 2009, 23 (19), 3031-3039.

109. Newland, T. G.; Moret, S.; Bécue, A.; Lewis, S. W., Further investigations into the single metal deposition (SMD II) technique for the detection of latent fingerprints. *Forensic Science International* 2016, 268, 62-72.
110. de la Hunty, M.; Moret, S.; Chadwick, S.; Lennard, C.; Spindler, X.; Roux, C., An effective Physical Developer (PD) method for use in Australian laboratories. *Australian Journal of Forensic Sciences* 2018, 50 (6), 666-671.
111. Bumbrah, G. S., Small particle reagent (SPR) method for detection of latent fingerprints: A review. *Egyptian Journal of Forensic Sciences* 2016, 6 (4), 328-332.
112. Paine, M.; Bandey, H. L.; Bleay, S. M.; Willson, H., The effect of relative humidity on the effectiveness of the cyanoacrylate fuming process for fingerprint development and on the microstructure of the developed marks. *Forensic Science International* 2011, 212 (1), 130-142.
113. Hinners, P.; Thomas, M.; Lee, Y. J., Determining Fingerprint Age with Mass Spectrometry Imaging via Ozonolysis of Triacylglycerols. *Analytical Chemistry* 2020, 92 (4), 3125-3132.
114. Yamashita, B.; French, M., Chapter 7: Latent Print Development. In *Fingerprint Sourcebook*, National Institute of Justice: Rockville, MD, United States of America, 2010.
115. Champod, C.; Lennard, C.; Margot, P.; Stoilovic, M., *Fingerprints and other ridge skin impressions*. Boca Raton : CRC Press: Boca Raton, 2004.
116. Goode, G. C.; Morris, J. R.; Establishment, A. W. R., *Latent Fingerprints: A Review of Their Origin, Composition and Methods for Detection*. Atomic Weapons Research Establishment: 1983.
117. Kent, T., *Sequential Treatment and Enhancement*. 2nd ed.; Academic Press: Waltham, 2013; p 104-110.

118. Stoilovic, M.; Lennard, C., NCFS workshop manual: fingermark detection & enhancement. 6th ed.; National Centre for Forensic Studies: Canberra, Australia, 2012.
119. Kent, T., Visualization or Development of Crime Scene Fingerprints. In Encyclopedia of Forensic Sciences (Second Edition), Siegel, J. A.; Saukko, P. J.; Houck, M. M., Eds. Academic Press: Waltham, 2013; pp 117-129.
120. Jelly, R.; Patton, E. L. T.; Lennard, C.; Lewis, S. W.; Lim, K. F., The detection of latent fingermarks on porous surfaces using amino acid sensitive reagents: A review. *Analytica Chimica Acta* 2009, 652 (1), 128-142.
121. Bicknell, D. E.; Ramotowski, R. S., Use of an Optimized 1,2-Indanedione Process for the Development of Latent Prints*. *Journal of Forensic Sciences* 2008, 53 (5), 1108-1116.
122. Wallace-Kunkel, C.; Lennard, C.; Stoilovic, M.; Roux, C., Optimisation and evaluation of 1,2-indanedione for use as a fingermark reagent and its application to real samples. *Forensic Science International* 2007, 168 (1), 14-26.
123. Stoilovic, M.; Lennard, C.; Wallace-Kunkel, C.; Roux, C., Evaluation of a 1,2-Indanedione Formulation Containing Zinc Chloride for Improved Fingermark Detection on Paper. *Journal of Forensic Identification* 2007, 57 (1), 4-18.
124. Spindler, X.; Shimmon, R.; Roux, C.; Lennard, C., The effect of zinc chloride, humidity and the substrate on the reaction of 1,2-indanedione–zinc with amino acids in latent fingermark secretions. *Forensic Science International* 2011, 212 (1–3), 150-157.
125. OdÉN, S.; Hofsten, B. V., Detection of Fingerprints by the Ninhydrin Reaction. *Nature* 1954, 173 (4401), 449-450.
126. Crown, D. A., The Development of Latent Fingerprints with Ninhydrin. *The Journal of Criminal Law, Criminology, and Police Science* 1969, 60 (2), 258-264.

127. Friedman, M.; Williams, D. L., Stoichiometry of formation of Ruhemann's purple in the ninhydrin reaction. *Bioorganic Chemistry* 1974, 3 (3), 267-280.
128. Lennard, C. J.; Margot, P. A.; Stoilovic, M.; Warrenner, R. N., Synthesis of Ninhydrin Analogues and Their Application to Fingerprint Development: Preliminary Results. *Journal of the Forensic Science Society* 1986, 26 (5), 323-328.
129. Kobus, H. J.; Stoilovic, M.; Warrenner, R. N., A simple luminescent post-ninhydrin treatment for the improved visualisation of fingerprints on documents in cases where ninhydrin alone gives poor results. *Forensic Science International* 1983, 22, 161-170.
130. Almog, J.; Levinton-Shamuilov, G.; Cohen, Y.; Azoury, M., Fingerprint Reagents with Dual Action: Color and Fluorescence. *Journal of Forensic Sciences* 2007, 52 (2), 330-334.
131. Ramotowski, R.; Cantu, A.; Joullié, M.; Petrovskaia, O., 1, 2-Indanediones: a preliminary evaluation of a new class of amino acid visualizing compounds. *Fingerprint Whorld* 1997, 23 (90), 131-140.
132. Hauze, D. B.; Petrovskaia, O.; Taylor, B.; Joullié, M. M.; Ramotowski, R.; Cantu, A., 1, 2-Indanediones: new reagents for visualizing the amino acid components of latent prints. *Journal of Forensic Science* 1998, 43 (4), 744-747.
133. de la Hunty, M.; Spindler, X.; Chadwick, S.; Lennard, C.; Roux, C., Synthesis and application of an aqueous Nile red microemulsion for the development of fingermarks on porous surfaces. *Forensic Science International* 2014, 244, e48-e55.
134. Ramotowski, R., A comparison of different physical developer systems and acid pre-treatments and their effects on developing latent prints. *Journal of Forensic Identification* 2000, 50 (4), 363-384.
135. Hardwick, S., User guide to physical developer—a reagent for detecting latent fingerprints. Great Britain Home Office Police Scientific Development Branch User Guide 1981, 14, 81.

136. De La Hunty, M.; Moret, S.; Chadwick, S.; Lennard, C.; Spindler, X.; Roux, C., Understanding Physical Developer (PD): Part II – Is PD targeting eccrine constituents? *Forensic Science International* 2015, 257, 488-495.
137. De La Hunty, M.; Moret, S.; Chadwick, S.; Lennard, C.; Spindler, X.; Roux, C., Understanding physical developer (PD): Part I – Is PD targeting lipids? *Forensic Science International* 2015, 257, 481-487.
138. Sauzier, G.; Frick, A.; Lewis, S., Investigation into the performance of physical developer formulations for visualizing latent fingerprints on paper. 2013.
139. Stauffer, E.; Becue, A.; Singh, K. V.; Thampi, K. R.; Champod, C.; Margot, P., Single-metal deposition (SMD) as a latent fingermark enhancement technique: An alternative to multimetal deposition (MMD). *Forensic Science International* 2007, 168 (1), e5-e9.
140. Sodhi, G. S.; Kaur, J., Multimetal deposition method for detection of latent fingerprints: a review. *Egyptian Journal of Forensic Sciences* 2017, 7 (1), 17.
141. Beaudoin, A., New technique for revealing latent fingerprints on wet, porous surfaces: Oil Red O. *Journal of Forensic Identification* 2004, 54 (4), 413.
142. Rawji, A.; Beaudoin, A., Oil red O versus physical developer on wet papers: a comparative study. *Journal of Forensic Identification* 2006, 56 (1), 33.
143. Salama, J.; Aumeer-Donovan, S.; Lennard, C.; Roux, C., Evaluation of the Fingermark Reagent Oil Red O as a Possible Replacement for Physical Developer. *Journal of Forensic Identification* 2008, 58 (2), 203-237.
144. Simmons, R. K.; Deacon, P.; Farrugia, K. J., Water-soaked porous evidence: a comparison of processing methods. *Journal of Forensic Identification* 2014, 64 (2), 157-173.
145. Braasch, K.; de la Hunty, M.; Deppe, J.; Spindler, X.; Cantu, A. A.; Maynard, P.; Lennard, C.; Roux, C., Nile red: Alternative to physical developer for the detection of latent fingermarks on wet porous surfaces? *Forensic Science International* 2013, 230 1-3, 74-80.

146. Ramotowski, R., Lee and Gaensslen's *Advances in Fingerprint Technology*. 3rd ed.; Hoboken : Taylor and Francis: 2012.
147. Frick, A. A.; Buseti, F.; Cross, A.; Lewis, S. W., Aqueous Nile blue: a simple, versatile and safe reagent for the detection of latent fingermarks. *Chemical Communications* 2014, 50 (25), 3341-3343.
148. Crocker, R. *Detection of Latent Fingermarks on Wetted Porous Surfaces*. Honours, Curtin University, 2015.
149. Bumrah, G. S., Cyanoacrylate fuming method for detection of latent fingermarks: a review. *Egyptian Journal of Forensic Sciences* 2017, 7 (1), 4.
150. Wargacki, S. P.; Lewis, L. A.; Dadmun, M. D., Understanding the Chemistry of the Development of Latent Fingerprints by Superglue Fuming. *Journal of Forensic Sciences* 2007, 52 (5), 1057-1062.
151. Lennard, C., FORENSIC SCIENCES | Fingerprint Techniques. In *Encyclopedia of Analytical Science (Second Edition)*, Worsfold, P.; Townshend, A.; Poole, C., Eds. Elsevier: Oxford, 2005; pp 414-423.
152. Farrugia, K. J.; Fraser, J.; Friel, L.; Adams, D.; Attard-Montalto, N.; Deacon, P., A comparison between atmospheric/humidity and vacuum cyanoacrylate fuming of latent fingermarks. *Forensic Science International* 2015, 257, 54-70.
153. Cheshier, B. K.; Stone, J. M.; Rowe, W. F., Use of the Omniprint™ 1000 alternate light source to produce fluorescence in cyanoacrylate-developed latent fingerprints stained with biological stains and commercial fabric dyes. *Forensic Science International* 1992, 57 (2), 163-168.
154. Chadwick, S.; Maynard, P.; Kirkbride, P.; Lennard, C.; Spindler, X.; Roux, C., Use of Styryl 11 and STaR 11 for the Luminescence Enhancement of Cyanoacrylate-Developed Fingermarks in the Visible and Near-Infrared Regions*. *Journal of Forensic Sciences* 2011, 56 (6), 1505-1513.

155. Batey, G.; Copeland, J.; Donnelly, D.; Hill, C.; Laturus, P.; McDiarmid, C.; Miller, K.; Misner, A.; Tario, A., Metal deposition for latent print development. *Journal of Forensic Identification* 1998, 48, 165-175.
156. Masters, N.; DeHaan, J., Vacuum metal deposition and cyanoacrylate detection of older latent prints. *Journal of Forensic Identification* 1996, 46, 32-48.
157. Flynn, J.; Stoilovic, M.; Lennard, C., Detection and enhancement of latent fingerprints on polymer banknotes: A preliminary study. *Journal of Forensic Identification* 1999, 49 (6), 594-613.
158. Kent, T.; Thomas, G. L.; Reynoldson, T. E.; East, H. W., A Vacuum Coating Technique for the Development of Latent Fingerprints on Polythene. *Journal of the Forensic Science Society* 1976, 16 (2), 93-101.
159. Jones, N.; Stoilovic, M.; Lennard, C.; Roux, C., Vacuum metal deposition: factors affecting normal and reverse development of latent fingerprints on polyethylene substrates. *Forensic Science International* 2001, 115 (1), 73-88.
160. Jones, N.; Mansour, D.; Stoilovic, M.; Lennard, C.; Roux, C., The influence of polymer type, print donor and age on the quality of fingerprints developed on plastic substrates using vacuum metal deposition. *Forensic Science International* 2001, 124 (2), 167-177.
161. Jones, N.; Stoilovic, M.; Lennard, C.; Roux, C., Vacuum metal deposition: developing latent fingerprints on polyethylene substrates after the deposition of excess gold. *Forensic Science International* 2001, 123 (1), 5-12.
162. Kanodarwala, F. K.; Moret, S.; Spindler, X.; Lennard, C.; Roux, C., Nanoparticles used for fingermark detection—A comprehensive review. *WIREs Forensic Science* 2019, 1 (5), e1341.
163. Becue, A., Emerging fields in fingermark (meta)detection - a critical review. *Analytical Methods* 2016, 8 (45), 7983-8003.
164. Moret, S.; Bécue, A.; Champod, C., Nanoparticles for fingermark detection: an insight into the reaction mechanism. *Nanotechnology* 2014, 25 (42), 425502.

165. Bécue, A.; Moret, S., Single-Metal deposition for Fingermark detection - A simpler and more efficient protocol. *Journal of Forensic Identification* 2015, 65 (2), 118-137.
166. Durussel, P.; Stauffer, E.; Becue, A.; Champod, C.; Margot, P., Single-Metal Deposition: Optimization of this Fingermark Enhancement Technique. *Journal of Forensic Identification* 2009, 59 (1), 80-96.
167. Becue, A.; Scoundrianos, A.; Moret, S., Detection of fingermarks by colloidal gold (MMD/SMD) – beyond the pH 3 limit. *Forensic Science International* 2012, 219 (1–3), 39-49.
168. Fairley, C.; Bleay, S. M.; Sears, V. G.; NicDaeid, N., A comparison of multi-metal deposition processes utilising gold nanoparticles and an evaluation of their application to ‘low yield’ surfaces for finger mark development. *Forensic Science International* 2012, 217 (1), 5-18.
169. González, M.; Gorziza, R. P.; de Cássia Mariotti, K.; Pereira Limberger, R., Methodologies Applied to Fingerprint Analysis. *Journal of Forensic Sciences* 2020, 65 (4), 1040-1048.
170. Wei, Q.; Zhang, M.; Ogorevc, B.; Zhang, X., Recent advances in the chemical imaging of human fingermarks (a review). *Analyst* 2016, 141 (22), 6172-6189.
171. Koenig, A.; Girod, A.; Weyermann, C., Identification of Wax Esters in Latent Print Residues by Gas Chromatography-Mass Spectrometry and Their Potential Use as Aging Parameters. *Journal of Forensic Identification* 2011, 61 (6), 652-676.
172. Croxton, R. S.; Baron, M. G.; Butler, D.; Kent, T.; Sears, V. G., Development of a GC-MS Method for the Simultaneous Analysis of Latent Fingerprint Components*. *Journal of Forensic Sciences* 2006, 51 (6), 1329-1333.
173. Dikshitulu, Y. S.; Prasad, L.; Pal, J. N.; Rao, C. V. N., Aging studies on fingerprint residues using thin-layer and high performance liquid chromatography. *Forensic Science International* 1986, 31 (4), 261-266.

174. Frick, A. A.; Kummer, N.; Moraleda, A.; Weyermann, C., Changes in latent fingerprint glyceride composition as a function of sample age using UPLC-IMS-QToF-MSE. *Analyst* 2020, 145 (12), 4212-4223.
175. Thomas, G. L.; Reynoldson, T. E., Some observations on fingerprint deposits. *Journal of Physics D: Applied Physics* 1975, 8 (6), 724-729.
176. Thomas, G. L., A fingerprint thin film. *Thin Solid Films* 1974, 24 (2), S52-S54.
177. Thomas, G. L.; Reynoldson, T. E. A Quantitative Study of Fingerprints using Interference Microscopy; Home Office Police Scientific Development Branch.
178. Moret, S.; Spindler, X.; Lennard, C.; Roux, C., Microscopic examination of fingerprint residues: opportunities for fundamental studies. *Forensic Science International* 2015, 255, 28-37.
179. Dorakumbura, B. N.; Becker, T.; Lewis, S. W., Nanomechanical mapping of latent fingerprints: A preliminary investigation into the changes in surface interactions and topography over time. *Forensic Science International* 2016, 267, 16-24.
180. Popov, K. T.; Sears, V. G.; Jones, B. J., Migration of latent fingerprints on non-porous surfaces: Observation technique and nanoscale variations. *Forensic Science International* 2017, 275, 44-56.
181. Goddard, A. J.; Hillman, A. R.; Bond, J. W., High Resolution Imaging of Latent Fingerprints by Localized Corrosion on Brass Surfaces. *Journal of Forensic Sciences* 2010, 55 (1), 58-65.
182. Jones, B. J.; Downham, R.; Sears, V. G., Effect of substrate surface topography on forensic development of latent fingerprints with iron oxide powder suspension. *Surface and Interface Analysis* 2010, 42 (5), 438-442.
183. Thomas, G., The physics of fingerprints and their detection. *Journal of Physics E: Scientific Instruments* 1978, 11 (8), 722.
184. Vongsvivut, J.; Pérez-Guaita, D.; Wood, B. R.; Heraud, P.; Khambatta, K.; Hartnell, D.; Hackett, M. J.; Tobin, M. J., Synchrotron macro ATR-FTIR

- microspectroscopy for high-resolution chemical mapping of single cells. *Analyst* 2019, 144 (10), 3226-3238.
185. Fritz, P.; van Bronswijk, W.; Lepkova, K.; Lewis, S. W.; Lim, K. F.; Martin, D. E.; Puskar, L., Infrared microscopy studies of the chemical composition of latent fingerprint residues. *Microchemical Journal* 2013, 111, 40-46.
186. Tahtouh, M.; Kalman, J. R.; Roux, C.; Lennard, C.; Reedy, B. J., The detection and enhancement of latent fingerprints using infrared chemical imaging. *Journal of forensic sciences* 2005, 50 1, 64-72.
187. Ricci, C.; Phiriyavityopas, P.; Curum, N.; Chan, K. L. A.; Jickells, S.; Kazarian, S. G., Chemical imaging of latent fingerprint residues. *Applied Spectroscopy* 2007, 61 (5), 514-522.
188. Bartick, E.; Schwartz, R.; Bhargava, R.; Schaeberle, M.; Fernandez, D.; Levin, I. In *Spectrochemical analysis and hyperspectral imaging of latent fingerprints*, 16th Meeting of the International Association of Forensic Sciences, 2002; pp 61-64.
189. Crane, N. J.; Bartick, E. G.; Perlman, R. S.; Huffman, S., Infrared Spectroscopic Imaging for Noninvasive Detection of Latent Fingerprints. *Journal of Forensic Sciences* 2007, 52 (1), 48-53.
190. Williams, D. K.; Brown, C. J.; Bruker, J., Characterization of children's latent fingerprint residues by infrared microspectroscopy: Forensic implications. *Forensic Science International* 2011, 206 (1), 161-165.
191. Francese, S.; Bradshaw, R.; Ferguson, L. S.; Wolstenholme, R.; Clench, M. R.; Bleay, S., Beyond the ridge pattern: multi-informative analysis of latent fingerprints by MALDI mass spectrometry. *Analyst* 2013, 138 (15), 4215-4228.
192. Bradshaw, R.; Denison, N.; Francese, S., Implementation of MALDI MS profiling and imaging methods for the analysis of real crime scene fingerprints. *Analyst* 2017, 142 (9), 1581-1590.

193. Connatser, R. M.; Prokes, S. M.; Glembocki, O. J.; Schuler, R. L.; Gardner, C. W.; Lewis Sr., S. A.; Lewis, L. A., Toward Surface-Enhanced Raman Imaging of Latent Fingerprints*. *Journal of Forensic Sciences* 2010, 55 (6), 1462-1470.
194. Pluháček, T.; Švidrnoch, M.; Maier, V.; Havlíček, V.; Lemr, K., Laser ablation inductively coupled plasma mass spectrometry imaging: A personal identification based on a gunshot residue analysis on latent fingerprints. *Analytica Chimica Acta* 2018, 1030, 25-32.
195. Wirtz, T.; Philipp, P.; Audinot, J. N.; Dowsett, D.; Eswara, S., High-resolution high-sensitivity elemental imaging by secondary ion mass spectrometry: from traditional 2D and 3D imaging to correlative microscopy. *Nanotechnology* 2015, 26 (43), 434001.
196. Garner, G. E.; Fontan, C. R.; Hobson, D. W., Visualization of Fingerprints in the Scanning Electron Microscope. *Journal of the Forensic Science Society* 1975, 15 (4), 281-288.
197. Nolan, P. J.; Brennan, J. S.; Keeley, R. H.; Pounds, C. A., The Imaging of Developed Fingerprint using the Scanning Electron-Microscope. *Journal of the Forensic Science Society* 1984, 24 (4), 419-419.
198. Mi Jung, C.; McBean, K. E.; Wuhrer, R.; McDonagh, A. M.; et al., Investigation into the Binding of Gold Nanoparticles to Fingermarks Using Scanning Electron Microscopy. *Journal of Forensic Identification* 2006, 56 (1), 24-32.
199. Erdoğan, A.; Esen, M.; Simpson, R., Chemical Imaging of Human Fingerprint by X-ray Photoelectron Spectroscopy (XPS). *J. Forensic Sci.* 2020, 65 (5), 1730-1735.
200. Watts, J. F., The potential for the application of X-ray photoelectron spectroscopy in forensic science. *Surface and Interface Analysis* 2010, 42 (5), 358-362.
201. Pushie, M. J.; Pickering, I. J.; Korbas, M.; Hackett, M. J.; George, G. N., Elemental and Chemically Specific X-ray Fluorescence Imaging of Biological Systems. *Chemical Reviews* 2014, 114 (17), 8499-8541.

202. Balerna, A.; Mobilio, S., Introduction to Synchrotron Radiation. In Synchrotron Radiation: Basics, Methods and Applications, Mobilio, S.; Boscherini, F.; Meneghini, C., Eds. Springer Berlin Heidelberg: Berlin, Heidelberg, 2015; pp 3-28.
203. Wiedemann, H., Overview of Synchrotron Radiation. In Synchrotron Radiation, Springer Berlin Heidelberg: Berlin, Heidelberg, 2003; pp 31-53.
204. Willmott, P., Synchrotron Physics. In An Introduction to Synchrotron Radiation, Willmott, P., Ed. 2011; pp 39-86.
205. Brown, T. L.; LeMay, H. E.; Bursten, B. E.; Murphy, C.; Woodward, P.; Langford, S.; Sagatys, D.; George, A., Chemistry: The Central Science. Pearson Higher Education AU: 2013.
206. Wiedemann, H., Synchrotron Radiation Physics. In Synchrotron Light Sources and Free-Electron Lasers: Accelerator Physics, Instrumentation and Science Applications, Jaeschke, E. J.; Khan, S.; Schneider, J. R.; Hastings, J. B., Eds. Springer International Publishing: Cham, 2016; pp 3-49.
207. Boldeman, J. W.; Einfeld, D., The physics design of the Australian synchrotron storage ring. Nuclear Instruments and Methods in Physics Research Section A: Accelerators, Spectrometers, Detectors and Associated Equipment 2004, 521 (2), 306-317.
208. Margaritondo, G., Characteristics and Properties of Synchrotron Radiation. In Synchrotron Radiation: Basics, Methods and Applications, Mobilio, S.; Boscherini, F.; Meneghini, C., Eds. Springer Berlin Heidelberg: Berlin, Heidelberg, 2015; pp 29-63.
209. Hare, D. J.; New, E. J.; de Jonge, M. D.; McColl, G., Imaging metals in biology: balancing sensitivity, selectivity and spatial resolution. Chem. Soc. Rev. 2015, 44 (17), 5941-5958.
210. Douglas, A. S.; Holler, F. J.; Stanley, R. C., Principles of Instrumental Analysis. Cengage: Mason, OH, United States, 2016.

211. Ozaki, Y., Infrared Spectroscopy—Mid-infrared, Near-infrared, and Far-infrared/Terahertz Spectroscopy. *Analytical Sciences* 2021, 37 (9), 1193-1212.
212. Vitha, M. F., *Spectroscopy : Principles and Instrumentation*. John Wiley & Sons, Incorporated: Newark, United States, 2018.
213. Plathe, R.; Martin, D.; Tobin, M. J.; Puskar, L.; Appadoo, D. In *The far-infrared/thz beamline at the Australian Synchrotron: Performance & applications, 2011 International Conference on Infrared, Millimeter, and Terahertz Waves, 2-7 Oct. 2011; 2011; pp 1-2*.
214. Colthup, N. B., Infrared Spectroscopy. In *Encyclopedia of Physical Science and Technology (Third Edition)*, Meyers, R. A., Ed. Academic Press: New York, 2003; pp 793-816.
215. Smith, B. C. a., *Fundamentals of Fourier transform infrared spectroscopy*. 2nd ed.. ed.; Boca Raton, Fla. : CRC Press: 2011.
216. Chan, K. L. A.; Kazarian, S. G., *New Opportunities in Micro- and Macro-Attenuated Total Reflection Infrared Spectroscopic Imaging: Spatial Resolution and Sampling Versatility*. *Applied Spectroscopy* 2003, 57 (4), 381-389.
217. Kazarian, S. G.; Chan, K. L. A., *ATR-FTIR spectroscopic imaging: recent advances and applications to biological systems*. *Analyst* 2013, 138 (7), 1940-1951.
218. Miller, L. M.; Dumas, P., *Chemical imaging of biological tissue with synchrotron infrared light*. *Biochimica et Biophysica Acta (BBA) - Biomembranes* 2006, 1758 (7), 846-857.
219. Holman, H.-Y. N.; Bechtel, H. A.; Hao, Z.; Martin, M. C., *Synchrotron IR Spectromicroscopy: Chemistry of Living Cells*. *Analytical Chemistry* 2010, 82 (21), 8757-8765.
220. Carr, G. L.; Reffner, J. A.; Williams, G. P., *Performance of an infrared microspectrometer at the NSLS*. *Review of Scientific Instruments* 1995, 66 (2), 1490-1492.

221. Nakano, T.; Kawata, S., Evanescent-field scanning microscope with fourier-transform infrared spectrometer. *Scanning* 1994, 16 (6), 368-371.
222. Milosevic, M., Internal reflection and ATR spectroscopy. *Applied Spectroscopy Reviews* 2004, 39 (3), 365-384.
223. Sommer, A. J.; Tisinger, L. G.; Marcott, C.; Story, G. M., Attenuated Total Internal Reflection Infrared Mapping Microspectroscopy Using an Imaging Microscope. *Applied Spectroscopy* 2001, 55 (3), 252-256.
224. Kazarian, S. G.; Chan, K. L. A., Applications of ATR-FTIR spectroscopic imaging to biomedical samples. *Biochimica et Biophysica Acta (BBA) - Biomembranes* 2006, 1758 (7), 858-867.
225. Chan, K. L. A.; Hammond, S. V.; Kazarian, S. G., Applications of Attenuated Total Reflection Infrared Spectroscopic Imaging to Pharmaceutical Formulations. *Analytical Chemistry* 2003, 75 (9), 2140-2146.
226. Ewing, A. V.; Kazarian, S. G., Infrared spectroscopy and spectroscopic imaging in forensic science. *Analyst* 2017, 142 (2), 257-272.
227. Chan, K. L. A.; Kazarian, S. G., Fourier Transform Infrared Imaging for High-Throughput Analysis of Pharmaceutical Formulations. *Journal of Combinatorial Chemistry* 2005, 7 (2), 185-189.
228. Tiernan, H.; Byrne, B.; Kazarian, S. G., ATR-FTIR spectroscopy and spectroscopic imaging for the analysis of biopharmaceuticals. *Spectrochimica Acta Part A: Molecular and Biomolecular Spectroscopy* 2020, 241, 118636.
229. Appadoo, D.; Plathe, R. In THz/Far-IR Astrophysical Studies at the Australian Synchrotron, 2019 44th International Conference on Infrared, Millimeter, and Terahertz Waves (IRMMW-THz), 1-6 Sept. 2019; 2019; pp 1-2.
230. Wilkinson, T., Perry, D., Martin, M., McKinney, W. Using synchrotron radiation to identify and characterize human chemical latent fingerprints - A novel forensic approach; Lawrence Berkeley National Laboratory: LBNL Report #: LBNL-51682 Abs. , 2002.

231. Wilkinson, T. J., Perry, D.L., Martin, M.C., McKinney, W.R.; , Applications of Synchrotron Infrared Microspectroscopy to the Study of Fingerprints. In National Meeting of the American Chemical Society Lawrence Berkeley National Laboratory: San Diego, 2001.
232. Williams, D. K.; Schwartz, R. L.; Bartick, E. G., Analysis of Latent Fingerprint Deposits by Infrared Microspectroscopy. *Applied Spectroscopy* 2004, 58 (3), 313-316.
233. Mou, Y.; Rabalais, J. W., Detection and Identification of Explosive Particles in Fingerprints Using Attenuated Total Reflection-Fourier Transform Infrared Spectromicroscopy. *Journal of Forensic Sciences* 2009, 54 (4), 846-850.
234. Banas, A.; Banas, K.; Breese, M. B. H.; Loke, J.; Lim, S. K., Spectroscopic detection of exogenous materials in latent fingerprints treated with powders and lifted off with adhesive tapes. *Analytical and Bioanalytical Chemistry* 2014, 406 (17), 4173-4181.
235. Chan, K. L. A.; Kazarian, S. G., Detection of trace materials with Fourier transform infrared spectroscopy using a multi-channel detector. *Analyst* 2006, 131 (1), 126-131.
236. Potts, P. J., X-ray Fluorescence and Emission | X-Ray Fluorescence Theory. In *Encyclopedia of Analytical Science (Second Edition)*, Worsfold, P.; Townshend, A.; Poole, C., Eds. Elsevier: Oxford, 2005; pp 408-418.
237. Eichert, D., X-Ray Microscopy. In *Synchrotron Radiation: Basics, Methods and Applications*, Mobilio, S.; Boscherini, F.; Meneghini, C., Eds. Springer Berlin Heidelberg: Berlin, Heidelberg, 2015; pp 409-436.
238. Margui, E.; Van Grieken, R., X-Ray Fluorescence Spectrometry and Related Techniques : An Introduction. Momentum Press: New York, United States, 2013.
239. Kramar, U., X-Ray Fluorescence Spectrometers*. In *Encyclopedia of Spectroscopy and Spectrometry (Second Edition)*, Lindon, J. C., Ed. Academic Press: Oxford, 1999; pp 2989-2999.

240. Szczerbowska-Boruchowska, M., Sample thickness considerations for quantitative X-ray fluorescence analysis of the soft and skeletal tissues of the human body – theoretical evaluation and experimental validation. *X-Ray Spectrom.* 2012, 41 (5), 328-337.
241. Adams, F., X-ray Fluorescence and Emission | Synchrotron X-Ray Fluorescence. In *Encyclopedia of Analytical Science (Second Edition)*, Worsfold, P.; Townshend, A.; Poole, C., Eds. Elsevier: Oxford, 2005; pp 458-462.
242. Lear, J.; Hare, D. J.; Fryer, F.; Adlard, P. A.; Finkelstein, D. I.; Doble, P. A., High-resolution elemental bioimaging of Ca, Mn, Fe, Co, Cu, and Zn employing LA-ICP-MS and hydrogen reaction gas. *Anal. Chem.* 2012, 84 (15), 6707-6714.
243. Becker, J. S.; Matusch, A.; Wu, B., Bioimaging mass spectrometry of trace elements – recent advance and applications of LA-ICP-MS: A review. *Anal. Chim. Acta* 2014, 835, 1-18.
244. Pozebon, D.; Scheffler, G.; Dressler, V., Recent applications of laser ablation inductively coupled plasma mass spectrometry (LA-ICP-MS) for biological sample analysis: a follow-up review. *J. Anal. At. Spectrom.* 2017, 32 (5), 890-919.
245. Chandra, S.; Smith, D. R.; Morrison, G. H., Subcellular Imaging by Dynamic SIMS Ion Microscopy. *Anal. Chem.* 2000, 72 (3), 104 A-114 A.
246. Jiang, H.; Kilburn, M. R.; Decelle, J.; Musat, N., NanoSIMS chemical imaging combined with correlative microscopy for biological sample analysis. *Curr. Opin. Biotechnol.* 2016, 41, 130-135.
247. Howard, D. L.; de Jonge, M. D.; Afshar, N.; Ryan, C. G.; Kirkham, R.; Reinhardt, J.; Kewish, C. M.; McKinlay, J.; Walsh, A.; Divitcos, J.; Basten, N.; Adamson, L.; Fiala, T.; Sammut, L.; Paterson, D. J., The XFM beamline at the Australian Synchrotron. *Journal of Synchrotron Radiation* 2020, 27 (5), 1447-1458.
248. Snigireva, I.; Snigireva, A., Microscopy Techniques | X-Ray Microscopy. In *Encyclopedia of Analytical Science (Second Edition)*, Worsfold, P.; Townshend, A.; Poole, C., Eds. Elsevier: Oxford, 2005; pp 151-158.

249. Ryan, C. G.; Kirkham, R.; de Jonge, M. D.; Siddons, D. P.; van der Ent, A.; Pagés, A.; Boesenberg, U.; Kuczewski, A. J.; Dunn, P.; Jensen, M.; Liu, W.; Harris, H.; Moorhead, G. F.; Paterson, D. J.; Howard, D. L.; Afshar, N.; Garrevoet, J.; Spiers, K.; Falkenberg, G.; Woll, A. R.; De Geronimo, G.; Carini, G. A.; James, S. A.; Jones, M. W. M.; Fisher, L. A.; Pearce, M., The Maia Detector and Event Mode. *Synchrotron Radiation News* 2018, 31 (6), 21-27.
250. Ryan, C. G.; Siddons, D. P.; Kirkham, R.; Li, Z. Y.; de Jonge, M. D.; Paterson, D. J.; Kuczewski, A.; Howard, D. L.; Dunn, P. A.; Falkenberg, G.; Boesenberg, U.; De Geronimo, G.; Fisher, L. A.; Halfpenny, A.; Lintern, M. J.; Lombi, E.; Dyl, K. A.; Jensen, M.; Moorhead, G. F.; Cleverley, J. S.; Hough, R. M.; Godel, B.; Barnes, S. J.; James, S. A.; Spiers, K. M.; Alfeld, M.; Wellenreuther, G.; Vukmanovic, Z.; Borg, S., Maia X-ray fluorescence imaging: Capturing detail in complex natural samples. *Journal of Physics: Conference Series* 2014, 499, 012002.
251. Paterson, D.; Jonge, M. D. d.; Howard, D. L.; Lewis, W.; McKinlay, J.; Starritt, A.; Kusel, M.; Ryan, C. G.; Kirkham, R.; Moorhead, G.; Siddons, D. P., The X-ray Fluorescence Microscopy Beamline at the Australian Synchrotron. *AIP Conference Proceedings* 2011, 1365 (1), 219-222.
252. James, S. A.; Burke, R.; Howard, D. L.; Spiers, K. M.; Paterson, D. J.; Murphy, S.; Ramm, G.; Kirkham, R.; Ryan, C. G.; de Jonge, M. D., Visualising coordination chemistry: fluorescence X-ray absorption near edge structure tomography. *Chemical Communications* 2016, 52 (79), 11834-11837.
253. James, S. A.; Roberts, B. R.; Hare, D. J.; de Jonge, M. D.; Birchall, I. E.; Jenkins, N. L.; Cherny, R. A.; Bush, A. I.; McColl, G., Direct in vivo imaging of ferrous iron dyshomeostasis in ageing *Caenorhabditis elegans*. *Chemical Science* 2015, 6 (5), 2952-2962.
254. Hollings, A. L.; Lam, V.; Takechi, R.; Mamo, J. C. L.; Reinhardt, J.; de Jonge, M. D.; Kappen, P.; Hackett, M. J., Revealing differences in the chemical form of zinc in brain tissue using K-edge X-ray absorption near-edge structure spectroscopy. *Metallomics* 2020, 12 (12), 2134-2144.

255. Hackett, M. J.; Ellison, G.; Hollings, A.; Colbourne, F.; de Jonge, M. D.; Howard, D. L., "A spectroscopic picture paints 1000 words" mapping iron speciation in brain tissue with "full spectrum per pixel" X-ray absorption near-edge structure spectroscopy. *Clinical Spectroscopy* 2021, 3, 100017.
256. Baruch, G.; Lior, N.; Joseph, A., Detection of firearms imprints on hands by the Ferrotrace spray: Profiles of some common weapons. *Journal of forensic identification* 1998, 48 (3), 257.
257. Hinder, S. J.; Watts, J. F., SIMS fingerprint analysis on organic substrates. *Surface and Interface Analysis* 2010, 42 (6-7), 826-829.
258. Cook, R.; Evett, I. W.; Jackson, G.; Jones, P. J.; Lambert, J. A., A hierarchy of propositions: deciding which level to address in casework. *Science & Justice* 1998, 38 (4), 231-239.
259. Taroni, F.; Biedermann, A.; Bozza, S.; Garbolino, P.; Aitken, C., *Bayesian Networks for Probabilistic Inference and Decision Analysis in Forensic Science*. John Wiley & Sons, Incorporated: New York, United Kingdom, 2014.
260. ANZPAA NIFS Research and Innovation Roadmap 2020-2025; Australia New Zealand Policing Advisory Agency: National Institute of Forensic Science 2020.
261. Sheridan, K. J.; Saltupyte, E.; Palmer, R.; Gallidabino, M. D., A study on contactless airborne transfer of textile fibres between different garments in small compact semi-enclosed spaces. *Forensic Science International* 2020, 315, 110432.
262. Kokshoorn, B.; Blankers, B. J.; de Zoete, J.; Berger, C. E. H., Activity level DNA evidence evaluation: On propositions addressing the actor or the activity. *Forensic Science International* 2017, 278, 115-124.
263. Buckingham, A. K.; Harvey, M. L.; van Oorschot, R. A. H., The origin of unknown source DNA from touched objects. *Forensic Science International: Genetics* 2016, 25, 26-33.

264. Gosch, A.; Euteneuer, J.; Preuß-Wössner, J.; Courts, C., DNA transfer to firearms in alternative realistic handling scenarios. *Forensic Science International: Genetics* 2020, 48.
265. Palmer, R.; Sheridan, K.; Puckett, J.; Richardson, N.; Lo, W., An investigation into secondary transfer—The transfer of textile fibres to seats. *Forensic Science International* 2017, 278, 334-337.
266. Bennett, S.; Roux, C. P.; Robertson, J., The significance of fibre transfer and persistence-A case study. *Australian Journal of Forensic Sciences* 2010, 42 (3), 221-228.
267. Hong, S.; Han, A.; Kim, S.; Son, D.; Min, H., Transfer of fibres on the hands of living subjects and their persistence during hand washing. *Science and Justice* 2014, 54 (6), 451-458.
268. Leifer, A.; Avissar, Y.; Berger, S.; Wax, H.; Donchin, Y.; Almog, J., Detection of Firearm Imprints on the Hands of Suspects: Effectiveness of PDT Reaction. *J Forensic Sci* 2001, 46 (6), 1442-1446.
269. Summers, K. L.; Fimognari, N.; Hollings, A.; Kiernan, M.; Lam, V.; Tidy, R. J.; Paterson, D.; Tobin, M. J.; Takechi, R.; George, G. N.; Pickering, I. J.; Mamo, J. C.; Harris, H. H.; Hackett, M. J., A Multimodal Spectroscopic Imaging Method To Characterize the Metal and Macromolecular Content of Proteinaceous Aggregates (“Amyloid Plaques”). *Biochemistry* 2017, 56 (32), 4107-4116.
270. Ryan, C. G.; Etschmann, B. E.; Vogt, S.; Maser, J.; Harland, C. L.; van Achterbergh, E.; Legnini, D., Nuclear microprobe – synchrotron synergy: Towards integrated quantitative real-time elemental imaging using PIXE and SXRF. *Nuclear Instruments and Methods in Physics Research Section B: Beam Interactions with Materials and Atoms* 2005, 231 (1), 183-188.
271. Ryan, C. G.; Laird, J. S.; Fisher, L. A.; Kirkham, R.; Moorhead, G. F., Improved Dynamic Analysis method for quantitative PIXE and SXRF element imaging of complex materials. *Nuclear Instruments and Methods in Physics Research Section B: Beam Interactions with Materials and Atoms* 2015, 363, 42-47.

272. Ryan, C. G., Quantitative trace element imaging using PIXE and the nuclear microprobe. *International Journal of Imaging Systems and Technology* 2000, 11 (4), 219-230.
273. Boseley, R. *Detection of Latent Fingermarks on Non-Porous Substrates using Cyanoacrylate Fuming and Luminescent Stains*. Curtin University, 2016.
274. Fritz, P.; Frick, A.; van Bronswijk, W.; Lewis, S.; Beaudoin, A.; Bleay, S.; Lennard, C., Variability and Subjectivity in the Grading Process for Evaluating the Performance of Latent Fingermark Detection Techniques. *Journal of Forensic Identification* 2015, 65 (5), 851-867.
275. Bandey, H., The powders process, study 1: Evaluation of fingerprint brushes for use with aluminium powder. *PSDB Fingerprint Development and Imaging Newsletter* 2004, 54 (4), 1-12.
276. International Fingerprint Research Group, Guidelines for the assessment of fingerprint detection techniques. *Journal of Forensic Identification* 2014, 64 (2), 174-200.
277. Frick, A. A.; Fritz, P. W.; Bronswijk, W. v.; Beaudoin, A.; Bleay, S. M.; Lennard, C.; Lewis, S. W. In *Investigations into the Influence of Donor Traits on Performance of Fingerprint Development Reagents. Part 2: Oil Red O and PD*, 2017.
278. Wilson, J.; Darke, D., The results of analyses of the mixtures of fatty acids found on the skin - Part 1 Commentary. *AERE Report No. G 1975*, 1154.
279. Pitera, M.; Sears, V. G.; Bleay, S. M.; Park, S., Fingerprint visualisation on metal surfaces: An initial investigation of the influence of surface condition on process effectiveness. *Science & Justice* 2018, 58 (5), 372-383.
280. Yaniv, Y. A.; Assaf, E. S.; Daniel, M.; Joseph, A., Identification of firearms holders by the $[FE(PDT)3]+2$ complex. Quantitative determination of iron transfer to the hand and its dependence on palmar moisture levels. *Journal of Forensic Sciences* 2004, 49 (6), 1215.

281. Kirkwood, H. J.; de Jonge, M. D.; Howard, D. L.; Ryan, C. G.; van Riessen, G.; Hofmann, F.; Rowles, M. R.; Paradowska, A. M.; Abbey, B., Polycrystalline materials analysis using the Maia pixelated energy-dispersive X-ray area detector. *Powder Diffraction* 2017, 32 (S2), S16-S21.
282. Fimognari, N.; Hollings, A.; Lam, V.; Tidy, R. J.; Kewish, C. M.; Albrecht, M. A.; Takechi, R.; Mamo, J. C. L.; Hackett, M. J., Biospectroscopic Imaging Provides Evidence of Hippocampal Zn Deficiency and Decreased Lipid Unsaturation in an Accelerated Aging Mouse Model. *ACS Chemical Neuroscience* 2018, 9 (11), 2774-2785.
283. Naim, F.; Khambatta, K.; Sanglard, L. M. V. P.; Sauzier, G.; Reinhardt, J.; Paterson, D. J.; Zerihun, A.; Hackett, M. J.; Gibberd, M. R., Synchrotron X-ray fluorescence microscopy-enabled elemental mapping illuminates the 'battle for nutrients' between plant and pathogen. *Journal of Experimental Botany* 2021, 72 (7), 2757-2768.
284. Smieska, L. M.; Twilley, J.; Woll, A. R.; Schafer, M.; Marcereau DeGalan, A., Energy-optimized synchrotron XRF mapping of an obscured painting beneath *Exit from the Theater*, attributed to Honoré Daumier. *Microchemical Journal* 2019, 146, 679-691.
285. Dredge, P.; Ives, S.; Howard, D. L.; Spiers, K. M.; Yip, A.; Kenderdine, S., Mapping Henry: Synchrotron-sourced X-ray fluorescence mapping and ultra-high-definition scanning of an early Tudor portrait of Henry VIII. *Applied Physics A* 2015, 121 (3), 789-800.
286. Rodrigues, E. S.; Gomes, M. H. F.; Duran, N. M.; Cassanji, J. G. B.; da Cruz, T. N. M.; Sant'Anna Neto, A.; Savassa, S. M.; de Almeida, E.; Carvalho, H. W. P., Laboratory Microprobe X-Ray Fluorescence in Plant Science: Emerging Applications and Case Studies. *Frontiers in Plant Science* 2018, 9 (1588).
287. Edwards, N. P.; Webb, S. M.; Krest, C. M.; van Campen, D.; Manning, P. L.; Wogelius, R. A.; Bergmann, U., A new synchrotron rapid-scanning X-ray

- fluorescence (SRS-XRF) imaging station at SSRL beamline 6-2. *Journal of Synchrotron Radiation* 2018, 25 (5), 1565-1573.
288. Osredkar, J.; Sustar, N., Copper and zinc, biological role and significance of copper/zinc imbalance. *J Clin Toxicol* 2011, 3 (2161), 0495.
289. Kozłowski, H.; Luczkowski, M.; Remelli, M.; Valensin, D., Copper, zinc and iron in neurodegenerative diseases (Alzheimer's, Parkinson's and prion diseases). *Coordination Chemistry Reviews* 2012, 256 (19), 2129-2141.
290. Crichton, R. R., *Biological Inorganic Chemistry* 2nd ed.; Elsevier: Oxford, 2012.
291. Aruoma, O. I.; Reilly, T.; MacLaren, D.; Halliwell, B., Iron, copper and zinc concentrations in human sweat and plasma; the effect of exercise. *Clinica Chimica Acta* 1988, 177 (1), 81-87.
292. Lu, P.-J.; Huang, S.-C.; Chen, Y.-P.; Chiueh, L.-C.; Shih, D. Y.-C., Analysis of titanium dioxide and zinc oxide nanoparticles in cosmetics. *Journal of Food and Drug Analysis* 2015, 23 (3), 587-594.
293. Zheng, L.-N.; Ma, R.-L.; Li, Q.; Sang, Y.-B.; Wang, H.-L.; Wang, B.; Yan, Q.-Q.; Chen, D.-L.; Wang, M.; Feng, W.-Y.; Zhao, Y.-L., Elemental analysis and imaging of sunscreen fingermarks by X-ray fluorescence. *Analytical and Bioanalytical Chemistry* 2019, 411 (18), 4151-4157.
294. Union, P., Regulation (EC) No 1223/2009 of the european parliament and of the council. *Official Journal of the European Union L* 2009, 342, 59.
295. Hartzell-Baguley, B.; Hipp, R. E.; Morgan, N. R.; Morgan, S. L., Chemical Composition of Latent Fingerprints by Gas Chromatography–Mass Spectrometry. An Experiment for an Instrumental Analysis Course. *Journal of Chemical Education* 2007, 84 (4), 689.
296. Lauzon, N.; Chaurand, P., Detection of exogenous substances in latent fingermarks by silver-assisted LDI imaging MS: perspectives in forensic sciences. *Analyst* 2018, 143 (15), 3586-3594.

297. Miller, L. M.; Wang, Q.; Telivala, T. P.; Smith, R. J.; Lanzirotti, A.; Miklossy, J., Synchrotron-based infrared and X-ray imaging shows focalized accumulation of Cu and Zn co-localized with β -amyloid deposits in Alzheimer's disease. *Journal of Structural Biology* 2006, 155 (1), 30-37.
298. Hackett, M. J.; Aitken, J. B.; El-Assaad, F.; McQuillan, J. A.; Carter, E. A.; Ball, H. J.; Tobin, M. J.; Paterson, D.; Jonge, M. D. d.; Siegele, R.; Cohen, D. D.; Vogt, S.; Grau, G. E.; Hunt, N. H.; Lay, P. A., Mechanisms of murine cerebral malaria: Multimodal imaging of altered cerebral metabolism and protein oxidation at hemorrhage sites. *Science Advances* 2015, 1 (11), e1500911.
299. Jasuja, O. P.; Toofany, M. A.; Singh, G.; Sodhi, G. S., Dynamics of latent fingerprints: The effect of physical factors on quality of ninhydrin developed prints — A preliminary study. *Science & Justice* 2009, 49 (1), 8-11.
300. Holder, E. H.; Robinson, L. O.; Laub, J. H., *The fingerprint sourcebook*. US Department. of Justice, Office of Justice Programs, National Institute of Justice: 2011.
301. Glattstein, B.; Nedivi, L.; Almog, J., Detection of firearms imprints on hands by the Ferrotrace spray: Profiles of some common weapons. *Journal of Forensic Identification* 1998, 48 (3), 257.
302. Smyth Wallace, J., *Chemical Analysis of Firearms, Ammunition, and Gunshot Residue*. Baton Rouge: CRC Press: Baton Rouge, 2008.
303. James, S. A.; Hare, D. J.; Jenkins, N. L.; de Jonge, M. D.; Bush, A. I.; McColl, G., ϕ XANES: In vivo imaging of metal-protein coordination environments. *Scientific Reports* 2016, 6 (1), 20350.
304. Maeng, S.; Axe, L.; Tyson, T. A., Characterization of gun-barrel steel corrosion as a function of time in concentrated hydrochloric acid solution. *Corrosion* 2002, 58 (4), 370.
305. Wilke, M.; Farges, F.; Petit, P.-E.; Brown, G. E.; Martin, F., Oxidation state and coordination of Fe in minerals: An Fe K-XANES spectroscopic study. *American Mineralogist* 2001, 86 (5-6), 714-730.

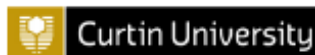
306. Dalby, O.; Butler, D.; Birkett, J. W., Analysis of Gunshot Residue and Associated Materials—A Review. *Journal of Forensic Sciences* 2010, 55 (4), 924-943.
307. D'Uva, J. A.; DeTata, D.; May, C. D.; Lewis, S. W., Investigations into the source attribution of party sparklers using trace elemental analysis and chemometrics. *Analytical Methods* 2020, 12 (41), 4939-4948.
308. Pounds, C. A.; Smalldon, K. W., The Transfer of Fibres Between Clothing Materials During Simulated Contacts and their Persistence During Wear: Part I—Fibre Transference. *Journal of the Forensic Science Society* 1975, 15 (1), 17-27.
309. Pounds, C. A.; Smalldon, K. W., The Transfer of Fibres between Clothing Materials During Simulated Contacts and their Persistence During Wear: Part II—Fibre Persistence. *Journal of the Forensic Science Society* 1975, 15 (1), 29-37.
310. Pounds, C. A.; Smalldon, K. W., The Transfer of Fibres Between Clothing Materials During Simulated Contacts and Their Persistence During Wear: Part III — A Preliminary Investigation of the Mechanisms Involved. *Journal of the Forensic Science Society* 1975, 15 (3), 197-207.
311. Pleik, S.; Spengler, B.; Schäfer, T.; Urbach, D.; Luhn, S.; Kirsch, D., Fatty Acid Structure and Degradation Analysis in Fingerprint Residues. *Journal of The American Society for Mass Spectrometry* 2016, 27 (9), 1565-1574.
312. Wisthaler, A.; Weschler, C. J., Reactions of ozone with human skin lipids: Sources of carbonyls, dicarbonyls, and hydroxycarbonyls in indoor air. *Proceedings of the National Academy of Sciences* 2010, 107 (15), 6568-6575.

Every reasonable effort has been made to acknowledge the owners of copyright material. I would be pleased to hear from any copyright owner who has been omitted or incorrectly acknowledged.

Appendix

Human Ethics Forms

Recovery and Enhancement of Fingermarks and other Physical
Evidence: Towards Improved Protocols for Crime Scene Investigation



PARTICIPANT INFORMATION SHEET

HREC Project Number:	HRE2018-0476
Project Title:	Recovery and Enhancement of Fingermarks and other Physical Evidence: Towards Improved Protocols for Crime Scene Investigation
Chief Investigator:	Professor Simon Lewis
Student researcher:	Rhiannon Boseley
Version Number:	1
Version Date:	02/07/2018

My name is Rhiannon Boseley. I am currently conducting a research project as part of my PhD at Curtin University under the supervision of Professor Simon Lewis.

Purpose of Research

This research will develop the scientific capabilities of fingerprint detection techniques to increase the recovery of fingerprint evidence and improve their effectiveness in crime scene investigations. This constitutes part of an on-going program of research at Curtin into latent fingerprints.

How You Can Help

This research depends upon a small collection of sample latent fingerprints to analyse. I am requesting you allow the research team to collect a sample of your fingerprints for this research. The fingerprints will be collected on a variety of surfaces with washed and unwashed hands.

Consent to Participate

Your involvement in the research is entirely voluntary. You have the right to withdraw at any stage without it affecting your rights or my responsibilities. When you have signed the consent form we will assume that you have agreed to participate and allow us to use your data in this research.

Storage

In adherence to Curtin University policy, the impressions will be kept in a locked cabinet within the School of Molecular and Life Sciences at Curtin for at least seven years, before a decision is made as to whether it should be destroyed.

Further Information

This study has been approved by the Curtin University Human Research Ethics Committee (Approval Number HRE2018-0476). If needed, verification of approval can be obtained either by writing to the Curtin University Human Research Ethics Committee, c/- Office of Research and Development, Curtin University of Technology, GPO Box U1987, Perth, 6845 or by telephoning 9266 2784.

If you would like further information about the study, please feel free to contact Professor Simon Lewis on 9266 2484 or s.lewis@curtin.edu.au.

Thank you very much for your involvement in this research.

Your participation is greatly appreciated.



CONSENT FORM

HREC Project Number:	HRE2018-0476
Project Title:	Recovery and Enhancement of Fingermarks and other Physical Evidence: Towards Improved Protocols for Crime Scene Investigation
Chief Investigator:	Professor Simon Lewis
Student researcher:	Rhiannon Boseley
Version Number:	1
Version Date:	02/07/2018

- I have read, the information statement version listed above and I understand its contents.
- I believe I understand the purpose, extent and possible risks of my involvement in this project.
- I voluntarily consent to take part in this research project.
- I have had an opportunity to ask questions and I am satisfied with the answers I have received.
- I understand that this project has been approved by Curtin University Human Research Ethics Committee and will be carried out in line with the National Statement on Ethical Conduct in Human Research (2007).
- I understand I will receive a copy of this Information Statement and Consent Form.

Participant Name	
Participant Signature	
Date	

To whom it may concern

I, **Rhiannon Boseley**, contributed conceptualization, investigation, methodology, visualisation, writing-original draft, writing-review & editing to the following paper:

Rhiannon E. Boseley, Buddhika N. Dorakumbura, Daryl L. Howard, Martin D. de Jonge, Mark J. Tobin, Jitraporn Vongsvivut, Tracey T. M. Ho, Wilhelm van Bronswijk, Mark J. Hackett and Simon W. Lewis

Revealing the Elemental Distribution within Latent Fingermarks Using Synchrotron Sourced X-ray Fluorescence Microscopy. Analytical Chemistry, 2019. 91, 16, pp 10622-10630

I as a Co-Author, endorse that this level of contribution by the candidate indicated above is appropriate.

Buddhika N. Dorakumbura

Daryl L. Howard

Martin D. de Jonge

Mark J. Tobin

Jitraporn Vongsvivut

Tracey T. M. Ho

Wilhelm van Bronswijk

Mark J. Hackett

Simon W. Lewis

To whom it may concern

I, **Rhiannon Boseley**, contributed Conceptualization; methodology; investigation; formal analysis; visualisation; writing - original draft; writing-review & editing:

Rhiannon E. Boseley, Daryl L. Howard, Mark J. Hackett and Simon W. Lewis

The transfer and persistence of metals in latent fingerprints. *The Analyst*, 2022. 147, pp 387-397

I as a Co-Author, endorse that this level of contribution by the candidate indicated above is appropriate.

Daryl L. Howard

Mark J. Hackett

Simon W. Lewis

To whom it may concern

I, **Rhiannon Boseley**, contributed conceptualization, investigation, methodology, visualisation, writing-original draft, writing-review & editing to the following paper:

Rhiannon E. Boseley, Jitraporn Vongsvivut, Dominique Appadoo, Mark J. Hackett and Simon W. Lewis

Monitoring the chemical changes in fingermark residue over time using synchrotron infrared spectroscopy. The Analyst, 2022. 147, pp 799-810

I as a Co-Author, endorse that this level of contribution by the candidate indicated above is appropriate.

Jitraporn Vongsvivut

Dominique Appadoo

Mark J. Hackett

Simon W. Lewis

To whom it may concern

I, **Rhiannon Boseley**, contributed conceptualization, investigation, methodology, visualisation, writing-original draft, writing-review & editing to the following paper:

Rhiannon E. Boseley, Jitraporn Vongsvivut, Daryl Howard, Mark J. Hackett and Simon W. Lewis

Leaving a mark on forensic science: how spectroscopic techniques have revealed new insights in fingerprint chemistry. Spectroscopy Europe, 2022 22

I as a Co-Author, endorse that this level of contribution by the candidate indicated above is appropriate.

Jitraporn Vongsvivut

Daryl Howard

Mark J. Hackett

Simon W. Lewis